

# T0007 : The Final CFHTLS Release

Patrick Hudelot, Yuliana Goranova, Yannick Mellier,  
Henry Joy McCracken, Frédéric Magnard,  
Mathias Monnerville, Gregory Sémah  
TERAPIX / INSTITUT D'ASTROPHYSIQUE DE PARIS

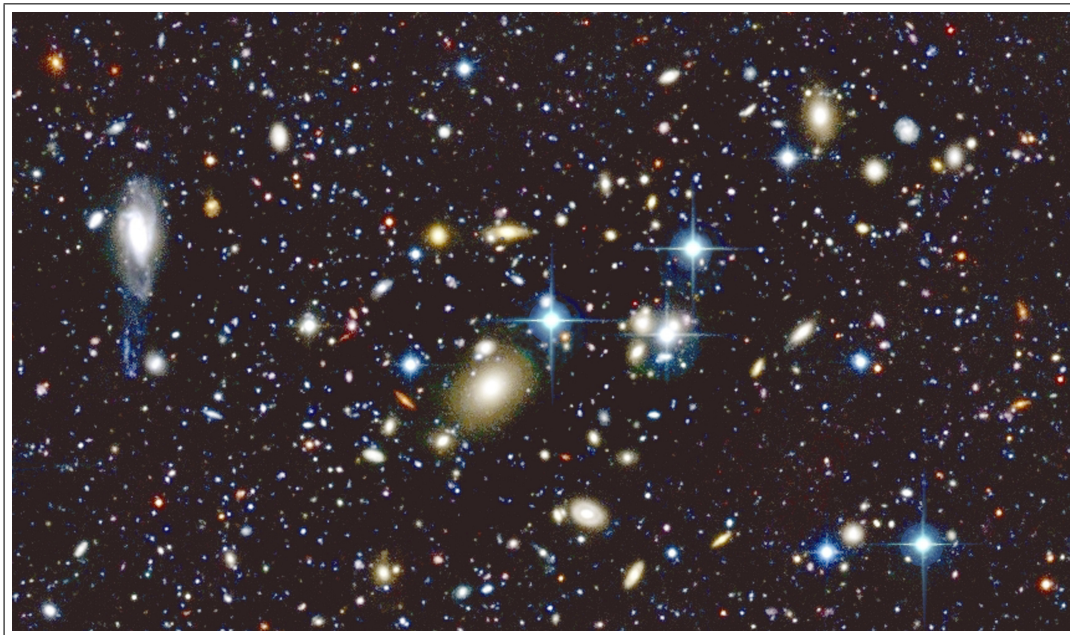
Jean-Charles Cuillandre, Kanoa Withington  
CANADA-FRANCE-HAWAII TELESCOPE CORPORATION

Nicolas Regnault, Marc Betoule  
LPNHE, CNRS-IN2P3 AND UNIVERSITÉS PARIS 6 & 7

Mathias Schultheis  
OBSERVATOIRE DE BESANÇON

Hervé Aussel  
AIM CEA CNRS, SACLAY

December 28, 2012





# 1 CFHTLS-T0007 Executive Summary

This document describes T0007, the 7<sup>th</sup> and final release of the Canada-France-Hawaii Telescope Legacy Survey CFHTLS<sup>1</sup>, produced by Terapix<sup>2</sup> based on a data set collected with MegaCam<sup>3</sup> on the CFHT. CFHTLS-T0007 is a deep sub-arcsecond (0.8'') wide-field (157 deg<sup>2</sup> total) optical survey ( $u^*$ ,  $g$ ,  $r$ ,  $i$ ,  $z$  bands) providing a high quality and homogeneous data set precisely calibrated photometrically (1.0%) and astrometrically (0.028''). This final release is directly public, open to the worldwide community.

CFHTLS-T0007 has two components: 1) the ‘‘CFHTLS Deep’’, four independent 1 deg<sup>2</sup> MegaCam ultra deep pointings, reaching a 80% completeness limit in AB of  $u^*=26.3$ ,  $g=26.0$ ,  $r=25.6$ ,  $i=25.4$ ,  $z=25.0$  for point sources, and 2) the ‘‘CFHTLS Wide’’ made of 171 MegaCam deep pointings which, due to overlaps between adjacent fields consists of a total of  $\sim 155$  deg<sup>2</sup> in four independent contiguous patches, reaching a 80% completeness limit in AB of  $u^*=25.2$ ,  $g=25.5$ ,  $r=25.0$ ,  $i=24.8$ ,  $z=23.9$  for point sources. The sky location of these fields is shown in Figure 1. This final release of the CFHTLS greatly benefits from vastly improved flat-fielding and photometric calibration techniques developed by the Supernova Legacy Survey (SNLS) team in collaboration with the CFHT. These new recipes significantly improve the precision of our photometric calibration compared to previous releases.

T0007 is derived from a parent sample comprising all validated images taken during the survey between May 26, 2003 and Feb. 02, 2009 and delivered by the CFHT pre-processing pipeline Elixir<sup>4</sup>. In addition, this release contains VIPERS-DDT (CFHT Director’s Discretionary Time) observations targeted to fill missing half-CCDs caused by malfunctioning detectors over the course of five months in 2003. All science stacks have been visually inspected; quality control information is available for each of them.

Observations were made in  $u^*$ ,  $g$ ,  $r$ ,  $z$  and either  $i$  or  $y$  filters ( $y$  is the Terapix designation for the replacement  $i$ -band filter, also known as  $i2$  at CFHT). Stacks are provided as MegaCam-size FITS images each covering 1 deg<sup>2</sup> with 0.186'' pixels. Each tile is located at each pre-defined center position listed in Table 31 for the Wide survey and Table 17 for the Deep survey. In addition, the Deep survey contains two sets of stacks, those comprising the ‘‘85%’’ best-seeing images (D85) and those comprising the ‘‘25%’’ best seeing images (D25). In total there are 48 Deep stacks corresponding to  $u^*$ ,  $g$ ,  $r$ ,  $i$ ,  $y$  and  $z$  bands, 12 for each field. There are 855 Wide stacks, in  $u^*$ ,  $g$ ,  $r$ ,  $i$ ,  $y$  and  $z$  bands or 360, 125, 245, 125 for W1–4. Over the 171 fields of the Wide, 141 are covered in  $i$ -band and 30 in  $y$ -band. The total volume of the T0007 release (stacks and catalogs) amounts to nearly 9 terabytes.

The internal astrometric errors of the stacks are between 1/15 and 1/3 of pixel, in  $x$  and  $y$ . The external astrometric errors are between 0.20'' and 0.27'' and are limited by the reference catalogue accuracy. The astrometric offsets between the CFHTLS and the astrometric reference catalogue are negligible. They are smaller than  $\pm 1/10$  of pixel in both axes and for all fields. Photometric errors have been estimated for all stacks using several independent methods. Based on external photometric comparisons with the SDSS, we find that our absolute photometric accuracy in the AB standard as well as the internal photometric homogeneity over the entire survey is at the 1.0% level or better in the  $g$ ,  $r$ ,  $i$  bands, 1.5% level in the  $z$  band, and 2% level in the  $u^*$  band.

Catalogues have been produced for each stack using a  $g-r-i$  selected ‘‘chi2’’ as a detection image and an associated mask. These data sets are complemented by a series of *merged catalogues* that combine information for each source in all filters into one file in addition to many different types of quality control data (tables, plots, figures). Merged catalogues for each of the four Deep fields and each of the four Wide

---

<sup>1</sup><http://www.cfht.hawaii.edu/Science/CFHTLS/>

<sup>2</sup><http://terapix.iap.fr/>

<sup>3</sup><http://www.cfht.hawaii.edu/Instruments/Imaging/MegaPrime/>

<sup>4</sup><http://www.cfht.hawaii.edu/Instruments/Elixir/>

patches are provided. Sources from overlapping tiles have been dealt with correctly and the parent tile information is recorded for each source. Aperture magnitudes, total magnitudes, and variable-aperture magnitudes (based on the image quality for each tile) are provided for each source.

For a concise overview of the survey, the reader should consult Tables 6, 18 and 19. These tables provide all basic data on the survey coverage, seeing, exposure times, depth and completeness, astrometric and photometric errors. This release document is complemented by practical information at the Terapix T0007 release page and the T0007 “synoptic table”<sup>5</sup>. All data sets are available worldwide directly from both Terapix and the Canadian Astronomy Data Centre (CADC). In addition, searchable catalogues are made available at the Centre de Données astronomiques de Strasbourg (CDS) through VizieR while the entire survey can now be explored visually through the Aladin sky atlas in the HEALPix format.

For users who prefer to produce their own stacks using the individual Elixir images, which are available at CADC along with their new weight-map produced by Terapix, a complete set of T0007 configuration files are listed in the Appendix A.2. In addition, a list of all images used in each Wide stack is given in Table 32. Weight maps and astrometric solution files are also provided for each individual image.

All T0007 data products are immediately available worldwide along with the photometric redshifts which are released simultaneously (Ibert et al. 2012). All the products can be downloaded from the CFHTLS T0007 release page at TERAPIX: [http://terapix.iap.fr/rubrique.php?id\\_rubrique=266](http://terapix.iap.fr/rubrique.php?id_rubrique=266)<sup>6</sup>

For further information, the Terapix team can be contacted at [terapix@iap.fr](mailto:terapix@iap.fr).

CFHT, with support from CEA, has provided outstanding MegaPrime/MegaCam support, ensuring the steady collection of data of uniform quality through CFHT’s Queued Service Observing. CFHT provided data pre-processing and calibration (Elixir) and distribution (DADS). Overall survey integrity has been ensured by the CFHTLS Steering Group and oversight by the CFHT Science Advisory Committee. Data have been archived and distributed by CADC. It is important to acknowledge this collective effort in all works using the CFHTLS data. Following recommendations of the CFHT Executive Director and the CFHT Board of Directors, the following acknowledgement should be part of any publication using CFHTLS data:

*”Based on observations obtained with MegaPrime/MegaCam, a joint project of CFHT and CEA/DAPNIA, at the Canada-France-Hawaii Telescope (CFHT) which is operated by the National Research Council (NRC) of Canada, the Institut National des Sciences de l’Univers of the Centre National de la Recherche Scientifique (CNRS) of France, and the University of Hawaii. This work is based in part on data products produced at Terapix and the Canadian Astronomy Data Centre as part of the Canada-France-Hawaii Telescope Legacy Survey, a collaborative project of NRC and CNRS.”*<sup>7</sup>

## 2 Key new features in T0007

The main goal of the T0007 release versus the T0006 release was to improve the absolute and internal photometric calibration of the survey. This has been done by applying recipes adopted by the Supernova Legacy Survey (SNLS) for the SNLS/Deep fields to both the Deep and Wide fields of the CFHTLS. These recipes were used to generate a new set of photometric flat-fields (known as “Elixir B5/SNLS”) which have been used to run a new pre-processing by Elixir at CFHT on the entire CFHTLS raw data set. Consequently, all individual weight-maps and object catalogues have been re-generated at Terapix

---

<sup>5</sup>[http://terapix.iap.fr/cplt/T0007/table\\_syn\\_T0007.html](http://terapix.iap.fr/cplt/T0007/table_syn_T0007.html)

<sup>6</sup>[http://terapix.iap.fr/rubrique.php?id\\_rubrique=266](http://terapix.iap.fr/rubrique.php?id_rubrique=266)

<sup>7</sup><http://www.cfht.hawaii.edu/Science/CFHTLS/cfhtlspublitext.html>



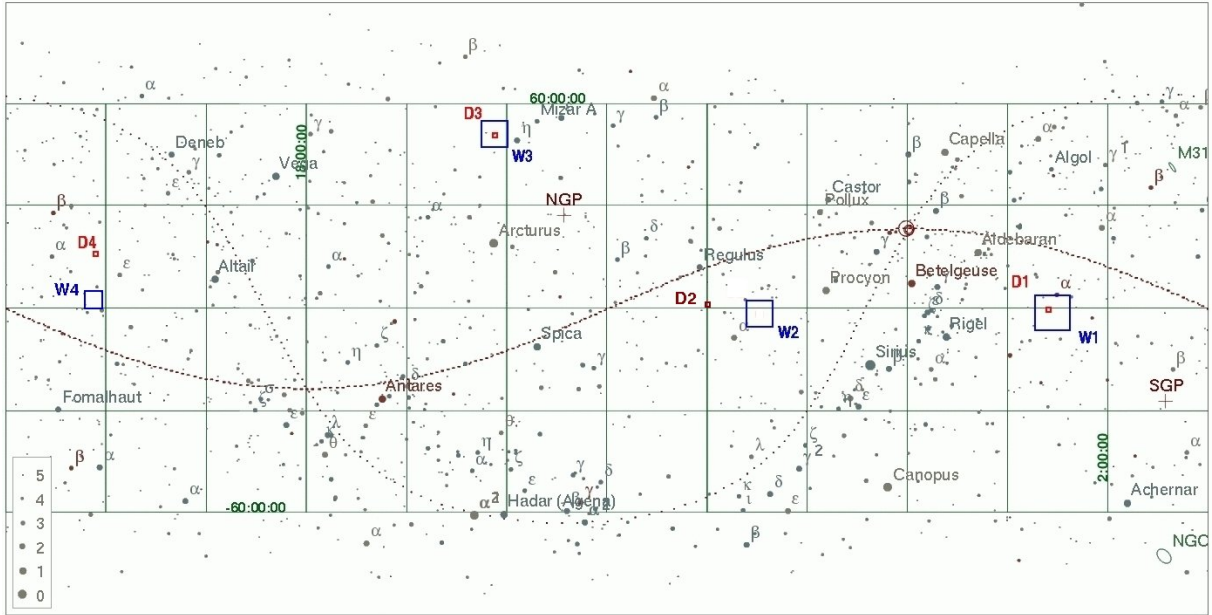


**Figure 1:** Location of the four Deep and four Wide CFHTLS fields on the sky.

for T0007.

A new series of shallow photometric calibration observations (a MegaCam program called “L99”) were made in photometric conditions towards the end of the CFHTLS survey. These observations pave in each filter the whole of the CFHTLS Wide within a short time window and are bracketed by observations of the SNLS tertiary standards on the Deep survey fields. These observations allowed the SNLS tertiary standards to be transferred to both the Deep and Wide surveys. This brings the absolute and relative photometric calibration over the entire survey at the 1% level or better in the  $g, r, i$  bands, 1.5% in the  $z$  band, and at the 2% level in the  $u^*$  band.

Several other key aspects of the processing have been revised and improved for T0007:

- A robust system is now used to correctly flag saturated objects at all stages of the processing;
- For the Deep fields, two sets of stacks are now provided, one generated using a sigma-clipped combination algorithm (leading to a slightly higher signal-to-noise) and one using the standard median combination;
- In the merged catalogues, object flags have been revised to provide object classification (star/galaxy), saturation, and masking in all bands;
- An effective seeing-scaled aperture magnitude,  $MAG\_IQ20$ , is introduced, although  $MAG\_AUTO$  magnitudes remain the best estimate for extended sources, i.e. not seeing dominated profiles;
- For each of the four Wide patches, merged catalogues have been generated and contain unique sources (overlapping objects from adjacent tiles are correctly dealt with);
- The CFHTLS catalogue data products are made available for the first time at the Centre de Données astronomiques de Strasbourg (CDS) through Vizier, while the entire survey can now be explored visually through the Aladin sky atlas in the HEALPix format;

Taken together, these changes represent a significant improvement in the scientific potential of the world-wide release T0007 (2012) compared to the six previous Terapix releases (2004-2009).

# Contents

<b>1</b>	<b>CFHTLS-T0007 Executive Summary</b>	<b>ii</b>
<b>2</b>	<b>Key new features in T0007</b>	<b>iii</b>
<b>3</b>	<b>T0007 processing description</b>	<b>1</b>
3.1	A note on CCD numbering and nomenclature . . . . .	1
3.2	Detrending at CFHT . . . . .	1
3.3	Overview of T0007 processing at Terapix . . . . .	3
3.4	Image evaluation and pre-selection . . . . .	4
3.5	Astrometric calibration and initial photometric rescaling . . . . .	6
3.6	Production of the Wide and Deep stacks . . . . .	9
3.7	Photometric calibration . . . . .	11
3.7.1	Overview . . . . .	11
3.7.2	Choice of magnitude measurement method for calibration . . . . .	13
3.7.3	Derivation of the MAG_IQ20 magnitudes . . . . .	15
3.7.4	Quantifying the improvements using MAG_IQ20 compared to MAG_SNLS . . . . .	17
3.7.5	SNLS standard star catalogue . . . . .	18
3.7.6	Calibrating the Deep survey . . . . .	19
3.7.7	Photometric calibration of the Wide survey . . . . .	21
3.7.8	Vega-AB conversion . . . . .	24
3.8	Final catalogue production . . . . .	25
3.9	Post-processing and quality control . . . . .	26
<b>4</b>	<b>Description of the CFHTLS T0007 Wide survey</b>	<b>27</b>
4.1	Overview . . . . .	27
4.2	Seeing and image quality . . . . .	36
4.3	Depth and completeness limits . . . . .	41
4.4	Photometric accuracy . . . . .	42
4.4.1	Internal photometric errors of Wide stacks from simulations . . . . .	44
4.4.2	Error estimation from overlapping Wide tiles . . . . .	48
4.4.3	Comparing CFHTLS-T0007 with SDSS-DR8 . . . . .	50
4.4.4	External photometric errors . . . . .	56
4.4.5	CFHTLS Wide photometric precision . . . . .	56
4.4.6	Stellar color-color plots . . . . .	57

4.4.7	Color offsets between CFHTLS and SDSS . . . . .	57
4.5	Astrometric accuracy . . . . .	58
4.5.1	Astrometric calibration errors . . . . .	59
4.5.2	Absolute astrometric accuracy of the CFHTLS stacks . . . . .	60
4.6	Outliers, stacks with exceptions or anomalies . . . . .	62
<b>5</b>	<b>Description of the CFHTLS T0007 Deep survey</b>	<b>69</b>
5.1	Overview . . . . .	69
5.2	Astrometric accuracy . . . . .	70
5.3	Photometric accuracy . . . . .	70
5.3.1	Comparison with SDSS-DR8 . . . . .	70
5.3.2	Internal photometric errors . . . . .	77
5.4	Depth and completeness limits . . . . .	80
<b>6</b>	<b>Data products</b>	<b>85</b>
6.1	Data set . . . . .	85
6.2	Data types and file naming conventions . . . . .	87
6.3	Content of CFHTLS source catalogues . . . . .	92
6.4	The QualityFITS input and output products . . . . .	98
6.5	Transfer to CADC and CDS . . . . .	103
6.5.1	Data products at CADC . . . . .	103
6.5.2	Data products at CDS . . . . .	103
<b>7</b>	<b>Acknowledgements</b>	<b>105</b>
<b>A</b>	<b>CFHTLS T0007 Wide supplementary information</b>	<b>106</b>
A.1	Complete list of Wide stacks coordinates, filters and exposure time . . . . .	106
A.2	List of images in each Wide stack . . . . .	110
A.3	CFHTLS T0007 Wide configuration files . . . . .	125
A.3.1	SCAMP configuration files for T0007 Wide . . . . .	125
A.3.2	SWarp stack configuration file for T0007 Wide . . . . .	133
A.3.3	SWarp chi2-image configuration file for T0007 Wide . . . . .	135
A.3.4	SExtractor .ldac catalogue configuration file for T0007 Wide . . . . .	137
A.3.5	SExtractor DUAL MODE .cat catalogue configuration file for T0007 Wide . . . . .	139
<b>B</b>	<b>CFHTLS T0007 Deep supplementary information</b>	<b>141</b>

B.1	Rescaling factors applied to deep stacks . . . . .	141
B.2	CFHTLS T0007 Deep configuration files . . . . .	142
B.2.1	SCAMP configuration files for T0007 Deep . . . . .	142
B.2.2	SWarp stack configuration file for T0007 Deep . . . . .	148
B.2.3	SWarp chi2-image configuration file for T0007 Deep . . . . .	150
B.2.4	SExtractor .ldac catalogue configuration file for T0007 Deep . . . . .	152
B.2.5	SExtractor DUAL MODE .cat catalogue configuration file for T0007 Deep . . . . .	154

## List of Figures

1	Location of the four Deep and four Wide CFHTLS fields on the sky. . . . .	iv
2	MegaCam readout layout and CEA-CFHT CCD numbering convention used in this report	2
3	Flow chart of the Terapix data processing pipeline for T0007. . . . .	5
4	The youpi-QualityFITS grading interface. . . . .	7
5	SCAMP photometric rescaling diagnostic plots . . . . .	10
6	SCAMP photometric rescaling diagnostic plots (cont'd) . . . . .	11
7	CFHTLS T0007 absolute photometric calibration . . . . .	12
8	Distribution of the Seeing of the L99 images and the CFHTLS Wide stacks . . . . .	14
9	Growth curve of the PSF models in the L99 r-band images . . . . .	15
10	Aperture correction dependence with image quality . . . . .	16
11	PSF shape in excellent and average seeing images . . . . .	16
12	PSF models in the four quadrants of a CFHTLS Wide stack . . . . .	17
13	Transmission of SNLS filters . . . . .	19
14	Flowchart of the calibration of the CFHTLS-Deep images . . . . .	20
15	Automatic determination of the saturation level . . . . .	21
16	Deep photometric calibration using SNLS standard stars . . . . .	21
17	Flowchart of the calibration of the CFHTLS Wide stacks . . . . .	22
18	Matching L99 and CFHTLS-Wide objects . . . . .	23
19	Positions and geometry of the CFHTLS Wide fields. . . . .	28
20	Positions, identification and naming conventions of stacks in the CFHTLS Wide survey. .	29
21	CFHTLS Wide pointings and dithering strategy. . . . .	31
22	W1 VIPERS-DDT field coverage. . . . .	33
23	Distribution of exposure times over the Wide fields. . . . .	36
24	Seeing FWHM mapped over the input <i>i</i> -band image 743065p.fits by QualityFITS-in	37
25	Distribution of the median seeing over the Wide tiles. . . . .	38
26	Maps of seeing (FWHM) in the CFHTLS Wide. . . . .	39
27	PSF variations as a function of the position and wavelength on MegaCam exposures . . .	40
28	Example completeness calculation for a W3 tile . . . . .	41
29	Distribution of completeness for the Wide fields . . . . .	43
30	Distribution of completeness . . . . .	43
31	Completeness as a function of seeing . . . . .	44
32	80% completeness limits maps in W1, W2, W3 and W4 . . . . .	45

33	Galaxy counts for the four Wide patches in all bands. The dotted red line corresponds to the 80% completeness for extended sources computed from the simulations. In $r$ and $i$ band counts are compared those in the VLT-VIRMOS deep field (McCracken et al., 2003).	46
34	Analysis of the internal photometric errors in CFHTLS_W_g_020241-041200_T0007 using simulations.	47
35	Analysis of the internal photometric errors using stacks overlapping regions.	51
36	Distributions of photometric offsets, $\delta_{m=u^*,g,r,i/y,z}$ , between CFHTLS Wide and SDSS-DR8 for W1, W2, W3 and W4.	53
37	Maps of photometric offsets between CFHTLS Wide and SDSS-DR8.	55
38	Comparison of one CFHTLS field with the Pickles stellar library (lower panel) and the Basel 3.1 stellar library using $[\text{Fe}/\text{H}]=-1.0$ (upper panel).	58
39	Mean RA-DEC offsets between the CFHTLS W1 and the 2MASS catalogues	63
40	Mean RA-DEC offsets between the CFHTLS W2 and the 2MASS catalogues (see comments on the caption of Fig. 39).	64
41	Mean RA-DEC offsets between the CFHTLS W3 and the 2MASS catalogues (see comments on the caption of Fig. 39).	65
42	Mean RA-DEC offsets between the CFHTLS W4 and the 2MASS catalogues (see comments on the caption of Fig. 39).	66
43	Comparison of the $(u^* - g)/(g - r)$ and $(g - r)/(r - i)$ stellar color-color tracks of the four Deep Dk-85 fields.	76
44	Estimation of the internal photometric accuracy in Deep stacks.	78
45	Weightmap images of the D2 field.	81
46	Locations of $u^*$ -band pointings used to produced the D2- $u^*$ stack.	82
47	Galaxy counts for the deep, sigma-weighted stacks in all bands for each of the four fields. The dotted lines show the 80% completeness for galaxies described in Section 5.4.	84
48	QFITS-out page of the W4 CFHTLS_W_i_222054+002300 stack.	100
49	QFITS-out page of the same field (cont'd).	101
50	QFITS-out page of the same field (cont'd).	102
51	CFHTLS all-sky previews from Aladin	104

## List of Tables

1	Influence of the aperture correction of the zero-point calibration of the Deep-L99 exposures.	18
2	AB offsets relative to the SNLS3 calibration of MegaCam.	25
3	Overview of the CFHTLS Wide fields.	30
4	Mean properties of the CFHTLS Wide survey.	30
5	Description of the additional VIPERS-DDT images.	32
6	Summary of the W1, W2, W3 and W4 mean survey parameters.	34
7	Summary of the W1, W2, W3 and W4 area covered by the survey in $deg^2$ ( $arcmin^2$ ).	35
8	Internal photometric errors per magnitude bins derived for each CFHTLS Wide field.	48
9	Internal photometric errors derived from overlapping Wide survey tiles	49
10	Internal photometric errors per magnitude bins derived for each CFHTLS Wide field.	50
11	Mean/Median magnitude offsets, $\langle \Delta_{m=u^*,g,r,i/y,z} \rangle$ , between the CFHTLS and the SDSS-DR8 surveys	54
12	External <i>rms</i> errors of the CFHTLS T0007 $u^*$ , $g$ , $r$ , $i$ and $z$ -band Wide surveys.	56
13	Mean RA and DEC differences between the external errors in each field and the mean external errors, averaged over the four Wide fields.	59
14	Mean astrometric position accuracy of each Wide stack. The Wide-averaged statistics is the ensemble average over all stacks of the mean CFHTLS-SDSS astrometric offset values computed for each stack (MegaCam mean), separately	61
15	CFHTLS Wide stacks with exceptions or anomalies.	67
16	CFHTLS Wide stacks with exceptions or anomalies (cont'd).	68
17	Overview of the CFHTLS Deep fields.	69
18	Summary of the “25%” best-seeing stack parameters.	71
19	Summary of the “85%” Deep stack parameters.	72
20	Summary of the “25%” best-seeing sigma-weighted stacks.	73
21	Summary of the “85%” best seeing sigma-combined stacks.	74
22	Analysis of the internal photometric errors in the CFHTLS T0007 Deep data from the comparison of source pairs in D-25 and D-85.	79
23	Mosaicing of D-25- $u^*$ and D-85- $u^*$ stacks.	83
24	CFHTLS files, point-of-access and naming convention.	88
25	CFHTLS files, point-of-access and naming conventions (cont'd).	89
26	CFHTLS files, point-of-access and naming conventions (cont'd).	90
27	CFHTLS files, point-of-access and naming conventions (cont'd).	91
28	Description of parameters listed in T0007 catalogues.	95
29	Description of parameters listed in T0007 catalogues (cond't).	96



30	Description of parameters listed in T0007 catalogues (cont'd). . . . .	97
31	The CFHTLS T0007 Wide stacks coordinates, filters and exposure time. . . . .	106
32	Full list of CFHTLS input images included in each Wide stack . . . . .	110
33	Deep images rescaling factors . . . . .	141

## 3 T0007 processing description

### 3.1 A note on CCD numbering and nomenclature

In what follows, the naming of MegaCam CCDs follows the CEA-CFHT naming convention. The camera is composed of 36 CCDs numbered from CCD00 to CCD35 (Boulade et al., 2000). CCD00 is at top-left (extreme North-East position) and numbers increase from left to right and top to bottom. When 1/2 missing CCDs are reported it means that one of the MegaCam output amplifiers did not work. In that case a 1/2-size CCD rectangle, as drawn in Fig. 2 has no data. These failures were very rare, limited to a 5 months long window in 2003, representing less than 0.3% of the data and are listed on the MegaPrime failures page<sup>8</sup>.

These failures demand special handling in the pipeline, but they have almost no impact on the science. In this document a “MegaCam pointing”, or a “tile” denotes a  $1 \times 1 \text{ deg}^2$  field corresponding to a target position of the Wide survey listed in Table31.

### 3.2 Detrending at CFHT

Removing the instrumental signature from the raw MegaCam frames taken at CFHT under the Queued Service Observing system falls under the responsibility of the Elixir<sup>9</sup> pipeline at CFHT. Correcting that signature is called “detrending” in Elixir parlance since it goes beyond what basic pre-processing usually encompasses. The steps involve, in a single pass, applying a bad pixel mask, correcting for the two-dimensional structures of the overscan, subtracting a master bias frame, and applying a flat-field including the illumination correction that makes the photometric zero point uniform across the entire image at the better than 1% level. The *i* and *z* images go through an extra step to subtract a scaled master fringe pattern. Finally the images are astrometrically calibrated on a per-CCD basis and photometric zero points information is fed into the final MEF (36 extensions) file based on the observing run global photometric analysis. The following paragraph cover some details of these operations in the context of the T0007 release.

At the end of each MegaCam run, master twilight flat-field frames and master fringe frames are built from selected exposures taken during the run, including non-CFHTLS data (which represents about half of the total dataset over the acquisition phase of the survey, 2003-2009). Elixir builds master flat-fields for each filter by stacking the individual twilight flat-field frames. Individual frames inadvertently contaminated by clouds or nearby moon light are rejected. They are identified by dividing each individual flat field exposure by the master flat, and inspecting the result visually. Typically, no more than one iteration is needed to reject the outliers and ensure consistent quality of this key calibration frame over the years. In order to mitigate possible non-linearity residuals at the sub-percent level, individual flat field images are acquired in the 10,000 to 15,000 ADU range. After two weeks, the typical length for a MegaCam run, there are typically 40 to 60 usable frames that can be stacked into a final normalized frame equivalent to a single 400,000 ADU counts per pixels, reducing photon noise to negligible levels.

If one measures the photometry of the same star on an image flat-fielded from the basic twilight flat-fields, the flux varies by about 15% in the *u* band and 10% in the *g*-, *r*-, *i*-, and *z*-bands when moving the star from center to edges of the field of view. The variation is monotonic and essentially follows a circular pattern. It is caused by scattered light in the optics (a combination of indirect illumination and

---

<sup>8</sup><http://www.cfht.hawaii.edu/Instruments/Imaging/MegaPrime/megaprimehistory.html>

<sup>9</sup><http://www.cfht.hawaii.edu/Instruments/Imaging/MegaPrime/dataprocessing.html>

B	AB	AB	AB	AB	AB	AB	AB	AB	A
00	01	02	03	04	05	06	07	08	
B	AB	AB	AB	AB	AB	AB	AB	AB	A
09	10	11	12	13	14	15	16	17	
18	19	20	21	22	23	24	25	26	
A	BA	BA	BA	BA	BA	BA	BA	BA	B
27	28	29	30	31	32	33	34	35	
A	BA	BA	BA	BA	BA	BA	BA	BA	B

**Figure 2:** MegaCam readout layout and CEA-CFHT CCD numbering convention used in this report. Each rectangle represents a MegaCam CCD. When mounted on MegaPrime, North is at the top, East to the left and each CCD covers a field of view of about  $6' \times 14'$ . The dotted lines separate the two 1/2 CCDs read by each amplifier of a detector. The positions of the two amplifiers are indicated by A or B. Note the organization of MegaCam into two sub-mosaics. They are separated by a large horizontal gap of 82" width.

light reflections) and the inherent geometrical distortion of the image. A photometric flat-field, which ought to deliver uniform photometry across the field of view is then created by multiplying the master flat-field frame by the maps of the imager photometric response non-uniformities. This composite flat-field is the one used for flattening the science images of the entire run, and allows for all multiplicative effects in the image to be corrected at once.

The data released by CFHT for the six previous Terapix releases of the CFHTLS were based on photometric flat-fields which were affected by 4% peak-to-peak residuals. While this was adequate for most science goals of the CFHTLS, it was not satisfactory for the SuperNova Legacy Survey (Astier et al., 2006). As a consequence, the SNLS team and CFHT have collaborated since 2005 to realize precision photometric measurements using MegaCam. The effort was instrumental in unlocking the potential of the SNLS survey (Regnault et al. (2009), Betoule et al, submitted).

This new recipe makes possible better than 1% peak-to-peak radial residuals within an image in all filters. This Elixir recipe version is named “B5”(or “B5/SNLS” in reference to its origins). All individual Elixir processed frames, available at CADC, used to build the Terapix T0007 release have a header indicating the photometric recipe used (in general the newly processed images indicate an Elixir version 3.0 or higher).

Fringe patterns are built by processing all  $i$  and  $z$ -band images corrected by the final flat-field. First the sky background is mapped at a large scale (100 pixels) and subtracted. Then, the exposures are scaled according to the fringe amplitudes measured on one hundred peak-valley pairs on each CCD. Since all

CCDs see the same sky and since the photometric zero-point is uniform across the entire field of view, a single scaling factor is derived from the 36 CCDs. The scaled exposures are stacked, and an iterative process similar to the one described above is carried out, with a visual control allowing the rejection of frames containing extended astrophysical sources such as large galaxies. The fringe correction is challenging at times in the  $z$ -band and some images get only partially corrected due to the extreme behavior of the OH emission lines in the upper atmosphere which cause a signature too different from the run master fringe frame. (A different observing strategy such as the one adopted for the MegaCam Next Generation Virgo Survey would have helped but was not available during CFHTLS observations.) Consequently the defringing recipe is unchanged for the T0007 data collection. All fringe patterns were however re-created since they must include the signature of the new photometric B5/SNLS flat-fields.

After these detrending steps, Elixir processes all the images of the run, and derives an astrometric solution per CCD only, at the pixel scale level ( $0.2''$ ). The goal at the Elixir level is to provide the users with a first order astrometric solution and no global solution over the mosaic is computed; this is a task handled by Terapix.

Following this step, all the frames containing Smith et al. (2002) photometric standards (the CFHT QSO “Q97” program. Please refer to the description of the Observing Programs Identificators<sup>10</sup>) are identified and processed using SExtractor. A median zero-point for the entire run is derived for each filter, since not enough observing time is available to derive enough standard star observations per night to derive solid zero-point solutions. Again, the intention is to provide MegaCam users with a reliable photometric scaling, offering a precision at the 4% level in absolute. But then again, since this default calibration was clearly not precise enough for their needs, the SNLS team developed in collaboration with CFHT new procedures to calibrate the images. This vast undertaking is the key to major improvements in T0007 compared to T0006: all knowledge acquired for the SNLS survey has been passed to the Deep and the Wide surveys. This calibration effort is described in detail in Section 3.7.

### 3.3 Overview of T0007 processing at Terapix

TERAPIX processing steps from the download of Elixir pre-processed CFHT images to the final stacked images and catalogues is illustrated in Fig. 3. The T0007 CFHTLS pre-processed images described in the previous section were transferred from CFHT and validated against the T0007 image lists. All Queued Service Observing validation flags archived at CFHT were also downloaded<sup>11</sup>.

For the T0007 release we use Elixir “B5/SNLS” pre-reduced images. The images were first ingested with the Terapix processing pipeline YouPI, producing weight-maps and input catalogues. We use quality grades from previous CFHTLS releases for images which were already in the database; new images from the “L99” photometric calibration program and the VIPERS Director’s Discretionary Time observations (described later) were graded using the Youpi grading interface, described below.

Images were then divided into each of the four Wide and four Deep fields and processed with SCAMP (Bertin, 2006) in order to derive the astrometric as well as the initial photometric calibrations. As explained below, as a consequence of the new calibration scheme based on L99 images, the astrometric and photometric calibrations were performed separately.

Once aligned astrometrically, images are co-added by SWARP (Bertin et al., 2002) using the SCAMP initial photometric rescaling. For the Deep field, images lists are derived using seeing and photometric rescaling constraints. Two series of Deep stacks are produced using two images combination schemes: median

<sup>10</sup><http://www.cfht.hawaii.edu/Science/CFHTLS-DATA/cfhtlsprograms.html>

<sup>11</sup><http://www.cfht.hawaii.edu/Science/CFHTLS-DATA>

and sigma-clipped, denoted throughout the current document as “MEDIAN” and “SIGWEI” stacks.

Because of the inherent limits in using a photometric calibration derived solely from the pre-existing CFHT survey photometric calibration (lists of observations previously flagged as photometric by the CFHT and photometric header calibration written by Elixir) in T0007 we use a different approach to calibrating the survey. Both Deep and Wide stacks are tied to the SNLS photometric system using photometric standards which lie within the CFHTLS Deep field (Regnault et al., 2009). For the Deep fields, which contain the Deep field calibrators, we can rescale images directly to the SNLS system, whereas for the CFHTLS Wide fields we use L99 short photometric exposures which are bracketed by observation of the Deep fields containing the calibrators. These L99 observations are then used to rescale the Wide tiles. The original SNLS Vega photometric system is finally converted to the natural AB system which has been used in previous CFHTLS releases (4.4).

Several types of final catalogues are produced: individual catalogues for each image, merged catalogues with all filters for each tile, Wide-patch merged catalogue (all tiles in all filters for each Wide patch). The objects are flagged according to the potential saturation in each filter and location in masked regions, object type (star or galaxy).

### 3.4 Image evaluation and pre-selection

In the first QualityFITS step (“QFTIS-in”), all individual CFHTLS input images are used to produce an input .ldac source catalogue (these are FITS binary tables containing an additional table derived from FITS header keywords present in the input images). This catalogue is used first for image quality assessment and subsequently in the astrometric and photometric calibration. QualityFITS also creates for each a image a “confidence map” or weight-map image, which corresponds to the relative inverse variance of each pixel. This weight is derived from the flat-field and mask images produced by the Elixir pipeline (Magnier & Cuillandre, 2004) at CFHT. This weight map is also used during image combination.

Saturated pixels are also flagged. This saturation cut is much lower than the CCD limit provided in the FITS header (SATURATE FITS keyword) to remove all bright stars and enable star-galaxy separation. During this step we discovered a previously overlooked problem: for some images the highest bit (16th) of the analog-to-digital encoders was stuck to 0, resulting in a 15 bits dynamic in one entire bank of the MegaCam focal plane (CCD27 → CCD35) versus the normal 16 bits<sup>12</sup>. This resulted in different saturation levels across the MegaCam mosaic (32000 instead of 64000). We have modified the .ldac catalogues of the affected exposures outside QFTIS-in with a proper flagging of the two-level saturation without rejecting too many bright sources which are essential for photometric calibration.

After QFTIS-in, images are visually inspected and evaluated through the Youpi image evaluation interface<sup>13</sup>. For T0007, grades were preserved from previous survey releases, and only new images were graded. For each image, Youpi provides a link to a QFITS-in web page which summarizes properties of each image. All QFITS-ed images are then graded “A”, “B” or “C”, after a visual inspection of each page (see Fig. 4), paying in particular special attention to the PSF and the seeing over the MegaCam field. Images with grade C are not within the CFHTLS specifications or show serious problems (such as missing CCDs or extensive scattered light over the whole MegaCam field, or obvious telescope guiding problems). “Grade B” represents acceptable images, within the specifications, but for which QFTIS-in revealed minor problems (such as unusual galaxy or stellar counts, or seeing values very close to the

<sup>12</sup>The problem was present during two observing runs in the winter 2004 before it was identified and corrected by CFHT. The source of this was a faulty video board which was subsequently replaced.

<sup>13</sup><http://youpi.terapix.fr>

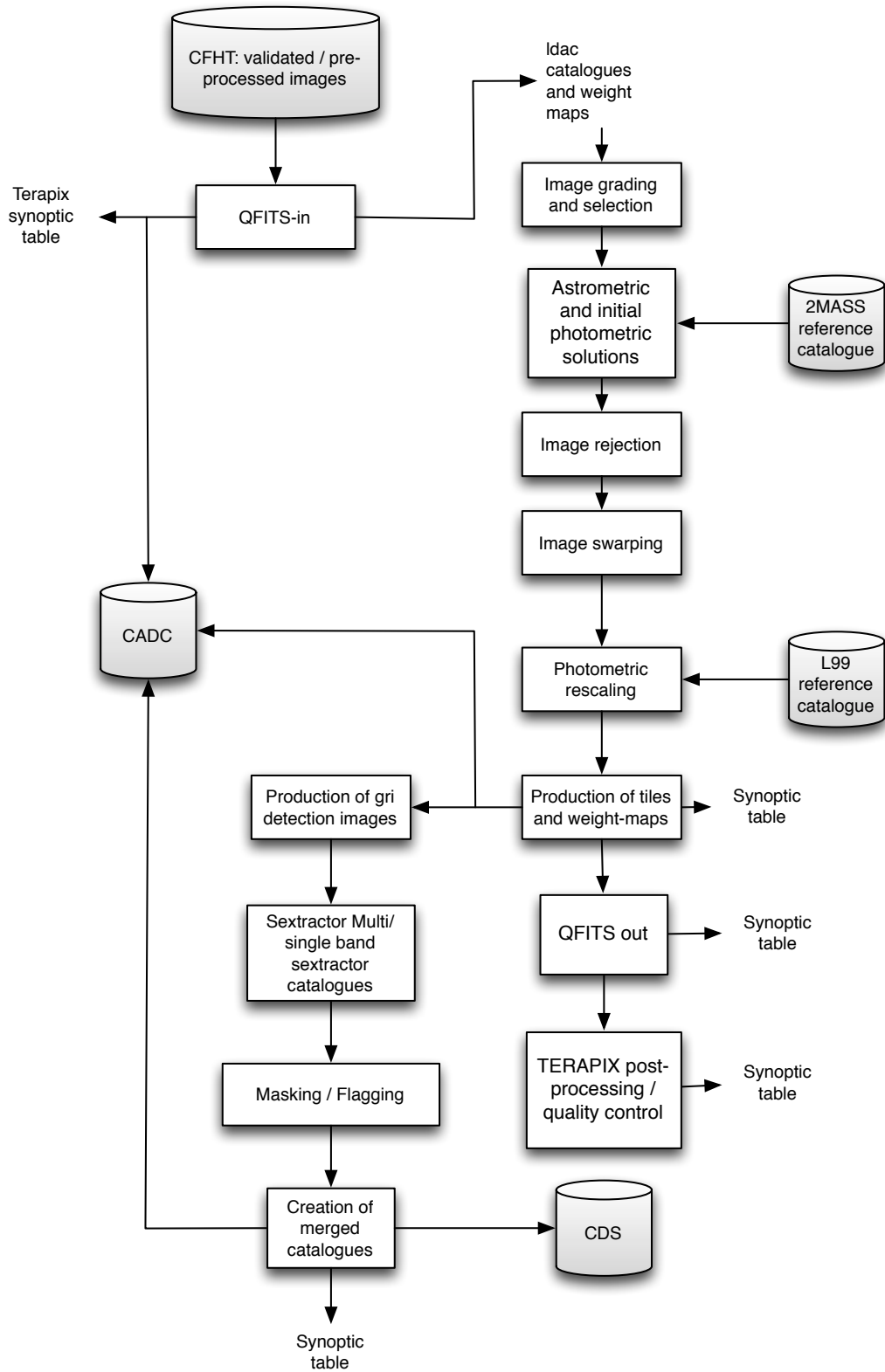


**Figure 3:** Flow chart of the Terapix data processing pipeline for T0007.

upper limit). The grading step is applied to all images which were validated (flag) at CFHT.

Based on the QualityFITS selection a initial selection of images is made by applying the following criteria:

- Terapix class: A or B grades;
- Exposure time longer than 60 seconds ;
- FWHM less than  $1.3''$ , except for  $u^*$  ( $< 1.4''$ ) ;
- Airmass less than 1.7;

(Note that the number of images with seeing  $> 1''$  in the CFHTLS survey is actually quite small since the observing requirements set the image quality upper limit at  $1.0''$ )

Rejected images are removed from the processing pipeline. In subsequent steps, the QFITS-in catalogues of the remaining sample are used to derive the astrometric and photometric calibrations.

The images used in the Wide survey are essentially these images, except that in certain stacks with missing detectors, they are supplemented by supplementary DDT observations mentioned above.

The selection of images used in the T0007 CFHTLS Deep survey starts from a pre-defined set of 85% best-seeing images which has been created in previous releases. It was verified that the seeing on these images (measured using a fit to the PSF with a Moffat function in PSFex) was less than  $1.1''$  in  $u^*$  and less than  $1.0''$  in all other bands. In addition, any image which had a field-to-field photometric rescaling (explained in the next section) which was larger than 0.15 mag was also rejected. The resulting list corresponds to our “85%” list. The “25%-best” seeing images were simply constructed from the 25% best seeing images *drawn from this list*. We verified that the effect of creating such list versus a list from the “best 25%” of all images has minimal effect on the completeness of the final stacks. Despite the name of “85%” and “25%” best seeing images, the lists do not strictly contain 85% and 25% of the total number of exposures as explained in this paragraph.

### 3.5 Astrometric calibration and initial photometric rescaling

The T0007 astrometric solutions and the initial photometric calibration were computed using Scamp in version 1.7.0. The configuration files which were used are presented in Appendix A.3.1. Scamp is a software developed by Emmanuel Bertin and available on Astromatic<sup>14</sup>.

Scamp first reads all image headers and then splits the exposures into a series of astrometric “contexts”. Each context isolates blocks of observing epochs where the instrument focal plane is in a fixed and (mostly) stable position; for the CFHTLS these contexts can be selected using the CFHT QRUNID FITS header keyword. Special care is taken to correctly flag saturated objects in particular for images for which saturation levels change significantly across the mosaic (described in Section 3.4).

An approximate first-guess for the position of astrometric sources is derived by the cross-identification of sources in the QFITS-in .ldac catalogues with the 2MASS external reference catalogue (Skrutskie et al., 2006). As in previous releases, 2MASS was chosen because astrometric solutions were stable and more accurate than using the USNO. (We note that ultimately an SDSS-based calibration would have been preferable because of the higher surface density of sources in SDSS and the similarity of SDSS and

---

<sup>14</sup><http://www.astromatic.net/software/scamp>

### Processing History

20 0 (20/15445)

Show all finished First Quality Evaluation processings

Show all images

Page 1 2 3 4 5 6 7 ... 752 > page 1

15093 of 15093 images already graded

First Quality Evaluation of 765143p	goranova	2009-08-06 18:56:13	Graded A
First Quality Evaluation of 766155p	goranova	2009-08-06 18:41:55	Graded B
First Quality Evaluation of 766153p	goranova	2009-08-06 18:33:32	Graded A
First Quality Evaluation of 765624p	goranova	2009-08-06 18:18:46	Graded A
First Quality Evaluation of 765622p	goranova	2009-08-06 18:11:58	Graded A
First Quality Evaluation of 765620p	goranova	2009-08-06 17:54:20	Graded A

### QualityFITS-in processing - 765143p.fits

2009-08-06 18:56:13  
2009-08-06 19:18:30  
Exit status: SUCCESS  
0:22:17 on  
fcix2.clic.iap.fr

Job initiated by goranova  
A ★★★★★ goranova  
Image graded 1 time

See full QFITS web page

USER PERMISSIONS

goranova/Terapix rwr---- (640)

CONDOR JOB LOGS

Cluster Id: 1144.0  
Condor out: --  
Condor log: --  
Condor error: --

QUALITYFITS-IN PROCESSING HISTORY (1)

Graded (x1) 2009-08-06 18:56:13 (0:22:17) fcix2.clic.iap.fr goranova [Reprocess]

QUALITYFITS RUN PARAMETERS

Image: /data/fcix/raid/T0005-Tp=release/D1-data/Images/i-dht/765143p.fits  
Flat: /data/fcix/raid/1youpi-INPUT/CFHTLS/T0006-Wide/AllFlat  
Mask: /data/fcix/raid/1youpi-INPUT/CFHTLS/T0006-Wide/AllMask  
Reg: --  
Results output dir: /data/fcix/raid/2youpi-OUTPUT/PROD/goranova/ftsini/D1-ext/

Toggle QualityFITS config file view

IMAGE INFORMATION

Object: D1	RunId: 04BL01	Filter: i.MP9701
ExpTime: 360.1	Ingestion Date: 2008-09-28 21:13:17	Air Mass: 1.140
Phot_c (header): -	Phot_c (custom): -	RA: 36.50612500
Dec: -4.49111100	UTC obs: 2004-10-09 00:00:00	Telescope: CFHT
Instrument: MEGACAM		

QUALITYFITS INFORMATION

RA offset: -	Dec offset: -	RA std dev: -	Dec std dev: -
Saturation level: 50000.0000 ADU	Median background: -	Min PSF FWHM: 2.781 arcsec	Avg PSF FWHM: 3.100 arcsec
Max PSF FWHM: 3.700 arcsec	Min PSF half-light diameter: -	Avg PSF half-light diameter: -	Max PSF half-light diameter: -
Min PSF elongation: 1.02	Avg PSF elongation: 1.21	Max PSF elongation: 1.46	Min PSF chi2/d.o.f: 1.41
Avg PSF chi2/d.o.f: 1.92	Max PSF chi2/d.o.f: 3.05	Min PSF residuals: 0.02	Avg PSF residuals: 0.04
Max PSF residuals: 0.08	Min PSF asymmetry: -	Avg PSF asymmetry: -	Max PSF asymmetry: -
Min number of PSF stars: 48	Avg number of PSF stars: 60	Max number of PSF stars: 75	Previous Release QFITS-in Grade: -

Toggle QFITS results ingestion log view

Previous Release Grade: No Grade. Grading history (1): ★★★★★ 2009-08-06 19:46:03 goranova Your grade: Grade: A ★★★★★

Comment unknown.

Your comment:

Custom:



### Evaluation of 765143p

- raw image weight map
- background map Background histogram
- PSF map PSF histogram
- Galaxy counts histogram Galaxy selection Rth-mag
- Star counts histogram Star selection Rth-mag
- PSF orientation and ellipticity map Rth-mag diagram

Keyword	Value
ORIGIN	CFHT
TELESCOP	CFHT 3.6m
DETECTOR	MegaCam
INSTRUME	MegaPrime
DATE	2004-10-09T10:39:17
RUNID	04BL01

Keyword	Value
OBJECT	D1
EXPTIME	360.05
FILTER	i.MP9701
RA	2:26:01.47
DEC	-4:29:26.0
EQUINOX	2000.0
AIRMASS	1.140

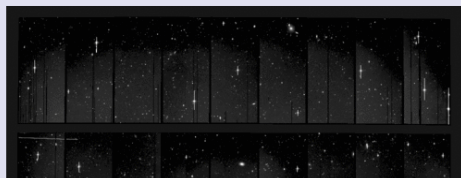


**Figure 4:** The youpi-QualityFITS grading interface. The top panels show the youpi-QualityFITS main page which displays the status of QualityFITS evaluations of all images (left), and the QualityFITS evaluation of a user-selected image (right). On the top right panel the grading status for the selected image is displayed. In this case the QualityFITS page (bottom panel) is loaded by youpi and options to grade a new image or to update the grade of an image are displayed. Users can then examine the data shown on Fig. 48 to 50. The grading interface minimizes the number of actions required to only three clicks per image. The youpi database preserves the evaluation history of all images and so it also archives the grades from previous releases. For the T0007 release, only new images have been graded.



CFHTLS filter sets; however the SDSS does not cover the whole CFHTLS survey; only W3 and D2 and D3 fields have complete coverage.)

To match CFHTLS and 2MASS catalogues we choose a source matching radius (CROSSID\_RADIUS) of 2.0 arcsec for all Wide and Deep fields. A 3<sup>rd</sup> order polynomial distortion model is then derived by minimizing a weighted quadratic sum of differences in positions between the 2MASS and the QFITS-in matched sources, and, internally, between different QFITS-in catalogues with overlapping regions of MegaCam images (see Fig. 21). Scamp then computes the astrometric internal errors from the differences of astrometric positions of sources inside the overlapping regions and the external errors from the comparisons of astrometric positions of MegaCam sources with the 2MASS catalogue.

Images are calibrated separately for each of the four Wide and four Deep fields. However, in order to take full advantage of L99 photometric images, processing is done in two steps:

- **Astrometric calibration** – this includes all types of images: science images, short and L99 photometric calibration images,  $r$ -band astrometric anchor pre-survey exposures and supplementary VIPERS-DDT (discretionary time) exposures for filling missing half-CCDs in W1.
- **Initial photometric rescaling** – this includes only science images and photometric bootstrapping (Q98 - Observing Programs Identifiers<sup>15</sup>) images and it uses the astrometric solution from the previous step. The primary goal of this step is to compute the relative rescaling of the individual images in each pointing before stacking. The absolute photometry is then anchored to the L99 exposures (see the procedure described in Section 3.7).

In addition, due to the large number of exposures in some of the fields the astrometric calibrations cannot be solved globally (due to memory requirements) and are additionally split by filter. For those fields the large number of observing runs produces too many astrometric contexts which cannot be handled by Scamp using current Terapix computing resources. For this reason, the astrometric calibration is computed in a field-dependent way.

For the W1 field, for which the astrometric solution is derived with respect to a reference catalogue we use this procedure:

- We first combine  $(r, i/y)$  .ldac catalogues of the science exposures as well as the  $r$ -band Wide pre-survey astrometric anchoring images and find an astrometric solution using the 2MASS reference catalogue and use this to produce an internal  $(r, i/y)$  astrometric reference catalogue, calibrated with 2MASS;
- We then run Scamp on all W1 exposures using this internal reference catalogue on the  $(u, g)$ ,  $(r, z)$ , and  $(i/y)$  samples separately. The homogeneity and consistency of the calibrations are ensured by the common  $r$ -band Wide pre-survey data used for all samples.

For W2, W3 and W4 fields, the astrometric solution is calculated once for each field by considering all selected images simultaneously, regardless the filter, exposure type or epoch, using 2MASS. In this way all images of a given Wide field are calibrated globally and in a homogeneous way.

All Deep fields are calibrated with SCAMP in a similar way as W1. However, the image selection used to construct the internal reference catalogue is done differently:

---

<sup>15</sup><http://www.cfht.hawaii.edu/Science/CFHTLS-DATA/cfhtlsprograms.html>

- First a sub-set of only two images per QRUNID is drawn from all science  $r, i, y$ -band exposures and supplemented with a set of all  $i$ -band astrometric anchoring fields surrounding the Deep pointing for D2, D3, and D4, and a sub-sample of W1 surrounding exposures for D1. The additional data sets are spread over many different observing periods and sample all QRUNIDs. As in W1, these internal reference catalogues are calibrated with respect to 2MASS;
- The astrometric solution for each filter is then calculated separately using the internal reference catalogue. The precision of the internal astrometric solution is assured by the common  $i$ -band astrometric anchoring exposures. In addition, due to the compact areas on the sky from which the Deep samples are drawn, the CROSSID\_RADIUS for this step is reduced to 0.5 arcsec.

The astrometric solution for the Deep fields is derived using the same recipe for each field, thus improving the consistency of the calibrations between the four Deep fields.

Astrometric solutions have been verified by examining the large range of check-plots produced by Scamp, in particular the 1D and 2D internal and external astrometric solutions as a function of RA and DEC, the reduced chi-squared for the astrometric solution, and the field-to-field photometric offset. After an optimal solution is calculated, this astrometric solution is written in a separate .head file for each input image.

In T0007, the initial photometric field-to-field rescaling is computed separately from the astrometric solution. Photometric flags are written in the .ahead files together with the default zero point provided by CFHT and derived from the astrometric solution computed in the previous step. As for the astrometric calibration, Scamp minimizes the quadratic sum of magnitudes using the overlapping regions between images. It then re-scales the flux of non photometric images accordingly (Fig. 5 and Fig. 6). After this step a “final” photometric rescaling is computed for each of the image tiles; this is described in detail in Section 3.7.

Finally, these astrometric and photometric solutions are combined into a single output .head file for each image (containing information for all of the 36 MegaCam extensions) which is then used for producing the Wide and Deep stacks using SWARP. All ScAMP output data including .xml tables, diagnostic plots, .ahead and .head files can be found in the T0007 synoptic table.

### 3.6 Production of the Wide and Deep stacks

Each stack comprises all images located inside a radius of 3' with respect to a tile center position. The shifts between each exposure in an observing sequence ensures that gaps between the CCDs are filled in the stacked image. Note that in the case of the Wide stacks, the overlapping pixels of nearest neighbor tiles are used for the field-to-field calibration but are not used during the combination process. (In the Deep D2- $u^*$  field, additional data from the COSMOS survey is used to make the final stacks). The software used for the image combination is SWARP (in version 2.17.6) developed by Emmanuel Bertin and available on Astromatic<sup>16</sup>.

The T0007 images and weight-maps are combined using the option COMBINE\_TYPE “MEDIAN” in SWarp for the Wide and Deep surveys. The weight-maps correspond to SWarp’s image type MAP\_WEIGHT which correspond to maps of relative inverse variance. Images are resampled using Lanczos-3 interpolation kernel. All resulting tiles and weight-maps have  $19354 \times 19354$  pixels of  $0.186''$ , corresponding  $1 \text{ deg} \times 1 \text{ deg}$ .

<sup>16</sup><http://www.astromatic.net/software/swarp>

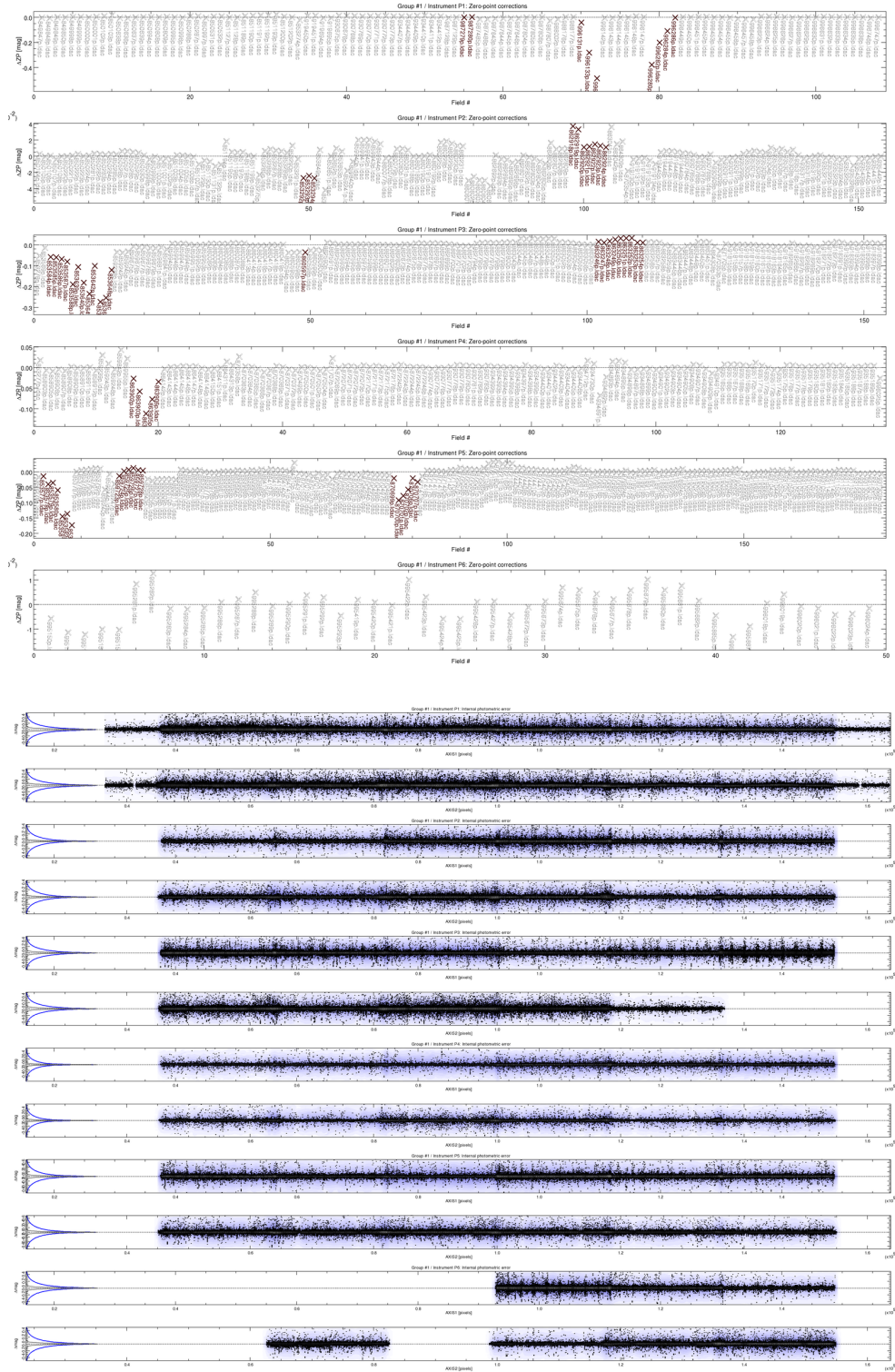


**Figure 5:** Outputs of the SCAMP calibration process of the W4 field (cont'd). Photometric rescaling and calibration of W4 images.

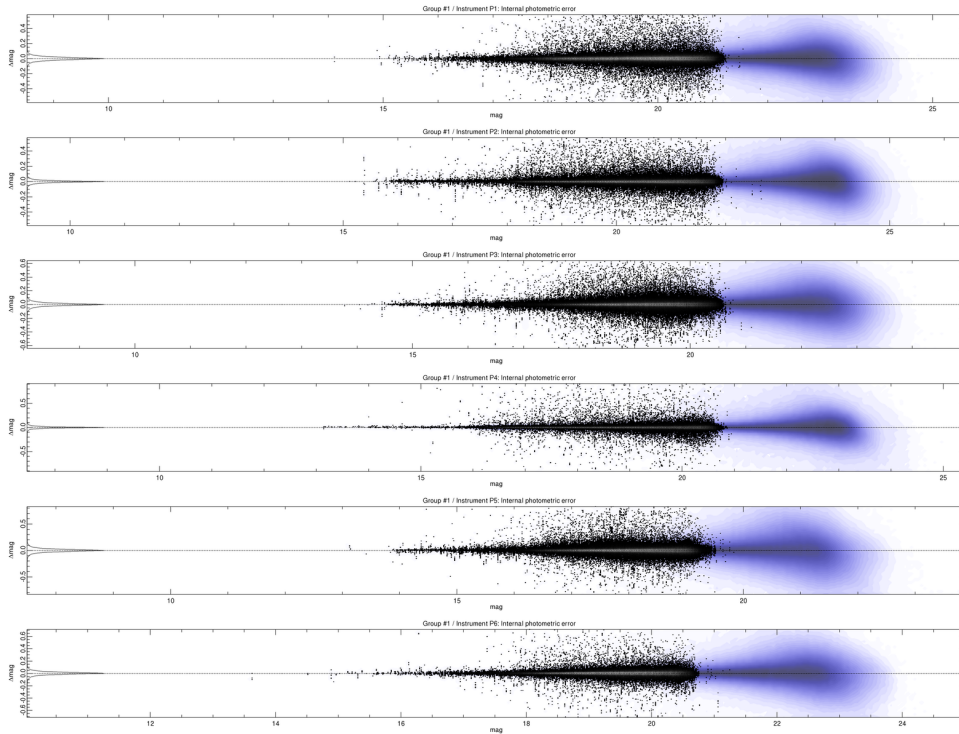


**Figure 6:** Outputs of the SCAMP calibration process of the W4 field (cont'd). Internal photometric error as function of magnitudes of W4 images.

Additionally, for the Deep fields, a second set of stacks is produced using a sigma-clipping pixel combination algorithm, selected by setting COMBINE\_TYPE “SIGWEI” in our modified version of SWarp supplied by S. Foucaud. The clipping parameter is set to  $\pm 3.0\sigma$ .

The complete list of images used in each Wide tile is presented in the Appendix A.2. For the Deep fields, similar lists can be made available on demand. For the Deep fields, images with seeing  $< 1.3''$  in  $u^*$ , and  $< 0.95''$  in  $griz$ , are selected for the stack production. From the lists, secondary lists are created containing the “85%” and “25%” best-seeing images.

All stacks have a zero-point of 30 in AB magnitudes. The magnitudes of objects in these stacks are computed as follows:  $m = 30 - 2.5 \log(\text{counts})$ . The SWarp configuration file is presented in Section B.2.2.

Once the  $g$ ,  $r$  and  $i$  band data are available they are combined into a “chisquare” or chi2 image which has the same position, scale and input size as the  $g$ ,  $r$  and  $i$  images. This chisquared image has been shown to be the optimal way to create a detection image from a series of images taken with different filters (Szalay et al., 1999). The SWarp configuration file for the production of the T0007 chi2 images is given in Section B.2.3.

## 3.7 Photometric calibration

### 3.7.1 Overview

CFHTLS T0007 photometry is anchored to the SNLS photometric system (Regnault et al., 2009) using a catalogue of tertiary standard stars supplied in this paper. This choice of calibrators implies that the filter bandpasses to be used in any scientific analysis are those defined by the SNLS team and described

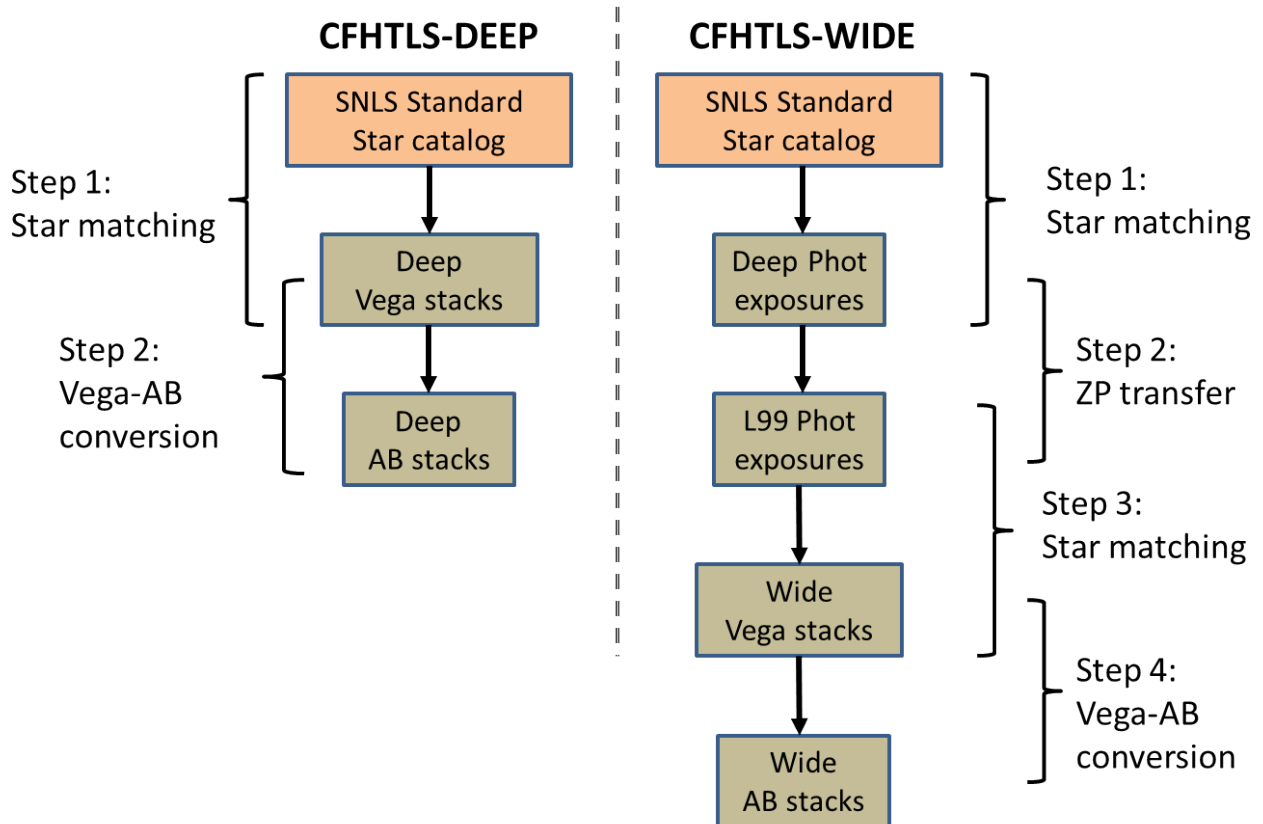


**Figure 7:** CFHTLS T0007 absolute photometric calibration. For the Deep fields, the calibration of the photometric zero-points can be made directly since the SNLS reference stars are inside the images. In the Wide, an intermediate set of photometric images (L99) is needed to apply the SNLS photometry to the stacks.

in section 3.7.5. The method to tie the CFHTLS to the SNLS reference system follows the method described in Regnault et al.:

- First the fluxes of the SNLS tertiary standard stars used as calibrators are measured using the same photometric technique used to estimate the flux for science objects;
- Secondly zero-points are derived for each image by comparing the instrumental magnitudes of the tertiary standards with the calibrated magnitudes;
- Lastly, the local “natural” magnitudes can be obtained by applying these zero-points to the science objects’ instrumental magnitudes.

The calibration process is different for the Wide and the Deep surveys.

The Deep stacks can be calibrated directly using SNLS tertiary standards inside the Deep fields. Zero-points can therefore be computed by comparing the instrumental magnitudes of the SNLS standard stars to the calibrated magnitudes published in Regnault et al. and applying the relevant Vega to AB magnitude offset (Table 2).

However, as there is no complete coverage of SNLS tertiary standards within the Wide fields, a special set of observations (“L99”) were acquired. These observations comprise series of short exposures taken during photometrically stable conditions to completely cover the Wide patches.

Each Wide tile is covered by at least one L99 exposure which covers 25% of the MegaCam field of view on each Wide tile. Given that the stacks are photometrically flat within 1% across the field of view due to the use of the Elixir B5/SNLS recipe, this guarantees that in turn all four quadrants are photometrically uniform.

Additionally, each L99 observation is preceded and followed by an observation of a CFHTLS Deep field containing the SNLS tertiary standards.

The photometric measurement method used to calibrate the Deep exposures taken before and after L99 observations follows the same procedure used for CFHTLS Deep stacks described above. The stable photometric conditions allows this zero-point to be used for the corresponding L99 exposures. In the last step, L99 images are used to compute rescaling factors which can be applied to the CFHTLS Wide stacks thanks to the large overlaps, 25% of a MegaCam field-of-view by design of the L99 observing program.

### 3.7.2 Choice of magnitude measurement method for calibration

In general, in any photometric calibration process, the method used to measure fluxes of the calibrating sources should be identical to the method used to measure the flux of the science objects. It is challenging to follow this procedure precisely as described in Regnault et al. for several reasons, none the least is that CFHTLS is a public survey which addresses many different science objectives, ranging from foreground stars to unresolved galaxies. In some cases, total magnitudes are important; in others, galaxy colors must be accurately measured. Ideally, the calibration process should introduce the smallest possible bias which should be documented and allow users to correct for this bias based on the kind of flux measurement they wish to perform.

A second important consideration comes from the intermediate step used to calibrate the CFHTLS Wide survey. The intermediate L99 photometric images have significantly different characteristics compared to the Wide stacks, as can be seen in Figure 8 which shows the distribution of seeing in L99 calibration images and in actual CFHTLS Wide images; the distribution of image seeing is quite different between the two kinds of images, with very large maximum values reported in the L99 stacks (the L99 were observed under poorer seeing conditions which would have provided out of specifications data for the Wide data set). Moreover, the exposure times are much shorter in the calibration images resulting in larger PSF variations across the field of view due to a less effective smoothing over time of the atmospheric turbulence over the one square degree MegaCam field of view. The method chosen to measure magnitudes scheme should be insensitive to these kinds of variations in exposure time and image quality.

Since the calibration is carried out using stars, aperture magnitudes are a natural photometric measurement scheme (and is also fully consistent with the aperture magnitudes scheme used for the SNLS photometric calibration). This is because, in principle, the correction to total flux is the same for all calibrating sources (unlike resolved galaxies which may have vastly differing light profiles).

In this work, as in Regnault et al. we choose an aperture magnitude where the aperture diameter scales with the image seeing:

$$\text{MAG\_SNLS} = \text{MAG\_APER}(7.5 \times \text{FWHM}) \quad (1)$$

The factor of 7.5 used by Regnault et al. implies an aperture correction, and in our case we also choose an aperture 20 times larger than the seeing to model and apply such correction to derive the total magnitude of stellar like sources, what we call MAG\_IQ20. We call seeing the image quality (IQ) based on measurements made using PSF fitting with PSFex during QualityFITS processing. IQ20 refers to actual

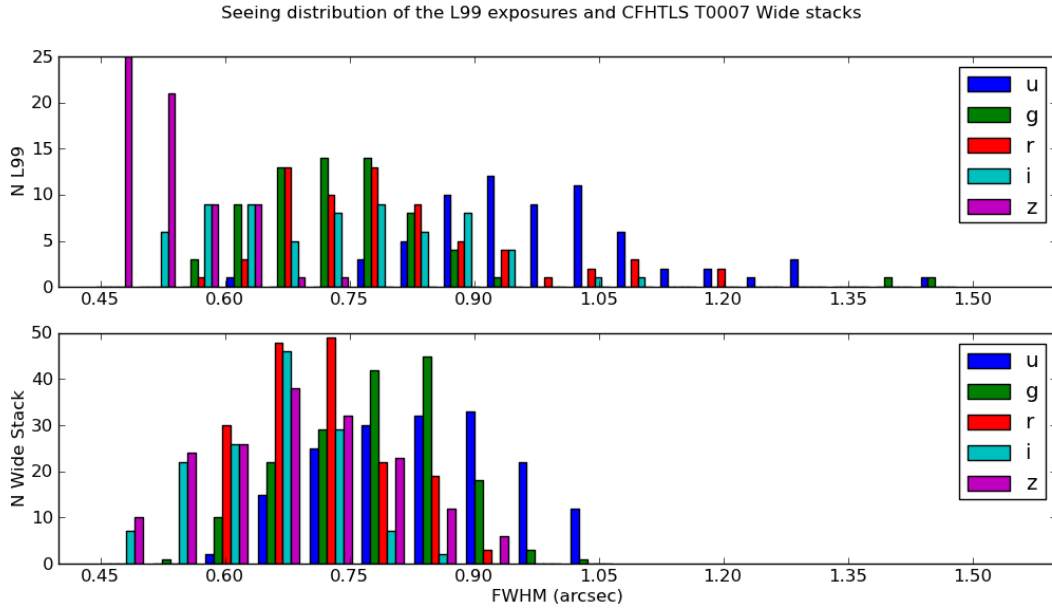


**Figure 8:** Seeing FWHM distribution for L99 individual exposures (top) and the CFHTLS-Wide stacks (bottom). In some specific pairs of overlapping images, the difference can reach  $0.4''$ .

measurements on the images using an aperture 20 times larger than the seeing. PSFex is a PSF modelling software developed by Emmanuel Bertin and available on Astromatic<sup>17</sup>.

This is motivated by the following considerations:

In extragalactic astronomy, one of the primary scientific aims of the CFHTLS, the pseudo-total MAG\_AUTO (Kron, 1980) is the one of the most commonly used estimators of the total flux of galaxies. Ideally, we should use this technique to calibrate our photometry. Unfortunately, our tests have shown that MAG\_AUTO measurements do not have the level of precision we require for our photometric calibration. But an alternative is to choose (more stable) aperture magnitudes which matches closely the magnitudes measured by MAG\_AUTO.

This is demonstrated in the right and left panels of Figure 9 which shows “Growth curves” for PSF models in the L99 *r*-band exposures using MAG\_SNLS and the measured IQ20 magnitudes to estimate the total magnitudes (left and right panels respectively). If we consider the “true” total flux as the measurement at  $40 \times \text{FWHM}$ , the SNLS flux underestimates the total flux by 3% (confirming the analysis from Regnault et al.). This is only 0.5% when the IQ20 aperture is used. Furthermore, the scatter for the total flux derived using the SNLS aperture magnitude is more than 3 times larger than with the IQ20 aperture (5.1 mmag compared to 1.6 mmag).

Secondly, the choice of magnitude measurement scheme is doubly important when using the SNLS tertiary standards to calibrate the (non-overlapping) L99 calibration fields. For this to work, the flux inside the IQ20 aperture must be as close as possible to a *constant fraction of the total flux of the star* whatever the shape and size of the PSF.

To test this assumption, we computed an aperture correction defined as the magnitude difference between the measured MAG\_SNLS and the measured IQ20 magnitude. This aperture correction is plotted against the image quality in Figure 10. It is important to note that the behavior in the regime of very good image

<sup>17</sup><http://www.astromatic.net/software/psfex>



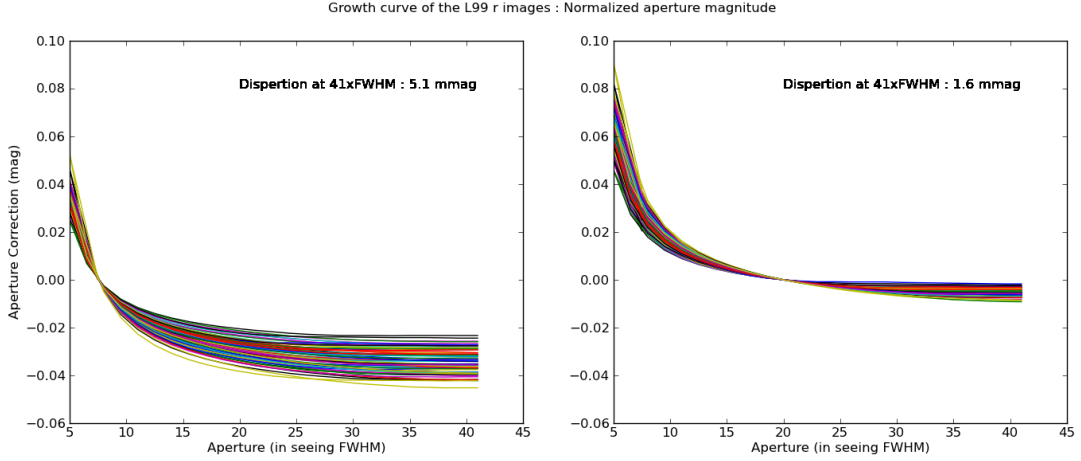


**Figure 9:** Growth curves for PSF models in the L99  $r$ -band exposures using MAG\_SNLS and IQ20 magnitudes to estimate the total magnitudes (left and right panels respectively). Each line corresponds to the difference in magnitude between the total flux and the flux at the stated aperture size (measured as a multiple of the FWHM) for each L99 exposure. As expected, when using the IQ20 aperture, the scatter at  $40 \times \text{FWHM}$  is considerably reduced (right panel)

quality clearly departs from a constant aperture correction.

For images taken in excellent seeing, the SNLS aperture is too small to capture the same flux versus total flux compared to poorer image quality, which makes the basic SNLS aperture photometry not reliable for our calibration. Figure 11 shows the shape of the PSF for two different FWHM rebinned to the same size. One can clearly notice that the overall shape is different : a boxy shape at good IQ due to flux in the spikes and a very symmetrical shape at larger IQ. A tangible explanation of the behavior of the aperture correction at low FWHM is the flux contained in the spikes which scale differently than the bulk of the flux of the PSF.

### 3.7.3 Derivation of the MAG\_IQ20 magnitudes

Measuring the flux inside a large aperture of  $20 \times \text{FWHM}$  is not a trivial task in the naturally deep CFHTLS stacks where objects are subject to crowding. Instead we chose to model the aperture correction on a per stack basis to go from the robust, but biased, MAG\_SNLS to the nearly total magnitude MAG\_IQ20.

The use of a master PSF model per image is adopted to ensure a robust estimation of the IQ20 aperture magnitudes. First a pixel-based model of the PSF is constructed using the PSFex software (Bertin, 2011) using a large set of stars. From this PSF model (which is produced as a FITS image) the fluxes inside a series of apertures are computed using SExtractor. The aperture correction (ApCorr) is defined as the magnitude difference between the flux inside the SNLS and IQ20 apertures:

$$\text{ApCorr} = -2.5 \times \log_{10} \frac{\text{Flux}(\text{Ap}_{\text{SNLS}})}{\text{Flux}(\text{Ap}_{\text{IQ20}})} \quad (2)$$

Since photometric rescaling from L99 to the CFHTLS stacks is carried out on only 25% of the MegaCam field of view, a unique PSF model is computed for each of the four quadrants of each L99 image. Despite the PSF variations across a quarter of a MEGACam field of view, a single PSF model is computed : this approximation is motivated by the small variation of the PSF shape and size across the MegaCam field



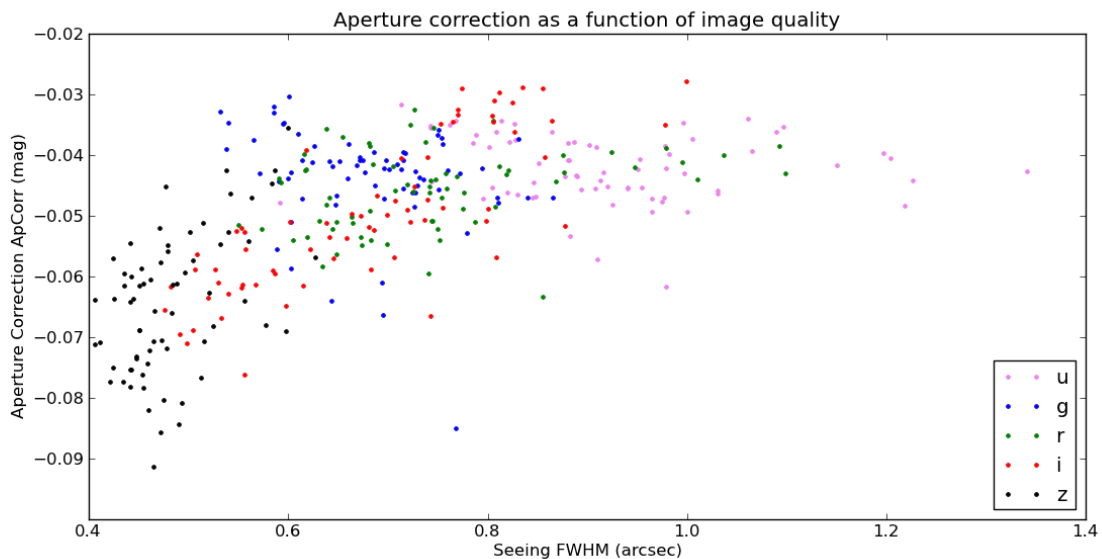


**Figure 10:** Aperture correction (defined as the magnitude difference between the flux in the SNLS and IQ20 apertures) as a function of image quality. In images of quality worse than  $0.7''$  the aperture correction is approximately constant; in better-seeing images the aperture correction show a clear trend. More flux falls outside the SNLS aperture in very good seeing images which results in a larger aperture correction.

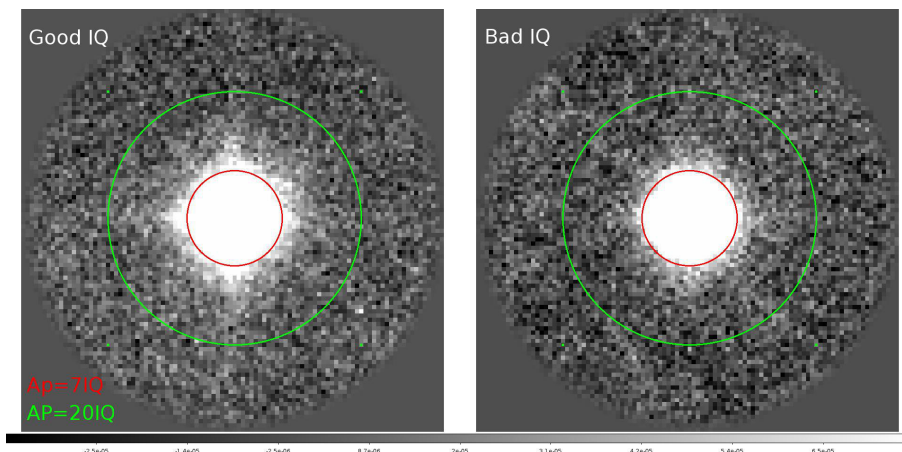


**Figure 11:** PSF model from two images with FWHM  $\sim 0.5''$  and  $\sim 0.9''$  (right and left panels respectively). Both PSFs have been resampled to a FWHM of 3 pixels. The “good-IQ” PSF has more flux in the “spikes” outside the SNLS aperture.

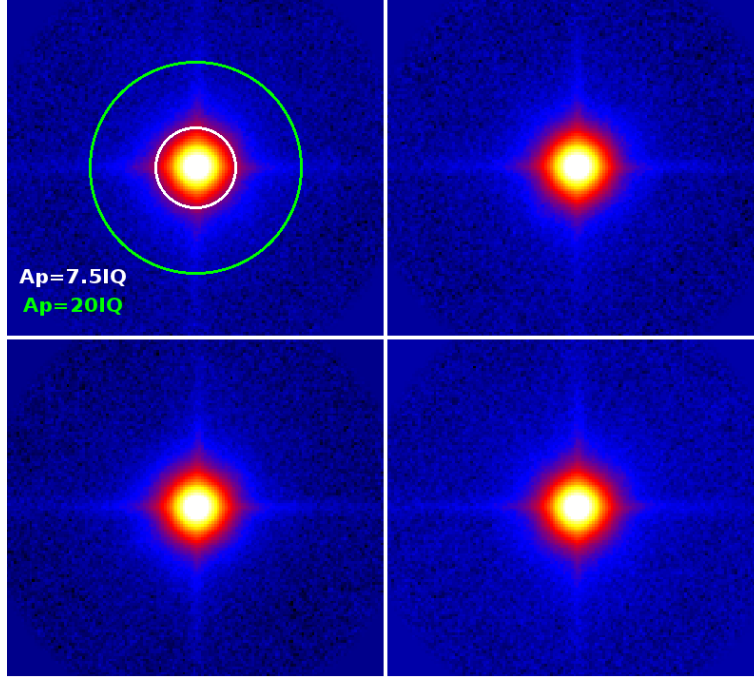


**Figure 12:** PSF model for the four quadrants of the CFHTLS-Wide stack CFHTLS\_w\_z\_222054-003100\_T0007. The circles represent the apertures used for the SNLS and IQ20 magnitudes.

of view compared to the (much larger) variations between the L99 images and the stacks.

The CFHTLS T0007 catalogues offer the `MAG_SNLS` magnitude since it is the measured value for each source on the image, but it is the aperture corrected magnitude based on the four PSF models for each stacks (and the corresponding four aperture corrections - `ApCorr`), `MAG_IQ20`, that ought to be used for any calibration or scientific purposes on point sources.

$$\text{MAG\_IQ20} = \text{MAG\_SNLS} + \text{ApCorr} \quad (3)$$

### 3.7.4 Quantifying the improvements using `MAG_IQ20` compared to `MAG_SNLS`

Deep fields observations bracket L99 observations. Since L99 observations were taken in photometric conditions, the zero-points derived from the comparison of the instrumental magnitudes and the SNLS tertiary standards catalogues should not change. By comparing the zero-points in these pairs of Deep observations (before and after L99 observations) in Table 1, one can see that the `MAG_IQ20` is a more stable estimator than `MAG_SNLS`. stability improves even for Deep images with identical seeing. This result indicates that the scatter in the aperture correction at a given seeing seen in Figure 10 captures real information on the varying PSF shape of identical size.

In conclusion, the variation of the aperture correction with the seeing shown in Figure 10 provides indication that the SNLS flux is not a truly valid proxy of the total flux (measured by the IQ20 aperture photometry) when the images have a large spread in image quality. Our current approach circumvent this obstacle.

Filter	u		g		r		i		z	
	-	ApCorr	-	ApCorr	-	ApCorr	-	ApCorr	-	ApCorr
D1	0.003	0.002	0.007	0.005	0.006	0.002	0.001	0.001	0.005	0.001
D2	0.002	0.001	0.002	0.002	0.004	0.002	0.001	0.002	0.004	0.002
D3	0.006	0.008	0.014	0.001	0.004	0.001	0.001	0.002	0.000	0.001
D4	0.014	0.007	0.033	0.003	0.015	0.007	0.002	0.000	0.008	0.001

**Table 1:** Zero-point difference for Deep field exposures before and after L99 observations, with and without the application of an aperture correction (left and right columns for each filter, respectively). In all cases except D3-*u*\* the application of the aperture correction reduces the difference.

### 3.7.5 SNLS standard star catalogue

The complete CFHTLS-T0007 release (both Deep and Wide) are photometrically calibrated using the SuperNova Legacy Survey (SNLS) tertiary standards catalogs. These catalogs have been produced and release as products of the SuperNova Legacy Survey. They have been made available at CDS in the catalog interface Vizier<sup>18</sup>. The detailed description of the production of the catalogs is described in (Regnault et al., 2009).

A summary of the description is reproduced here.

This is the photometric calibration of the SuperNova Legacy Survey (SNLS) three year dataset. The SNLS corresponds to the DEEP component of the larger Canada-France-Hawaii Telescope Legacy Survey (CFHTLS). The SNLS repeatedly monitors four one square degree fields (labeled D[1-4]) with the MegaCam wide-field imager, in the g, r, i and z bands. u-band observations of the same fields are also available, although not formally part of the SNLS dataset.

(...)

The SNLS 3 year calibration relies on the ((Landolt, 1992)) standard star catalog. Landolt fields are observed during each photometric night along with the SNLS fields. Zero-points are derived from these observations. Stable and isolated stars are detected on the SNLS fields and selected as "tertiary standards". The calibrated magnitudes of each tertiary standard obtained under photometric conditions are combined to produce a calibration catalog for each SNLS field.

(...)

To interpret the tertiary standard magnitudes as physical fluxes, we need a primary standard, i.e. a star with known MegaCam magnitudes and whose spectral energy distribution has been measured absolutely. The SNLS uses BD+17 4708 whose SED has been measured in Bohlin & Gilliland, 2004, Cat. J/AJ/128/3053 using the HST STIS and NICMOS spectrographs. BD+17 4708 has not been directly observed by SNLS, however, its MegaCam magnitudes were inferred from its known Landolt magnitudes ((Regnault et al., 2009), table 7).

(...)

The u-band observations of the SNLS DEEP fields are not formally part of the SNLS. Nevertheless we give u-band magnitudes for a subset of the SNLS tertiary stars.

<sup>18</sup><http://cdsarc.u-strasbg.fr/viz-bin/Cat?J/A%2bA/506/999>

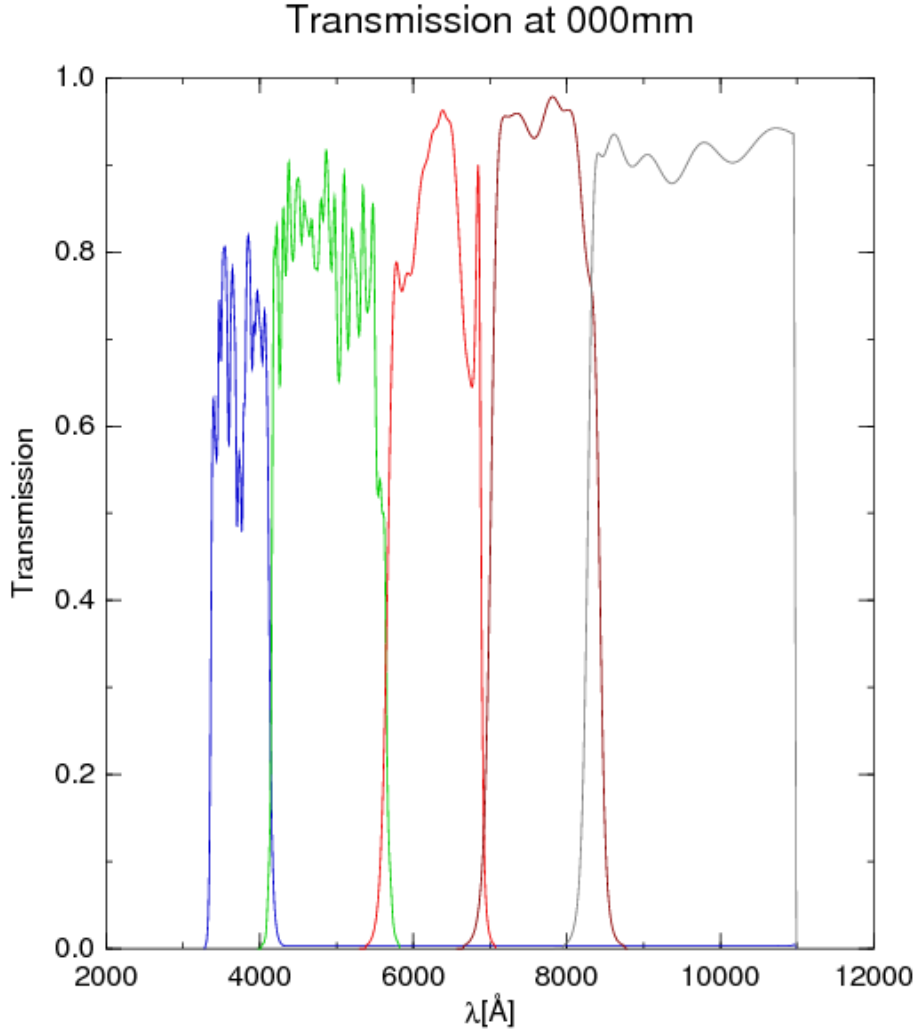


**Figure 13:** Transmission of SNLS filters in the center of the MEGACam field of view.

The Megacam imager transmission curves are published in the form on tables at CDS : Megacam transmission<sup>19</sup>. The filters transmission are shown in figure 13.

### 3.7.6 Calibrating the Deep survey

The calibration process for the Deep fields is summarized in Figure 14. In the first step, an object catalogue is produced using SExtractor on the Deep images. This catalogue is then used to produce a PSF model using PSFex. The calibration magnitudes `MAG_IQ20` are derived from this catalogue and the PSF model. Next, saturated objects are flagged and are removed. The diagnostic plots used in this procedure are presented in Figure 15. The algorithm first locates the 45 degrees angled thin stellar branch in the `MU_MAX` (magnitude of the brightest pixel) against `MAG` diagram (left plot). The saturation level is identified in the `MU_MAX` axis from the broadening of the distribution along the `MAG` direction. The resulting saturation level is also plotted in the `FLUX_RADIUS` versus `MAG` scatter plot. This estimator is quite robust but can still fail for 1% of the fields for several reasons (such as heterogeneous seeing due to the stacking

<sup>19</sup><http://vizier.u-strasbg.fr/viz-bin/VizieR?-source=J/A%2BA/506/999>

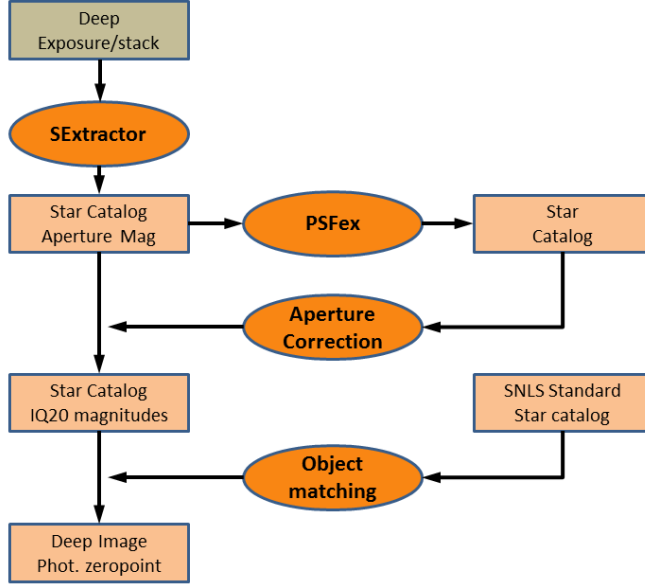


**Figure 14:** Photometric calibration process of the CFHTLS-Deep stacks and Deep calibration images used for L99.

of images with different image quality or higher number of objects close to the saturation level which blur the determination of the saturation limit). For this reason all plots are manually inspected. Finally, to ensure the cleanest possible calibration sample, an additional 0.5 magnitude margin is subtracted from the MU\_MAX magnitude saturation limit.

Sources in the Deep stacks are matched with the SNLS standards using a nearest neighbor procedure with a 2'' matching radius. All stars with a non-zero SExtractor flag are discarded (to avoid blended objects with potentially corrupted photometry). Figure 16 shows the magnitude difference distribution as a function of reference magnitude after matching. The scatter is low, around 1% in average. The 2- $\sigma$  clipping applied only removes a small fraction of objects (as can be seen in the in the right panel).

The final estimator is the median offset after an iterative two-pass 2 $\sigma$  clipping. A linear regression is used to verify that the estimator does not depend strongly on the magnitude of the selected objects (which would be a sign of systematic biases in our magnitude measurement scheme).

The list of rescaling factors applied to the stacks are given in the Appendix in Table 33. Images are rescaled to keep a final zero-point of Vega 30.0. In a last step, these pixels are scaled to a zero-point of 30.0 in AB. Given a magnitude offset of  $\delta_{\text{SNLS}}$  versus the published total magnitude (CAT\_SNLS), we get:

$$\delta_{\text{SNLS}} = \text{Median\_Clipped}(\text{MAG\_IQ20}_i - \text{CAT\_SNLS}_i) \quad (4)$$

And we can compute a pixel scaling factor of  $F_{\text{SNLS}}$  as follows:

$$F_{\text{SNLS}} = 10^{0.4 \times \delta_{\text{SNLS}}} \quad (5)$$

We note that pixel rescaling using this factor implies that the photometric measurement technique (MAG\_AUTO for example) used is identical to the measurement method used for calibration (aperture photometry).

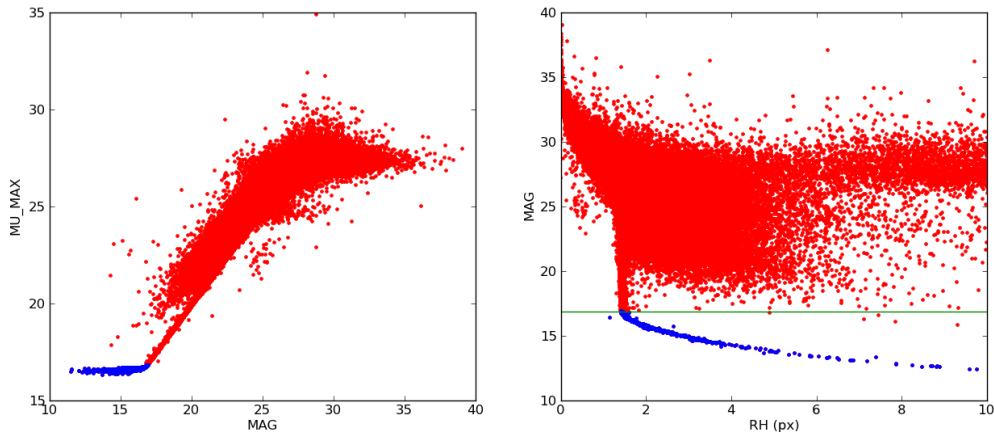


**Figure 15:** Diagnostic plots used to determine the saturation level and to flag saturated objects. Blue points represent discarded objects, the green line shows the saturation limit.

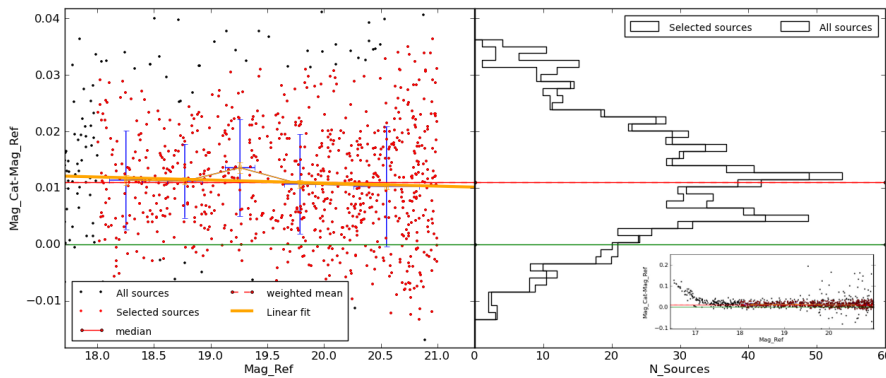


**Figure 16:** Calibration of Deep photometric stacks using the SNLS standard stars catalog. Stellar sources are cross-matched with SNLS catalogues and outliers are removed using an iterative two-pass  $2\sigma$  clipping. The median of the magnitude difference of the remaining objects is used as the rescaling factor.

This approximation is widely used in astronomy and should be suitable for most science cases. But it does not follow the recipe described in (Regnault et al., 2009). If CFHTLS users require a more precise calibration, the best photometric accuracy will be attained by recalibrating the source magnitudes (measured for instance using `MAG_AUTO` for example) to the provided `MAG_IQ20` CFHTLS star catalogs using a procedure analogous to the calibration transfer from (Regnault et al., 2009) to the CFHTLS.

### 3.7.7 Photometric calibration of the Wide survey

The flowchart of the photometric calibration procedure for the CFHTLS Wide stacks is presented in Figure 17. The key aspect of this procedure is the use of the L99 calibration observations to “transfer” the photometry from the SNLS standard stars to the Wide stacks. The L99 fields are observations “bracketed” (preceded and followed) by an exposure on the Deep survey field closest on the sky to the observed Wide patch. The zero-point of the Deep exposures are calculated in the exact same procedure than described in the previous section. Assuming a perfect stability of the photometric conditions during the series of L99

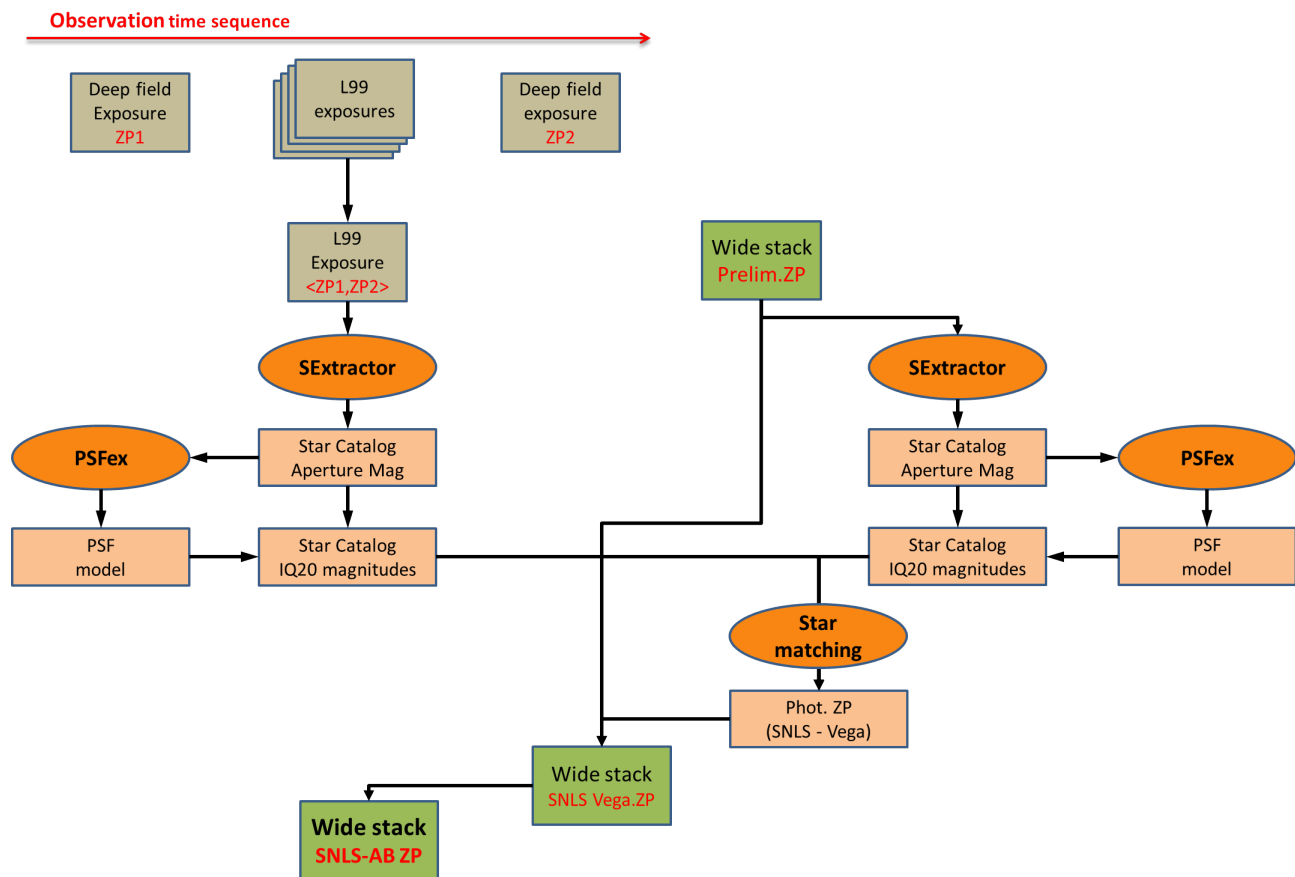


**Figure 17:** Photometric calibration process of the CFHTLS Wide stacks.

and Deep observations, the Deep data zero-points are used to calculate the corresponding zero points for the L99 images (taking into account airmass differences).

The zero-point applying to all L99 image taken in the sequence is computed from the mean value of the bracketing Deep fields. In the next step, catalogues with `MAG_IQ20` are extracted from both the L99 calibrated images and the Wide stacks. As before, saturated objects are carefully flagged and only stellar objects for which `MAG_IQ20` can be reliably measured are selected. The catalogues of overlapping L99-Wide pairs are then matched with the following object selection:

- Magnitude ranges (u:15.0-20.5, g:15.0-21.5, r:15.5-21.5, i:15.5-20.5, y:15.5-20.5, z:15.0-20.0)
- Stellar objects: `SExtractor CLASS_STAR > 0.95`;
- Unblended objects: `SExtractor FLAGS==0`;
- Object with good signal-to-noise : `SExtractor MAG_ERR < 0.02`;

From this clean sample rescaling factors are derived from the mean, median or weighted mean. This is illustrated in Figure 18 The resulting median offset, used for the rescaling, is shown as the dashed red line in the main panel of Figure 18. The inset panel shows a linear fit to the bin-averaged statistics (red dots) of the clean sample. Each plot for each L99-Wide pair is visually inspected to ensure a clean calibration sample.

T0007 z-band: W1-72 / L99-037  
mag\_aper limits=[(16.67) 16.68, 18.49]; n\_tot stars: 1887

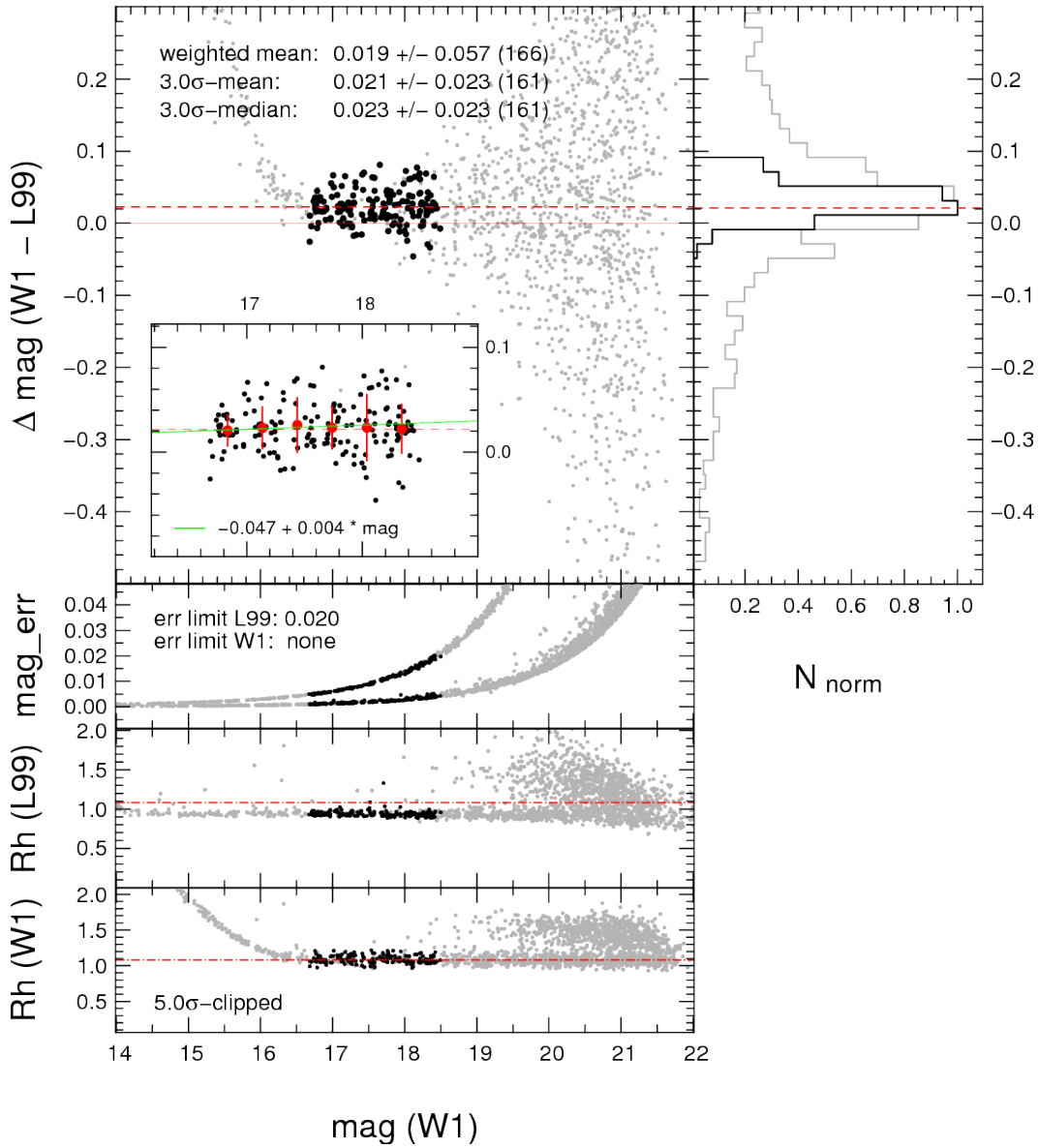


**Figure 18:** Matching between one L99 image and a CFHTLS Wide tile (stacks are represented by a simplified notation). Upper panel and inset: magnitude difference between W1 and L99; lower panels, magnitude errors and FLUX\_RADIUS measurements for both stacks; right panel, histogram of differences. Grey and black dots represent all objects and those used for computation of statistics and rescaling factors respectively. Visual inspection of these control plots allows one to ensure that the sample for final statistics is drawn from non-saturated stars with unblended photometry in both catalogues, following the selection criteria outlined in the text.



When more than one L99 image overlap with a single Wide stack, the final rescaling factor is a simple average of each separate rescaling factor. The comparison of the individual factors on a Wide stacks is a useful quality assessment of the quality of the calibration and will be discussed in the photometric accuracy section.

For practical reasons, since all objects in a given L99-Wide pair share the same aperture correction, the rescaling offset is computed using SNLS magnitudes (instead of IQ20) and the final rescaling offset includes both the matching offset and the two aperture corrections of the L99 and the Wide catalogues. The final rescaling in magnitude is therefore given by :

$$\delta = \delta_{\text{L99-Wide}} - \text{ApCorr(L99)} + \text{ApCorr(Wide)} \quad (6)$$

After calibration, image pixels are first rescaled to a zero-point of Vega 30.0 using the SNLS rescaling factors. In a second step, these pixels are scaled to a zero-point of 30.0 in AB.

### 3.7.8 Vega-AB conversion

The SNLS photometric system is Vega-based using BD+17 4708. We want the CFHTLS releases in a true AB system, in consequence the final processing step converts all images to the AB system by scaling the pixel values using Vega to AB conversion factors. The conversion offsets have been derived by the SNLS Team (Betoule, private communication, 2011); they are listed in Table 2.

Regnault et al.'s calibration system is linked to the HST white dwarf system through the primary spectroscopic standard star BD+17 4708. The Vega magnitudes (at an airmass of 1) for a star of spectral flux density  $\phi$  can be calculated as:

$$m_{|x_0} = -2.5 \log_{10} \frac{\int \lambda T(\lambda) \phi(\lambda) d\lambda}{\int \lambda T_{x_0}(\lambda) \phi_{bd17}(\lambda) d\lambda} + m_{\text{BD17}} \quad (7)$$

where  $T_{x_0}(\lambda)$  is the effective filter passband,  $\phi_{bd17}$  is the spectral flux density of the photometric standard BD+17 4708 and  $m_{bd17}$  is the magnitude of BD+17 4708 in the MegaCam instrumental system.

From the definition of the AB system (Oke, 1974), the broadband AB magnitude of a star of SED  $\phi(\lambda)$  is :

$$m_{ab} = -2.5 \log_{10} \frac{\int \lambda T(\lambda) \phi(\lambda) d\lambda}{\int \lambda T(\lambda) \phi_{ab}(\lambda) d\lambda} \quad (8)$$

where

$$\phi_{ab}(\lambda) = 10^{-48.6/2.5} c \lambda^2 \quad (9)$$

It follows that the AB offsets required to bring SNLS magnitudes to AB system,  $\delta_{ab} = m_{ab} - m_{|x_0}$ , are :

$$\delta_{ab} = -2.5 \log_{10} \frac{\int \lambda T(\lambda) \phi_{bd17}(\lambda) d\lambda}{\int \lambda T(\lambda) \phi_{ab}(\lambda) d\lambda} - m_{bd17} \quad (10)$$

The pixels in the images are scaled following this relation:

filter	u	g	r	i.MP9701 (i)	i.MP9702 (y)	z
$m_{ab}$	10.211	9.592	9.343	9.253	9.256	9.241
$m_{bd17}$	9.769	9.691	9.218	8.914	8.947	8.774
$\delta_{ab}$	0.442	-0.099	0.125	0.339	0.309	0.467

**Table 2:** Offsets between AB magnitudes and the SNLS Vega-based MegaCam calibration.

$$p_{AB} = p_{VEGA} \times 10^{0.4 \times \delta_{AB}} \quad (11)$$

### 3.8 Final catalogue production

In the Wide and Deep surveys, a `.ldac` `SExtractor` source catalogue is produced immediately after the final rescaling of the stacks (using L99 images for the Wide and the SNLS standard star catalogue for the Deep). The T0007 Wide and Deep `.ldac` source catalogues have been produced using a 128 pixels mesh size to derive the local sky background (`BACK_SIZE` parameter in `SExtractor`). These catalogues are the inputs of the QFITS-out processing. The `SExtractor` configuration file for the production of the T0007 `.ldac` catalogues are presented in Appendix B.2.4 and Appendix A.3.4 for Wide and Deep respectively.

After the production of the `chi2` image, `SExtractor` is run in dual-image mode on the  $u^*g, r, i, y$  and  $z$  stacks using the `chi2` image as reference. The Wide and Deep `chi2 .cat` catalogues are produced with a using a background mesh size in `SExtractor` of 256 pixels. All catalogues contain parameter values for all quantities listed in Tables 28, 29 and 30. For each source, aperture magnitudes are computed within 27 (26+SNLS) apertures, following same procedure as for the previous T0006 release. The `SExtractor` configuration file used for the production of the T0007 `.cat` dual-image mode catalogues is listed in the Appendix B.2.5 and Appendix A.3.5 for Deep and Wide surveys respectively. Based on its measured `MAG_SNLS`, each source is corrected for aperture, leading to the `MAG_IQ20` magnitude.

Additionally, for each survey pointing, the following data products are produced:

- a  $(u, g, r, i/y, z)$  Wide or  $(u, g, r, i, y, z)$ -merged Deep catalogues that includes a restricted number of parameters. These catalogues are produced in two versions with either `MAG_AUTO`, `MAG_SNLS` and `MAG_IQ20` magnitudes. They also contain the  $E(B - V)$  value at each source position derived from dust map images (Schlegel et al., 1998) and the  $dk$  cell number for the given position on the image, an estimate of a second order term of the photometric flatness of the image, meant to account for the slight variation in bandwidth of the MegaCam filters from center to edge. See Regnault et al. (2009) for a full explanation. Since it did not bring any significant gain, the  $dk$  term is not used within T0007.
- a  $(u, g, r, i/y, z)$ -merged Wide, or  $(u, g, r, i, y, z)$ -merged Deep multi-aperture (`.ape`) extended catalogue that only includes the data concerning the 27 `MAG_APER` informations in all filters.
- four  $(u, g, r, i/y, z)$  Wide patch merged catalogues (one for each Wide patch). These catalogues are produced by matching the objects from the previous multi-aperture merged catalogues in right ascension and declination. The matching is done across each patch of the Wide with the following constraints:

- Objects closer than 250 pixels from the tile edges are discarded. This helps removing spurious objects and is small enough to ensure that the complete area is covered without holes.
- The matching tolerance is set to 1.5 arcsec
- When an object is detected in more than one tile, the object which is kept is the one with the highest signal to noise ratio (defined as the *i*-band FLUX\_AUTO/FLUXERR\_AUTO ratio.)

### 3.9 Post-processing and quality control

Finally, a series of quality assessments are made for:

- all individual  $u^*$ ,  $g$ ,  $r$ ,  $i/y$ ,  $z$  Deep and Wide stacks,
- all Wide patches,  $W_k$  ( $k=1-4$ ), and
- the whole Wide survey.

The QFITS-in, Scamp, QFITS-out output files are part of the overall quality assessments. Other assessment files which are generated include completeness limit plots, stellar color-color tracks, three-color stacked images, survey maps, Stellar Locus Regression (SLR) color fitting plots and are all available from the T0007 synoptic table.

## 4 Description of the CFHTLS T0007 Wide survey

### 4.1 Overview

The T0007 release of the Wide survey covers 171 MegaCam pointings (or tiles) divided into the W1, W2, W3 and W4 fields and is complete in all filters. In total there are 855  $u^*$ ,  $g$ ,  $r$ ,  $i/y$  and  $z$  stacks and 171 chisquared images (2052 including the weight-maps). The positions and geometry of the four Wide fields comprising T0007, namely W1, W2, W3 and W4, are shown on Fig. 19 and summarized in Table 3. Table 7 lists the effective area, after masking, of the four Wide patches in each of the filters.

The image selection criteria applied to the 6378 CFHTLS *Validated* images for the production of the T0007 CFHTLS Wide survey are the following:

- CFHTLS L02 and L05 Wide observation period: between May 26, 2003 and November, 2008; VIPERS-DDT images (2009BD97);
- TERAPIX selection of CFHT *Validated* images, with QualityFITS grade A or B (images within the survey specifications);
- exposure time  $> 60$  s;
- airmass  $< 1.7$ ;
- few images with missing data on more than one entire CCD have been removed from the parent sample. However, all images with missing data on only half of CCD detectors have been preserved;
- all pre-Wide survey images and all photometric short exposures. They will be included in the set of images used for the SCAMP astrometric/photometric calibration process;
- images with seeing (FWHM<sup>20</sup>)  $< 1.4''$  in  $u^*$ , and  $< 1.2''$  in  $g$ ,  $r$ ,  $i$  and  $z$  are selected for the calibration process;
- images with seeing (FWHM)  $< 1.3''$  in  $u^*$ , and  $< 0.95''$  in  $g$ ,  $r$ ,  $i$  and  $z$ , are selected for the stack production;

The parent sample of images after the QualityFITS selections is composed of 1000  $u^*$ , 1059  $g$ , 1728  $r$ , 1064  $i$ , 291  $y$  and 1236  $z$ -band images. 25% of the sample are short photometric or Pre-Wide exposures that are only used for calibration but are not combined into stacks.

All stacks have the same pixel scale and cover exactly  $1 \times 1$  deg<sup>2</sup> ( $19354 \times 19354$  pixels of  $0.1860''$ ). The stacks only combine images that are part of a CFHTLS Wide observing sequence and that are within 3 arcminutes of the CFHTLS pre-defined stack center

Each stack comprises a sequence of medium exposures a few hundred seconds long each. After each exposure the telescope is shifted by a small amount (typically a few tens of arcseconds, see the right panel of Fig. 21) in order to fill the gaps between CCDs and enable the rejection of bad pixels and cosmic rays during subsequent processing steps.

The adjacent fields have an overlapping region of several arcminutes width to constrain the field-to-field astrometric and photometric calibrations. The size of the overlaps is 4 arcmin in DEC and 3 arcmin in RA (see Fig. 21). The overlaps between fields reduce the sky coverage of the 171 CFHTLS Wide tiles to approximately 155 deg<sup>2</sup>.

---

<sup>20</sup>As defined in Section 4.2

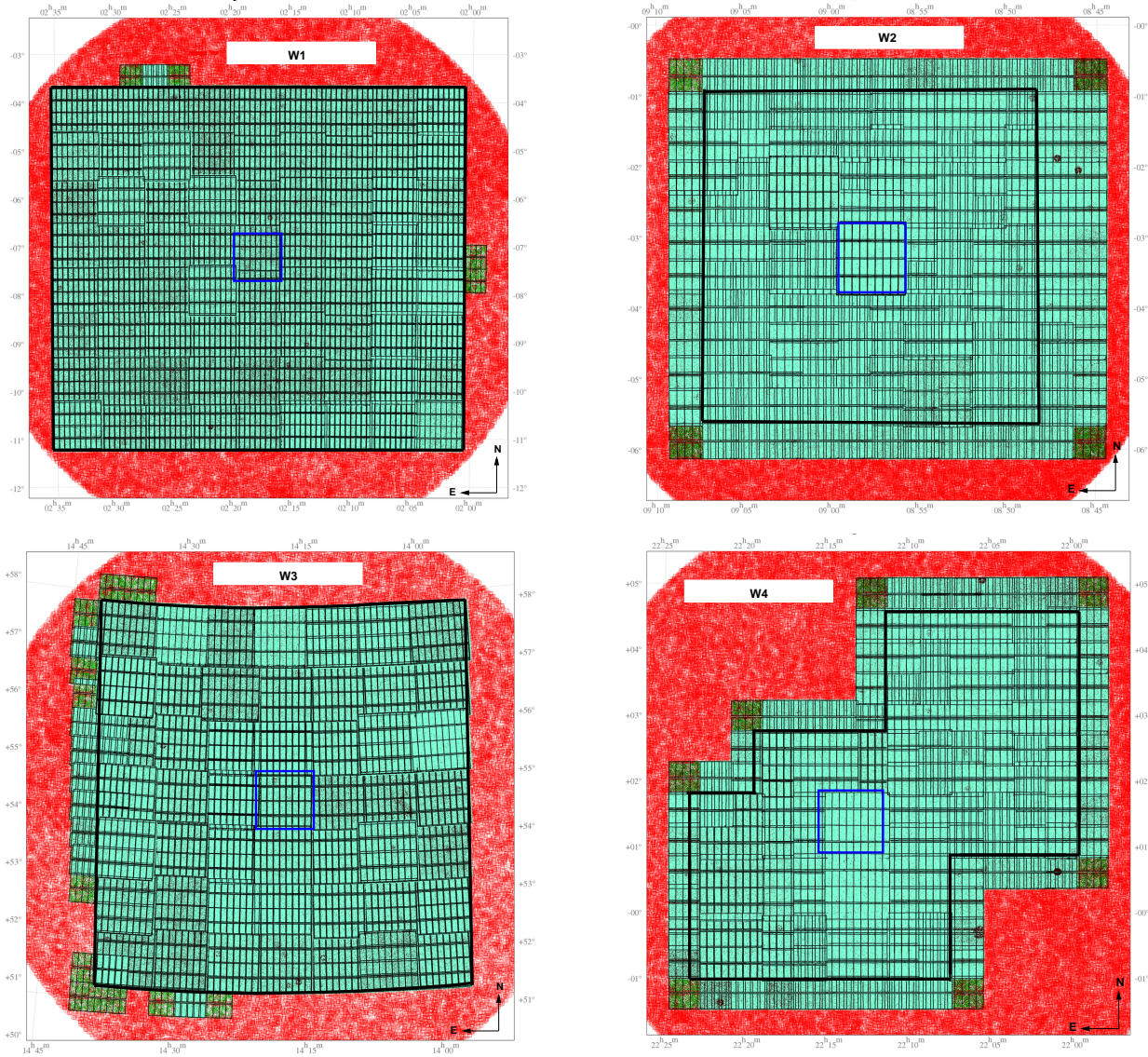


**Figure 19:** Positions and geometry of the CFHTLS Wide fields. The black thick contours show the total field of view composing the  $u^*$ ,  $g$ ,  $r$ ,  $i/y$  and  $z$  stacks of the T0007 release. The fields located outside these regions are supplementary astrometric calibration data but are not included in the stacks. W1, W2, W3 and W4 do not cover the same field of view, so the four Wide regions are not shown with the same scale in this figure. The blue squares show a typical MegaCam field of view and indicate the positions of the reference center field. The MegaCam images included in the release are in green. They reveal the tiling and mosaicing of each CFHTLS Wide area. The small rectangles indicate individual MegaCam CCDs. These plots have been produced by SCAMP during the calibration step of W1, W2, W3 and W4.

**W1**

W1(+4+3)	W1(+3+3)	W1(+2+3)	W1(+1+3)	W1(0+3)	W1(-1+3)	W1(-2+3)	W1(-3+3)	W1(-4+3)
023319-041200	022929-041200	022539-041200	022150-041200	021800-041200	021410-041200	021021-041200	020631-041200	020241-041200
W1(+4+2)	W1(+3+2)	W1(+2+2)	W1(+1+2)	W1(0+2)	W1(-1+2)	W1(-2+2)	W1(-3+2)	W1(-4+2)
023319-050800	022929-050800	022539-050800	022150-050800	021800-050800	021410-050800	021021-050800	020631-050800	020241-050800
W1(+4+1)	W1(+3+1)	W1(+2+1)	W1(+1+1)	W1(0+1)	W1(-1+1)	W1(-2+1)	W1(-3+1)	W1(-4+1)
023319-060400	022929-060400	022539-060400	022150-060400	021800-060400	021410-060400	021021-060400	020631-060400	020241-060400
W1(+4+0)	W1(+3+0)	W1(+2+0)	W1(+1+0)	W1(0+0)	W1(-1+0)	W1(-2+0)	W1(-3+0)	W1(-4+0)
023319-070000	022929-070000	022539-070000	022150-070000	021800-070000	021410-070000	021021-070000	020631-070000	020241-070000
W1(+4-1)	W1(+3-1)	W1(+2-1)	W1(+1-1)	W1(0-1)	W1(-1-1)	W1(-2-1)	W1(-3-1)	W1(-4-1)
023319-075600	022929-075600	022539-075600	022150-075600	021800-075600	021410-075600	021021-075600	020631-075600	020241-075600
W1(+4-2)	W1(+3-2)	W1(+2-2)	W1(+1-2)	W1(0-2)	W1(-1-2)	W1(-2-2)	W1(-3-2)	W1(-4-2)
023319-085200	022929-085200	022539-085200	022150-085200	021800-085200	021410-085200	021021-085200	020631-085200	020241-085200
W1(+4-3)	W1(+3-3)	W1(+2-3)	W1(+1-3)	W1(0-3)	W1(-1-3)	W1(-2-3)	W1(-3-3)	W1(-4-3)
023319-094800	022929-094800	022539-094800	022150-094800	021800-094800	021410-094800	021021-094800	020631-094800	020241-094800
W1(+4-4)	W1(+3-4)	W1(+2-4)	W1(+1-4)	W1(0-4)	W1(-1-4)	W1(-2-4)	W1(-3-4)	W1(-4-4)
023319-104400	022929-104400	022539-104400	022150-104400	021800-104400	021410-104400	021021-104400	020631-104400	020241-104400

**W2**

W2(+3+3)	W2(+2+3)	W2(+1+3)	W2(0+3)	W2(-1+3)
090526-012700	090137-012700	085749-012700	085400-012700	085011-012700
W2(+3+2)	W2(+2+2)	W2(+1+2)	W2(0+2)	W2(-1+2)
090526-022300	090137-022300	085749-022300	085400-022300	085011-022300
W2(+3+1)	W2(+2+1)	W2(+1+1)	W2(0+1)	W2(-1+1)
090526-031900	090137-031900	085749-031900	085400-031900	085011-031900
W2(+3+0)	W2(+2+0)	W2(+1+0)	W2(0+0)	W2(-1+0)
090526-041500	090137-041500	085749-041500	085400-041500	085011-041500
W2(+3-1)	W2(+2-1)	W2(+1-1)	W2(0-1)	W2(-1-1)
090526-051100	090137-051100	085749-051100	085400-051100	085011-051100

**W3**

W3(+3+3)	W3(+2+3)	W3(+1+3)	W3(0+3)	W3(-1+3)	W3(-2+3)	W3(-3+3)
143756+571831	143115+571831	142435+571831	141754+571831	141113+571831	140433+571831	135752+571831
W3(+3+2)	W3(+2+2)	W3(+1+2)	W3(0+2)	W3(-1+2)	W3(-2+2)	W3(-3+2)
143728+562231	143057+562231	142425+562231	141754+562231	141123+562231	140451+562231	135820+562231
W3(+3+1)	W3(+2+1)	W3(+1+1)	W3(0+1)	W3(-1+1)	W3(-2+1)	W3(-3+1)
143702+552631	143040+552631	142417+552631	141754+552631	141131+552631	140509+552631	135846+552631
W3(+3+0)	W3(+2+0)	W3(+1+0)	W3(0+0)	W3(-1+0)	W3(-2+0)	W3(-3+0)
143638+543031	143023+543031	142409+543031	141754+543031	141139+543031	140525+543031	135910+543031
W3(+3-1)	W3(+2-1)	W3(+1-1)	W3(0-1)	W3(-1-1)	W3(-2-1)	W3(-3-1)
143615+533431	143008+533431	142401+533431	141754+533431	141147+533431	140540+533431	135933+533431
W3(+3-2)	W3(+2-2)	W3(+1-2)	W3(0-2)	W3(-1-2)	W3(-2-2)	W3(-3-2)
143553+523831	142953+523831	142354+523831	141754+523831	141155+523831	140555+523831	135955+523831
W3(+3-3)	W3(+2-3)	W3(+1-3)	W3(0-3)	W3(-1-3)	W3(-2-3)	W3(-3-3)
143532+514231	142939+514231	142347+514231	141754+514231	141202+514231	140609+514231	135752+514231

**W4**

W4(+1+3)	W4(+2+3)	W4(+3+3)
220930+040700	220542+040700	220154+040700
W4(+1+2)	W4(+2+2)	W4(+3+2)
220930+031100	220542+031100	220154+031100
W4(+1+1)	W4(+2+1)	W4(+3+1)
221706+021500	221318+021500	220930+021500
W4(+2+0)	W4(+1+0)	W4(+3+0)
222054+011900	221706+011900	220930+011900
W4(+2-1)	W4(+1-1)	W4(+3-1)
222054+002300	221706+002300	221318+002300
W4(+2-2)	W4(+1-2)	W4(+3-2)
222054-003100	221706-003100	221318-003100

**Figure 20:** Positions, identification and naming conventions of stacks in the CFHTLS Wide survey. The figure shows the positions of each “tile” (blue square corresponding to the field of view of Mega-Cam) covering the W1 and W2 Wide fields. Each tile is labelled by its Cartesian name on top (see <http://terapix.iap.fr/cplt/oldSite/Descart/summarycfhtlswide.html>) and the official CFHTLS below. Field W\*(0,0) (in red) at the approximate center field of each survey patch, before the survey strategy changes.

CFHTLS field name	Reference center		Total pointings [n×p]	Total sky coverage [deg <sup>2</sup> ]	Filters	Comment
	RA [J2000]	DEC [J2000]				
W1	02:18:00	−07:00:00	9×8	8.5×7.5	$u^*, g, r, i/y, z$	16 y
W2	08:57:49	−03:19:00	5×5	4.8×4.7	$u^*, g, r, i/y, z$	New center; 2y
W3	14:17:54	+54:30:31	7×7	6.7×6.6	$u^*, g, r, i/y, z$	7 y
W4	22:13:18	+01:19:00	25	23.3	$u^*, g, r, i/y, z$	SE-NW elongated; 7 y

**Table 3:** Overview of the CFHTLS Wide fields. The pointings “n×p” refer to the numbers of tiles along the horizontal and vertical axes of MegaCam (*i.e.* the E-W and N-S axes). Sky coverage is expressed along RA and DEC axes.

Filter	Median number of exposures	Median exposure time [seconds]	Mean limiting magnitude [MegaCam AB system]	Mean image quality [′′]
$u^*$	5	3000	25.2	0.85
$g$	5	2500	25.5	0.78
$r$	4	2000	25.0	0.71
$i/y$	7	4300	24.8	0.64
$z$	6	3600	23.9	0.68

**Table 4:** Mean properties of the CFHTLS Wide survey. The  $i$  and  $y$  are not split into two sub-samples. The Mean limiting magnitude corresponds to the 80% completeness limit for point-like sources. The Mean image quality is the mean FWHM of stellar sources over all stacks.



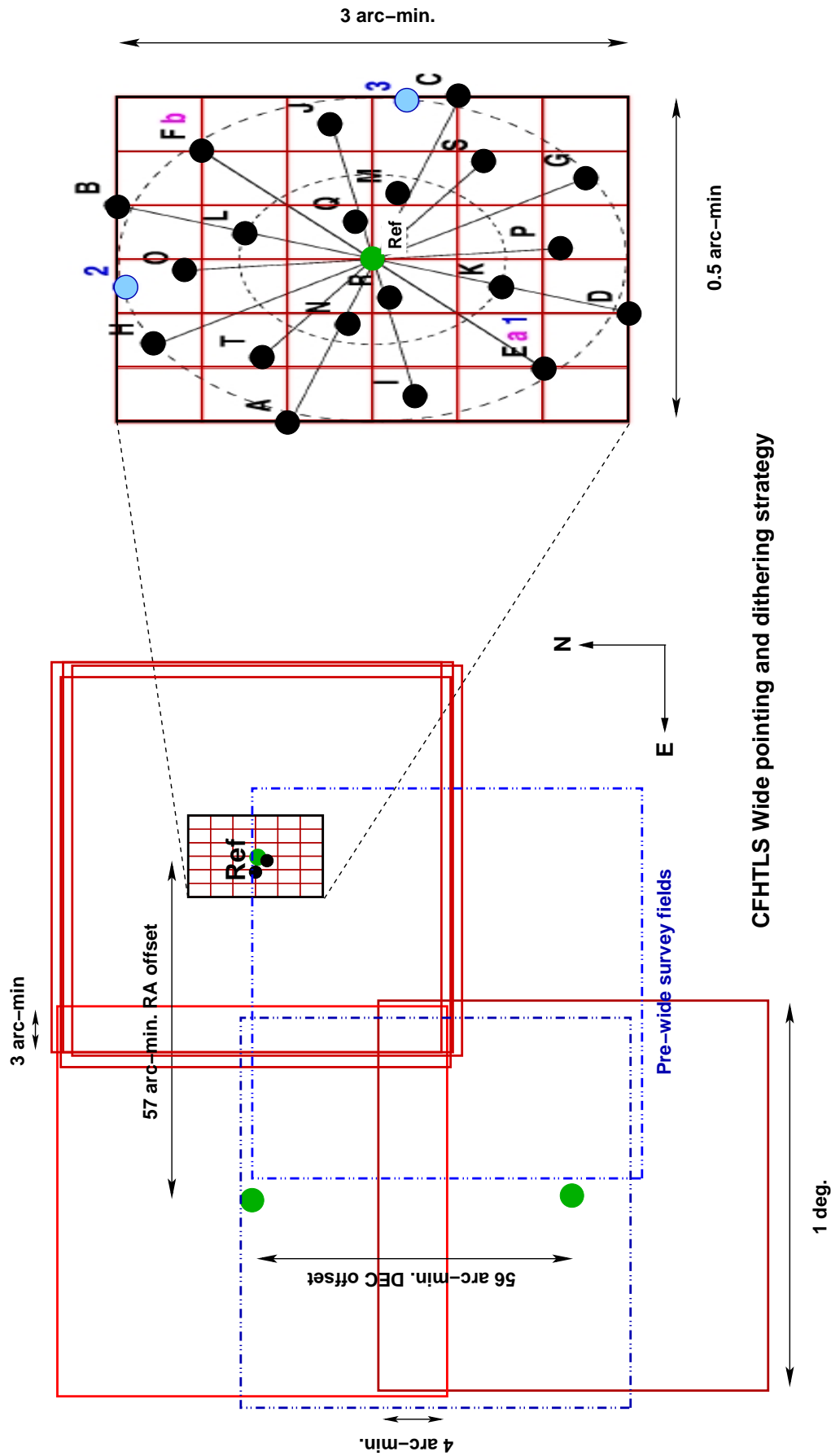


**Figure 21:** Offsets between adjacent pointings (left) and dithering (right) inside a pointing of the CFHTLS Wide survey. Each pointing (or tile) overlaps along the RA and DEC directions with its nearest neighbors. In addition to the large offsets, the observations at each CFHT Wide reference position ("Ref" and green filled circles) are split into an observing sequence of exposures, with a small dither between each. The dithering pattern depends on the number of exposure per sequence and is different for each filter (see Table 4). In all configurations the dithered positions (black filled circles) are among those located inside a  $30'' \times 180''$  ellipse centered at the reference position of a Wide pointing. This is illustrated on the right hand of the figure (drawn from this figure are given at this URL). The offsets <http://www.cfht.hawaii.edu/Instruments/Imaging/MegaPrime/specsinformati.on.html>. The details of this figure are given at this URL). The offsets and the dithers along the DEC direction are sufficiently large to fill the central horizontal gap ( $83''$  high) between the CCDs (see Fig. 2) with a fraction of exposures of each sequence. The dash-dot-dot blue squares on the left show the positions of Pre-Wide images. They are shifted by a half-MegaCam field of view, in both directions, in order to provide very large overlaps between pointings and ease the astrometric calibration. The Pre-Wide images are short exposures ( $3\text{ min}$ ) only done in  $r$ -band.



Each tile is centered at a well-defined position. The coordinates of a stack center position are identical for all filters. W1, W2, W3 and W4 are therefore composed of a complete set of  $u^*$ ,  $g$ ,  $r$ ,  $i$ ,  $y$  and  $z$  adjacent square tiles of  $1 \text{ deg}^2$  each.

The integer part of the center position of each tile is used to name the final stacks and other data products. This naming convention was agreed by CADAC, Terapix and the CFHTLS Steering Group and is valid for all CFHTLS releases.

In addition to the official astronomical CFHTLS naming convention, Terapix defined in 2002 a shorter naming convention based on a Cartesian grid coordinate system, where the increment unit is a MegaCam-size field and the center positions of the grid points are the center positions of the tiles<sup>21</sup>.

The reference center of each Wide field of view is defined as the reference W[1, 2, 3, 4](0,0) and the Cartesian field names increase toward the East and North. The tiling and field naming conventions are drawn on Fig. 20 and the complete list of the T0007 Wide stacks is given in Tables 31.

The total exposure time per filter is approximately the same for each tile (see Table 31 and the synoptic table). For some tiles, the exposure time is longer than the nominal value, because exposures that were considered out of spec by QSO and hence immediately reobserved have been later on salvaged at the post processing time. It produces very sharp exposure time distributions for all filters (see Fig. 23). Some observations have been adjusted to take into account unexpected events (like absorption by clouds/cirrus or technical problems). There are a few fields that have deeper  $u^*$ -band and  $z$ -band exposures which explains the small tails shown in the inset of Fig. 23. These longer exposures were taken before it was decided to cut the  $u^*$  and  $z$  exposure times by a factor of two at the survey mid-term review (2005).

In addition to the original CFHTLS exposures, the VIPERS consortium took complementary exposures to fill in the holes in W1 which were caused by malfunctioning CCDs later in 2003. These images (distributed in 6 pointings and three filters  $u$ ,  $g$  and  $y$ ) have been added to T0007. As a result, these pointing are deeper than the rest of the survey. A detailed description of the added VIPERS-DDT images can be found in Table 5. Their position on the W1 patch are shown in Figure 22.

Wide position	Filter	Exposure time (per image) [s]	Number of exposures
W1+2+2	u.MP9301	600	6
W1+4+2	g.MP9401	290	7
W1+3+1	g.MP9401	290	5
W1+3+1	g.MP9401	290	5
W1+4+1	g.MP9401	290	5
W1+2+1	i.MP9702	300.096	7
W1+3+2	i.MP9702	300.092	5

**Table 5:** Description of the 40 additional VIPERS-DDT images.

All  $r$ -band stacks combine data taken during two epochs separated by at least two years and totalling

<sup>21</sup><http://terapix.iap.fr/cplt/oldSite/Descart/summarycfhtlswide.html>

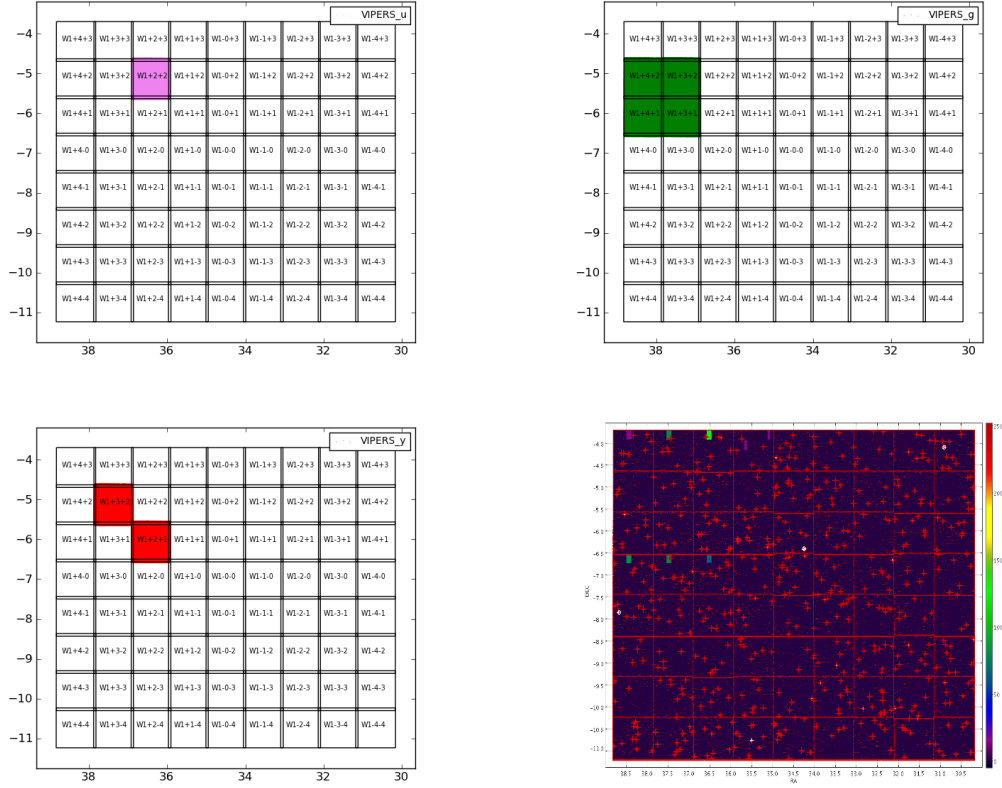


**Figure 22:** Position of the additional VIPERS-DDT exposures used to fill in the holes in the survey. Top left:  $u^*$ -band, top-right:  $g$ -band, lower left:  $y$ -band. lower-right: filter mask coverage of the W1 Wide patch (See Section 6 for the meaning of the flags). Seven fields still remain with half-CCD holes in one or more filters due to the malfunctioning of some CCDs late 2003. These anomalies are listed in Tables 15 and 16.

$2 \times 500$  s each. In all filters except  $u^*$ , observations were carried out only when the seeing (FWHM) was below  $0.95''$ . For the  $u^*$ -band, this rule was relaxed to  $1.3''$ .

The complete list of CFHTLS input images that were combined into the Wide stacks is given in the Appendix A.2, in Table 32.

The global properties of the CFHTLS Wide survey are summarized in Table 4 and in more detail in Table 6. Overall, they meet the survey specifications but the homogeneity of the survey over a Wide patch scale must be assessed carefully. The Wide field-to-field and MegaCam tile-to-tile scatters will be explored in detail in the following sections. The depth, the seeing, the photometric errors analysis are presented in the next parts of the document.

Finally, the complete set of configuration files used for the T0007 release is presented in the Appendix. They are intended for users who would prefer to re-process the pre-processed or the stacked images with parameters tuned for their own scientific projects. The configuration files are available on request from Terapix.

Field	Parameter	$u^*$	$g$	$r$	$i$	$y$	$z$	
W1	Nb stacks	72	72	72	56	16	72	
	Seeing ["]	$0.84 \pm 0.11$	$0.77 \pm 0.10$	$0.70 \pm 0.07$	$0.65 \pm 0.08$	$0.66 \pm 0.10$	$0.69 \pm 0.13$	
	80% Compl. (stellar)	$25.27 \pm 0.21$	$25.52 \pm 0.18$	$25.03 \pm 0.16$	$24.73 \pm 0.18$	$24.82 \pm 0.22$	$23.90 \pm 0.26$	
	80% Compl. (extended)	$24.45 \pm 0.15$	$24.67 \pm 0.14$	$24.00 \pm 0.10$	$23.69 \pm 0.13$	$23.78 \pm 0.20$	$22.91 \pm 0.15$	
	Int. astrom. err.	$(0.031", 0.029")$	$(0.031", 0.029")$	$(0.025", 0.022")$	$(0.020", 0.017")$	$(0.020", 0.017")$	$(0.025", 0.022")$	
	Ext. astrom. err.	$(0.237", 0.227")$	$(0.254", 0.244")$	$(0.259", 0.247")$	$(0.252", 0.243")$	$(0.272", 0.254")$	$(0.260", 0.247")$	
	Mag. err. [mag.]	$0.05 \pm 0.01$	$0.03 \pm 0.01$	$0.03 \pm 0.01$	$0.03 \pm 0.01$	$0.03 \pm 0.01$	$0.04 \pm 0.01$	
	cFHTLS-sdss $\langle \delta_m \rangle$ [mag.]	$-0.020 \pm 0.015$	$+0.003 \pm 0.006$	$+0.041 \pm 0.014$	$+0.000 \pm 0.007$	$-0.002 \pm 0.008$	$+0.015 \pm 0.011$	
	W2	Nb stacks	25	25	25	23	2	25
		Seeing ["]	$0.88 \pm 0.10$	$0.79 \pm 0.08$	$0.72 \pm 0.09$	$0.64 \pm 0.08$	$0.59 \pm 0.05$	$0.72 \pm 0.09$
80% Compl. (stellar)		$25.16 \pm 0.20$	$25.51 \pm 0.18$	$25.04 \pm 0.18$	$24.81 \pm 0.13$	$24.96 \pm 0.15$	$23.88 \pm 0.16$	
80% Compl. (extended)		$24.36 \pm 0.17$	$24.66 \pm 0.16$	$24.00 \pm 0.13$	$23.76 \pm 0.10$	$23.84 \pm 0.09$	$22.94 \pm 0.11$	
Int. astrom. err.		$(0.024", 0.021")$	$(0.024", 0.021")$	$(0.024", 0.021")$	$(0.024", 0.021")$	$(0.024", 0.021")$	$(0.024", 0.021")$	
Ext. astrom. err.		$(0.183", 0.186")$	$(0.208", 0.211")$	$(0.211", 0.213")$	$(0.207", 0.210")$	$(0.224", 0.228")$	$(0.211", 0.212")$	
Mag. err. [mag.]		$0.05 \pm 0.01$	$0.03 \pm 0.01$	$0.03 \pm 0.01$	$0.03 \pm 0.01$	$0.03 \pm 0.01$	$0.04 \pm 0.01$	
cFHTLS-sdss $\langle \delta_m \rangle$ [mag.]		$-0.040 \pm 0.011$	$-0.008 \pm 0.005$	$+0.007 \pm 0.004$	$-0.007 \pm 0.005$	-	$+0.018 \pm 0.012$	
W3		Nb stacks	49	49	49	42	7	42
		Seeing ["]	$0.85 \pm 0.11$	$0.81 \pm 0.09$	$0.75 \pm 0.08$	$0.66 \pm 0.08$	$0.59 \pm 0.08$	$0.67 \pm 0.09$
	80% Compl. (stellar)	$25.20 \pm 0.22$	$25.48 \pm 0.16$	$24.99 \pm 0.15$	$24.67 \pm 0.16$	$24.95 \pm 0.15$	$23.93 \pm 0.22$	
	80% Compl. (extended)	$24.35 \pm 0.21$	$24.64 \pm 0.12$	$23.98 \pm 0.10$	$23.63 \pm 0.12$	$23.89 \pm 0.11$	$22.92 \pm 0.17$	
	Int. astrom. err.	$(0.036", 0.035")$	$(0.036", 0.035")$	$(0.036", 0.035")$	$(0.036", 0.035")$	$(0.036", 0.035")$	$(0.036", 0.035")$	
	Ext. astrom. err.	$(0.235", 0.225")$	$(0.248", 0.242")$	$(0.258", 0.249")$	$(0.246", 0.242")$	$(0.275", 0.269")$	$(0.258", 0.250")$	
	Mag. err. [mag.]	$0.05 \pm 0.01$	$0.03 \pm 0.01$	$0.03 \pm 0.01$	$0.03 \pm 0.01$	$0.03 \pm 0.01$	$0.04 \pm 0.01$	
	cFHTLS-sdss $\langle \delta_m \rangle$ [mag.]	$-0.012 \pm 0.009$	$+0.003 \pm 0.004$	$+0.010 \pm 0.005$	$-0.013 \pm 0.004$	$+0.000 \pm 0.004$	$+0.001 \pm 0.005$	
	W4	Nb stacks	25	25	25	18	7	25
		Seeing ["]	$0.81 \pm 0.11$	$0.75 \pm 0.06$	$0.67 \pm 0.07$	$0.61 \pm 0.07$	$0.59 \pm 0.06$	$0.64 \pm 0.10$
80% Compl. (stellar)		$25.22 \pm 0.21$	$25.57 \pm 0.17$	$25.02 \pm 0.16$	$24.81 \pm 0.19$	$24.97 \pm 0.11$	$23.91 \pm 0.20$	
80% Compl. (extended)		$24.35 \pm 0.17$	$24.71 \pm 0.15$	$23.94 \pm 0.12$	$23.73 \pm 0.19$	$23.88 \pm 0.08$	$22.90 \pm 0.13$	
Int. astrom. err.		$(0.023", 0.020")$	$(0.023", 0.020")$	$(0.023", 0.020")$	$(0.023", 0.020")$	$(0.023", 0.020")$	$(0.023", 0.020")$	
Ext. astrom. err.		$(0.193", 0.186")$	$(0.218", 0.213")$	$(0.222", 0.217")$	$(0.217", 0.215")$	$(0.221", 0.217")$	$(0.214", 0.212")$	
Mag. err. [mag.]		$0.05 \pm 0.01$	$0.03 \pm 0.01$	$0.03 \pm 0.01$	$0.03 \pm 0.01$	$0.03 \pm 0.01$	$0.04 \pm 0.01$	
cFHTLS-sdss $\langle \delta_m \rangle$ [mag.]		$-0.030 \pm 0.009$	$+0.009 \pm 0.003$	$+0.010 \pm 0.007$	$-0.001 \pm 0.006$	-	$+0.022 \pm 0.005$	

**Table 6:** Summary of the W1, W2, W3 and W4 mean survey parameters. The  $i$  and  $y$  data have been combined. "80% Compl." is the 80% completeness limit. The seeing is the median FWHM and the errors is the field-to-field scatter. Astrometric errors are given along the two  $(x,y)=(\text{ns,ew})$  axes. The internal astrometric errors are from the (global) astrometric calibration errors step; the external astrometric errors are from the (ensemble average) astrometric accuracy of cFHTLS stacks. The "cFHTLS-sdss  $\langle \delta_m \rangle$  mag." denotes the mean magnitude offset between the cFHTLS and the sdss surveys, averaged over a Wide field. It is derived from a sample of common stars to both surveys in W1, W3 and W4 (no data for W2). The "Mag. err." is estimated from the external and internal magnitude errors discussed in the document. For W2, it is based on the internal mag. error and extrapolated from the W1, W3 and W4 cFHTLS-sdss comparisons.

Field	Parameter	$u^*$	$g$	$r$	$i$	$y$	$z$	$ugriz$ coverage
W1	Nb stacks	72	72	72	56	16	72	72
	Raw observed area	-	-	-	-	-	-	64.16
	Final unmasked area	58.47 (210500)	58.41 (210267)	58.49 (210581)	45.41 (163490)	13.08 (47096)	58.47 (210504)	58.33 (209975)
W2	Nb stacks	25	25	25	23	2	25	25
	Raw observed area	-	-	-	-	-	-	22.22
	Final unmasked area	18.60 (66952)	18.51 (66624)	18.60 (66952)	17.19 (61878)	1.43 (5152)	18.60 (66952)	18.50 (66622)
W3	Nb stacks	49	49	49	42	7	42	49
	Raw observed area	-	-	-	-	-	-	41.91
	Final unmasked area	37.04 (133351)	37.04 (133351)	37.04 (133351)	31.74 (114277)	5.56 (20018)	37.04 (133351)	37.04 (133340)
W4	Nb stacks	25	25	25	18	7	25	25
	Raw observed area	-	-	-	-	-	-	22.09
	Final unmasked area	19.66 (70777)	19.66 (70777)	19.66 (70777)	14.10 (50754)	5.62 (20218)	19.66 (70777)	18.50 (66622)
Wide	Nb stacks	171	171	171	129	32	171	25
	Raw observed area	-	-	-	-	-	-	22.09
	Final unmasked area	133.77 (481580)	133.616 (481019)	133.795 (481661)	108.44 (390399)	25.69 (92484)	133.78 (481584)	132.38 (476559)

**Table 7:** The raw observed area is the surface covered by MegaCam the sky. The Final unmasked area is the surface observed by the CFHTLS which is not masked (due to foreground star and instrumental defects). The surface is given in square degrees and square arcminutes.

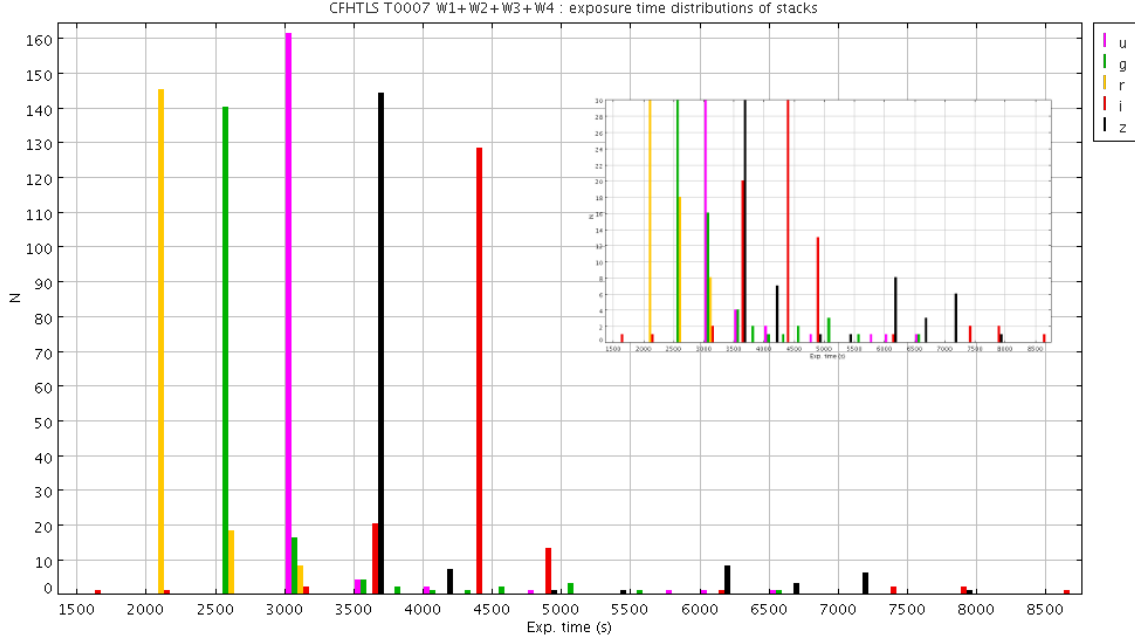


**Figure 23:** Distribution of exposure times over the Wide fields. The inset is a close-up view of the long exposure tails.

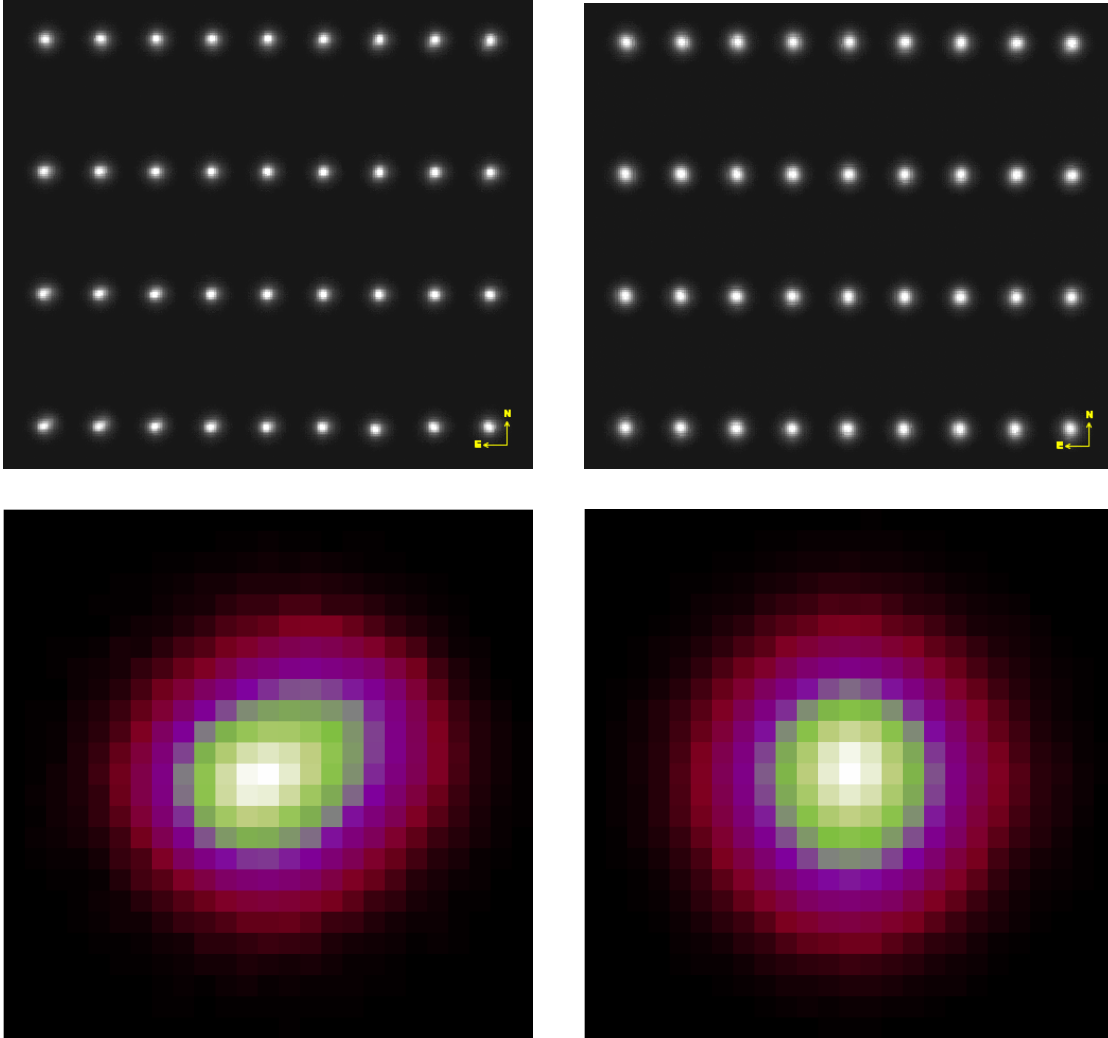
## 4.2 Seeing and image quality

All seeing values reported in this document and in tables are computed using PSFex (Bertin, 2011). The seeing is measured from a two-dimensional Moffat model of the PSF and the FWHM is defined from the ellipticity parameters of the PSF as  $\text{FWHM} = \sqrt{a b}$ , where  $a$  and  $b$  are the size of the major and minor axes derived from the model. For single CFHTLS input images, the seeing is sampled over a CCD ( $\sim 7' \times 14'$ , see Fig. 24), and for T0007 stacks it is sampled over a  $5' \times 5'$  grid. (Note that in T0006 and anterior releases, the seeing was measured from the radius enclosing half the object flux.)

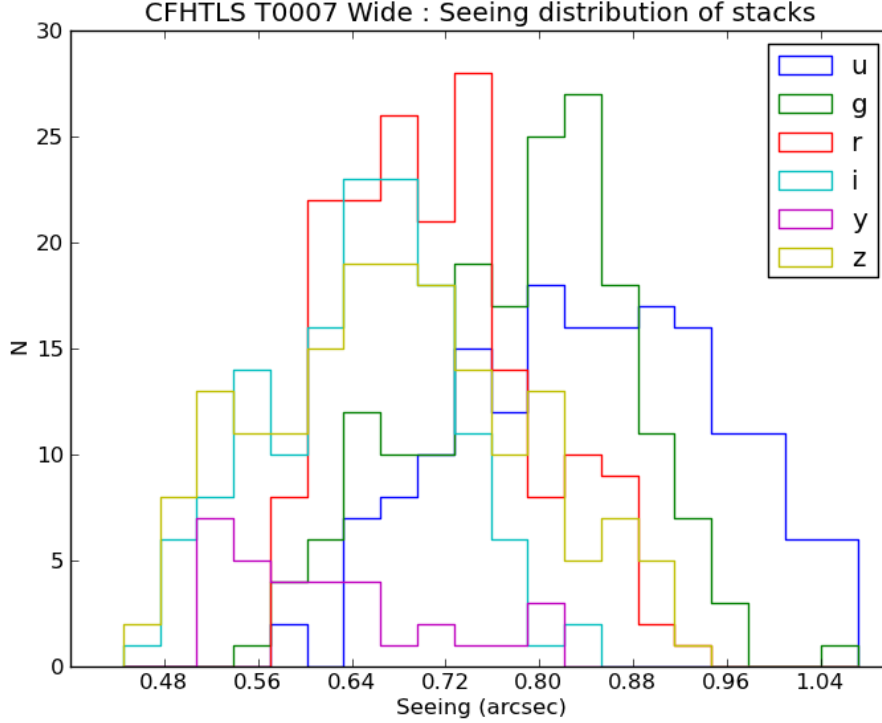
The PSF model of each stack (Wide and Deep) is determined using stellar sources selected by PSFex. All unsaturated and sufficiently bright stellar sources identified over the entire MegaCam field are used. The median seeing values of the survey are given in Table 4 and Table 6.

Overall, the CFHTLS Wide is within or better than expectations, thanks to the high ranking of the program which meant most observations were made in good-seeing conditions (i.e. close to median conditions at CFHT). The histograms drawn in Fig. 25 show the median seeing increases from  $z$  to  $u^*$ . However, more than 98% of  $g, r, i, y, z$  and more than 70% of  $u^*$  band stacks have seeing better than  $0.9''$ . Note that the histograms show the distributions of seeing over the whole period of the survey. They merge together data obtained before and after the flip of the L3 lens of the MegaPrime Wide Field Corrector (Dec. 4, 2004). This tuning produced an unexpected and unexplained, but spectacular, improvement of the image quality and our merging of the pre-flip and post-flip periods contribute to the large scatter of the seeing distributions. However, the Wide survey had not made much observing progress by late 2004 compared to the SNLS/Deep survey which remained a top priority within the CFHTLS, hence “contamination” by poorer image quality images is quite minimal in the Wide survey. In consequence, despite this extra-scatter term, the image quality of the CFHTLS Wide survey is excellent and unique compared to other current wide field surveys.

Figure 26 shows maps of the spatial distribution of seeings in all Wide stacks and for each filter. No bias



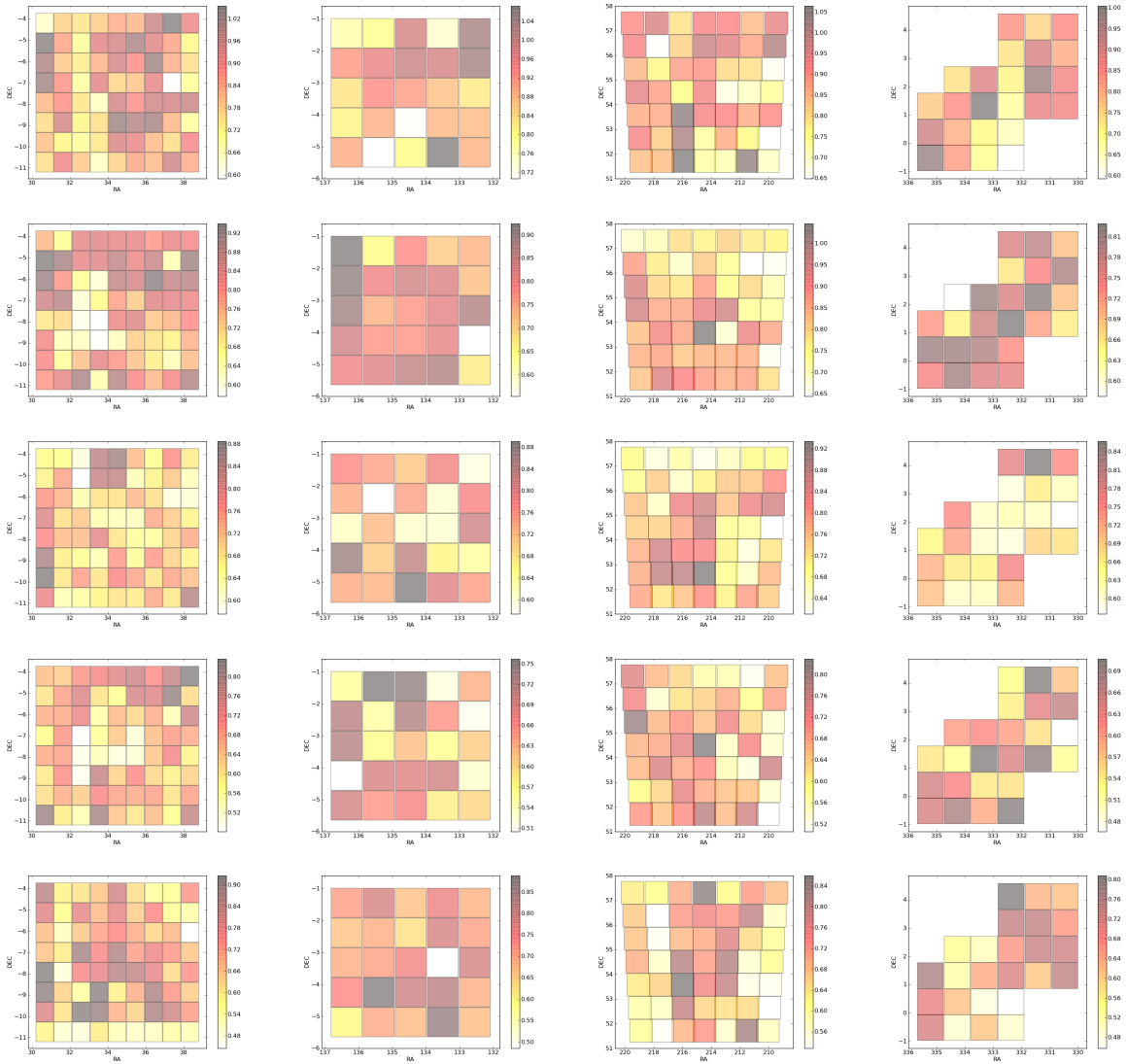
**Figure 24:** (Top Left) Seeing (FWHM) mapped over the input *i*-band image 743065p.fits by QualityFITS-in. This image was taken before the MegaPrime optics were optimized (fall 2004) to deliver a uniform PSF across the entire field. It is used as an illustration of the image quality issue on MegaCam from May 2003 to Nov. 2004. Each spot shows an image of the PSF computed by PSFex from a model of stars detected on the CCD. The optical distortion of the wide field corrector is clearly visible from PSF variation over the field. The median seeing over the MegaCam field is 0.692", but it is 0.642" at the center, on CCD#22 (spot 23 from the top left corner), and 0.795" at the bottom left corner. (Top Right) Seeing (FWHM) mapped over the input *i*-band image 980090p.fits by QualityFITS-in. This second image was taken after the MegaPrime optics were optimised (fall 2004). The lower part shows the clear improvement of the average PSF shape over the whole field: the tuning of the wide field corrector reduced to less than 0.05" the typical image quality degradation from the center to the edge of the field.



**Figure 25:** Distribution of the median seeing over the Wide tiles. The seeing is the  $\text{FWHM} = \sqrt{a b}$  derived with PSFEX, from the fitting of a 2-dimension Moffat model of the PSF. The mean seeing value over the MegaCam field of each stack is available at [http://terapix.iap.fr/cplt/T0007/table\\_syn\\_T0007.html](http://terapix.iap.fr/cplt/T0007/table_syn_T0007.html).

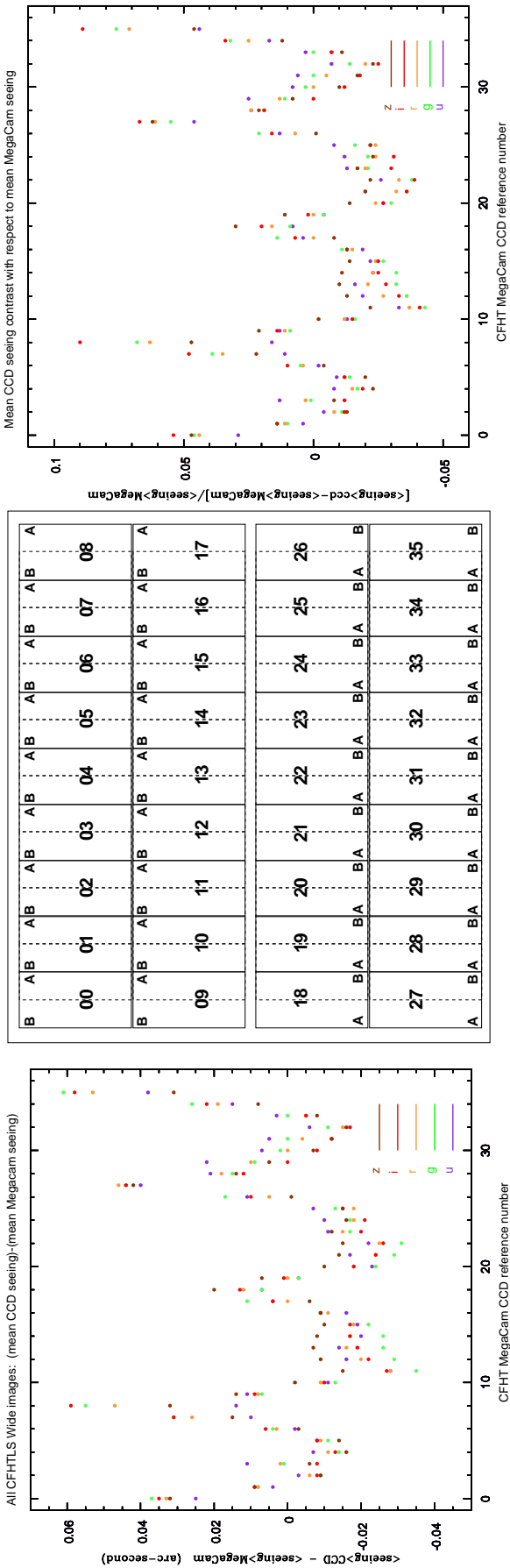
is observed, the median seeing of each stack appears randomly distributed over the four Wide fields.

Figure 27 shows the seeing fluctuations on MegaCam. The seeing is averaged over a CCD field of view and compared to the mean seeing over the whole MegaCam field. The statistics is based on 6378 input images used for the CFHTLS Wide T0007 release. For CCDs at the edges of the detector, the differences are important but never exceed  $0.065''$ , and the maximum peak-to-peak amplitude is less than  $0.1''$ . This upper limit is acceptable. It still preserves the mean seeing over the whole MegaCam field of view below one arcsecond for all input images that will be combined into stacks. The legend of Figure 27 elaborates on the extreme corners of the MegaCam field of view which exhibit a rapid image quality degradation, but represent an area limited to just 3% of each image.



**Figure 26:** Maps of seeing (FWHM) in the CFHTLS Wide. Each small square represents a median seeing value over a  $1^\circ \times 1^\circ$  tile (or a stack) of the Wide survey. The panels show, from left to right: W1, W2, W3 and W4; from top to bottom: the  $u^*$ ,  $g$ ,  $r$ ,  $i/y$  and  $z$  CFHTLS stacks.





**Figure 27:** PSF variations as a function of the position on MegaCam (CCD positions) and wavelength (filters), produced by the optical distortion of the MegaPrime wide field corrector. These statistics are based on 935  $u^*$ , 978  $g$ , 1669  $r$ , 1064  $i$  and 1177  $z$ -band images (the 220  $y$ -band images have been ignored here). The variations are estimated from the comparison between the mean seeing (FWHM) averaged over the MegaCam field of view and the mean seeing averaged over a CCD field of view. The statistics are computed over the 36 CCDs composing the mosaic. The CCDs are numbered using the CEA-CFHT CCD reference number laid out on the central figure. The left panel shows the difference  $\langle \text{FWHM} \rangle_{\text{CCD}} - \langle \text{FWHM} \rangle_{\text{MegaCam}}$  expressed in arcseconds. The horizontal axis is the CEA-CFHT CCD reference number. One can see that for the CCDs at the edges of the detector, the differences never exceed 0.065", and the highest peak-to-peak amplitude is less than 0.1". The right panel shows the seeing contrast  $\frac{\langle \text{FWHM} \rangle_{\text{CCD}} - \langle \text{FWHM} \rangle_{\text{MegaCam}}}{\langle \text{FWHM} \rangle_{\text{MegaCam}}}$ . The contrast is always lower than 10% and the highest peak-to-peak contrast amplitudes are always less than 15%. Overall, the range of seeing values over the MegaCam field of view is acceptable. However, at the extreme corners of MegaCam, the seeing difference with the mean value can be as large as 0.25". Only the most extreme positions have a large PSF degradation and images that no longer meet the specifications of the surveys. We discard these regions by adding extra polygons to the T0007 .reg files that mask the edges of all stacks. The fraction of the MegaCam field discarded is less than 3%.

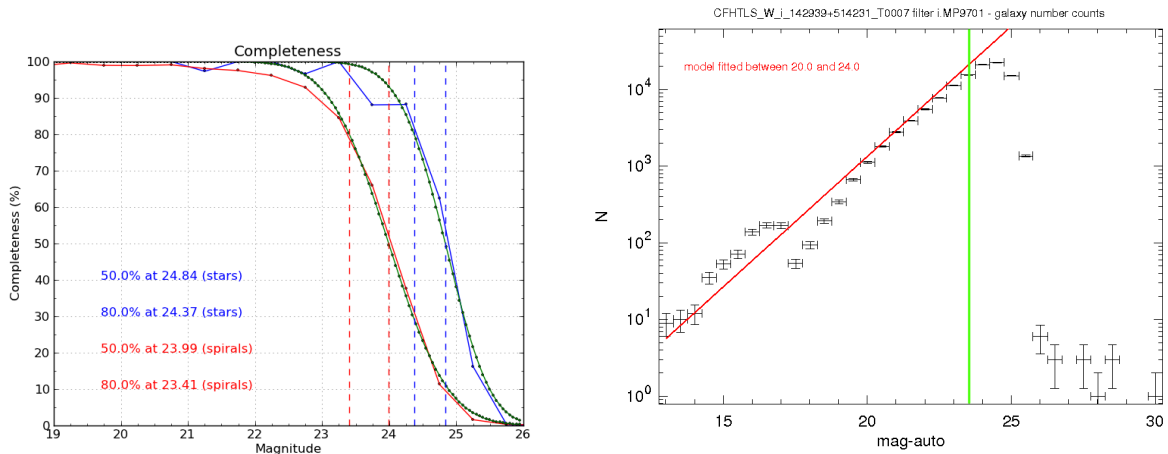


**Figure 28:** Completeness calculation for the W3 stack CFHTLS\_W\_i\_142939+514231. Left panel: The blue and red lines shows the completeness for point-like and extended sources respectively. The green dots show the best fitting functions which are used to derive the completeness values. Right panel: galaxy counts derived automatically by `QualityFITS` from this stack. The red line shows the expectations for the MegaCam *i*-filter. The green line is the 80% completeness limit of extended objects.

### 4.3 Depth and completeness limits

The depth of the survey tile is measured by the completeness limit. It is determined for each stack and each filter separately. The depth is also checked by using the galaxy counts computed after the production of each stack, as part of the `QualityFITS` analysis. All completeness galaxy count plots are available from the T0007 synoptic table<sup>22</sup>.

To compute the completeness limit, we used image simulations produced by `SkyMaker`(Bertin, 2009). Noiseless images of point-like (stars or galaxy bulges) and disk-like (spiral galaxies) sources have been simulated by combining spheroid and disk models, using de Vaucouleur and exponential light profiles, respectively. The star and galaxy number densities of simulated sources correspond to the expectations for typical CFHTLS exposure times. Their slope and normalization are based on realistic luminosity function in a standard  $\Lambda$ -CDM cosmology (for galaxies), and are produced according to the transmission of the MegaCam filters.

The sources are then convolved by a PSF that takes into account the pupil of the CFHT telescope (mirrors and arms) and other components of the PSF. The PSF is built by using the diffraction and the simplest aberration components of the CFHT telescope, as well as the typical atmospheric contributions that degrade long exposures. A set of simulations are produced with PSF FWHM ranging from 0.4'' to 1.3''. For each stack, the simulated images with the closest PSF in FWHM size is then used to compute the final completeness. This “adaptive FWHM” method gives rise to larger dispersion in the completeness distribution compared to T0006. The T0007 completeness encompass both the exposure time and depth effect, as well as the image quality. The point source completeness is therefore more affected than the extended objects one.

The completeness limit is then derived from the averaged completeness value over the central 10000×10000 MegaCam fields. The statistics are computed in each field separately and for each filter. The output is the fraction of sources detected and measured as a function of magnitude. The magnitudes at 80% and

<sup>22</sup>[http://terapix.iap.fr/cpl/t0007/table\\_syn\\_T0007.html](http://terapix.iap.fr/cpl/t0007/table_syn_T0007.html)

50% completeness are given for point-like (star or bulge) and for extended (disks) sources.

The 80% and 50% completeness values are calculated from an automated fitting process applied to the catalogues of real and simulated sources without tuning. The limiting magnitudes are derived automatically by an empirical two parameter ( $x_0; \alpha$ ) fitting function

$$y = 100.0 \times \left( 1 - \frac{\text{erf} [x - x_0]^\alpha + 1.0}{2.0} \right) \quad (12)$$

where  $x_0$  provides the turn-over position of the completeness function and  $\alpha$  is the function slope at  $x_0$ . The parameters ( $x_0; \alpha$ ) are found from a standard  $\chi^2$  minimization. The 50% and 80% completeness limits are derived from a linear interpolation. An example of fit is given in Fig. 28. In some cases, the fit and the interpolation are not good and the completeness value is then poorly estimated.

The completeness distributions over all the Wide fields and inside a Wide field are presented in Table 6. The left panel of Figure 29 shows the completeness distribution for the entire Wide survey for all four fields. Figure 30 shows the completeness distributions for each of the four Wide patches.

The histograms coupled to a detailed inspection of the data show that the mean scatter in completeness is  $\pm 0.20$  magnitudes, with significant variations from filter to filter. The completeness distribution in  $z$ -band is broader than other filters, with a tail that extends over one magnitude. In contrast, the  $r$  band distribution is narrower ( $\pm 0.15$  mag.). This is due primarily to the large variations of the sky brightness through the years in that photometric band (OH emission lines), causing the variable depth on observations following a fixed exposure time model. Erratic behavior of the OH emission lines also leads to poorer correction of the fringes, aggravating the situation in the  $z$ -band.

Figure 32 shows a series of completeness maps over the entire Wide fields. The maps are produced for each Wide field and for each filter.

The left and right panels of Figure 31 shows that the completeness distribution are dominated by seeing, both for point sources and extended objects : better image quality corresponds to deeper images. Compared to the seeing contribution, the exposure time (even with double exposure time) has a smaller influence on the final depth measurement. For the  $u^*$  band, the range of limiting depth is likely broadened by the diversity of observing conditions (Moon, extinction, seeing). Nevertheless, (other than exposure time) the main factor affecting image completeness is the Seeing FWHM.

The comparison with T0006 completeness is not straightforward. In T0006, the simulations were produced using a PSF of fixed FWHM equal to 0.9 arcsec. In T0007, the simulated PSF size matches the real PSF size of each tile. Since the actual seeing distribution peaks at an image quality better than 0.9 arcsec, the T0007 measured completeness of point sources is deeper than T0006. This increase in depth (around 0.02 to 0.03mag in riyz) is therefore largely due to the measurement technique rather than changes in the images.

Finally, Figure 33 shows the galaxy counts for the four Wide patches for each of the six bands, appropriately normalized in each case to the effective area after masking. The field-to-field agreement between the different patches is excellent, as is the match to the literature values.

#### 4.4 Photometric accuracy

In this Section we attempt to make a robust estimate of the internal photometric errors of the CFHTLS using a variety of methods. Although Scamp provides an estimate of the internal photometric error (between individual MegaCam images), we instead focus on the photometric errors in the final tiles.

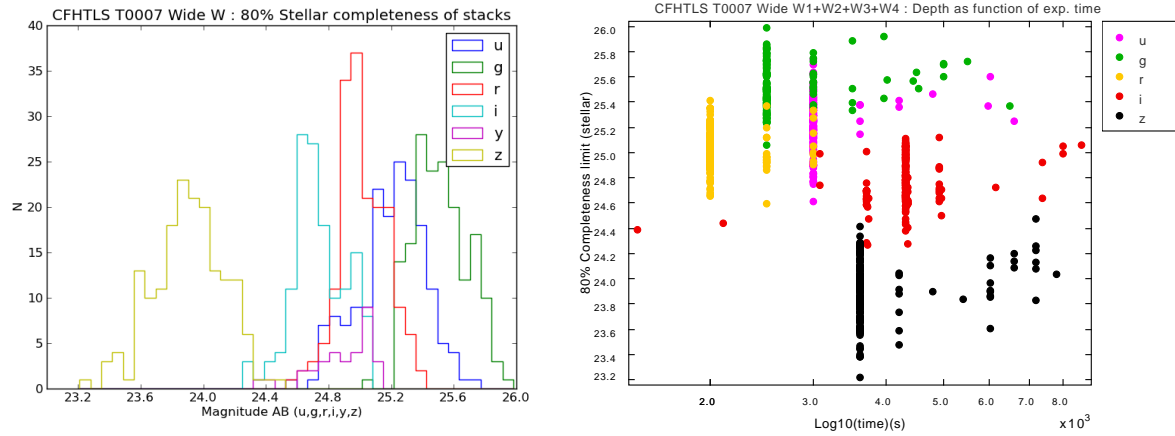


**Figure 29:** Left panel: overall distribution of completeness on the Wide fields. Right panel: completeness limit of Wide stacks as a function of exposure time. A trend of increasing depth with increasing observing time is apparent. There is however a broad spread in depths at a given exposure time. due to other factors such as image quality, sky brightness and weather conditions (cirrus). The depth of some z-band stacks is also reduced by residuals from the fringe subtraction.

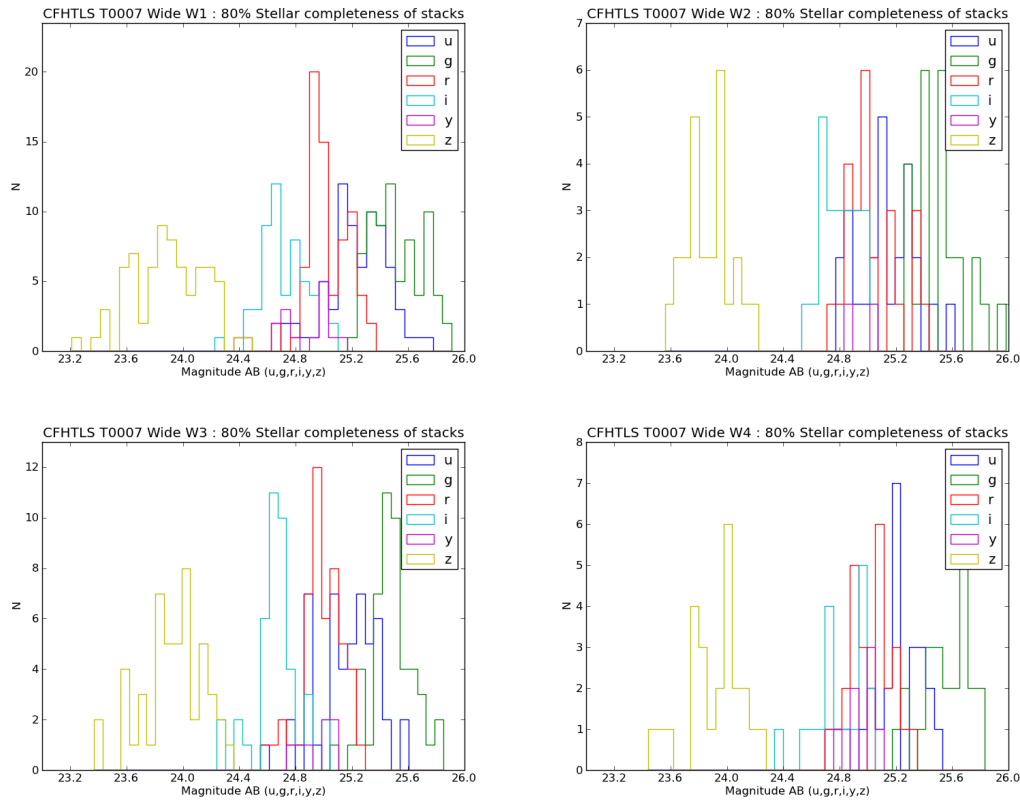


**Figure 30:** Distribution of 80% stellar completeness over the Wide fields. The horizontal axes are MegaCam AB magnitudes.

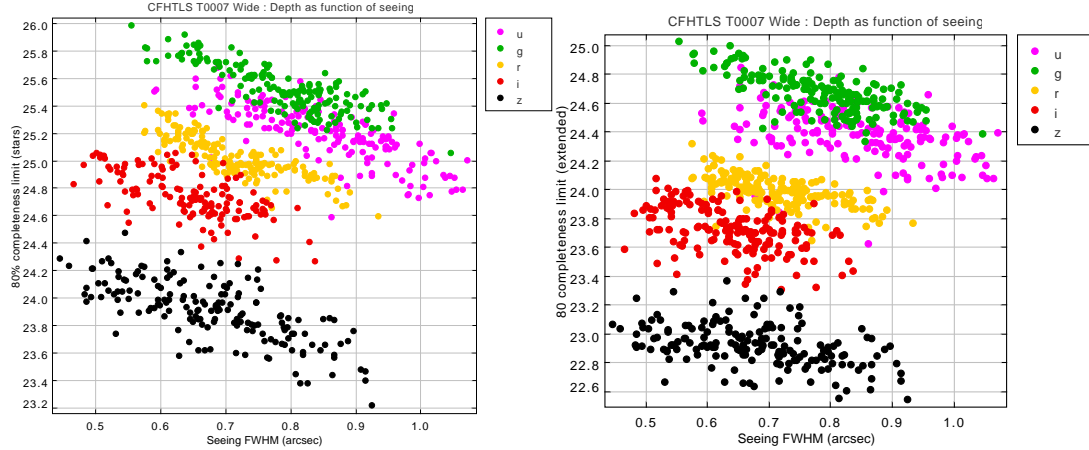


**Figure 31:** Left and right panels respectively: Stellar and extended sources completeness limit of Wide stacks as a function of seeing FWHM. As expected, the point source completeness is a clear function of the image quality: the better the seeing, the deeper the image.

This way, initial calibration errors and any other subsequent source of errors, inside each stack and field-to-field are better taken into account, leading to a more realistic estimation of the errors.

#### 4.4.1 Internal photometric errors of Wide stacks from simulations

The internal photometric errors are derived using the same simulations used in the completeness analysis described in Section 4.3. The use of simulations enables a better control of the input and output sources and ensures that all Wide stacks are evaluated consistently. As before, simulated sources are added to the real T0007 Wide stacks and processed the same way as real sources. Their photometry is then compared to the input simulated values. The simulated sources are added within the central  $10000 \times 10000$  pixel and consequently are expected to be free from edge effects.

This procedure has been applied to the 855 Wide stacks, using simulated stars generated on a grid of FWHM in steps of  $0.05''$  using the Skymaker software (Bertin, 2009). In each case, stars with a FWHM closest to the stack in question are selected. For each sample, the magnitude difference between the input and the output simulated sources as a function of magnitude is computed and the FWHM of the magnitude distribution is derived after  $3\text{-}\sigma$  clipping. The internal error is then given by  $\sigma_{mag} = \text{FWHM}/2.35$ .

Error estimates are computed for sources selected with signal-to-noise ratios of 10, 30 and 100, respectively, or as a function of magnitude Fig. 34 shows an example result for internal photometric analysis of the CFHTLS T0007 Wide stack CFHTLS\_w\_g\_020241-041200\_T0007. The statistics compare the MAG\_AUTO magnitude calculated by SExtractor for several thousands of stellar sources. It is interesting to note that the results are very stable down to signal-to-noise values of 10. Note that the difference between the input and output magnitudes as function of magnitude is not flat, but tilted. The tilt may artificially increase the dispersion inside a magnitude bin and may contaminate the internal error estimates, if the bin is large. The mean inside a bin is then corrected from the tilt prior to deriving an errors or FWHM.

The internal errors per magnitude bin are listed in Table 8.



**Figure 32:** Maps of 80% completeness limits in W1, W2, W3 and W4 (from left to right). Each colored square represents a  $1 \times 1 \text{ deg}^2$  tile. Square color indicates the seeing value, with darker squares have poorer seeing. From top to bottom:  $u^*$ ,  $g$ ,  $r$ ,  $i$ ,  $y$  and  $z$  bands.

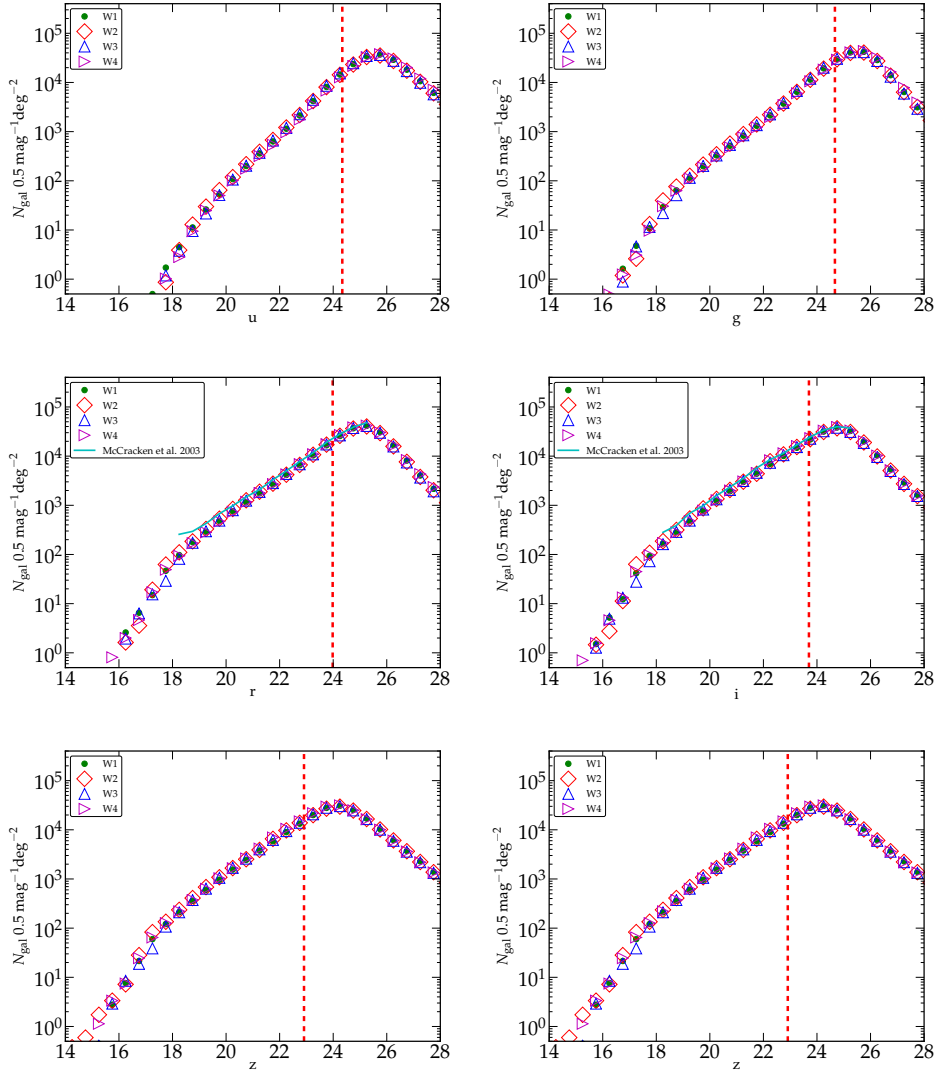


**Figure 33:** Galaxy counts for the four Wide patches in all bands. The dotted red line corresponds to the 80% completeness for extended sources computed from the simulations. In  $r$  and  $i$  band counts are compared those in the VLT-VIRMOS deep field (McCracken et al., 2003).

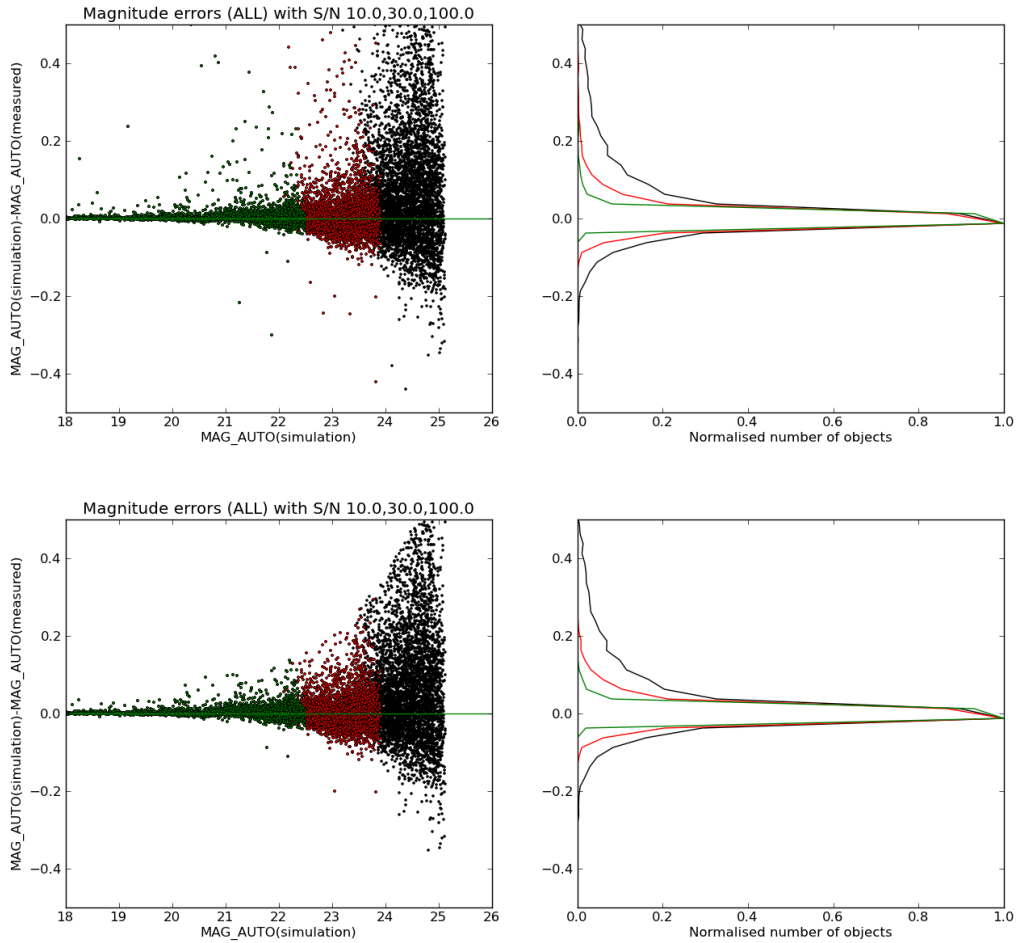


**Figure 34:** Analysis of the internal photometric errors in CFHTLS\_W\_g\_020241-041200\_T0007 using simulations of stars. The top panels are analyzed without clipping and the bottom panels after a  $3\text{-}\sigma$  clipping. The figures show the results for three sub-samples selected from signal-to-noise ratio (not magnitudes):  $S/N=10$  (black), 30 (red) and 100 (green). Each panel is split into two plots. On the left the magnitude differences between the *true* input and the *measured* output magnitudes of simulated sources are drawn as a function of magnitude. The sub-samples are shown in green, red and black colors. On the right, the normalized distributions for the three sub-samples are shown. The FWHM, errors,  $\sigma = \text{FWHM}/2.35$ , in table 8 are derived from the histograms. Note that a magnitude dependant offset has been corrected prior to computing the FWHM and the errors inside a magnitude bin quoted in Table 8.



Wide Field	Magnitude range [MegaCam AB]	$u^*$ [mag.]	$g$ [mag.]	$r$ [mag.]	$i$ [mag.]	$y$ [mag.]	$z$ [mag.]
W1	[19.0 – 20.0]	0.002	0.002	0.003	0.006	0.003	0.008
	[20.0 – 21.0]	0.005	0.003	0.010	0.007	0.007	0.017
	[21.0 – 22.0]	0.008	0.009	0.011	0.016	0.014	0.043
	[22.0 – 23.0]	0.020	0.015	0.025	0.037	0.035	0.098
	[23.0 – 24.0]	0.046	0.035	0.061	0.089	0.083	0.159
W2	[19.0 – 20.0]	0.002	0.002	0.003	0.003	-	0.009
	[20.0 – 21.0]	0.004	0.004	0.005	0.007	-	0.018
	[21.0 – 22.0]	0.009	0.009	0.012	0.016	-	0.041
	[22.0 – 23.0]	0.020	0.016	0.027	0.038	-	0.097
	[23.0 – 24.0]	0.050	0.038	0.067	0.087	-	0.161
W3	[19.0 – 20.0]	0.002	0.001	0.002	0.003	0.002	0.008
	[20.0 – 21.0]	0.004	0.003	0.005	0.007	0.007	0.018
	[21.0 – 22.0]	0.008	0.007	0.011	0.017	0.015	0.040
	[22.0 – 23.0]	0.020	0.015	0.025	0.039	0.034	0.095
	[23.0 – 24.0]	0.049	0.035	0.060	0.094	0.084	0.140
W4	[19.0 – 20.0]	0.002	0.001	0.002	0.003	0.003	0.009
	[20.0 – 21.0]	0.004	0.003	0.005	0.007	0.007	0.019
	[21.0 – 22.0]	0.008	0.007	0.013	0.017	0.015	0.044
	[22.0 – 23.0]	0.020	0.015	0.028	0.041	0.035	0.098
	[23.0 – 24.0]	0.049	0.035	0.057	0.094	0.088	0.142

**Table 8:** Internal photometric errors per magnitude bins derived for each CFHTLS Wide field. The simulated sources include only stars and are detected and analyzed in the same way as real sources. The errors are the  $\text{FWHM}/2.35$ , as shown in Fig. 34. They are corrected from the amplitude of the tilt from horizontal of the difference between of the input and output magnitudes as function of magnitude inside the bin. The magnitude ranges quoted in the table only comprise bins with all sources below the completeness limits and with all sources having a signal-to-noise ratio larger than 10. The W2 y-band is not quoted because it only concerns two stacks and the statistics are meaningless for these fields.

#### 4.4.2 Error estimation from overlapping Wide tiles

An estimation of the internal photometric errors of the Wide survey can also be made using common sources in overlapping tiles. Since each tile is shifted by  $56'$  in RA and  $57'$  in DEC with respect to its nearest tiles overlap regions are stripes of  $4' \times 60'$  or  $3' \times 60'$  (see Fig. 21). We use the  $u^*$ ,  $g$ ,  $r$ ,  $i$  and  $z$ -band `MAG_IQ20` stars located in these regions to compare the photometry of sources detected in two adjacent stacks. The analysis is restricted to stars to avoid the specific issues involved in the use of `MAG_AUTO` for galaxies. Furthermore, it can only be applied on thin strips located at the edges of images where sources have lower signal-to-noise due to the adopted dithering strategy; therefore, this analysis should be regarded as secondary to our previous simulation-based estimations.

The first estimate of internal errors is derived by calculating for each pair of overlapping tiles the median of the magnitude differences of all source pairs in the overlapping regions. This value is the *field to field photometric offset* between the two contiguous tiles. For a complete Wide patch, the standard deviation

Wide field	$\sigma_{u^*}$ [mag.]	$\sigma_g$ [mag. ]	$\sigma_r$ [mag. ]	$\sigma_i$ [mag. ]	$\sigma_z$ [mag. ]
W1	0.020	0.010	0.015	0.013	0.020
W2	0.020	0.010	0.012	0.011	0.023
W3	0.025	0.010	0.015	0.011	0.019
W4	0.016	0.009	0.008	0.013	0.016

**Table 9:** Internal field-to-field photometric errors in the T0007 CFHTLS Wide release derived from sources in adjacent tiles. These internal errors are computed from the T0007 “merged source catalogues” (M-SC, see Section 6.3) which contains MAG\_IQ20 for sources detected on the  $u^*$ ,  $g$ ,  $r$ ,  $i/y$ ,  $z$  and chi2 images. They are derived from the mean of the absolute magnitude differences of source pairs, averaged over overlapping regions of neighboring stacks. Only bright stars are used to derive a robust field-to-field offset for each contiguous tile pair. The limiting magnitudes are  $u < 19, g < 22, r < 20, i < 21, z < 19$ . These values should be regarded as an upper estimate of the errors as they are calculated using the stack edges which have lower signal-to-noise due to the dithering.

of these field to field offsets is a estimator of the field to field scatter. The values for each field and filter are listed in Table 9. To compare these errors with estimators calculated from a comparison to a reference catalogue used in Section 4.4.3, a hypothesis has to be made on the distribution of this random variable. If we assume that photometric measurement are Gaussian-distributed around the “true” photometry with a dispersion of  $\sigma$ , then the dispersion of the field to field offsets is a Gaussian with a dispersion  $\sqrt{2}\sigma$ . The values of Table 9 must be divided by  $\sqrt{2}$  to be compared with the field to field estimations of Table 12. The errors are larger in  $u^*$  and  $z$  bands for several reasons: the residuals from fringe subtractions in  $z$ , the poorer image quality in  $u^*$ , especially at the edges of the stacks, and the residuals from the internal calibration errors. Considering the factor of  $\sqrt{2}$ , these errors are completely consistent with an overall photometric field to field scatter of 1% in  $g, r$  and  $i$  and 1.5% in  $u^*$  and  $z$ .

The second estimate of internal photometric errors which can be determined from the analysis of objects observed in multiple tiles is the measurement error. Since the images are photometrically flat, the dispersion of the magnitude offsets around the mean field-to-field shift of objects detected in multiple tiles is dominated by statistical measurements errors. This dispersion as a function of magnitude is plotted as the vertical error bars in Figure 35 for each of the four Wide patches and is listed in Table 10. In this analysis, both stars and galaxies are included; magnitudes are estimated using MAG\_AUTO to yield a realistic estimate of measurement errors for both stars and galaxies. We also note the plots are broadly similar for each of the four patches, confirming the homogeneous nature of the Wide survey. The  $z$ -band errors are several times higher than other bands; for these longer wavelengths fringing residuals become an true issue.

The dispersion distributions are fitted with third order polynomials. To compare these values to the direct estimation of measurement errors in the simulations, one has to assume a gaussian distribution (dispersion  $\sigma_M$ ) of the measured magnitude around the true magnitude. The distribution of the magnitude differences is then a Gaussian distribution with a dispersion equal to :

$$\sigma_{\text{diff}} = \sqrt{2} \times \delta_M \quad (13)$$

These errors are listed in Table 10.

Comparing these errors with those derived from the simulations shows that the errors from the overlaps

Wide Field	Magnitude range [MegaCam AB]	$u^*$ [mag.]	$g$ [mag.]	$r$ [mag.]	$i$ [mag.]	$z$ [mag.]
W1	[19.0 – 20.0]	0.013	0.007	0.009	0.010	0.025
	[20.0 – 21.0]	0.016	0.008	0.013	0.016	0.054
	[21.0 – 22.0]	0.024	0.014	0.023	0.031	0.112
	[22.0 – 23.0]	0.039	0.026	0.043	0.062	0.210
	[23.0 – 24.0]	0.065	0.046	0.078	0.114	0.359
W2	[19.0 – 20.0]	0.010	0.006	0.010	0.009	0.020
	[20.0 – 21.0]	0.014	0.009	0.015	0.015	0.045
	[21.0 – 22.0]	0.024	0.016	0.025	0.030	0.100
	[22.0 – 23.0]	0.043	0.027	0.047	0.059	0.195
	[23.0 – 24.0]	0.074	0.044	0.083	0.108	0.344
W3	[19.0 – 20.0]	0.011	0.007	0.009	0.010	0.023
	[20.0 – 21.0]	0.016	0.009	0.013	0.016	0.049
	[21.0 – 22.0]	0.025	0.014	0.022	0.033	0.101
	[22.0 – 23.0]	0.040	0.023	0.043	0.066	0.189
	[23.0 – 24.0]	0.062	0.036	0.079	0.123	0.324
W4	[19.0 – 20.0]	0.008	0.006	0.008	0.010	0.019
	[20.0 – 21.0]	0.012	0.008	0.013	0.016	0.044
	[21.0 – 22.0]	0.023	0.013	0.024	0.031	0.097
	[22.0 – 23.0]	0.044	0.022	0.046	0.061	0.189
	[23.0 – 24.0]	0.079	0.036	0.083	0.111	0.332

**Table 10:** Internal photometric errors per magnitude bins derived for each CFHTLS Wide field. The magnitudes of the objects detected in two stacks are compared. For each pair of stacks, a mean offset and dispersion is calculated from the magnitude differences of each pair of objects. Assuming a gaussian distribution of errors, the listed values are estimated as the dispersion divided by  $\sqrt{2}$ .

are larger. This is to be expected and can be explained by several reasons: the statistics on the objects in the overlaps rely on sources detected at field edges where image quality and signal-to-noise is lowest due to dithering and PSF degradation at the edge of the field. Furthermore, the flatness of the photometry across the field of view show a departure from the reference central photometry on the very edges. This effect is slightly non-symmetric and affects the reliability of the magnitude measurements at the field edges. Therefore these error estimates should be considered as upper limits and contain residual systematic effects which add to the pure statistical flux measurement errors.

#### 4.4.3 Comparing CFHTLS-T0007 with SDSS-DR8

As a further check of our reduction and calibration procedures we wish to compare photometric measurements on the CFHTLS Wide with an external and well-characterized survey. Our aim is to check both the relative tile-to-tile calibration and the absolute photometric calibration. At the present time, the best candidates are the surveys conducted using the Sloan telescope at Apache Point Observatory. The latest release of the main Sloan survey, SDSS-DR8, overlaps at least partially with all four Wide patches of the CFHTLS.

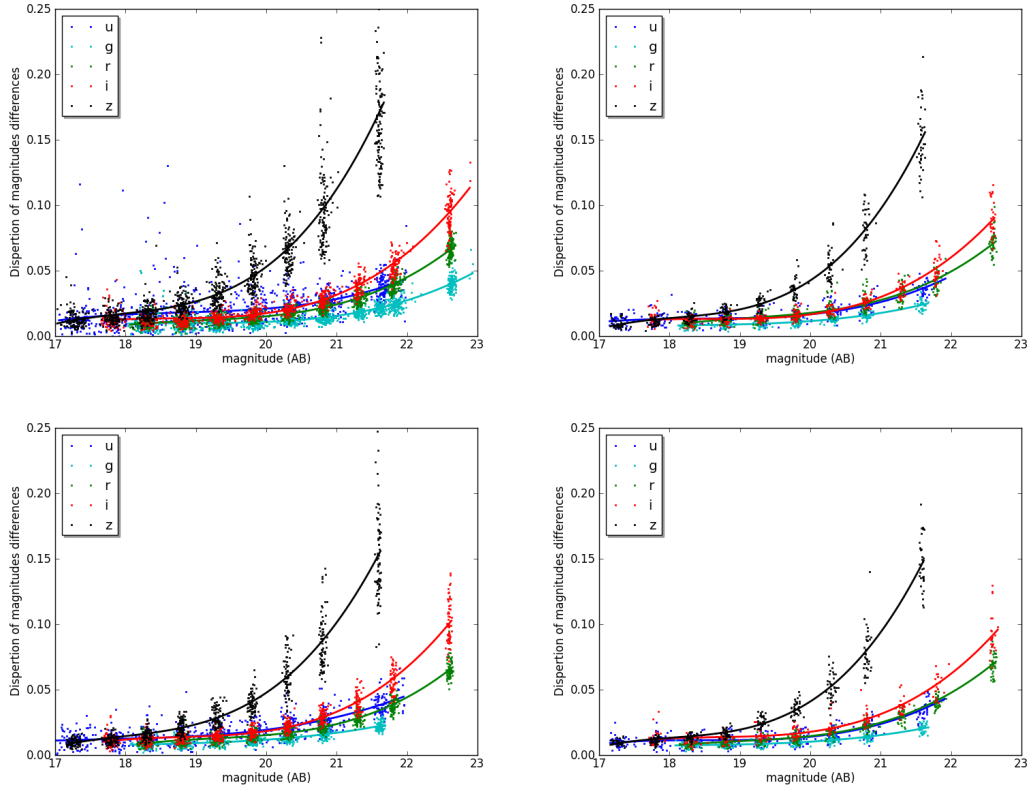


**Figure 35:** Magnitude errors as a function of magnitude derived from sources from overlapping regions for W1, W2, W3 and W4 (top left and top right and bottom left and bottom right fields respectively).

As thoroughly documented in Betoule et al. (submitted), the final release of the SNLS (SNLS5) compares in absolute to the SDSS Supernova Survey on Stripe 82 at better than 1% in the *griz* bands, and 2% for the  $u^*$  band. The MegaCam to SDSS transformation provided below for all MegaCam filters is based on that specific effort. The MegaCam T0007 photometry is exclusively in the AB system (Oke & Gunn, 1983). The following offsets used to convert the SDSS AB magnitude to the MegaCam AB magnitude are based on values presented in Table 1 from Holtzman et al. (2008), derived from observed and synthetic measurements of Solar analogs for the SDSS Supernova Survey. They have been produced in narrow color ranges :

$$\begin{aligned}
 u_{\text{CFHTLS}} - u_{\text{SDSS}} &= -0.189 \times (u - g)_{\text{SDSS}} - 0.099 & , 0.5 < u - g < 2 \\
 g_{\text{CFHTLS}} - g_{\text{SDSS}} &= -0.158 \times (g - r)_{\text{SDSS}} + 0.024 & , 0.0 < g - r < 0.4 \\
 r_{\text{CFHTLS}} - r_{\text{SDSS}} &= -0.071 \times (r - i)_{\text{SDSS}} + 0.000 & , 0 < r - i < 0.4 \\
 i_{\text{CFHTLS}} - i_{\text{SDSS}} &= -0.102 \times (r - i)_{\text{SDSS}} + 0.024 & , \text{ for the } i \text{ (i.9701) filter, } 0 < r - i < 0.4 \\
 y_{\text{CFHTLS}} - i_{\text{SDSS}} &= -0.020 \times (r - i)_{\text{SDSS}} + 0.032 & , \text{ for the } y \text{ (i.9702) filter, and} \\
 z_{\text{CFHTLS}} - z_{\text{SDSS}} &= +0.069 \times (i - z)_{\text{SDSS}} + 0.030 & .0.1 < i - z < 0.3
 \end{aligned}
 \tag{14}$$

It is important to realize the SDSS Supernova Survey on the SDSS Southern equatorial stripe 82 (SS82) is the result of a different effort from the general SDSS survey, the SDDS-DR8 catalogue as of 2012, to which the T0007 is being compared to in this section. The two SDSS surveys follow different calibration paths. From the joint effort between the SNLS and the SDSS Supernova Survey, that survey is known

for being precisely anchored in a true AB system. This is however not the case for the general SDSS survey which is known to suffer from systematic offsets to a true AB system<sup>23</sup>, while the internal relative photometry of the SDSS-DR8 across the sky is about 1% in gri and about 2% in u and z, the systematic offsets in respect to the true AB system are known to be larger:

In consequence, one should expect systematic residuals when comparing T0007 to SDSS-DR8 using the present transformation equations established on the the true SDSS AB system. To assess this fundamental differences between SDDS SS82 (to which the SNLS compares at better than the percent) and SDSS-DR8, we compared the offsets between the magnitude of the SNLS tertiary standards located on two Deep fields which overlap with SDSS-DR8 (D2 and D3 CFHTLS fields). We found the following offsets for the difference between the true MegaCam-AB magnitude of the SNLS tertiary standards (including their conversion from their published Vega magnitude to AB) and the SDSS-DR8 magnitudes of the SNLS tertiary standards converted to the MegaCam-AB system using Equation 14:

- -0.033 to -0.055 offset in  $u^*$
- less than 1% offset in  $g, r, i$
- +0.000 to +0.011 offset in  $z$

Based on the photometric consistency of the CFHTLS Wide with the Deep/SNLS, such systematic offsets should in consequence be found between the Wide and SDSS-DR8. A generous 115 amongst the 171 Wide fields have sources in common with SDSS on all four Wide patches. As in previous releases, the photometric calibration has been verified by comparing the CFHTLS and SDSS bright sources in regions where the SDSS-DR8 overlaps with the Wide fields.

The CFHTLS and SDSS-DR8 sources have been cross-identified using the public SDSS catalogue (Data Release 8; <http://www.sdss.org>) and the `MAG_AUTO` magnitudes of the CFHTLS merged source catalogue. The CFHTLS and SDSS photometry data have been compared using a well-defined common sample bright stars in unmasked regions of CFHTLS stacks. For W1, W2 and W3, only unsaturated stellar objects with  $17 < i < 21$  (i.e the limiting magnitude for a clear star/galaxy separation) located inside a cross-identification radius of  $2''$  have been used. For W4, which is more contaminated by very bright stars, we only used stellar sources with  $17 < i < 20$ .

The mean offset for the  $m$ -band inside a MegaCam field,  $\delta_m$ , is calculated using a weighted mean :

$$\delta_m = \frac{\sum_i w_i (m_{\text{CFHTLS}_i} - m_{\text{SDSS}_i})}{\sum_i w_i}, \quad \text{with } w_i = \frac{1}{\sigma_{\text{CFHTLS}_i}^2 + \sigma_{\text{SDSS}_i}^2}, \quad (15)$$

where  $i$  is the index for each common star,  $m_i$  denote the magnitudes, and  $\sigma_i$  the magnitude errors as listed in the CFHTLS and the SDSS catalogues. Note that the offsets calculated here are averaged over a full MegaCam field.

From this star sample, we define two different mean magnitude offset values, depending on the angular scale over which the offset is averaged:

- the 115 mean offsets,  $\delta_{m=u^*,g,r,i/y,z}$ , averaged over a MegaCam field. They are computed for all stacks with common stars between T0007 and SDSS-DR8. The offset values are listed in the appendix as well as in the synoptic table.

<sup>23</sup>[www.sdss3.org/dr9/algorithms/fluxcal1.php#SDSStoAB](http://www.sdss3.org/dr9/algorithms/fluxcal1.php#SDSStoAB)

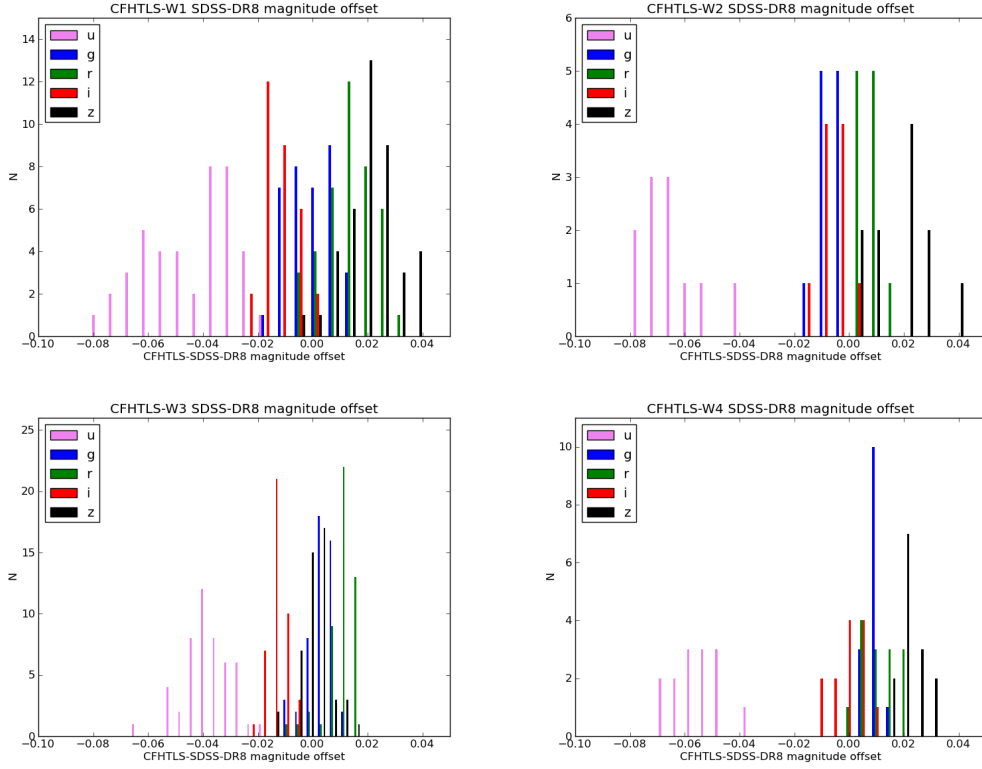


**Figure 36:** Distributions of photometric offsets,  $\delta_{m=u^*,g,r,i/y,z}$ , between CFHTLS Wide and SDSS-DR8 for W1, W2, W3 and W4.

- the W1, W2, W3 and W4 offsets, averaged over each Wide field,  $\langle \delta_{m=u^*,g,r,i/y,z} \rangle$ . They are summarized in Table 6 and in the histograms of Figure 36;

The external photometric errors are then derived by applying the 115 mean offset values for each tile and by computing the *rms* of the distribution. The results are presented in the next section following the discussion of magnitude offsets.

Fig. 36 separates W1, W2, W3 and W4. There is no significant difference between the four fields: the histograms show that the mean and *rms* offset values are consistent from field to field in all bands. The  $u^*$  and  $z$  bands exhibit however a stronger dispersion than the  $g$ ,  $r$ ,  $i$  bands. Table 11 presents this histogram data averaged per Wide patch: the expected offset between T0007 and SDSS-DR8 is found in the  $u^*$  band (-0.05 mag on average) and the  $z$  band (+0.02 mag) while the  $g$ ,  $r$ ,  $i$  bands exhibit an offset lower than 1%. Identifying these systematic offsets between SDSS-DR8 and the MegaCam AB system confirms the proper photometric bootstrapping of the Wide patches.

The higher offset found in the  $u^*$  and  $z$  bands (resp. 5% and 2% compared to less than 1% for  $g$ ,  $r$ ,  $i$ ) is also in line with the uncertainty estimates of the SNLS tertiary standards calibration. The respective contributions to these discrepancies from the SNLS and the SDSS is still unclear. We remind that the anchoring of the DR8 to AB is thought to be off by about  $u_{AB} = u_{SDSS} - 0.04$ . The precision of the  $z$  band calibration is limited by the precision of the color transformation of BD+17.4708 at the 2% level. The larger offset seen in the  $u^*$  band stems from the fairly significant difference between the filters used in those two cameras, coupled to the large spectral range of stars used as calibrators.

---

Wide field	External magnitude offsets with respect to SDSS-DR8				
	$\delta_{u^*}$ [mag.]	$\delta_g$ [mag.]	$\delta_r$ [mag.]	$\delta_i$ [mag.]	$\delta_z$ [mag.]
W1	-0.044/-0.038	0.000/0.000	0.013/0.012	-0.012/-0.014	0.020/0.020
W2	-0.064/-0.066	-0.008/-0.009	0.006/0.006	-0.007/-0.004	0.019/0.021
W3	-0.038/-0.037	0.003/0.004	0.010/0.010	-0.013/-0.013	0.001/0.001
W4	-0.055/-0.053	0.009/0.010	0.010/0.012	-0.001/0.000	0.022/0.021

---

**Table 11:** Mean magnitude offsets,  $\langle \Delta_{m=u^*,g,r,i/y,z} \rangle$ , between the CFHTLS and the SDSS-DR8 surveys, using the whole sample of common stars found in W1, W2, W3 and W4. The mean offsets for W1, W3 and W4 are also given in Table 6, The distribution over the 115 fields are shown on Fig. 36.

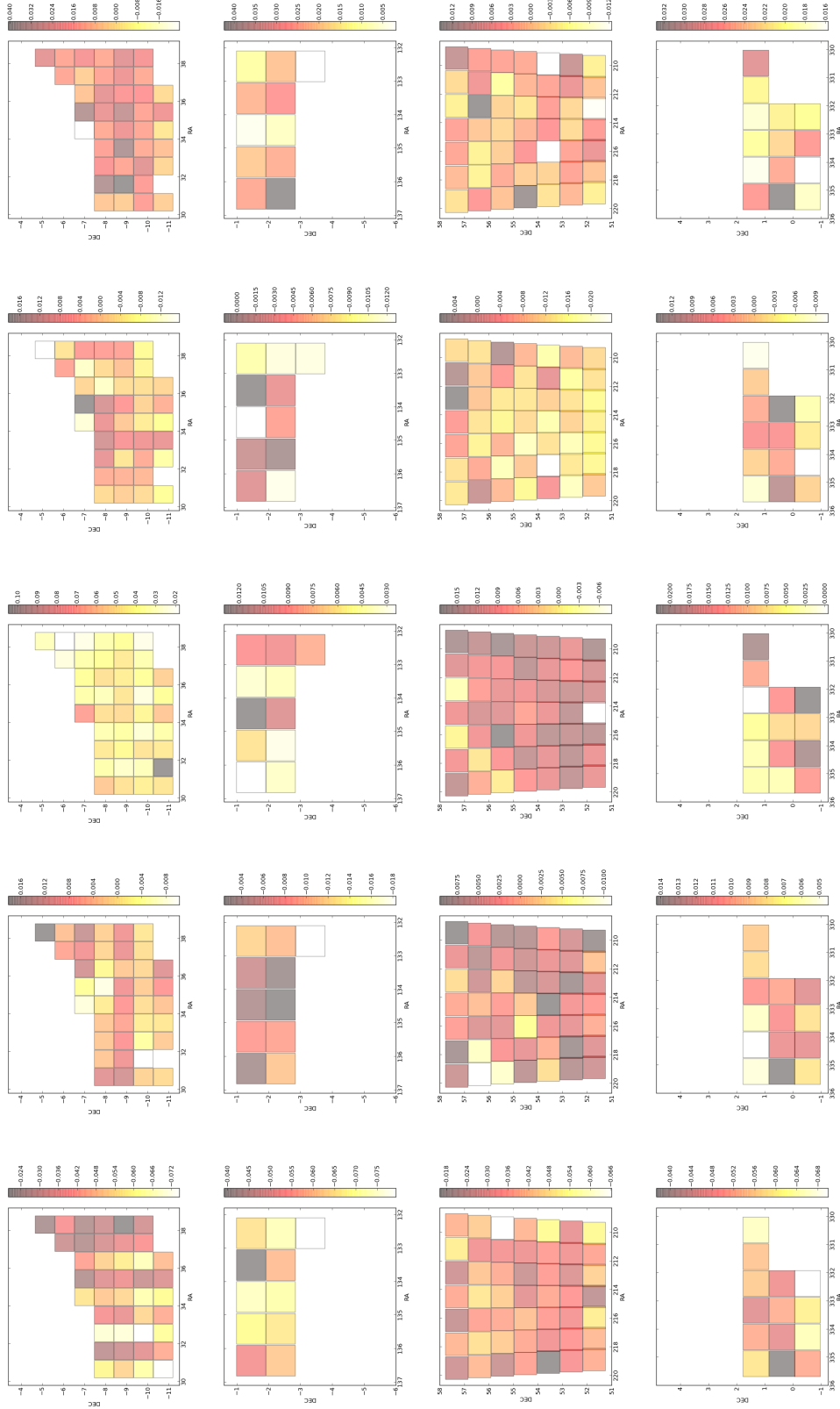


**Figure 37:** Maps of photometric offsets between CFHTLS Wide and SDSS-DR8, based on stars common to both surveys (115 Wide stacks). Each square represents a  $1^\circ \times 1^\circ$  tile (or a stack) of the CFHTLS Wide. The top panels show, from left to right, the  $u^*$ ,  $r$ ,  $i/y$  and  $z$  magnitude offsets for W1. The middle panels are the same for W2 and W3, and the bottom for W4.



Wide field	External <i>rms</i> errors with respect to SDSS-DR8				
	$\sigma_{u^*}$ <i>rms</i> [mag.]	$\sigma_g$ <i>rms</i> [mag.]	$\sigma_r$ <i>rms</i> [mag.]	$\sigma_i$ <i>rms</i> [mag.]	$\sigma_z$ <i>rms</i> [mag.]
W1	0.016	0.008	0.009	0.006	0.010
W2	0.011	0.005	0.004	0.005	0.012
W3	0.009	0.005	0.005	0.004	0.005
W4	0.009	0.003	0.007	0.006	0.005

**Table 12:** External *rms* errors of the CFHTLS T0007  $u^*$ ,  $g$ ,  $r$ ,  $i$  and  $z$ -band Wide surveys. They are derived from the variance of the magnitude offset distributions between the SDSS-DR8 and CFHTLS-T0007, in the W1, W2, W3 and W4 fields. The error estimates only use 115/171 Wide fields. In contrast with the internal errors, most common source loci are outside the noisy overlapping regions, and the selected stellar sources used for the comparison are brighter.

#### 4.4.4 External photometric errors

The external photometric errors are derived from the *rms* of the mean CFHTLS-SDSS magnitude offset values,  $\delta_{m=u^*,g,r,i/y,z}$ , in each Wide field separately. They are measured by adding the 115 offsets to CFHTLS-SDSS common sources of each relevant tile and then by computing the *rms* of the CFHTLS-SDSS residual over the tile.

The external errors are quoted for each Wide in Table 12. As expected the  $g$ ,  $r$  and  $i$ -bands are on the average better than the  $u^*$  and  $z$ . W1 seems slightly worse than W2, W3 and W4, probably due to contamination by several outliers reported in the previous section. The overall external field to field calibration is around 1.5% in  $u^*$  and  $z$ , and below 1.0% in  $g$ ,  $r$  and  $i/y$ .

#### 4.4.5 CFHTLS Wide photometric precision

To summarize, the systematic photometric precision in the CFHTLS Wide T0007 calibration (or field to field scatter) can be measured using :

- the dispersion of the tile magnitude offsets with SDSS (section 4.4.4 and table 12)
- the dispersion of the the magnitude offsets between adjacent fields measured in the overlapping regions (section 4.4.2 and table 9)

These two measurements are in good agreement and show field to field scatters of :

- 1.5% in  $u^*$  and  $z$  bands
- 1% in  $g$ ,  $r$  and  $i/y$  bands

#### 4.4.6 Stellar color-color plots

The nearly blackbody emission spectra of stars places them in a narrow line in optical and infrared color-color space. Under the assumption that stellar loci in the *ugriz* color space are intrinsically universal, one can identify this locus and use it to calibrate the colors (and magnitudes) of the CFHTLS sources. As in previous releases, a comparison between the CFHTLS point-source colors and stellar model tracks have been used in order to assess the stability of survey photometry from tile to tile and across the whole Wide area.

The stellar color-color loci are derived from a sample of well-defined bright stars selected from the T0007 merged catalogues. Only unsaturated objects with  $17 < i < 21$  and located in unmasked regions are considered (i.e. objects with FLAG=1. The MAG\_AUTO as well as as the MAG\_IQ20 magnitudes of the sources are plotted in the  $(u * -g)/(g - r)$ ,  $(g - r)/(r - i)$  and  $(r - i)/(i - z)$  color-color diagrams with the color tracks of the stellar models (Pickles, 1998).

We wish to remind the reader that the Pickles stellar library is not complete in the  $(T_{eff}, \log g)$  stellar parameter space, especially in the  $\log g$  range. In addition, the stellar library covers only stars with *solar metallicity*. As shown in Schultheis et al. (2006), the CFHTLS fields are a mixture of different stellar populations with different metallicities, i.e. the thin disc, the thick disc and the halo population. The effects of metallicity is largest in the  $(u - g)$  color and therefore systematic offsets compared to Pickles are to be expected. Sesar et al. (2011) studied the metallicities of the CFHTLS Wide fields and they found clearly a mean metallicity below solar ( $[Fe/H]=-1.5$ ). However, the metallicity variation over the Wide fields has yet to be determined.

To illustrate the effect of metallicity, Figure 38 shows the Basel 3.1 model track (Westera et al., 2002) with  $[Fe/H]=-1.0$  (i.e. low metallicity) in comparison to the Pickles models (bottom panels) with solar metallicity. While we see clearly an offset in  $(u - g)$  and  $(g - r)$  from the Pickles stars, this offset completely disappears using the Basel 3.1  $[Fe/H]=-1.0$  track. We therefore conclude that these offsets seen with respect to the Pickles stars do not represent a photometric calibration problem and can instead be explained from metallicity variations. Furthermore, realistic models of the galaxy indicate that the variations in metallicity expected in fields of sizes comparable to the CFHTLS Wide patches could correspond to displacements in color-color space of a few percent or larger,

#### 4.4.7 Color offsets between CFHTLS and SDSS

In the previous CFHTLS release (T0006), the stellar locus in the Wide tiles has been used to recalibrate the photometry and improve the final field to field scatter. The differences between the loci of CFHTLS and SDSS stars in color-color tracks can be used to determine the color offsets,  $\Delta_{m-m'}^{SLR}$ , between the two surveys. However, as we have seen in the previous sections, the expected percent-level photometric precision of the CFHTLS Wide survey now exceeds the metallicity-induced field-to-field variations in color which we would expect in a survey the size of the CFHTLS. Consequently, this raises doubts concerning the ability of the ‘‘Stellar Locus Regression’’ (SLR) fitting techniques to enable further reductions in the photometric scatter of the CFHTLS wide.

To test this, we checked the potential improvement on the color offsets compared to SDSS using the SLR recalibration. First, we computed the color offsets with respect to the SDSS reference catalog  $\delta_{m-m'}$ . We then computed the correcting color offsets from the SLR method as described in the T0006 documentation  $\Delta_{m-m'}^{SLR}$ . We finally compared the *rms* of the color offsets across the Wide patch compared to SDSS before and after the application of the SLR corrections. Before re-calibration, the scatter in  $(u - g)$ ,  $(g - r)$ ,  $(r - i)$  and  $(i - z)$  with respect to the transformed SDSS stellar locus is 0.011, 0.005, 0.008

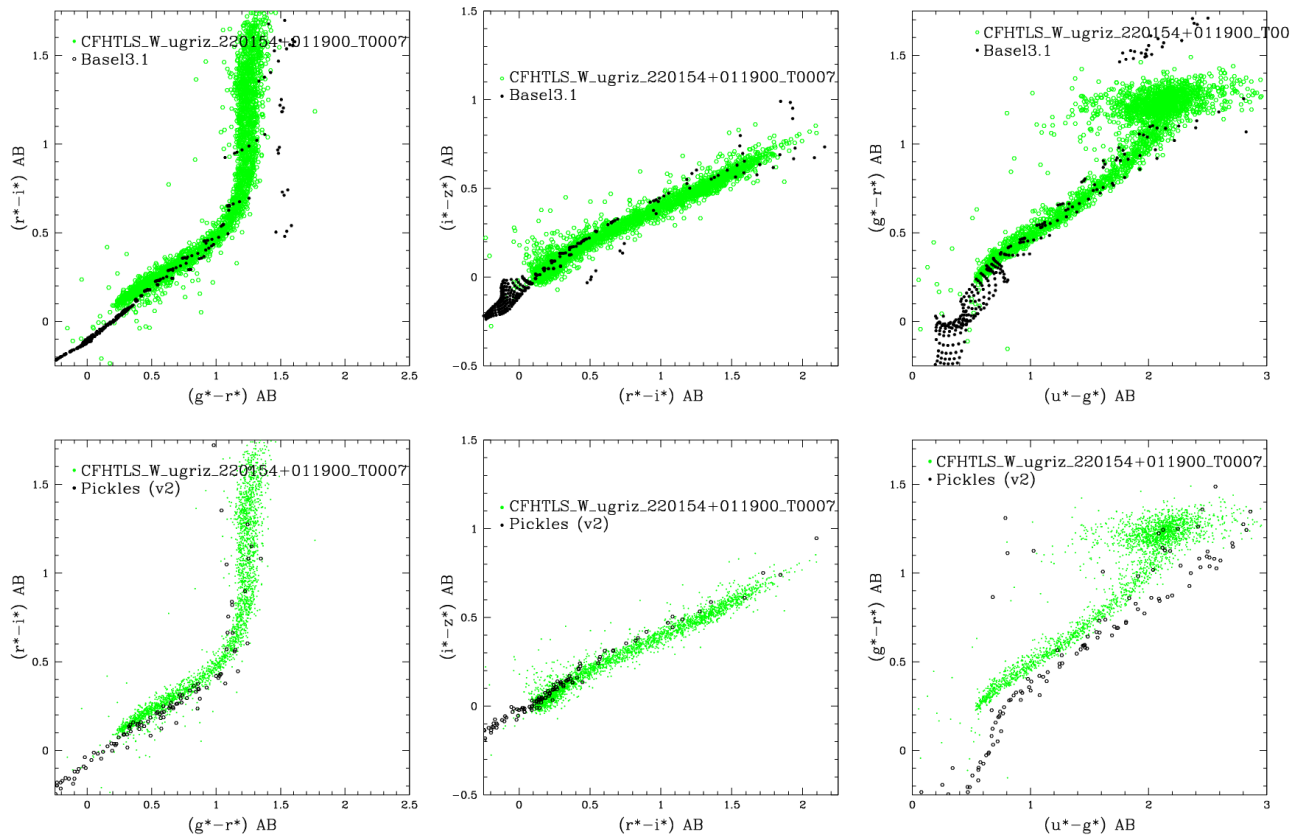


**Figure 38:** Comparison of one CFHTLS field with the Pickles stellar library (lower panel) and the Basel 3.1 stellar library using  $[Fe/H]=-1.0$  (upper panel).

and 0.008 respectively; after the application of the SLR regression, this becomes 0.014, 0.011, 0.010 and 0.008.

The use of SLR clearly makes no improvement to our W3 photometric calibration, and demonstrates in our case the SLR calibration is limited to a precision larger than 1%. Without a detailed knowledge of the stellar population variations across the Wide patches, it is difficult to see how this could be improved further.

Considering the lack of improvement in the recalibration of W3 using the SLR, we chose not to use this method in T0007.

#### 4.5 Astrometric accuracy

The astrometric accuracy is measured in two different ways.

- Firstly, at the end of the global astrometric calibration process, by comparing the astrometric positions of sources in all single CFHTLS images with sources in an internal and an external reference catalogue. This *astrometric calibration error* represents the upper limit for the astrometric accuracy of the survey.
- Secondly, by comparing position of sources inside each CFHTLS Wide stack with respect to an

Field	RA diff. ["]	DEC diff. ["]
W1	+0.014	+0.010
W2	-0.035	-0.025
W3	+0.011	+0.010
W4	-0.026	-0.023

**Table 13:** Mean RA and DEC differences between the external errors in each field and the mean external errors, averaged over the four Wide fields.

external reference catalogue. This *astrometric accuracy of CFHTLS stacks* measures the final absolute astrometric accuracy of each stack and their corresponding catalogues.

The astrometric calibration of the Wide survey is described in Section 3.5.

#### 4.5.1 Astrometric calibration errors

The mean internal astrometric calibration errors are derived using the cross-identifications of sources inside the overlapping regions of adjacent fields (see Fig. 21). All single input MegaCam Wide, Pre-Wide (see Fig. 21) and short photometric exposures images remaining after selection are included. The cross-identifications and the internal errors are obtained during the SCAMP calibration process. The calibrations outputs of the Wide fields W1, W2, W3 and W4 are available from the synoptic table.

Over the whole survey, the mean internal *rms* error is

$$\sigma_{\text{RA}} = 0.0279'' \pm 0.0049'', \text{ and } , \sigma_{\text{DEC}} = 0.0256 \pm 0.0057'', \quad (16)$$

where the reported errors are not the SCAMP internal errors, but the mean absolute difference of the internal errors between the four Wide fields and the mean error values. Since the four fields are calibrated independently, the errors quoted above are approximate; the internal errors for W1, W2, W3 and W4 are given in Table 6.

For each field, the mean *rms* external RA and DEC errors of the astrometric solution are derived during the SCAMP calibration process, using the cross-identification of sources inside each single CFHTLS Wide image with the 2MASS catalogue. The mean external calibration errors over the whole survey are  $\sigma_{\text{RA}} = 0.239''$  and  $\sigma_{\text{DEC}} = 0.232''$ . They roughly correspond to the internal errors of the 2MASS catalogue.

The mean scatter from one Wide field to another is uncertain, because the CFHTLS is made of only four independent fields. It can be estimated from the offsets of the mean external errors of each field separately with respect to the mean value over the four fields. The offsets are listed in Table 13. The amplitudes are very close to the internal astrometric calibration errors of the Wide fields, hence we conclude that the internal astrometric accuracy for the CFHTLS Wide does not have significant field-to-field scatter.

### 4.5.2 Absolute astrometric accuracy of the CFHTLS stacks

The astrometric accuracy inside each stack is measured by comparing the source positions in the final CFHTLS catalogues produced from all stacks with the 2MASS source catalogue. The results are given in the QualityFITS-out (QFITS-out) evaluation web pages. The mean external astrometric errors inside each stack are given by the *rms* of the the positions of each source inside a stack with respect to an external reference catalogue (2MASS). The results are listed in Table 14. They are in excellent agreement with the external errors from the internal astrometric calibration.

To control whether systematic offsets of source coordinates are present inside each Wide catalogue, we inspected and averaged over all stacks composing each Wide field the mean offsets  $\langle \Delta RA_{\text{CFHTLS-2MASS}} \rangle$  and  $\langle \Delta DEC_{\text{CFHTLS-2MASS}} \rangle$ , between the the CFHTLS and 2MASS positions inside a stack. The significance of the offsets is given by comparing the *rms* of the average of the mean offset value with the *rms* of the mean external errors, averaged over the number of field per Wide tile (72 for W1, 25 for W2, 49 for W3 and 25 for W4). The results are listed in Table 14 and detailed in Fig. 39, 40, 41, and 42, for the four Wide patches, globally and as a function of filter. All fields with the exception of W1 show small offsets. They are perceptible in both amplitude and direction and in all filters, but vary from a Wide tile to another. The amplitude is nevertheless small (about 1/10 of the CFHTLS pixel size) and never larger than the  $1\text{-}\sigma$  *rms* offset error, the  $1\text{-}\sigma$  *rms* error of the external error or the mean internal astrometric errors of the Wide astrometric calibration. Furthermore, we do not see significant chromatic effects.

Figures 39 to 42 also show only a few outliers stacks with large astrometric offsets with respect to the 2MASS source positions. The most extreme fields are listed in the next sections. However, the number of outliers with an amplitude of the deviation of more than  $3\text{-}\sigma$  deviations in at least one direction is close to Gaussian expectations (9/360 for W1, 1/245 for W3, 0/125 for W2 and W4).

Wide Field - Filter	Wide-averaged MegaCam-mean astrometric offset with respect to 2MASS	$\langle \Delta RA_{\text{CFHTLS-2MASS}} \rangle$ ["]	$\langle \Delta DEC_{\text{CFHTLS-2MASS}} \rangle$ ["]	$\sigma_{\text{RA}}$ ["]	$\sigma_{\text{DEC}}$ ["]	Wide-averaged MegaCam mean external $rms$ astrometric error
W1 - all bands	0.009 ± 0.028	0.004 ± 0.029	0.004 ± 0.029	0.253 ± 0.019	0.242 ± 0.021	
W1 <i>u</i> -band	0.006 ± 0.028	-0.004 ± 0.029	0.004 ± 0.029	0.237 ± 0.019	0.227 ± 0.023	
W1 <i>g</i> -band	0.013 ± 0.028	0.002 ± 0.029	0.002 ± 0.029	0.254 ± 0.016	0.244 ± 0.019	
W1 <i>r</i> -band	0.009 ± 0.028	0.008 ± 0.029	0.008 ± 0.029	0.259 ± 0.014	0.247 ± 0.016	
W1 <i>i</i> -band	0.011 ± 0.027	0.006 ± 0.028	0.006 ± 0.028	0.252 ± 0.014	0.243 ± 0.017	
W1 <i>y</i> -band	0.002 ± 0.028	0.015 ± 0.027	0.015 ± 0.027	0.272 ± 0.014	0.254 ± 0.020	
W1 <i>z</i> -band	0.008 ± 0.027	0.007 ± 0.028	0.007 ± 0.028	0.260 ± 0.017	0.248 ± 0.019	
W2 - all bands	-0.006 ± 0.018	0.015 ± 0.013	0.015 ± 0.013	0.204 ± 0.014	0.207 ± 0.013	
W2 <i>u</i> -band	-0.008 ± 0.017	0.014 ± 0.014	0.014 ± 0.014	0.183 ± 0.009	0.186 ± 0.011	
W2 <i>g</i> -band	-0.005 ± 0.018	0.015 ± 0.014	0.015 ± 0.014	0.208 ± 0.008	0.211 ± 0.007	
W2 <i>r</i> -band	-0.005 ± 0.019	0.015 ± 0.012	0.015 ± 0.012	0.211 ± 0.009	0.213 ± 0.008	
W2 <i>i</i> -band	-0.004 ± 0.019	0.016 ± 0.013	0.016 ± 0.013	0.207 ± 0.007	0.210 ± 0.006	
W2 <i>y</i> -band	-0.004 ± 0.020	0.020 ± 0.008	0.020 ± 0.008	0.224 ± 0.009	0.228 ± 0.010	
W2 <i>z</i> -band	-0.007 ± 0.019	0.013 ± 0.013	0.013 ± 0.013	0.211 ± 0.008	0.212 ± 0.008	
W3 - all bands	-0.002 ± 0.018	-0.013 ± 0.024	-0.013 ± 0.024	0.250 ± 0.017	0.242 ± 0.016	
W3 <i>u</i> -band	-0.003 ± 0.018	-0.005 ± 0.022	-0.005 ± 0.022	0.235 ± 0.014	0.225 ± 0.014	
W3 <i>g</i> -band	-0.002 ± 0.019	-0.011 ± 0.022	-0.011 ± 0.022	0.248 ± 0.015	0.242 ± 0.012	
W3 <i>r</i> -band	-0.002 ± 0.018	-0.016 ± 0.023	-0.016 ± 0.023	0.258 ± 0.013	0.249 ± 0.012	
W3 <i>i</i> -band	-0.002 ± 0.018	-0.016 ± 0.022	-0.016 ± 0.022	0.246 ± 0.014	0.242 ± 0.013	
W3 <i>y</i> -band	0.008 ± 0.018	-0.047 ± 0.020	-0.047 ± 0.020	0.275 ± 0.016	0.269 ± 0.012	
W3 <i>z</i> -band	-0.002 ± 0.018	-0.014 ± 0.023	-0.014 ± 0.023	0.258 ± 0.012	0.250 ± 0.012	
W4 - all bands	0.015 ± 0.019	0.010 ± 0.018	0.010 ± 0.018	0.213 ± 0.015	0.209 ± 0.017	
W4 <i>u</i> -band	0.014 ± 0.019	0.009 ± 0.017	0.009 ± 0.017	0.193 ± 0.012	0.186 ± 0.015	
W4 <i>g</i> -band	0.015 ± 0.020	0.010 ± 0.018	0.010 ± 0.018	0.218 ± 0.010	0.213 ± 0.012	
W4 <i>r</i> -band	0.017 ± 0.019	0.010 ± 0.018	0.010 ± 0.018	0.222 ± 0.011	0.217 ± 0.013	
W4 <i>i</i> -band	0.014 ± 0.020	0.010 ± 0.021	0.010 ± 0.021	0.217 ± 0.011	0.215 ± 0.014	
W4 <i>y</i> -band	0.020 ± 0.015	0.006 ± 0.014	0.006 ± 0.014	0.221 ± 0.009	0.217 ± 0.010	
W4 <i>z</i> -band	0.012 ± 0.018	0.011 ± 0.018	0.011 ± 0.018	0.214 ± 0.012	0.212 ± 0.013	

**Table 14:** Mean astrometric position accuracy of each Wide stack. The Wide-averaged statistics is the ensemble average over all stacks of the mean CFHTLS-SDSS astrometric offset values computed for each stack (MegaCam mean), separately

## 4.6 Outliers, stacks with exceptions or anomalies

Several images show unusual properties with respect to the bulk sample of stacks. This is the case for the 32 *y*-band stacks that are expected to have slightly different (photometric) properties compared to the other 139 *i*-band tiles due to the slightly different bandwidth of that replacement filter after the original one broke in 2007.

The most common technical anomaly is an amplifier failure during an observing sequence. Since all CCDs have two outputs, several images show missing data from a half or a full CCD area. Usually, each observing sequence is done only once, so the data from the missing CCD cannot be recovered. However, since the CCD failures are intermittent, the *r*-band observations which have been split into two observing sequences normally do not experience this missing data problem. We note furthermore that many of the pointings originally affected by this problem have been re-observed by in Director's Discretionary Time (images with more than one full CCD missing have been rejected during the image selection stack.)

Problematic T0007 stacks are listed in Tables 15 and 16, with a short description. None of these problems are critical for the scientific exploitation of the survey, but there are some half-CCD size regions of the CFHTLS Wide where one or two filters are missing.

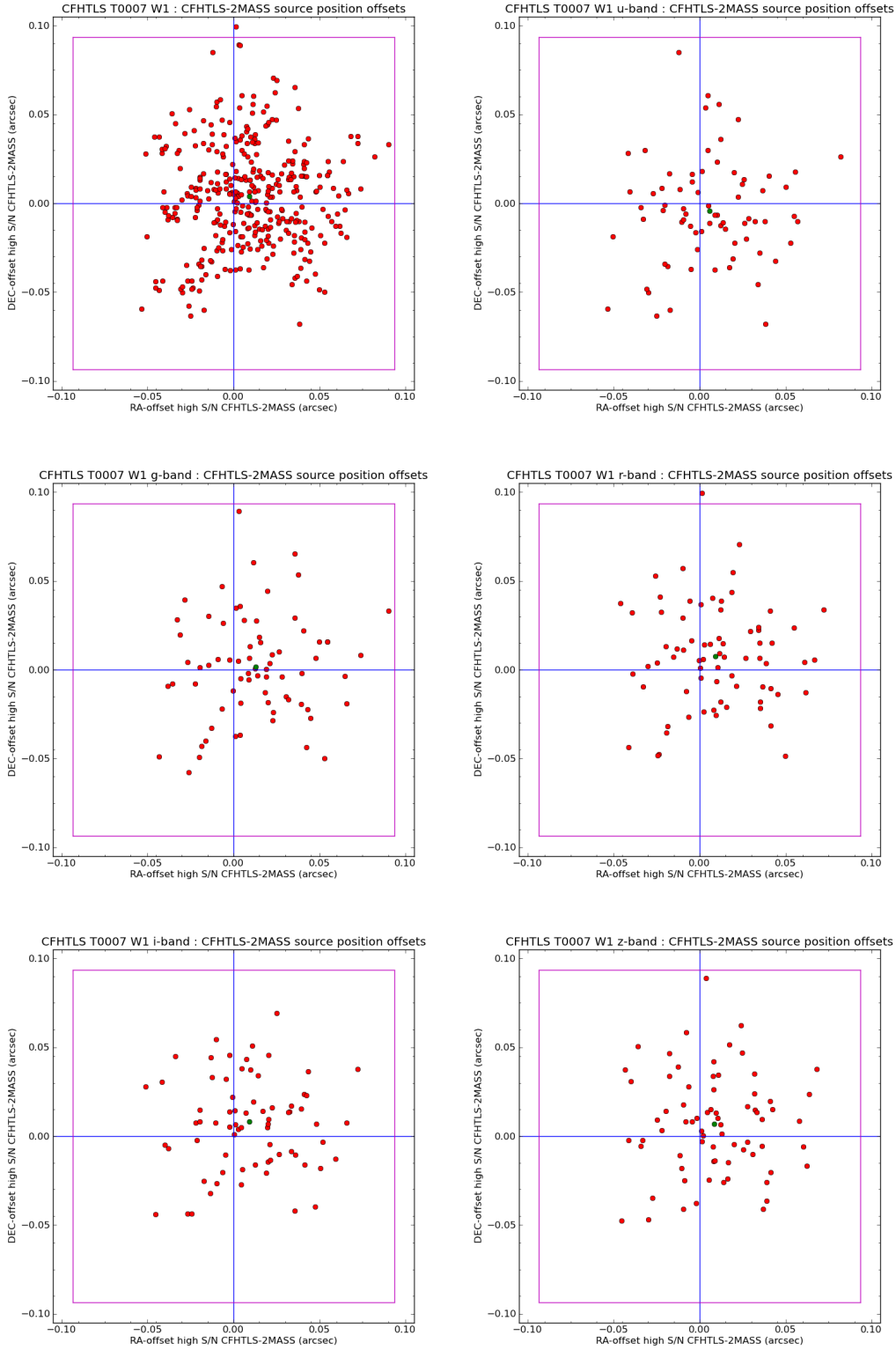


**Figure 39:** Mean RA-DEC offsets between the CFHTLS W1 and the 2MASS catalogues. The offset is derived from the ensemble average over all Wide W1 stacks of the mean offset inside each W1 stack. The top left plot shows the offset using all filters together (360 stacks). The other plots show the offsets in each filter (72 stacks per filter). The red dots show the mean offset in each stack. The green dot show the ensemble average of all stacks. The magenta square shows the MegaCam pixel size (0.186").



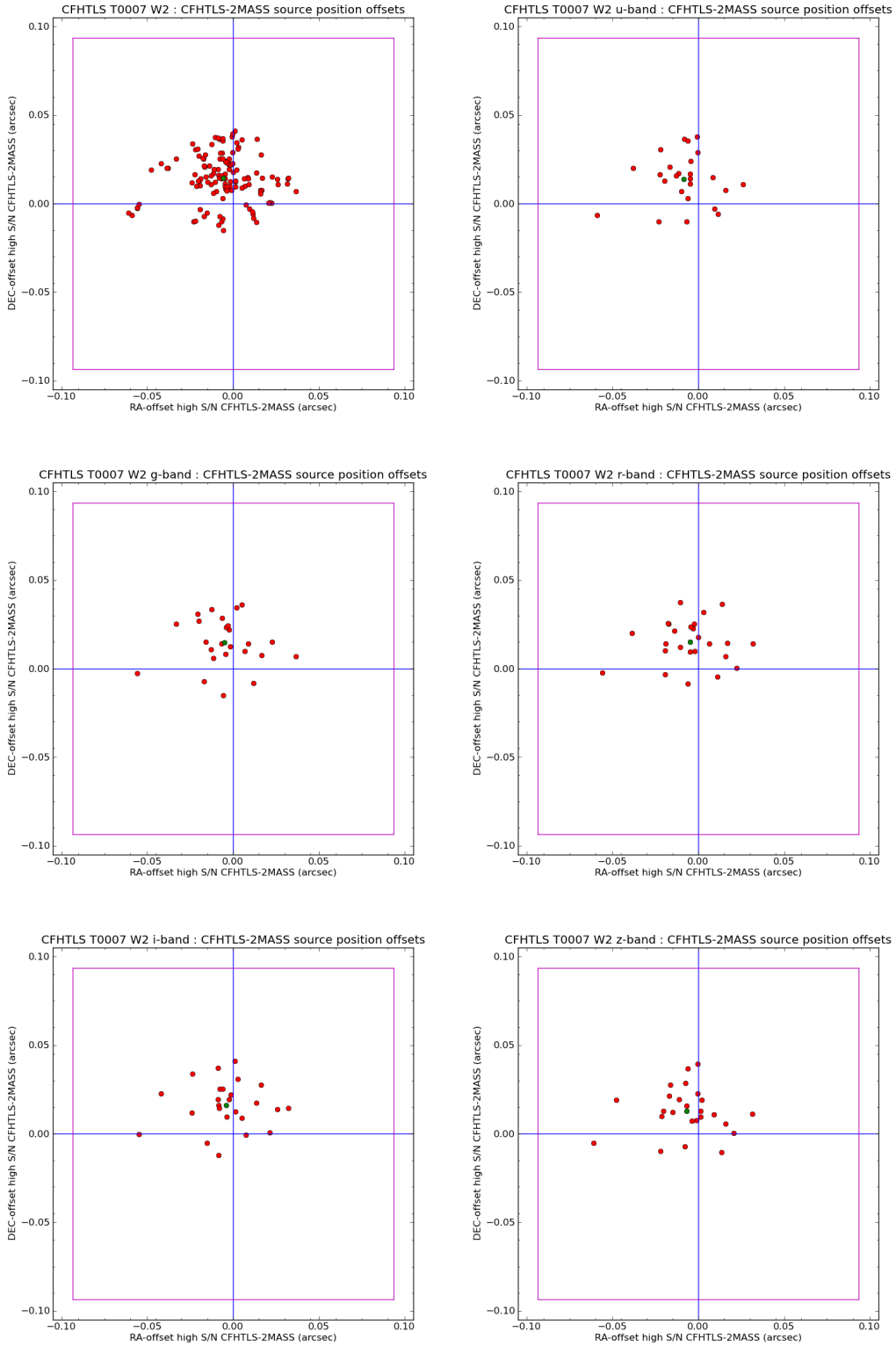


**Figure 40:** Mean RA-DEC offsets between the CFHTLS W2 and the 2MASS catalogues (see comments on the caption of Fig. 39).

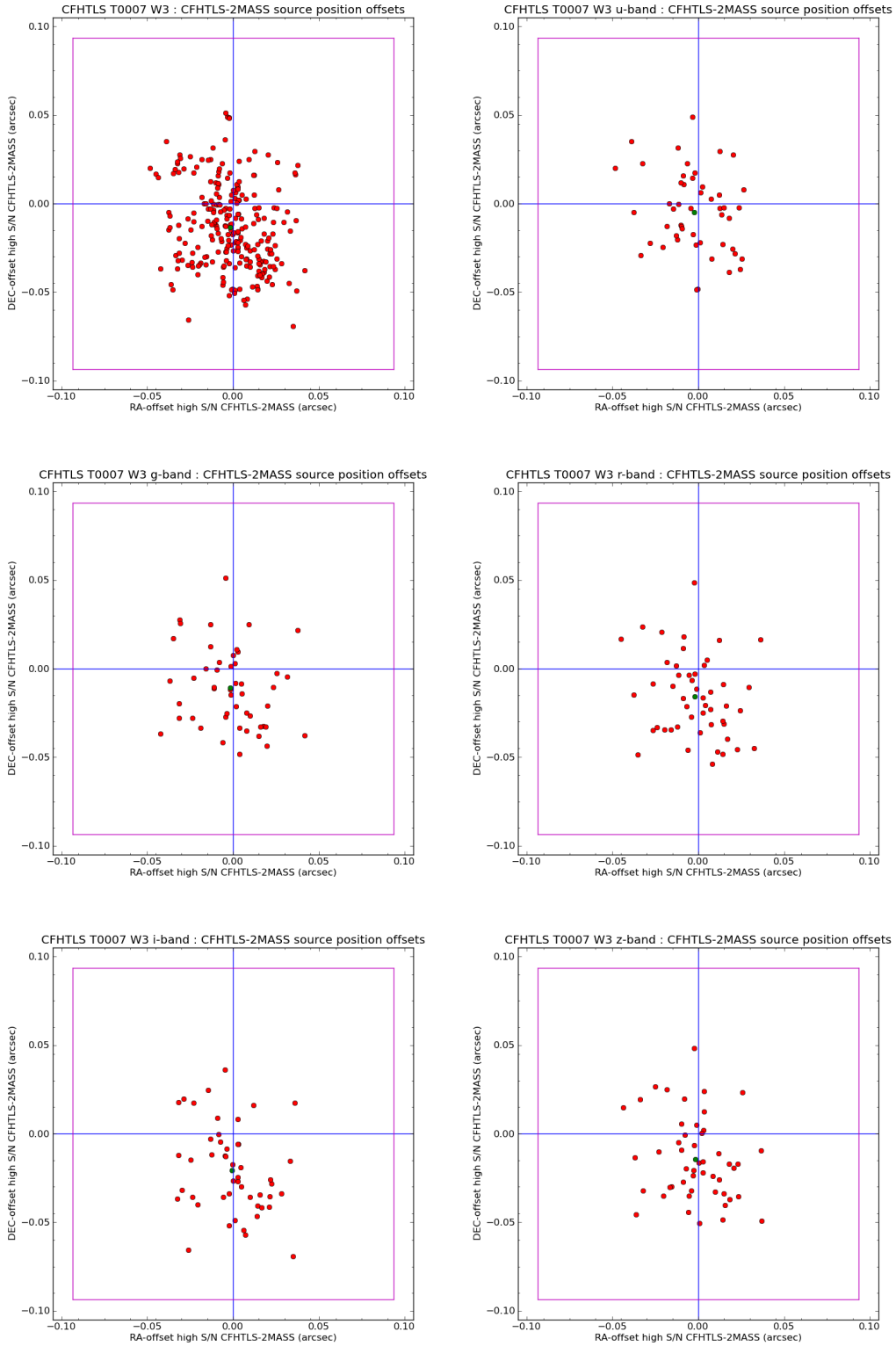


**Figure 41:** Mean RA-DEC offsets between the CFHTLS W3 and the 2MASS catalogues (see comments on the caption of Fig. 39).

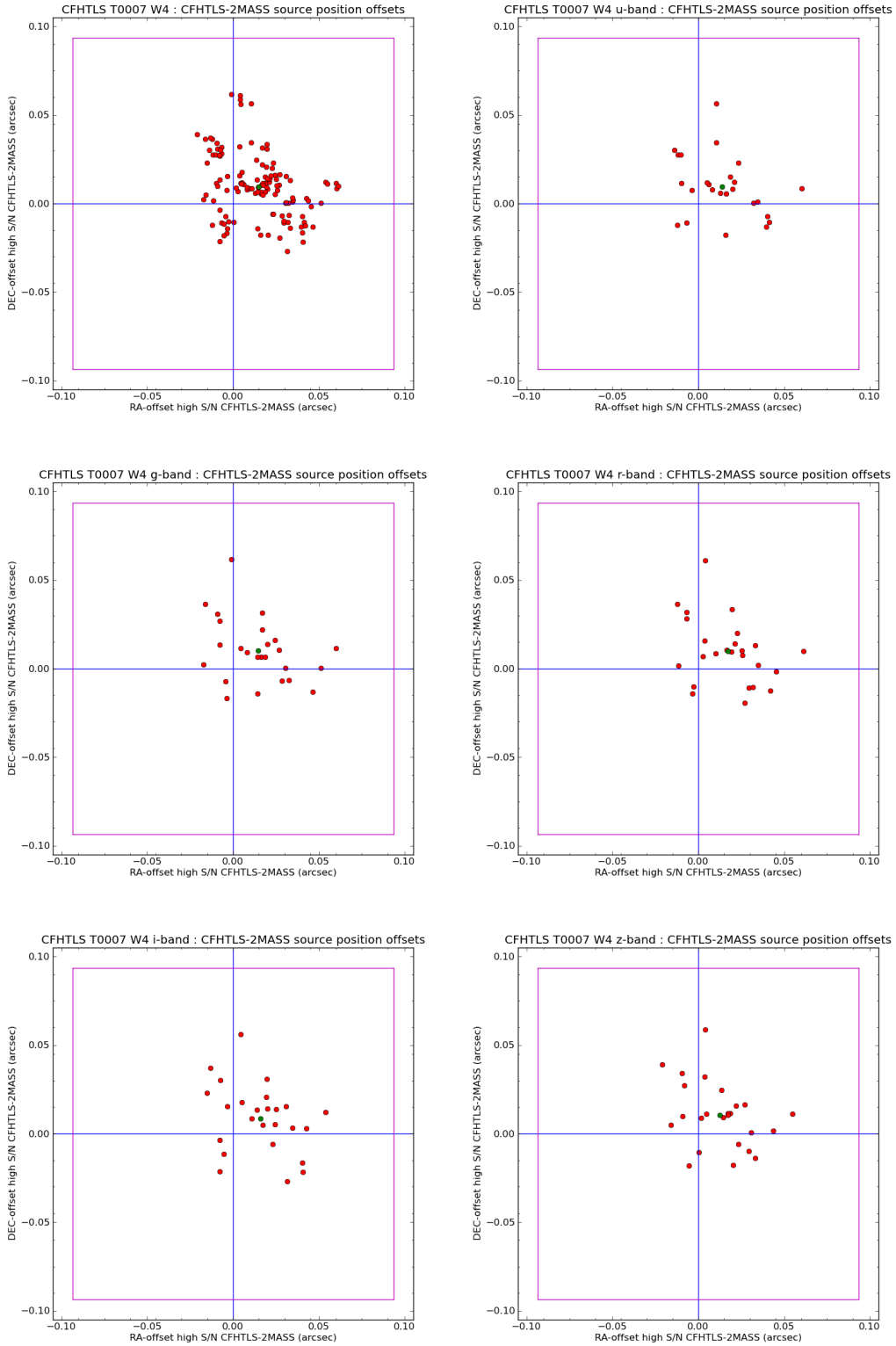


**Figure 42:** Mean RA-DEC offsets between the CFHTLS W4 and the 2MASS catalogues (see comments on the caption of Fig. 39).

W Cartesian Ident name	CFHTLS Ident name	Special filter	VIPERS-DDT images	Comments
W1(-4 - 4)	020241-104400	y-band observations	y-band exp. time is 7380 s.	
W1(-3 - 4)	020631-104400	y-band observations		
W1(-2 - 0)	021021-070000			radial astrometric offset around 0.090" in all bands
W1(-2 - 4)	021021-104400	y-band observations		
W1(+2 - 0)	022539-070000			g-band: CCD#03 missing
W1(+2 + 1)	022539-060400	y-band observations	y-band	
W1(+2 + 2)	022539-050800	y-band observations	$i^*$ -band	
W1(+2 + 3)	022539-041200			$i^*$ -band and z-band: CCD#03 missing ;
W1(-1 - 4)	021410-104400	y-band observations		
W1(-0 - 4)	021800-104400	y-band observations		
W1(+1 - 4)	022150-104400	y-band observations		
W1(+1 - 1)	022150-075600	y-band observations		
W1(+1 + 1)	022150-060400	y-band observations		
W1(+1 + 3)	022150-041200			i-band : two 1/2 CCD missing (CCD#07 and CCD#11) $i^*$ -band radial astrometric offset 0.084"
W1(+2 - 4)	022539-104400	y-band observations		
W1(+3 - 4)	022929-104400	y-band observations		
W1(+3 - 0)	022929-070000			g-band and t-band : CCD#03 missing ;
W1(+3 + 1)	022929-060400	y-band observations	g-band	
W1(+3 + 2)	022929-050800	y-band observations	g-band, y-band	
W1(+3 + 3)	022929-041200			g-band and t-band : CCD#03 missing
W1(+4 - 4)	023319-104400	y-band observations		
W1(+4 - 0)	023319-070000			g-band and t-band : CCD#03 missing ; $u, g$ and $i$ -band radial astrometric around 0.079"

**Table 15:** CFHTLS Wide stacks with exceptions or anomalies.

W Cartesian Ident name	CFHTLS Ident name	Special filter	VIPERS-DDT images	Comments
W1(+4 + 1)	023319-060400			
W1(+4 + 2)	023319-050800	y-band observations	g-band	
W1(+4 + 3)	023319-041200			<i>i</i> -band : CCD#03 missing
W2(-1 + 3)	085011-012700			g-band : CCD#03 missing
W2(+1 + 1)	085749-031900	y-band observations		
W2(+3 + 1)	090526-031900			g-band : CCD#03 missing
W2(+3 + 2)	090526-022300			g-band : CCD#03 missing
W2(+3 + 3)	090526-012700			g-band : CCD#03 missing
W2(+2 + 2)	090137-022300	y-band observations		
W3(-3 + 1)	135846+552631	y-band observations		
W3(-2 - 0)	140525+543031			$u^*$ , <i>g</i> , <i>r</i> , <i>i</i> , <i>z</i> contamination: Messier 101 galaxy on the 4 <sup>th</sup> (bottom right) MegaCam quadrant
W3(-2 - 1)	140540+533431	y-band observations		
W3(-2 + 1)	140509+552631	y-band observations		
W3(-2 + 3)	140433+571831	y-band observations		
W3(-1 + 3)	141113+571831	y-band observations		
W3(-0 - 1)	141754+533431			y-band radial astrometric offset 0.077"
W3(+3 - 1)	143615+533431	y-band observations		g-band seeing anomaly: 1.045"
W3(+3 + 2)	143728+562231	y-band observations		
W4(+1 - 1)	221706+002300			
W4(-1 - 1)	220930+002300	y-band observations		
W4(-1 + 1)	220930+021500	y-band observations		
W4(-1 + 2)	220930+031100	y-band observations		
W4(-1 + 3)	220930+040700	y-band observations		
W4(-2 + 2)	220542+031100	y-band observations		
W4(-2 + 3)	220542+040700	y-band observations		
W4(-3 + 3)	220154+040700	y-band observations		

**Table 16:** CFHTLS Wide stacks with exceptions or anomalies (cont'd).

Field name	Reference center		Comment
	RA (J2000)	DEC (J2000)	
D1	02:25:59.00	-04:29:40	
D2	10:00:28.00	+02:12:30	COSMOS $u^*$ data included
D3	14:19:27.00	+52:40:56	
D4	22:15:31.00	-17:43:56	

**Table 17:** Location of the CFHTLS Deep fields. All fields cover  $1 \text{ deg}^2$  and are taken in all six filters.

## 5 Description of the CFHTLS T0007 Deep survey

### 5.1 Overview

The CFHTLS Deep survey is composed of four independent MegaCam pointings in the D1, D2, D3 and D4 fields, whose sky location is shown in Figure 1, observed in all six MegaCam filters. It is composed of 96  $u^*$ ,  $g$ ,  $r$ ,  $i$ ,  $y$  and  $z$  stacks and 16 chi2 images (that is 112 images including the weight-maps). There are two types of stacks per Deep field: the “85%” best seeing images (hereafter the  $Dk-85$  sample,  $k = 1 - 4$ ) and the “25%” best seeing images ( $Dk-25$ ). The two  $Dk$  series of stacks have exactly the same center positions.

The image selection criteria applied to the 10632 CFHTLS images for the production of the CFHTLS Deep survey has already been described in Section 3.4. Note that in addition to the CFHTLS images taken between May 26, 2003 and February 02, 2009 on the  $D2-u^*$  field contains MegaCam images taken by the COSMOS consortium (Capak et al., 2007).

The T0007 CFHTLS Deep survey contains in total 8916 images. After proper selection, the remaining 8638 images were combined into stacks as follows: 634  $u^*$ , 1457  $g$ , 1932  $r$ , 1990  $i$ , 691  $y$  and 1934  $z$ .

All stacks have the same pixel scale and cover exactly  $1 \times 1 \text{ deg}^2$  ( $19354 \times 19354$  pixels of  $0.1860''$ ). For all fields with the exception of  $D2-u^*$  the stacks are only composed of images that are part of a CFHTLS Deep observing sequence and that are within a radius of 3 arc-minutes with respect to the CFHTLS Deep center fields. For the  $D2-u^*$ , we included all  $u^*$ -COSMOS images that passed the selection, without restriction on the radial distance.

The Deep stacks combine sets of images obtained during sequences of medium exposures (few hundreds of seconds). Each exposure is followed by a small shift of the telescope to fill the physical gaps between CCDs. The shifts are within a box of  $4'$  in DEC and 3 arcminutes in RA. The  $D2-u^*$  stacks COSMOS data are shifted by 30 arcminutes in both RA and DEC directions in order to pave the  $1.4 \times 1.4 \text{ deg}^2$  of the cosmos survey. These images are combined with CFHTLS  $D2-u^*$  observations and cut to provide the  $1 \times 1 \text{ deg}^2$  centered on the CFHTLS D2.

The center position of each stack is predefined. The coordinates of a stack center position are given in Table 17, and are exactly the same for all filters. D1, D2, D3 and D4 are therefore composed of a complete set of  $u^*$ ,  $g$ ,  $r$ ,  $i$ ,  $y$  and  $z$  images of  $1 \text{ deg}^2$  each.

Tables 18 and 19 summarize the properties of Deep median-combined stacks; the characteristics of the sigma-combined stacks are given in Tables 20 and 21. (Note that the exposure time  $u^*$ -band does not

accurately reflect the integration time per pixel because most COSMOS images are shifted by 30' and only fill one quadrant of the CFHTLS  $u^*$ -band stack. The D2- $u^*$  corresponds to the innermost regions of Fig. 46, delimited by the black contours. Table 23 describes each sub-field in more detail).

## 5.2 Astrometric accuracy

The astrometric accuracy is derived in the same way as for the Wide survey. We refer to the beginning of Section 4.5 for a description of the method. The Deep analysis is however simpler than the Wide because there is only one single position per field. The astrometric calibration of the Deep fields is detailed in Section 3.5, so we only focus on the accuracy in this section.

The results of the internal and external error analysis are given in Tables 18 and 19. The internal errors have been measured by SCAMP, from the astrometric solutions of each Deep field, for each filter separately. In contrast, the external errors quoted in Tables 18 and 19 are not the values derived from the astrometric solutions. They are computed separately as well, but after the production of the Deep images, in order to get the true astrometric errors of sources in each stack. The reference external catalogue is 2MASS, and the external errors found are very similar to the Wide survey.

On average, the mean internal astrometric *rms* errors in the Deep fields are

$$\sigma_{\text{RA}} = 0.056'' \pm 0.011'' , \text{ and } , \sigma_{\text{DEC}} = 0.056 \pm 0.011'' , \quad (17)$$

and the mean external errors

$$\sigma_{\text{RA}} = 0.283'' \pm 0.017'' , \text{ and } , \sigma_{\text{DEC}} = 0.232 \pm 0.014'' , \quad (18)$$

where, the dispersions are the *rms* errors. Since the four fields are calibrated independently, the values quoted above are only rough estimates; the errors for D1, D2, D3 and D4 are given in Tables 18 and 19. The rather large scatter in the internal errors is due to the different ways each Deep field has been calibrated (either using an internal catalogue based on the  $i$  band data, or using the external 2MASS catalogue, see Section 3.5). The external astrometric errors are similar to the Wide survey and correspond to the expectations, considering the astrometric errors in the 2MASS reference catalogue.

## 5.3 Photometric accuracy

### 5.3.1 Comparison with SDSS-DR8

The photometric calibration of the Deep survey fields is fully described in Section 3.7. We aim in this section at conducting an external comparison to the SDSS survey: wherever possible, magnitude offsets between common stars in the CFHTLS Deep and SDSS-DR8 have been measured. SDSS magnitudes are first converted to the MegaCam AB system using the MegaCam-SDSS color transformation equations presented in the section comparing the Wide to SDSS-DR8 (Section 4.4.3, Equation 13).

The offsets are quoted in Tables 18 and 19 and in the synoptic table. Only fields D2 and D3 have sources in common with SDSS-DR8. The offsets are found to be similar to the means  $\langle \Delta_{m=u^*,g,r,i/y,z} \rangle$  (Table 11) or  $\langle \delta_{m=u^*,g,r,i/y,z} \rangle$  (Table 6) found for the Wide fields.

In both the Deep and the Wide surveys, the CFHTLS to SDSS-DR8 comparisons are made using stars with  $17 < i < 21$ . The signal-to-noise ratio of all common stars on the Deep fields is much higher than for the Wide, hence it is reassuring to find very similar offsets in all filters for both the Deep and the

Field	Parameter	$u^*$	$g$	$r$	$i$	$y$	$z$
D1-25	Nb images	29	96	134	138	37	142
	Exp. time [s]	19142	23106	42429	66490	13961	51129
	Seeing ["]	0.72	0.66	0.62	0.62	0.52	0.56
	80% Compl. (stellar)	$26.24 \pm 0.10$	$26.31 \pm 0.10$	$25.92 \pm 0.10$	$25.43 \pm 0.10$	$25.39 \pm 0.10$	$25.11 \pm 0.10$
	80% Compl. (extended)	$25.43 \pm 0.10$	$25.48 \pm 0.10$	$24.94 \pm 0.10$	$24.57 \pm 0.10$	$24.32 \pm 0.10$	$23.98 \pm 0.10$
	Int. astrom. err.	(0.042",0.042")	(0.049",0.048")	(0.048",0.048")	(0.047",0.047")	(0.041",0.040")	(0.050",0.050")
	Ext. astrom. err.	(0.25",0.23")	(0.26",0.25")	(0.25",0.24")	(0.25",0.24")	(0.27",0.25")	(0.26",0.24")
Mag. int. err. [mag.]	0.03	0.02	0.02	0.02	0.02	0.03	
D2-25	Nb images	128	83	114	107	60	104
	Exp. time [s]	~25000	18680	34208	51808	24483	37446
	Seeing ["]	0.75	0.64	0.58	0.57	0.57	0.56
	80% Compl. (stellar)	$26.26 \pm 0.10$	$26.31 \pm 0.10$	$25.91 \pm 0.10$	$25.51 \pm 0.10$	$25.65 \pm 0.10$	$25.14 \pm 0.10$
	80% Compl. (extended)	$25.55 \pm 0.10$	$25.42 \pm 0.10$	$24.93 \pm 0.10$	$24.63 \pm 0.10$	$24.55 \pm 0.10$	$24.07 \pm 0.10$
	Int. astrom. err.	(0.070",0.068")	(0.068",0.065")	(0.065",0.063")	(0.062",0.060")	(0.054",0.052")	(0.024",0.024")
	Ext. astrom. err.	(0.21",0.21")	(0.23",0.22")	(0.22",0.22")	(0.22",0.22")	(0.23",0.22")	(0.21",0.22")
Mag. int. err. [mag.]	0.03	0.02	0.02	0.02	0.02	0.03	
CFHTLS-SDSS $\langle \delta_m \rangle$ [mag.]	-0.051	-0.005	+0.010	+0.003	-0.004	+0.009	
D3-25	Nb images	29	96	134	138	37	142
	Exp. time [s]	19806	20717	36623	64425	19209	45023
	Seeing ["]	0.75	0.67	0.63	0.61	0.61	0.54
	80% Compl. (stellar)	$26.12 \pm 0.10$	$26.29 \pm 0.10$	$25.76 \pm 0.10$	$25.48 \pm 0.10$	$25.42 \pm 0.10$	$25.07 \pm 0.10$
	80% Compl. (extended)	$25.30 \pm 0.10$	$25.44 \pm 0.10$	$24.90 \pm 0.10$	$24.58 \pm 0.10$	$24.46 \pm 0.10$	$23.94 \pm 0.10$
	Int. astrom. err.	(0.060",0.058")	(0.065",0.064")	(0.065",0.064")	(0.064",0.063")	(0.054",0.053")	(0.075",0.074")
	Ext. astrom. err.	(0.23",0.23")	(0.25",0.25")	(0.25",0.25")	(0.25",0.25")	(0.26",0.25")	(0.25",0.25")
Mag. int. err. [mag.]	0.03	0.02	0.02	0.02	0.02	0.04	
CFHTLS-SDSS $\langle \delta_m \rangle$ [mag.]	-0.042	-0.002	+0.014	+0.003	-0.001	-0.004	
D4-25	Nb images	31	96	118	123	29	120
	Exp. time [s]	20462	23345	39066	57088	11561	43207
	Seeing ["]	0.74	0.70	0.60	0.57	0.57	0.55
	80% Compl. (stellar)	$26.01 \pm 0.10$	$26.14 \pm 0.10$	$25.76 \pm 0.10$	$25.42 \pm 0.10$	$25.45 \pm 0.10$	$25.06 \pm 0.10$
	80% Compl. (extended)	$25.22 \pm 0.10$	$25.33 \pm 0.10$	$24.93 \pm 0.10$	$24.60 \pm 0.10$	$24.28 \pm 0.10$	$23.87 \pm 0.10$
	Int. astrom. err.	(0.053",0.054")	(0.063",0.062")	(0.061",0.060")	(0.060",0.060")	(0.046",0.054")	(0.067",0.066")
	Ext. astrom. err.	(0.22",0.21")	(0.23",0.23")	(0.23",0.22")	(0.22",0.22")	(0.24",0.23")	(0.23",0.22")
Mag. int. err. [mag.]	0.04	0.02	0.02	0.02	0.02	0.03	

**Table 18:** Summary of the “25%” best=seeing stack parameters. “80% Compl.” is the 80% completeness limit. The seeing is the median  $\text{FWHM}$ . Astrometric errors are given along the two  $(x,y)=(\text{NS,EW})$  axes. The internal astrometric errors are derived from SCAMP calibrations, and the external errors are QuLi tyFITS-out outputs, from the comparison of source positions on each stack with the 2MASS astrometric positions. The “Mag. int. err.” are the mean internal photometric errors from the mean of the three magnitude ranges of Table 22. The  $\langle \delta_m \rangle$  magnitude is the mean magnitude offset between CFHTLS-T0007 and the SDSS-DR8 survey, averaged over a Deep field.



Field	Parameter	$u^*$	$g$	$r$	$i$	$y$	$z$
D1-85	Nb images	113	382	528	551	148	553
	Exp. time [s]	74590	89334	171876	264804	61768	199116
	Seeing ["]	0.87	0.83	0.77	0.76	0.71	0.72
	80% Compl. (stellar)	$26.44 \pm 0.10$	$26.07 \pm 0.10$	$25.61 \pm 0.10$	$25.33 \pm 0.10$	$25.38 \pm 0.10$	$24.99 \pm 0.10$
	80% Compl. (extended)	$25.72 \pm 0.10$	$25.33 \pm 0.10$	$24.75 \pm 0.10$	$24.40 \pm 0.10$	$24.48 \pm 0.10$	$24.16 \pm 0.10$
	Int. astrom. err.	$(0.042", 0.042")$	$(0.049", 0.048")$	$(0.048", 0.048")$	$(0.047", 0.047")$	$(0.041", 0.040")$	$(0.050", 0.050")$
	Ext. astrom. err.	$(0.26", 0.23")$	$(0.26", 0.25")$	$(0.26", 0.24")$	$(0.25", 0.24")$	$(0.26", 0.25")$	$(0.25", 0.23")$
Mag. int. err. [mag.]	0.03	0.02	0.02	0.02	0.02	0.03	
D2-85	Nb images	282	332	449	422	235	410
	Exp. time [s]	~45000	74723	135875	199655	99176	147628
	Seeing ["]	0.84	0.80	0.75	0.72	0.69	0.68
	80% Compl. (stellar)	$26.42 \pm 0.10$	$26.08 \pm 0.10$	$25.66 \pm 0.10$	$25.30 \pm 0.10$	$25.51 \pm 0.10$	$25.01 \pm 0.10$
	80% Compl. (extended)	$25.77 \pm 0.10$	$25.33 \pm 0.10$	$24.74 \pm 0.10$	$24.49 \pm 0.10$	$24.54 \pm 0.10$	$24.15 \pm 0.10$
	Int. astrom. err.	$(0.070", 0.068")$	$(0.068", 0.065")$	$(0.065", 0.063")$	$(0.062", 0.060")$	$(0.054", 0.052")$	$(0.024", 0.024")$
	Ext. astrom. err.	$(0.21", 0.22")$	$(0.22", 0.22")$	$(0.22", 0.22")$	$(0.22", 0.22")$	$(0.23", 0.23")$	$(0.21", 0.22")$
Mag. int. err. [mag.]	0.03	0.02	0.02	0.02	0.02	0.03	
CFHTLS-SDSS $\langle \delta_m \rangle$ [mag.]	-0.056	-0.006	+0.011	+0.007	-0.008	-0.011	
D3-85	Nb images	118	361	483	527	192	500
	Exp. time [s]	77904	80977	146374	249016	82276	180097
	Seeing ["]	0.88	0.85	0.78	0.76	0.78	0.69
	80% Compl. (stellar)	$26.26 \pm 0.10$	$26.11 \pm 0.10$	$25.58 \pm 0.10$	$25.32 \pm 0.10$	$25.54 \pm 0.10$	$25.03 \pm 0.10$
	80% Compl. (extended)	$25.63 \pm 0.10$	$25.29 \pm 0.10$	$24.69 \pm 0.10$	$24.39 \pm 0.10$	$24.46 \pm 0.10$	$24.13 \pm 0.10$
	Int. astrom. err.	$(0.060", 0.058")$	$(0.065", 0.064")$	$(0.065", 0.064")$	$(0.064", 0.063")$	$(0.054", 0.053")$	$(0.075", 0.074")$
	Ext. astrom. err.	$(0.24", 0.24")$	$(0.25", 0.25")$	$(0.25", 0.25")$	$(0.24", 0.25")$	$(0.26", 0.26")$	$(0.25", 0.25")$
Mag. int. err. [mag.]	0.03	0.02	0.02	0.02	0.02	0.04	
CFHTLS-SDSS $\langle \delta_m \rangle$ [mag.]	-0.042	-0.004	+0.016	+0.001	-0.003	-0.004	
D4-85	Nb images	121	382	472	490	116	471
	Exp. time [s]	77269	89541	155609	235153	45767	169588
	Seeing ["]	0.89	0.82	0.73	0.69	0.69	0.66
	80% Compl. (stellar)	$26.14 \pm 0.10$	$25.99 \pm 0.10$	$25.61 \pm 0.10$	$25.35 \pm 0.10$	$25.40 \pm 0.10$	$25.09 \pm 0.10$
	80% Compl. (extended)	$25.53 \pm 0.10$	$25.34 \pm 0.10$	$24.85 \pm 0.10$	$24.49 \pm 0.10$	$24.45 \pm 0.10$	$24.17 \pm 0.10$
	Int. astrom. err.	$(0.053", 0.054")$	$(0.063", 0.062")$	$(0.061", 0.060")$	$(0.060", 0.060")$	$(0.046", 0.054")$	$(0.067", 0.066")$
	Ext. astrom. err.	$(0.22", 0.22")$	$(0.23", 0.23")$	$(0.23", 0.22")$	$(0.22", 0.22")$	$(0.24", 0.23")$	$(0.22", 0.22")$
Mag. int. err. [mag.]	0.04	0.02	0.02	0.02	0.02	0.03	

**Table 19:** Summary of the “85%” Deep stack parameters. “80% Compl.” is the 80% completeness limit. The seeing is the median FWHM. Astrometric errors are given along the two (X,Y)=(NS,EW) axes. The internal photometric errors are from the SCAMP calibrations, and the external errors are QualityFITS-out outputs, from the comparison of source positions on each stack with the 2MASS astrometric positions. The “Mag. int. err.” are the mean internal photometric errors from the mean of the three magnitude ranges of Table 22. The  $\langle \delta_m \rangle$  magnitude is the mean magnitude offset between CFHTLS-T0007 and the SDSS-DR8 survey, averaged over a Deep field.

Field	Parameter	$u^*$	$g$	$r$	$i$	$y$	$z$
D1-25	Seeing ["]	0.71	0.67	0.63	0.61	0.54	0.56
	80% Compl. (stellar)	$26.43 \pm 0.10$	$26.36 \pm 0.10$	$25.86 \pm 0.10$	$25.55 \pm 0.10$	$25.43 \pm 0.10$	$25.23 \pm 0.10$
	80% Compl. (extended)	$25.61 \pm 0.10$	$25.54 \pm 0.10$	$24.95 \pm 0.10$	$24.63 \pm 0.10$	$24.41 \pm 0.10$	$24.14 \pm 0.10$
	Mag. int. err. [mag.]	0.03	0.02	0.02	0.02	0.02	0.03
D2-25	Seeing ["]	0.76	0.64	0.60	0.58	0.58	0.55
	80% Compl. (stellar)	$26.43 \pm 0.10$	$26.34 \pm 0.10$	$25.94 \pm 0.10$	$25.59 \pm 0.10$	$25.44 \pm 0.10$	$25.22 \pm 0.10$
	80% Compl. (extended)	$25.74 \pm 0.10$	$25.51 \pm 0.10$	$24.99 \pm 0.10$	$24.60 \pm 0.10$	$24.58 \pm 0.10$	$24.21 \pm 0.10$
	Mag. int. err. [mag.]	0.03	0.02	0.02	0.02	0.02	0.03
	CFHTLS-SDSS $\langle \delta_m \rangle$ [mag.]	-0.057	-0.005	+0.011	+0.004	-0.009	+0.010
D3-25	Seeing ["]	0.76	0.68	0.65	0.62	0.62	0.53
	80% Compl. (stellar)	$26.24 \pm 0.10$	$26.34 \pm 0.10$	$25.84 \pm 0.10$	$25.49 \pm 0.10$	$25.46 \pm 0.10$	$25.14 \pm 0.10$
	80% Compl. (extended)	$25.49 \pm 0.10$	$25.47 \pm 0.10$	$24.97 \pm 0.10$	$24.64 \pm 0.10$	$24.56 \pm 0.10$	$24.11 \pm 0.10$
	Mag. int. err. [mag.]	0.03	0.02	0.02	0.02	0.02	0.04
	CFHTLS-SDSS $\langle \delta_m \rangle$ [mag.]	-0.041	+0.004	+0.015	+0.007	-0.012	-0.001
D4-25	Seeing ["]	0.72	0.68	0.60	0.56	0.56	0.54
	80% Compl. (stellar)	$26.28 \pm 0.10$	$26.27 \pm 0.10$	$25.86 \pm 0.10$	$25.51 \pm 0.10$	$25.50 \pm 0.10$	$25.20 \pm 0.10$
	80% Compl. (extended)	$25.49 \pm 0.10$	$25.43 \pm 0.10$	$25.00 \pm 0.10$	$24.69 \pm 0.10$	$24.43 \pm 0.10$	$24.03 \pm 0.10$
	Mag. int. err. [mag.]	0.04	0.02	0.02	0.02	0.02	0.03

**Table 20:** Characteristics of the "25%" best-seeing sigma-combined stacks. "80% Compl." is the 80% completeness limit. The seeing is the median  $\text{FWHM}$ . Astrometric errors are given along the two  $(x, y) = (\text{ns}, \text{EW})$  axes. The "Mag. int. err." are the mean internal photometric errors from the mean of the three magnitude ranges of Table 22. The  $\langle \delta_m \rangle$  magnitude is the mean magnitude offset between CFHTLS-T0007 and the SDSS-DR8 survey, averaged over a Deep field.

Field	Parameter	$u^*$	$g$	$r$	$i$	$y$	$z$
D1-85	Seeing ["]	0.84	0.81	0.77	0.74	0.71	0.72
	80% Compl. (stellar)	$26.51 \pm 0.10$	$25.98 \pm 0.10$	$25.62 \pm 0.10$	$25.32 \pm 0.10$	$25.47 \pm 0.10$	$24.98 \pm 0.10$
	80% Compl. (extended)	$25.87 \pm 0.10$	$25.32 \pm 0.10$	$24.71 \pm 0.10$	$24.37 \pm 0.10$	$24.54 \pm 0.10$	$24.22 \pm 0.10$
	Mag. int. err. [mag.]	0.03	0.02	0.02	0.02	0.02	0.03
D2-85	Seeing ["]	0.82	0.78	0.74	0.72	0.70	0.66
	80% Compl. (stellar)	$26.56 \pm 0.10$	$26.05 \pm 0.10$	$25.56 \pm 0.10$	$25.22 \pm 0.10$	$25.48 \pm 0.10$	$25.15 \pm 0.10$
	80% Compl. (extended)	$25.95 \pm 0.10$	$25.32 \pm 0.10$	$24.72 \pm 0.10$	$24.46 \pm 0.10$	$24.55 \pm 0.10$	$24.28 \pm 0.10$
	Mag. int. err. [mag.]	0.03	0.02	0.02	0.02	0.02	0.03
	cFFTLs-sdss $\langle \delta_m \rangle$ [mag.]	-0.057	-0.004	+0.011	+0.002	-0.011	+0.010
D3-85	Seeing ["]	0.87	0.84	0.78	0.75	0.77	0.69
	80% Compl. (stellar)	$26.51 \pm 0.10$	$26.06 \pm 0.10$	$25.54 \pm 0.10$	$25.20 \pm 0.10$	$25.51 \pm 0.10$	$25.14 \pm 0.10$
	80% Compl. (extended)	$25.86 \pm 0.10$	$25.26 \pm 0.10$	$24.66 \pm 0.10$	$24.35 \pm 0.10$	$24.46 \pm 0.10$	$24.20 \pm 0.10$
	Mag. int. err. [mag.]	0.03	0.02	0.02	0.02	0.02	0.04
	cFFTLs-sdss $\langle \delta_m \rangle$ [mag.]	-0.040	+0.005	+0.016	+0.000	-0.012	-0.004
D4-85	Seeing ["]	0.86	0.81	0.72	0.69	0.66	0.65
	80% Compl. (stellar)	$26.44 \pm 0.10$	$25.95 \pm 0.10$	$25.53 \pm 0.10$	$25.31 \pm 0.10$	$25.53 \pm 0.10$	$25.16 \pm 0.10$
	80% Compl. (extended)	$25.79 \pm 0.10$	$25.32 \pm 0.10$	$24.82 \pm 0.10$	$24.48 \pm 0.10$	$24.47 \pm 0.10$	$24.26 \pm 0.10$
	Mag. int. err. [mag.]	0.04	0.02	0.02	0.02	0.02	0.03

**Table 21:** Characteristics of the “85%” best-seeing sigma-combined stack parameters.

Wide surveys. As explained in the Section 4.4.3 on the comparison between the Wide and SDSS-DR8, the CFHTLS is anchored to the SDSS Supernova Survey which is established in a true AB magnitude system, while SDSS-DR8 is known to exhibit some offsets to the AB system, especially in the  $u^*$  and the  $z$  bands (Equation 14), offsets that we identify indirectly here. Please refer to Section 4.4.3 for a complete discussion on the topic.

---

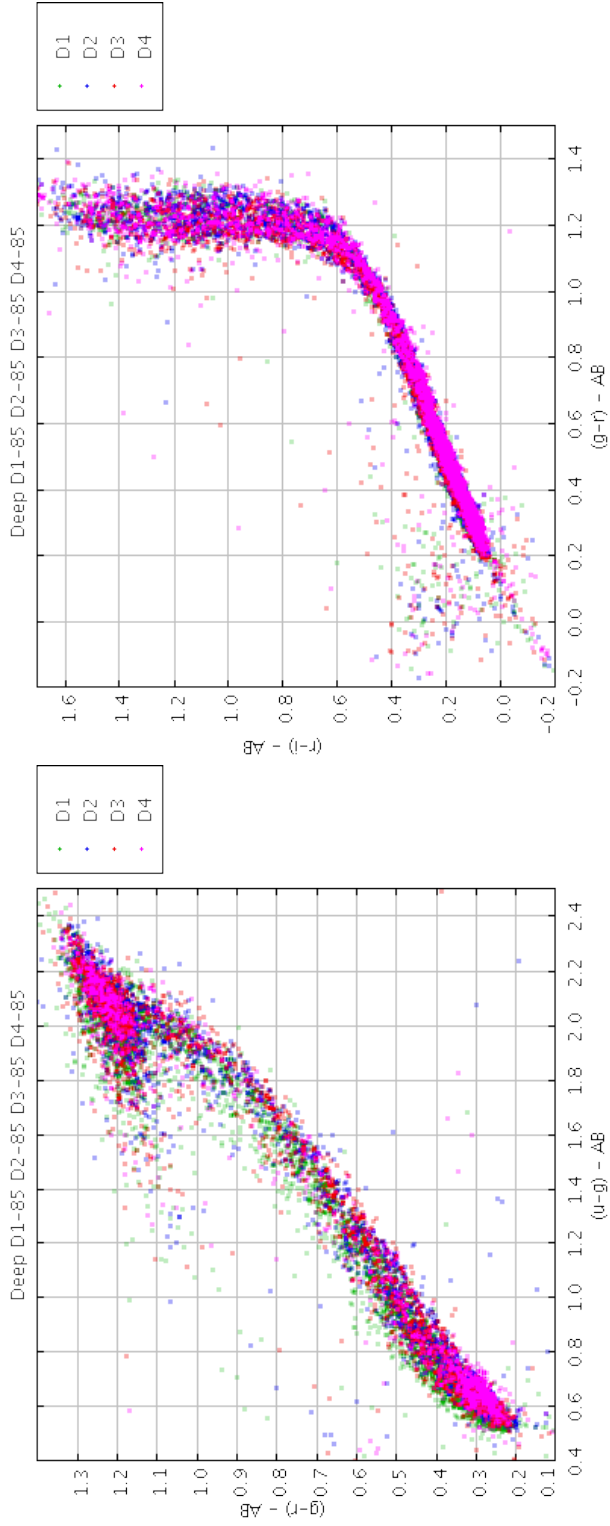


**Figure 43:** Comparison of the  $(u^* - g)/(g - r)$  (left) and  $(g - r)/(r - i)$  (right) stellar color-color tracks of the four Deep Dk-85 fields. The tracks are shown in different colors to make shifts between fields easier to see. Green, blue red and magenta points are D1-85, D2-85, D3-85 and D4-85. The agreement is excellent. All points overlap and the distinction between the color-color tracks is difficult. The left panel show D4-D3-D2-D1 over-plotted, in that order, so D4 (magenta) is background, and D1 (green) is foreground. The right panel presents the opposite.

The stellar color-color tracks of the four fields are remarkably similar. No color offsets can be measured between D1, D2, D3 and D4. This is illustrated on Fig. 43. It shows a superimposition of the  $(u^* - g)/(g - r)$  and  $(g - r)/(r - i)$  color-color plots for the four D-85 stacks together.

### 5.3.2 Internal photometric errors

The internal errors have been measured by comparing the photometry of common sources in the D-25 and D-85 stacks. The D-25 and D-85 parent samples comprise all source pairs listed in the merged catalogues of the four Deep fields. The selected sources must have magnitudes measured in all filters (no objects with magnitude/mag\_err = 99.0 in any  $u^*$ ,  $g$ ,  $r$ ,  $i$ ,  $y$  and  $z$  filters, for both the D-25 and D-85 catalogues), with a SExtractor extraction flag FLAGS=0 (objects with good photometry) and a Terapix object flag=1 or 0 (i.e. stellar or extended sources, only non-saturated objects in non-masked regions). Only sources fainter than  $u^*, g=20.5$  and  $r, i, y, z=19.5$ , and brighter than the D-25 80% completeness limit of extended sources are selected. This cut ensures the homogeneity and completeness of the D-25 and D-85 populations.

The internal photometric errors are derived from the distributions of magnitude differences of source pairs between the D-25 and D-85 catalogues, D25–D85, as a function of D-25 magnitudes. The analysis are carried out in three magnitude ranges, for all filters, and after a  $3\text{-}\sigma$  clipping over the distributions of magnitude differences. The statistics use the MAG\_AUTO magnitudes to derive first the median and mean systematic magnitude offsets between D-25 and D-85, then the mean scatter, based on the *rms*. We verified that the median systematic offset is randomly distributed around zero and never exceeds 0.013 mag., for all sub-samples.

The distributions are then fitted by a Gaussian, which gives the FWHM of the mean magnitude difference of cross-identified sources in D-25 and D-85. The mean internal photometric error is then defined as  $\sigma_{\text{D25-D85}} = \text{FWHM}/2.35$ . We checked that the error estimate based on the Gaussian fitting is very close to the *rms* errors. The results are summarized in Table 22. Overall, they look very similar to the Wide survey, when sources with same signal-to-noise ratio are compared.

We use the results quoted in Table 22 to compute the photometric errors listed in the summary Tables 18 and 19. The internal photometric errors are the mean values of the three magnitude ranges. This is a reasonable but probably optimistic estimate because it does not take into account there are many more faint than bright objects. Note that these results are valid for both stellar and extended sources.

In contrast with the Wide survey, we do not have many sources in common between CFHTLS and SDSS in D2 and D3 to estimate accurately external errors. In addition, we do not have any common sources at all for D1 and D4. However taking into account the statistics for the internal errors and the remarkable consistency of the results with the Wide survey, conclusions for the Wide survey apply equally: we consider the following errors are reasonably accurate and conservative estimates of the *rms* photometric errors over a rather broad magnitude range of the CFHTLS Deep survey down to the 80% completeness limit (details in Table 22):

- 5% in  $u^*$ ; 3% in  $g, r$  and  $i/y$ , 4% in  $z$  .

For faint sources beyond the 80% completeness limit, photometric errors rise by a factor of  $\sim 2$  in all bands with respect to the magnitude range quoted above and in Tables 18 and 19.

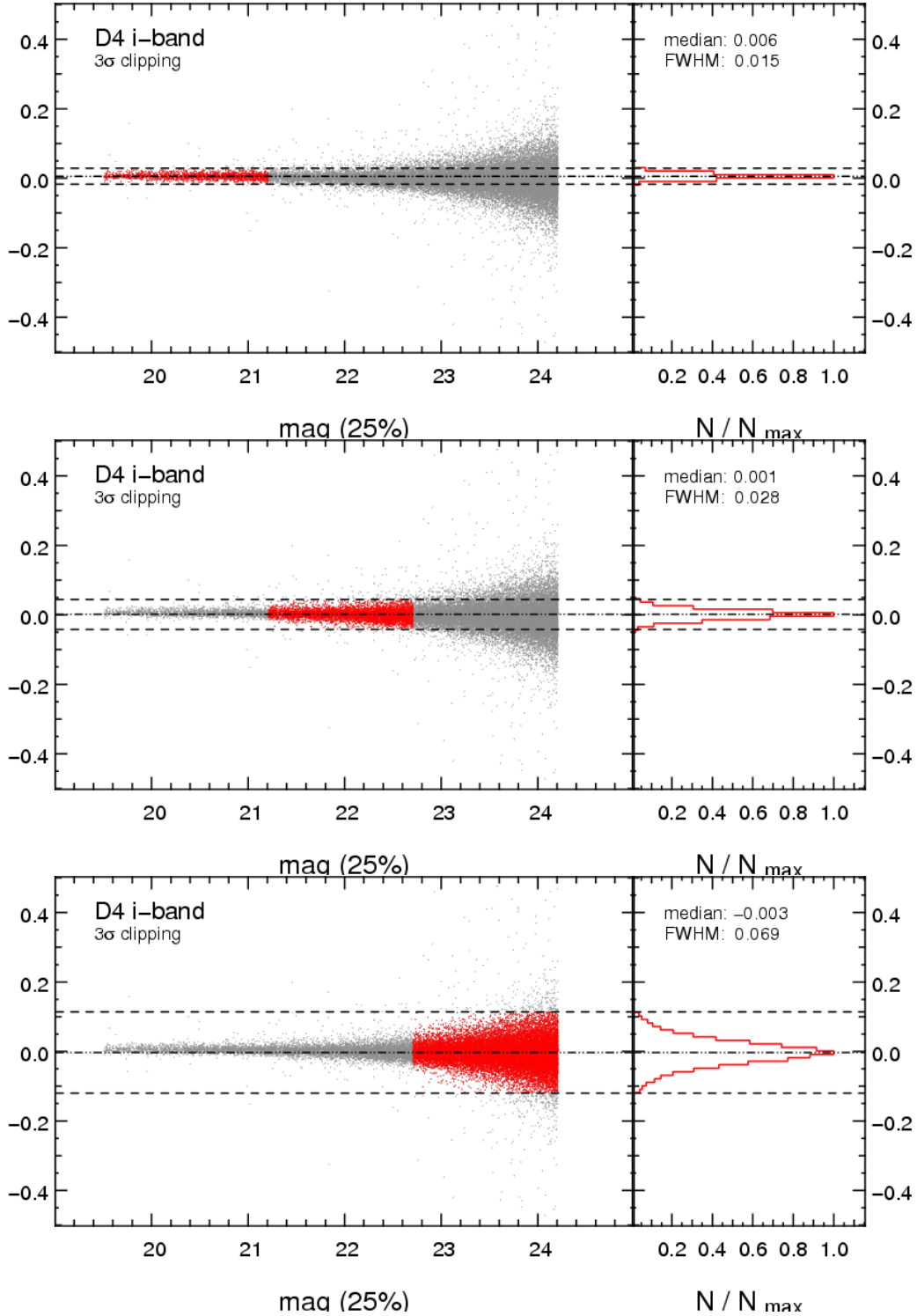


**Figure 44:** Estimation of the internal photometric accuracy in Deep stacks by comparing the the `MAG_AUTO` magnitudes of sources in D4-25-*i* and D-85-*i*. The sample comprises all (stars and galaxies) common sources down to the 80% completeness limits for extended sources of the D-25 stack (sharp cuts on the left panels). The catalogue is then split into three magnitude bins (from top to bottom, the red dots:  $19.5 < i < 21.21$ ,  $21.21 < i < 22.71$ ,  $22.71 < i < 24.21$ ), and for each bin we analyze the *i*-band magnitude differences D25–D85 as a function of magnitude (left panels). The right panels show the distribution of magnitude differences. The histograms are first sigma-clipped and then fit by a Gaussian that returns the FWHM of the distribution. The mean internal photometric error is then defined as  $\sigma_{D25-D85} = \text{FWHM}/2.35$ .

Filter	CFHTLS T0007 Deep data											
	D1			D2			D3			D4		
	mag. range [AB MegaCam]	$\sigma_{D25-D85}$ [mag.]	mag. range [AB MegaCam]	$\sigma_{D25-D85}$ [mag.]	mag. range [AB MegaCam]	$\sigma_{D25-D85}$ [mag.]	mag. range [AB MegaCam]	$\sigma_{D25-D85}$ [mag.]	mag. range [AB MegaCam]	$\sigma_{D25-D85}$ [mag.]	mag. range [AB MegaCam]	$\sigma_{D25-D85}$ [mag.]
$u^*$	20.50 - 22.42	0.011	20.50 - 22.54	0.011	20.50 - 22.35	0.013	20.50 - 22.27	0.014	20.50 - 22.27	0.013	20.50 - 22.27	0.014
	22.42 - 23.92	0.023	22.54 - 24.04	0.021	22.35 - 23.85	0.025	22.27 - 23.77	0.026	22.27 - 23.77	0.025	22.27 - 23.77	0.026
	23.92 - 25.42	0.062	24.04 - 25.54	0.053	23.85 - 25.35	0.060	23.77 - 25.27	0.068	23.77 - 25.27	0.060	23.77 - 25.27	0.068
$g$	20.50 - 22.19	0.008	20.50 - 22.20	0.006	20.50 - 22.19	0.007	20.50 - 22.16	0.007	20.50 - 22.16	0.007	20.50 - 22.16	0.007
	22.19 - 23.69	0.014	22.20 - 23.70	0.012	22.19 - 23.69	0.015	22.16 - 23.66	0.014	22.16 - 23.66	0.015	22.16 - 23.66	0.014
	23.69 - 25.19	0.035	23.70 - 25.20	0.030	23.69 - 25.19	0.037	23.66 - 25.16	0.037	23.66 - 25.16	0.037	23.66 - 25.16	0.037
$r$	19.50 - 21.58	0.007	19.50 - 21.58	0.006	19.50 - 21.59	0.006	19.50 - 21.55	0.007	19.50 - 21.55	0.006	19.50 - 21.55	0.007
	21.58 - 23.08	0.012	21.58 - 23.08	0.010	21.59 - 23.09	0.011	21.55 - 23.05	0.012	21.55 - 23.05	0.011	21.55 - 23.05	0.012
	23.08 - 24.58	0.030	23.08 - 24.58	0.026	23.09 - 24.59	0.029	23.05 - 24.55	0.031	23.05 - 24.55	0.029	23.05 - 24.55	0.031
$i$	19.50 - 21.22	0.008	19.50 - 21.28	0.007	19.50 - 21.29	0.007	19.50 - 21.21	0.008	19.50 - 21.21	0.007	19.50 - 21.21	0.008
	21.22 - 22.72	0.016	21.28 - 22.78	0.011	21.29 - 22.79	0.014	21.21 - 22.71	0.014	21.21 - 22.71	0.014	21.21 - 22.71	0.014
	22.72 - 24.22	0.040	22.78 - 24.28	0.027	22.79 - 24.29	0.034	22.71 - 24.21	0.034	22.71 - 24.21	0.034	22.71 - 24.21	0.034
$y$	19.50 - 21.18	0.012	19.50 - 21.29	0.010	19.50 - 21.26	0.007	19.50 - 21.12	0.007	19.50 - 21.12	0.007	19.50 - 21.12	0.007
	21.18 - 22.68	0.019	21.29 - 22.79	0.012	21.26 - 22.76	0.015	21.12 - 22.62	0.016	21.12 - 22.62	0.015	21.12 - 22.62	0.016
	22.68 - 24.18	0.040	22.79 - 24.29	0.028	22.76 - 24.26	0.037	22.62 - 24.12	0.042	22.62 - 24.12	0.037	22.62 - 24.12	0.042
$z$	19.50 - 20.73	0.010	19.50 - 20.80	0.008	19.50 - 20.61	0.011	19.50 - 20.66	0.009	19.50 - 20.66	0.011	19.50 - 20.66	0.009
	20.73 - 22.23	0.023	20.80 - 22.30	0.020	20.61 - 22.11	0.026	20.66 - 22.16	0.020	20.66 - 22.16	0.026	20.66 - 22.16	0.020
	22.23 - 23.73	0.061	22.30 - 23.80	0.050	22.11 - 23.61	0.071	22.16 - 23.66	0.059	22.16 - 23.66	0.071	22.16 - 23.66	0.059

**Table 22:** Analysis of the internal photometric errors in the CFHTLS T0007 Deep data from the comparison of source pairs in D-25 and D-85. For each Deep field, the internal error is estimated from the mean  $\text{MAG\_AUTO}$  magnitude differences of common sources in D-25 and D-85. The statistics are based on a  $3\text{-}\sigma$  clipping and a Gaussian fitting of the distribution of magnitude differences. The best fit returns the  $\text{FWHM}$  of the distribution. The mean internal photometric error is then defined as  $\sigma_{D25-D85} = \text{FWHM}/2.35$ . Each sample is split into three magnitude ranges, but does not make any morphological selection, so the internal errors quoted in this table are valid for any sources. The bright cuts are  $\text{AB}=20.5$  for  $u^*$  and  $g$  and  $\text{AB}=19.5$  for  $r, i, y$  and  $z$ , while for the faint sources, the cut is set by the 80% completeness limits of extended sources in the D-25 stacks, so both D-85 and D-25 are complete up to the depth of the analysis.



## 5.4 Depth and completeness limits

The depth is measured the same way as in Section 4.3. The completeness limits and galaxy count plots are available in the synoptic table.

The depths of D-25 and D-85 are given in Tables 18 and 19 for the median combined stacks and Tables 20 and 21 for the sigma-combined stacks. These numbers are also presented in the synoptic table. The errors quoted for the completeness limits in the Tables are dominated by the fitting error. For the 80% and 50% values, this is due to sparse sampling of the curve in the magnitude range where the variations of the completeness as a function of magnitude are important.

From Figure 47, the 80% completeness limits of stellar sources is a good indicator of the turn-over magnitude for the galaxy counts. Similarly, the 80% completeness limits of extended sources corresponds well to the turnover point where the galaxy counts begin to be incomplete. This is however not true for the  $u^*$ -band data, where both depth parameters have similar values and also for the  $z$ -band, where the completeness limit value is lower than the turnover point and appears to be a pessimistic estimate of depth.

We note that the completeness limit measurements with simulated sources in the Deep data seem to be in poorer agreement with the galaxy counts plots in comparison to the Wide survey (see Fig. 28). Furthermore, the Deep D-25 estimates are closer to expectations than D-85. This is most likely a consequence of increased crowding in deeper images. In these D-85 images, the fraction of blended sources indeed increases and makes the unambiguous detection of simulated sources more and more difficult.

The D2- $u^*$  should be interpreted with caution. As it contains a mix of CFHTLS and cosmos images that are shifted by 30 arc-minutes, the center of the stacks is deeper and the corners are shallower than the mean depth of the stack (see Fig. 45). Note that the total exposure times and the depths quoted in the Tables and on the figures for the D2-25- $u^*$  and D2-85- $u^*$  do *not* apply to the entire image.

The D2- $u^*$  is the only Deep stack with a non-uniform field coverage. The observing sequences were split into five positions of MegaCam with respect to the Deep D2 center field. They are referenced as:

- the D2-cc- $u^*$  center pointing;
- the D2-u1- $u^*$  upper left pointing, located North-East from the center field;
- the D2-ur- $u^*$  upper right pointing, located North-West;
- the D2-l1- $u^*$  lower left pointing, located South-East; and
- the D2-lr- $u^*$  lower right pointing, located South-West.

The relative positions of D2-cc, D2-u1, D2-ur, D2-l1 and D2-lr are shown on Fig. 46. The black contours outline the shape of the D2- $u^*$  stacks. All colored areas located inside are combined to produce the D-25- $u^*$  and D-85- $u^*$ , which explains the complex weightmap shown on the left panel of Fig. 45.

The complex mosaic pattern and the division of observations amongst several observing runs results in a non-uniform completeness for the D2- $u^*$  stacks. The exposure time and depth can only be defined locally over for the D2- $u^*$  MegaCam field. Table 23 describes the observations in sub-quadrants drawn on Fig. 46. Each quadrant of D-25- $u^*$  and D-85- $u^*$  combines the cc images with either D2-u1, or D2-ur, or D2-l1, or D2-lr, while the central part combines them all. A global estimation of exposure time and depth for D2- $u^*$  is clearly impossible. Note that the exposure times inside the bold contours of Fig. 46 are 51012 s. and 142970 s., for the D2- $u^*$ -25 and D2- $u^*$ -85 stacks, respectively.

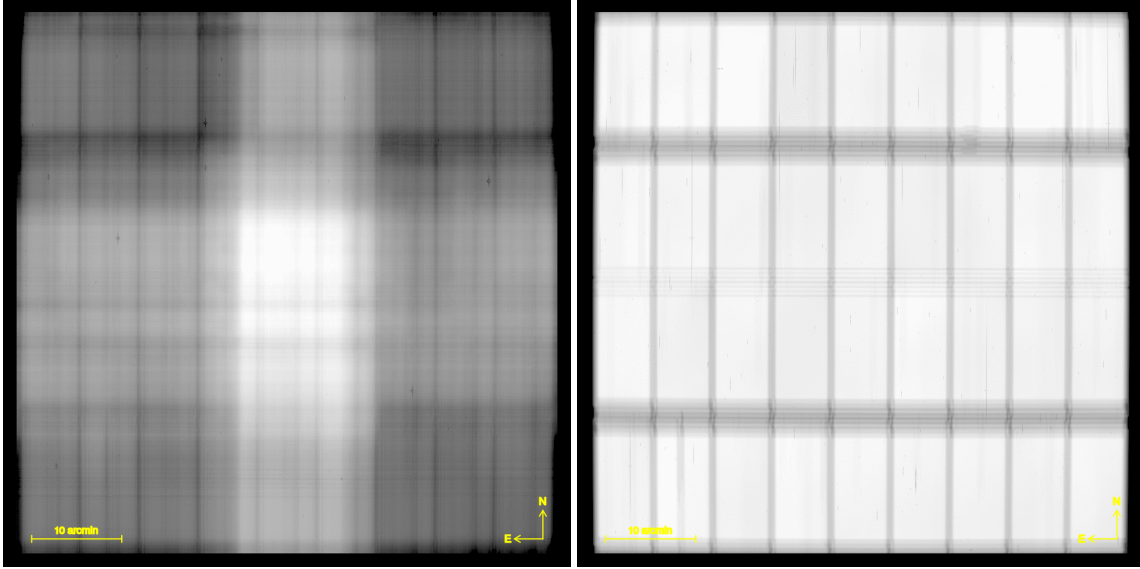


**Figure 45:** Weightmap images of the D2 CFHTLS\_D-85\_u\_100028+021230\_T0007 (left) and CFHTLS\_D-85\_i\_100028+021230\_T0007 (right) stacks. The mosaicing of the D2- $u^*$  field by CFHTLS and COSMOS data produces a heterogeneous stack, with significant variations of the exposure times and depths over the field. The contrast with the  $i$ -band (and other filters) is striking. The innermost bright region of the D2- $u^*$  weight-map corresponds to the central squares inside the bold contours drawn on Fig. 46, and the numbers quoted on Tables 18 and 19 for the D2- $u^*$  stacks are only relevant for the regions inside the black contours.

In contrast, the seeing is more uniform. The last column of Table 23 provides the mean seeing, as derived from the median seeing value of the single MegaCam exposures comprising D2-cc, D2-u1, D2-ur, D2-l1 and D2-lr. The errors are the *rms* of the mean. None of the seeing values are further than  $1-\sigma$  from the mean.

Stacks labelled SIGWEI have been combined using a sigma-clipping method. Sources in such a sigma-clipped image combination should have slightly better signal-to-noise ratios (around 20%) compared to a median-combined image. Our results do show a modest improvement in  $u$  and  $z$  (0.1 to 0.2 mag) but almost no improvement within the error bars in  $r$  and  $i$ . We note that this result has to be considered with caution since the  $gri$  bandpasses suffer from crowding, and the technique of adding simulated objects to a field where a large fraction of pixels are already masked (due to the presence of objects) is necessarily problematic. Other methods should be investigated to test the improvement of depth with the combination method.

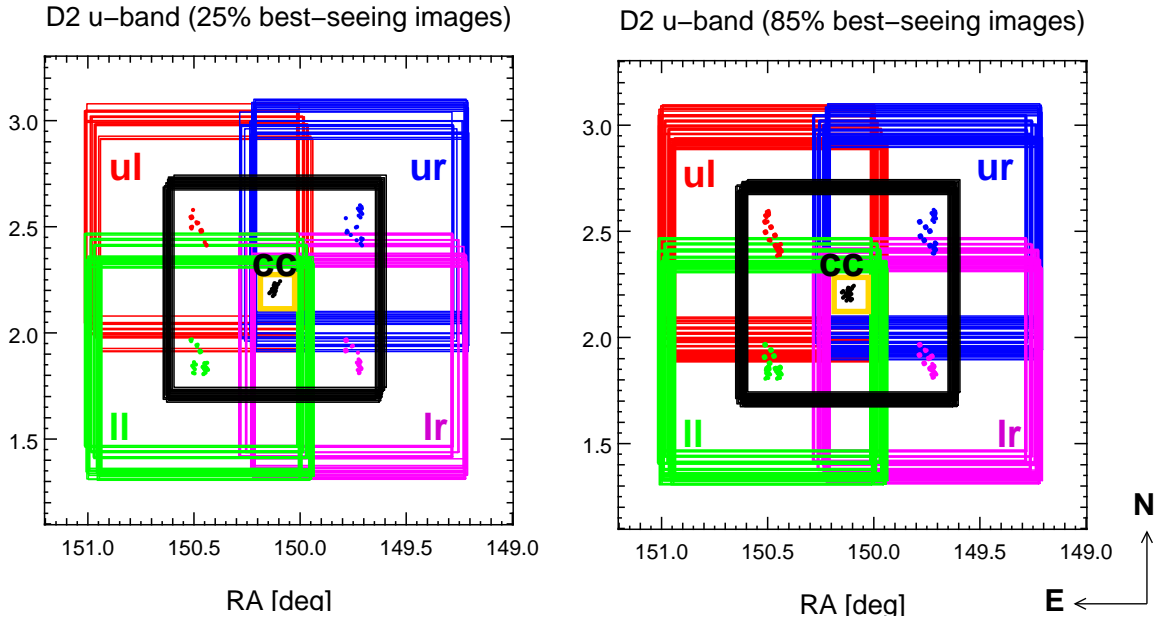


**Figure 46:** Locations of  $u^*$ -band pointings used to produced the D2- $u^*$  stack. The colored squares represent the different MegaCam fields, and the colored points are the center positions of each CFHTLS and COSMOS images that are combined to produce the D-25- $u^*$  and D-85 $u^*$  images. The dark squares are located at the D2 center position and outline the contour of the final D2- $u^*$ . The D2- $u^*$  characteristics quoted in Tables 18 and 19 only refer to the central regions delimited by the black squares. The bold squares show the central region containing all exposures. The stacks inside this narrow region are extremely deep: 51012 s. for D2- $u^*$ -25, and 142970 s. for D2- $u^*$ -85.

cfHTLS+cosmos D2- $u^*$ field name	Reference center RA ; DEC [J2000]	Number of Exposures	Total Exp. time [s]	Mean Seeing $\pm$ <i>rms</i> ["]
D2-cc-25	10:00:28.00 ; +02:12:30	37	19663	$0.827 \pm 0.133$
D2-cc-85		37	19663	$0.827 \pm 0.133$
D2-ul-25	10:01:48.00 ; +02:24:44	15	6393	$0.812 \pm 0.019$
D2-ul-85		61	31004	$0.909 \pm 0.080$
D2-ur-25	09:58:50.00 ; +02:24:44	15	12482	$0.730 \pm 0.059$
D2-ur-85		58	27892	$0.853 \pm 0.099$
D2-11-25	10:01:48.00 ; +01:49:47	15	19299	$0.716 \pm 0.019$
D2-11-85		64	32805	$0.840 \pm 0.098$
D2-1r-25	09:58:50.00 ; +01:49:47	15	12866	$0.690 \pm 0.044$
D2-1r-85		62	28325	$0.865 \pm 0.124$

**Table 23:** Overview of the mosaicing of  $u^*$ -band observations over the five pointings that are used to produce D-25- $u^*$  and D-85- $u^*$ . The total field of view covered by the five pointings is  $1.4 \times 1.4 \text{ deg}^2$ , but we only keep the  $1. \times 1. \text{ deg}^2$  field at the D2 T0007 reference position. Only the very central region of stacks contains all data and corresponds to the D2- $u^*$  properties quoted in Tables 18 and 19. This region is roughly contained within the bold squares of Fig. 46. The seeing is not the same, but the scatter is large and all stacks agree with the same mean seeing, within  $1-\sigma$ .

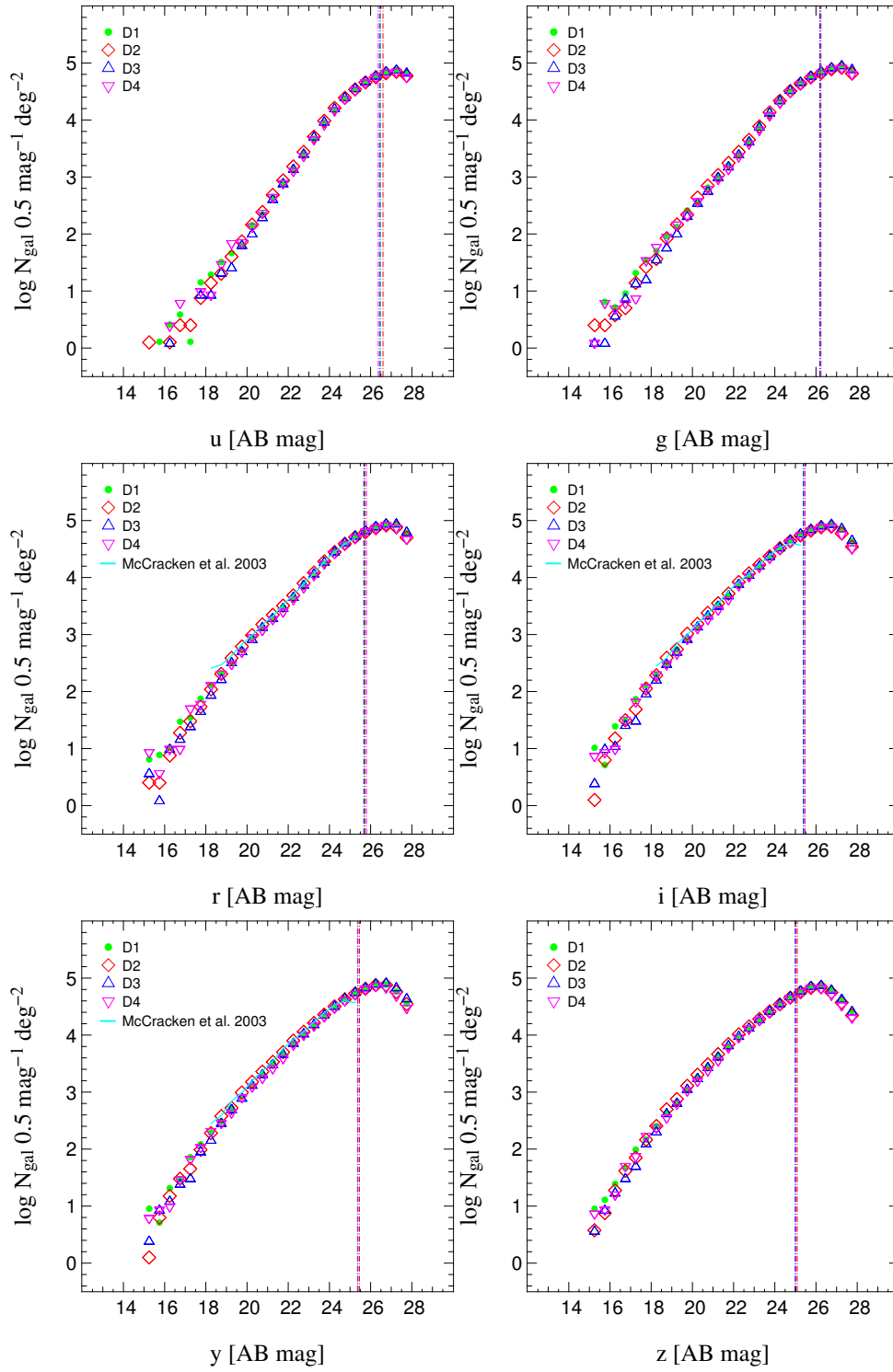


**Figure 47:** Galaxy counts for the deep, sigma-weighted stacks in all bands for each of the four fields. The dotted lines show the 80% completeness for galaxies described in Section 5.4.

## 6 Data products

### 6.1 Data set

Unlike the previous CFHTLS releases, T0007 is immediately public. The T0007 synoptic table<sup>24</sup> is an easy way to access all the data and presents a complete summary of the release. These images and catalogues form the core of the T0007 release. These data are:

- the complete set of individual weight-map images corresponding to the 6378 and 8916 single images used during the production of the CFHTLS Wide and Deep releases. The Terapix weight-map images are Multi-Extension FITS (MEF), like the native CFHT images.
- Stacked images with their corresponding weight-maps;
- 855 Wide stacks, corresponding to  $u^*$ ,  $g$ ,  $r$ ,  $i$  or  $y$  and  $z$  bands:
  - 360 for W1,
  - 125 for W2,
  - 245 for W3 and
  - 125 for W4;
- 96 Deep stacks corresponding to  $u^*$ ,  $g$ ,  $r$ ,  $i$ ,  $y$  and  $z$  bands, consisting of:
  - 24 for D1 (6 D-25 MEDIAN, 6 D-25 SIGWEI, 6 D-85 MEDIAN, 6 D-85 SIGWEI),
  - 24 for D2,
  - 24 for D3 and
  - 24 for D4;
- each stack corresponds to a tile of 1 deg.×1 deg. field (19354×19354 pixels of 0.1860"), centered at the positions listed in Tables 31 (Wide), and in 17 (Deep);
- the Equatorial coordinate system is J2000 (ICRS) and the projection type is the distorted tangential TAN. Stacks are produced using a median filter, are weighted accordingly using the weight-map images, and combined using a Lanczos3 interpolation kernel.
- the “chi2” detection images ( $g-r-i/y$  for the Wide and  $g-r-i$  for the Deep data) images with their weight-map (FITS image).
  - the chi2 image only combines  $g$ ,  $r$  and  $i/y$ <sup>25</sup> (Wide) or  $g$ ,  $r$  and  $i$  (Deep) images;
  - As for the Wide stacks, they are produced in two versions, sigma-clipped and median-combined;
  - each has the same size, pixel scale and projection type as the native stacks;
  - the pixel values are actually  $\sqrt{\text{chi2}}$ , not chi2

---

<sup>24</sup>[http://terapix.iap.fr/cplt/T0007/table\\_syn\\_T0007.html](http://terapix.iap.fr/cplt/T0007/table_syn_T0007.html)

<sup>25</sup>We  $i/y$  means either  $i$  or (exclusive)  $y$  data.

- there is one chi2 image per Wide tile and Deep field. Since T0007 is complete, there are 171 chi2 images for the Wide and 16 chi2 images for the Deep.

In total the T0007 release is therefore composed of 2052 Wide and 224 Deep MegaCam-size science, chi2 or weight-map images;

- the catalogues of sources extracted from each stack, prior to producing catalogues from the chi2 reference image (855 .1dac Wide and 96 .1dac Deep FITS table);
- single filter catalogues, one per stack. They are created by running SExtractor in dual-image mode using the chi2 image as the reference source detection image and the  $u^*$ ,  $g$ ,  $r$ ,  $i$ ,  $y$  or a  $z$ -stack as a photometry image ( $*u/g/r/i/z*.cat$  ASCII tables). The T0007 single filter catalogues contain all parameters listed in Tables 28, 29 and 30. There is one source catalogue per chi2 source detection and per filter, that is 855 Wide and 96 Deep catalogues. So, for each MegaCam stack position, the Wide ( $u^*$ ,  $g$ ,  $r$ ,  $i/y$ ,  $z$ ) and the Deep ( $u^*$ ,  $g$ ,  $r$ ,  $i$ ,  $y$ ,  $z$ ) catalogues have the same number of sources;
- ASCII merged source catalogues (M-SC) are also provided:
  - 342 Wide merged 5-filters  $u^*gr[i/y], z$  catalogues (either  $i$  or  $y$  band data inside), and
  - 32 Deep merged 6-filters  $u^*griyz$  catalogues (both  $i$  and  $y$  band inside),

in ASCII table format. The Wide catalogues are named  $*urgiz*.cat$  or  $*urgyz*.cat$ ; the Deep are all named  $*ugriyz*.cat$ , and contain  $i$  and  $y$  data. They contain all objects with a restricted list of parameters from the parent single filter catalogues, but include  $e(b - v)$  values for each object. They are estimated at each source position from interpolation of the Schlegel et al. (1998) maps; Two sets of catalogues are produced containing either MAG\_AUTO magnitudes or SNLS aperture magnitudes (SNLS and IQ20 magnitudes). Please refer to section 6.3 for a detailed catalogue content description.

- The ASCII Wide patch merged catalog. These four catalogues (one for each Wide patch) contain all parameters in all filters for each object detected in the corresponding Wide patch. The parent catalogues are the Chi2 catalogues which are merged together. For objects in overlapping regions which are detected on several tiles, the parameters are kept from the largest i-band signal to noise detection (FLUX\_AUTO/FLUX\_ERR). Note that these catalogues are huge (40 to 130 GB).
- the DS9 compliant masks (.reg ASCII file), *one for each stack*. The masks are produced automatically. The masking uses the USNO source catalogues to locate bright stars in CFHTLS stacks and draw a polygon that delimits a polluted region. The size of the polygon depends on the magnitude of the stars. After the stellar source masking, polygons are added automatically to all mask, to exclude the edges of fields. Masks are then tuned manually with additional polygons that exclude regions with missing CCDs.

*It is important to notice that the mask needs depend on the science goals. The T0007 masks may therefore be tuned accordingly. We recommend to CFHTLS users to overlay the masks on a DS9 view of each stack image and have a first look prior to use them.*

All quality control files produced during Terapix processing are public. The supplementary data available are:

- a set of 855 Wide and 96 Deep binary masks images (FITS), one per filter, based on the ASCII .reg masks;

- the 6378 Wide and 8916 Deep individual QualityFITS evaluation files attached to each input image (QFITS-in). Only QFITS-in data of images that were selected for stacks in T0007 are available;
- the astrometric and photometric initial rescaling calibration files attached to each image during the SCAMP calibration step. There are 6378 Wide and 8916 Deep .ahead and .head (ASCII) files;
- the complete list of MegaCam images contained in each stack (upon request);
- the list of the L99 stack rescaling factors;
- the 855 Wide and 96 Deep individual QualityFITS evaluation files for each final stack (QFITS-out);
- a series of quality assessment files: tables, images, plots and statistics for any image are available from the T0007 synoptic table [http://terapix.iap.fr/cplt/T0007/table\\_syn\\_T0007.html](http://terapix.iap.fr/cplt/T0007/table_syn_T0007.html). They include:
  - all stellar colour-colour plots. There are three color-color plots per Wide stack, and five color-color plots per Deep stack;
  - all three-filter colour (.jpg) images. There are three color images per stack that combines the five filters in different ways;
  - all completeness limit (.png) plots, one per stack. The ASCII .dat data tables used to make these plots are also available, upon request to TERAPIX;
  - all galaxy count (.ps) plots, one per stack;
  - the complete QualityFITS QFITS-out quality control files (.html page); one per stack;
  - the complete set of SCAMP output and quality control files (.html page); between one (all image together) and six (one per filter) per field;

## 6.2 Data types and file naming conventions

All files provided with the T0007 release are listed and briefly described in Tables 24 to 27. The CFHT input image names are the native CFHT odometer numbers. Terapix preserves this naming convention for all relevant files attached to single images, such as the weight-maps, the QualityFITS .ldac catalogues or the astrometric calibration files.



File name	Content	Data type	Size	Number of files	Access
#[CFHT-odometer]p.fits	Individual input images	MEF-FITS binary	16 0.7 GB	6378 Wide 8916 Deep	CADC
#[CFHT-odometer]p_weight.fits	Individual weight-map images	MEF-FITS binary	-32 1.4 GB	6378 Wide 8916 Deep	CADC
#[CFHT-odometer]p.ldac	Single image early catalogues	FITS binary-table	8 11 MB	6378 Wide 8916 Deep	TERAPIX
#[CFHT-odometer]p.ahead	Individual astrometric calibration files	ASCII	100 kB	6378 Wide 8916 Deep	TERAPIX
#[CFHT-odometer]p.head	Individual photometric calibration files	ASCII	1.5 kB	6378 Wide 8916 Deep	TERAPIX
#[CFHT-odometer]p/	QFITS-in directories	QA files, various type	350 MB	6378 Wide 8916 Deep	TERAPIX
CFHTLS_w_[f]_RA-DEC_T0007_MEDIAN.fits	Wide stack science images	FITS binary	-32 1.4 GB	855	CADC
CFHTLS_w_[f]_RA-DEC_T0007_MEDIAN_weight.fits	Wide stack weight maps	FITS binary	-32 1.4 GB	855	CADC
CFHTLS_w_gri_RA-DEC_T0007_MEDIAN.fits	Wide chi2 stacks, for <i>i</i> stacks <i>gri</i> combined	FITS binary	-32 1.4 GB	139	CADC
CFHTLS_w_gri_RA-DEC_T0007_MEDIAN_weight.fits	Wide chi2 weight map for <i>i</i> stacks, <i>gri</i> combined	FITS binary	-32 1.4 GB	139	CADC
CFHTLS_w_gry_RA-DEC_T0007_MEDIAN.fits	Wide chi2 image for <i>y</i> stacks, <i>gry</i> combined	FITS binary	-32 1.4 GB	32	CADC
CFHTLS_w_gry_RA-DEC_T0007_MEDIAN_weight.fits	Wide chi2 weight map for <i>y</i> stacks, <i>gry</i> combined	FITS binary	-32 1.4 GB	32	CADC
CFHTLS_w_[f]_RA-DEC_T0007_MEDIAN.ldac	Wide stack catalogues	FITS binary-table	8 50 MB	855	CADC
CFHTLS_w_[f]_RA-DEC_T0007_MEDIAN.cat	Wide stack chi2 catalogues	ASCII 181 columns	450 MB	855	CADC
CFHTLS_w_ugriz_RA-DEC_T0007_MEDIAN_MAGAUTO.cat	Wide chi2 merged band catalogues, MAG_AUTO magnitudes	ASCII 24 columns	50 MB	171	CADC

**Table 24:** CFHTLS files, point-of-access and naming conventions. The first line of the table gives the input images delivered from CFHT. Successive lines refer to Terapix T0007 data products. Access to restricted CADC and Terapix data sets, public figures and plots are possible from the T0007 synoptic table. The number of files for QFITS-in/out refers to the number of directories, each containing around 100 files per directory).

File name	Content	Data type	Size	Number of files	Access
CFHTLS_w_ugtiz_RA-DEC_t0007_MEDIAN_MAGSNLS.cat	Wide chi2 merged band catalogues, MAG_SNLS magnitudes	ASCII 29 columns	60 MB	171	CADC
CFHTLS_w_ugtiz_RA-DEC_t0007_MEDIAN.apc	Wide chi2 27+MAG_SNLS aperture merged band catalogues	ASCII 556 columns	1.3 GB	171	TERAPIX
CFHTLS_w_[f]_RA-DEC_t0007_MEDIAN.reg	Wide DS9 compliant mask $f$ -band	ASCII	100 kB	855	CADC
CFHTLS_w_[f]_RA-DEC_t0007_MEDIAN_binmask.fits	Wide binary mask image $f$ -band	FITS binary -32	1.4 GB	855	TERAPIX
CFHTLS_w_[f]_RA-DEC_t0007_MEDIAN/	Wide $f$ -band stack	QA files, various type	50 MB	855	TERAPIX
CFHTLS_w_[f]_RA-DEC_t0007_MEDIAN/qFITS-out directory	qFITS-out directory				
CFHTLS_w_[fff]_RA-DEC_t0007.jpg	Wide stacks 3-color image ( $u^*gr$ ); ( $gr[i/y]$ ); ( $r[i/y]z$ )	JPEG	50 MB	513	TERAPIX
CFHTLS_w_ugtiz_RA-DEC_t0007_MEDIAN_MAGAUTO_fff.png	Wide stellar color-color tracks plots ( $u^*-g$ )/( $g-r$ ); ( $g-r$ )/( $r-i$ ); ( $r-i$ )/( $i-z$ )	PNG	50 kB	417	TERAPIX
CFHTLS_w_ugtiz_RA-DEC_t0007_MEDIAN_MAGSNLS_fff.png	Wide stellar color-color tracks plots ( $u^*-g$ )/( $g-r$ ); ( $g-r$ )/( $r-i$ ); ( $r-i$ )/( $i-z$ )	PNG	50 kB	417	TERAPIX
CFHTLS_w_ugtyz_RA-DEC_t0007_MEDIAN_MAGAUTO_fff.png	Wide stellar color-color tracks plots ( $u^*-g$ )/( $g-r$ ); ( $g-r$ )/( $r-y$ ); ( $r-y$ )/( $y-z$ )	PNG	50 kB	96	TERAPIX
CFHTLS_w_ugtyz_RA-DEC_t0007_MEDIAN_MAGSNLS_fff.png	Wide stellar color-color tracks plots ( $u^*-g$ )/( $g-r$ ); ( $g-r$ )/( $r-y$ ); ( $r-y$ )/( $y-z$ )	PNG	50 kB	96	TERAPIX
CFHTLS_w_[f]_RA-DEC_t0007_MEDIAN_Complim.png	Wide stacks completeness limit plots $f$ -band	PNG	60 kB	855	TERAPIX
CFHTLS_w_[f]_RA-DEC_t0007_MEDIAN_Complim.dat	Wide stacks completeness data points $f$ -band	ASCII	0 kB	855	TERAPIX
CFHTLS_w_[f]_RA-DEC_t0007_gal_histo.ps	Wide stacks galaxy counts $f$ -band	PS	50 kB	855	TERAPIX

**Table 25:** CFHTLS files, point-of-access and naming conventions (cont'd).

File name	Content	Data type	Size	Number of files	Access
Each DEEP product is produced in 4 flavours (D-[28]5 and COMB=MEDIAN/SIGWEI)					
CFHTLS_D-[28]5_[f]_RA-DEC_T0007_[COMB].fits	Deep [28]5% best seeing stack science image <i>f</i> -band	FITS binary -32	1.4 GB	24 * 4	CADC
CFHTLS_D-[28]5_[f]_RA-DEC_T0007_[COMB]_weight.fits	Deep [28]5% best seeing stack weight maps <i>f</i> -band	FITS binary -32	1.4 GB	24 * 4	CADC
CFHTLS_D-[28]5_gri_RA-DEC_T0007_[COMB].fits	Deep [28]5% best seeing chi2 image for <i>i</i> stacks, chi2- <i>gri</i> combined	FITS binary -32	1.4 GB	4 * 4	CADC
CFHTLS_D-[28]5_gri_RA-DEC_T0007_[COMB]_weight.fits	Deep [28]5% best seeing chi2 weight map for <i>i</i> stacks, chi2- <i>gri</i> combined	FITS binary -32	1.4 GB	4 * 4	CADC
CFHTLS_D-[28]5_[f]_RA-DEC_T0007_[COMB].ldac	Deep [28]5% best seeing stack catalogue <i>f</i> -band	FITS binary-table 8	50 MB	24 * 4	CADC
CFHTLS_D-[28]5_[f]_RA-DEC_T0007_[COMB].cat	Deep [28]5% best seeing stack chi2 catalogue <i>f</i> -band	ASCII 181 columns	500 MB	24 * 4	CADC
CFHTLS_D-[28]5_ugtiyz_RA-DEC_T0007_[COMB]_MAGAUTO.cat	Deep [28]5% best seeing chi2 catalogue merged band (in MAGAUTO)	ASCII 27 columns; e(b-v)	100 MB	4 * 4	CADC
CFHTLS_D-[28]5_ugtiyz_RA-DEC_T0007_[COMB]_MAGSNLS.cat	Deep [28]5% best seeing chi2 catalogue merged band (in MAGAUTO)	ASCII 27 columns; e(b-v)	100 MB	4 * 4	CADC
CFHTLS_D-[28]5_ugtiyz_RA-DEC_T0007_[COMB].ape	Deep [28]5% best seeing chi2 27 aperture photometry catalogue merged band	ASCII 618 columns	3.1 GB	4 * 4	TERAPIX
CFHTLS_D-[28]5_[f]_RA-DEC_T0007_[COMB].reg	Deep [28]5% best seeing DS9 compliant mask <i>f</i> -band	ASCII	100 kB	24 * 4	CADC
CFHTLS_D-[28]5_[f]_RA-DEC_T0007_[COMB]_binmask.fits	Deep [28]5% best seeing binary mask image <i>f</i> -band	FITS binary -32	1.4 GB	24 * 4	TERAPIX
CFHTLS_D-[28]5_[f]_RA-DEC_T0007_[COMB]/	Deep [28]5% best seeing <i>f</i> -band stack QA: QFITS-out directory	QA files, various type	(2.3 MB .gz) 75 MB	24 * 4	TERAPIX
CFHTLS_D-[28]5_[fff]_RA-DEC_T0007_[COMB].jpg	Deep [28]5% best seeing 3-color image of stacks	JPEG	50 MB	12 * 4	TERAPIX

**Table 26:** CFHTLS files, point-of-access and naming conventions (cont'd).

File name	Content	Data type	Size	Number of files	Access
CFHTLS_D-[28]15_ugriz_RA-DEC_T0007_[COMB]_MAGAUTO_fff.png	Deep [28]15% best seeing stellar color plots (in MAGAUTO) $(u^*-g)/(g-r);(g-r)/(r-i);(r-i)/(i-z);(g-r)/(r-y);(r-y)/(y-z)$	PNG	200 kB	4 * 4	TERAPIX
CFHTLS_D-[28]15_ugriz_RA-DEC_T0007_[COMB]_MAGSNLS_fff.png	Deep [28]15% best seeing stellar color plots (in MAGSNLS) $(u^*-g)/(g-r);(g-r)/(r-i);(r-i)/(i-z);(g-r)/(r-y);(r-y)/(y-z)$	PNG	200 kB	4 * 4	TERAPIX
CFHTLS_D-[28]15_[f]_RA-DEC_T0007_[COMB]_CompLim.png	Deep [28]15% best seeing stacks completeness limit plots $f$ -band	PNG	60 kB	24 * 4	TERAPIX
CFHTLS_D-[28]15_[f]_RA-DEC_T0007_[COMB]_CompLim.dat	Deep [28]15% best seeing stacks completeness data points $f$ -band	ASCII	0 kB	24 * 4	TERAPIX
CFHTLS_D-[28]15_[f]_RA-DEC_T0007_[COMB]_gal_histo.ps	Deep stacks galaxy counts $f$ -band	PS	50 kB	24 * 4	TERAPIX

**Table 27:** CFHTLS files, point-of-access and naming conventions (cont'd).

### 6.3 Content of CFHTLS source catalogues

Five types of source catalogue are provided:

- “.ldac” source catalogues for individual images. There is one .ldac catalogue per CFHT input image. For T0007, 6378 .ldac Wide and 8916 .ldac Deep are produced;
- the FITS-table output-ldac source catalogues of each individual stack. There is one catalogue per tile and per filter. So 855 .ldac-Wide (171 tiles, 5 filters per tiles) and 96 .ldac-Deep (4 fields, 6 filters per field, D-25 and D-85 seeing selections, MEDIAN and SIGWEI combination) source catalogues are produced;
- the ASCII-table chi2-image reference source catalogues (chi2-RSC), produced from the aperture-matched detections in the five Wide ( $u^*gri/yz$ ) or six Deep ( $u^*griyz$ ) stacked images of each tile. There is one catalogue per tile and per filter, but each filter has the same number of sources, located at the same positions, as measured in the chi2 image. These catalogues are not corrected for galactic extinction. 855 Wide and 96 Deep  $[f].cat$  catalogues are produced, where  $[f]$  denotes the filter, and they all contain the `Sextractor` parameters listed in Tables 28, 29 and 30;
- the ASCII merged source catalogues (M-SC), produced by merging the chi2-RSC for each filter into one single catalogue ( $u^*griz$ , or  $u^*gryz$ , or  $u^*griyz$ ). The Wide  $*ugriz*.cat$ ,  $*ugryz*.cat$  and Deep  $*ugriyz*.cat$  catalogues are more concise, but may be more convenient for most CFHTLS users. Note that the Wide and Deep catalogues do not have the same number of columns.
  - The ASCII merged source catalogues are produced in two versions. The “MAGAUTO” version contains `MAG_AUTO` magnitudes and is suitable for science topics involving galaxies. The “MAGSNLS” version contains two sorts of aperture magnitudes: `MAG_SNLS` (aperture magnitude with a diameter of  $7.5 * FWHM$ ) and `MAG_IQ20` (`MAG_SNLS` magnitude with an aperture correction). These are the magnitudes used for the photometric calibration of star catalogues (mainly IQ20 magnitudes). For a detailed description of these magnitudes, please refer to the photometric calibration section.
  - The Wide merged catalogues contain the following parameters, extracted from the either the chi2-RSC  $ugriz$  or the  $ugryz$  catalogues (`id,x,y,ra,dec,r2,flag,u*,g,r,i/y,z,u_err,g_err,r_err,(i/y)_err,z_err,e(b-v),u*_SEx-flag,g*_SEx-flag,r*_SEx-flag,(i/y)_SEx-flag,z*_SEx-flag,dk`), where
    - \* `id` : `SExtractor` object ID. This corresponds to the object ID which appears in the chi2 catalogue;
    - \* `x,y (pixels)` : object pixel coordinates. The pixel scale is 0.186";
    - \* `RA,DEC` : right ascension and declination in J2000 coordinates;
    - \* `r2 (pixels)` : radius enclosing half the flux;
    - \* `flag` : Terapix object flag, derived from the `Sextractor r2` parameter, the saturation and the masking. The flag value is a combination of the following binary flags :
      - 0/1 : galaxy/star
      - 0/2 : saturated object in at least one filter
      - 0/4 : masked in z band
      - 0/8 : masked in y band
      - 0/16 : masked in i band

- 0/32 : masked in  $r$  band
- 0/64 : masked in  $g$  band
- 0/128 : masked in  $u$  band

For example, an object with flag 37 is a star which is in a masked region in the  $r$  and  $z$  bands.

- \*  $u^*, g, r, i/y, z$  : Depending on the catalog, object MAG\_AUTO or MAG\_SNLS magnitudes in the MegaCam instrumental reference frame. When magnitude and its error are missing, these values are set to 99. Note that the  $i$  or  $y$  magnitudes are both listed in a column labelled  $i$  on the top header of each catalog.
  - \*  $u_{err}^*, g_{err}, r_{err}, (i/y)_{err}, z_{err}$ : Object magnitude errors;
  - \*  $e(b-v)$ : the values of the galactic extinction are calculated using the Schlegel et al. (1998) dust map at the object's position. The extinction,  $E(B - V)$ , is derived at each source position using a linearly interpolated dust value from the four nearest pixels. The  $E(B - V)$  is then added in the last column of the merged catalogue;
  - \*  $u_{SEX-flag}^*, g_{SEX-flag}, r_{SEX-flag}, (i/y)_{SEX-flag}, z_{SEX-flag}$  : SExtractor extraction flags, for each filter. Each flag is set to zero when no source extraction problem is encountered, or follows the sum of power-of-two rule<sup>26</sup>;
  - \*  $dk$  : object cell number for the spatially variable color-term (see photometric calibration).
  - \*  $u_{IQ20}^*, g_{IQ20}, r_{IQ20}, i/y_{IQ20}, z_{IQ20}$  (only in the SNLS catalogues). IQ20 magnitudes are MAG\_SNLS aperture magnitudes corrected by an aperture correction factor to estimate the flux in an aperture of  $20 * FWHM$ . This magnitude is a better measurement for stellar total flux.
- The Deep merged catalogues also contain the parameters extracted from the chi2-RSC, but for six filters instead of five, as for the Wide. All catalogues have *ugriyz* data for all sources.

342 Wide merged catalogues are produced, one per tile, two for MAG\_AUTO, MAG\_SNLS, and 32 Deep merged catalogues are produced, two per field (D-25 and D-85), two for MEDIAN/SIGWEI, two for MAG\_AUTO, MAG\_SNLS;

- the ASCII multi-aperture merged source catalogues (MAM-SC), produced like the (M-SC), but the catalogues only include the data from the 27 apertures (SNLS+26 apertures) and aperture magnitudes of each sources of the chi2-RSC catalogue. The aperture sizes range from 10 to 60 pixels. As the M-SC, 171 Wide catalogues and 16 Deep catalogues are produced. These catalogues are very large (1-3 GB). They have 536 columns per source for the Wide and 642 for the Deep.
- The ASCII Wide patch merged catalog (WPM-SC). These four catalogues (one for each Wide patch) contain all parameters in all filters for each object detected in the corresponding Wide patch. The parent catalogues are the Chi2 catalogues (27 apertures) which are merged together.

All catalogues have a header on that describes the meaning of each column.

All data of the two last catalogues with the exception of the  $E(B - V)$  for the merged source catalogue, are extracted from the large chi2-RSCs. They are produced only for convenience. All of them have been produced using SExtractor, but with different configuration files and output parameter lists. Most  $i$  stacks are made with the first  $i$  ( $i.MP9702$ ) filter. However, there are 16 W1, 2 W2, 7 W3 and 7 W4

<sup>26</sup><http://astromatic.iap.fr/software/sextractor>

stacks made with the  $y$ -( $i$  .MP9702) filter. The  $y$  stacks are listed in Tables 31 and quoted in Tables 15 and 16. All Deep fields comprise both  $i$  and  $y$ -band stacks, but the  $i$  stacks contain much more images and are much deeper.

The two input-ldac and output-ldac catalogues as well as the chi2-RSC catalogue contain the 75 parameters described in Table 28 to 30. However, they do not have the same input nor the same of output parameter values. Some of them are vectors, so the number of entries are also not the same and can be much higher than 75. In particular, they do not have the same detection threshold, or the same number of MAG\_APER aperture magnitudes. Columns of catalogues with both the '.cat' or the '.ldac' extensions are defined in the '.param' files. For the Wide survey, there are 77 columns in the .ldac catalogues, 181 columns in the chi2-RSC, 24 (resp 30) in the merged MAG\_AUTO (resp MAG\_SNLS) M-SC catalogues, 536 in the merged MAM-SC catalogues and 827 in the patch-merged catalogues WPM-SC.

All images have a new magnitude ZP set to 30 AB magnitudes. The magnitudes of objects in the final stacks are computed as follows:

$$m = 30 - 2.5 \log(counts) . \quad (19)$$

It is important to realise that the .cat catalogues are produced using specific selection criteria or filters selected by TERAPIX from past experience and after discussions with experienced users and the CFHTLS Steering Group. They are certainly not suitable for all scientific goals. Please examine the configuration and parameter list files and check they meet your needs. In case different selections or configuration parameters are needed, it may be better to produce a new and more suitable catalogue, or to produce a new chi2 image. TERAPIX can provide specific help to users who want to produce their own images or catalogues.

Id	Parameter	Description	Units	Comments
1	NUMBER	Running object number	-	
2	X_IMAGE	Object position along x	[pixel]	
3	X_IMAGE	Object position along y	[pixel]	
4	ERRA_IMAGE	RMS position error along major axis	[pixel]	Error-ellipse shape parameter. Generic SExtractor parameter naming construction: ERR[-] refers to error-ellipse properties, while [-]ERR refers to error on SExtractor object parameters.
5	ERRB_IMAGE	RMS position error along minor axis	[pixel]	
6	ERRTHETA_IMAGE	Error ellipse position angle (CCW/x)	[deg]	
7	A_IMAGE	Profile RMS along major axis	[pixel]	
8	B_IMAGE	Profile RMS along minor axis	[pixel]	
9	POLAR_IMAGE	$(A\_IMAGE^2 - B\_IMAGE^2)/(A\_IMAGE^2 + B\_IMAGE^2)$		
10	THETA_IMAGE	Position angle (CCW/x)	[deg]	
11	X_WORLD	Barycenter position along world x axis	[deg]	
12	Y_WORLD	Barycenter position along world y axis	[deg]	
13	ERRA_WORLD	World RMS position error along major axis	[deg]	
14	ERRB_WORLD	World RMS position error along minor axis	[deg]	
15	ERRTHETA_WORLD	Error ellipse pos. angle (CCW/world-x)	[deg]	
16	A_WORLD	Profile RMS along major axis (world units)	[deg]	
17	B_WORLD	Profile RMS along minor axis (world units)	[deg]	
18	POLAR_WORLD	$(A\_WORLD^2 - B\_WORLD^2)/(A\_WORLD^2 + B\_WORLD^2)$		
19	THETA_WORLD	Position angle (CCW/world-x)	[deg]	
20	ALPHA_J2000	Right ascension of barycenter (J2000)	[deg]	
21	DELTA_J2000	Declination of barycenter (J2000)	[deg]	
22	ERRTHETA_J2000	J2000 error ellipse pos. angle (east of north)	[deg]	
23	THETA_J2000	Position angle (east of north) (J2000)	[deg]	
24	XWIN_IMAGE	Windowed position estimate along x	[pixel]	
25	YWIN_IMAGE	Windowed position estimate along y	[pixel]	
26	ERRWIN_IMAGE	RMS windowed pos error along major axis	[pixel]	
27	ERRWIN_IMAGE	RMS windowed pos error along minor axis	[pixel]	
28	ERRTHETAWIN_IMAGE	Windowed error ellipse pos angle (CCW/x)	[deg]	

**Table 28:** Description of parameters listed in T0007 catalogues.



Id	Parameter	Description	Units	Comments
29	AWIN_IMAGE	Windowed profile RMS along major axis	[pixel]	
30	BWIN_IMAGE	Windowed profile RMS along minor axis	[pixel]	
31	POLARWIN_IMAGE	$(AWIN^2 - BWIN^2)/(AWIN^2 + BWIN^2)$		
32	THETAWIN_IMAGE	Windowed position angle (CCW/x)	[deg]	
33	XWIN_WORLD	Windowed position along world x axis	[deg]	
34	YWIN_WORLD	Windowed position along world y axis	[deg]	
35	ERRAWIN_WORLD	World RMS windowed pos error along major axis	[deg]	
36	ERRBWIN_WORLD	World RMS windowed pos error along minor axis	[deg]	
37	ERRTHETAWIN_WORLD	Windowed error ellipse pos. angle (CCW/world-x)	[deg]	
38	AWIN_WORLD	Windowed profile RMS along major axis (world units)	[deg]	
39	BWIN_WORLD	Windowed profile RMS along minor axis (world units)	[deg]	
40	POLARWIN_WORLD	$(AWIN^2 - BWIN^2)/(AWIN^2 + BWIN^2)$		
41	THETAWIN_WORLD	Windowed position angle (CCW/world-x)	[deg]	
42	ALPHAWIN_J2000	Windowed right ascension (J2000)	[deg]	
43	DELTAWIN_J2000	Windowed declination (J2000)	[deg]	
44	ERRTHETAWIN_J2000	J2000 windowed error ellipse pos. angle (east of north)	[deg]	
45	THETAWIN_J2000	Windowed position angle (east of north) (J2000)	[deg]	
46	FLUX_ISO	Isophotal flux	[count]	
47	FLUXERR_ISO	RMS error for isophotal flux	[count]	
48	MAG_ISO	Isophotal magnitude	[mag]	
49	MAGERR_ISO	RMS error for isophotal magnitude	[mag]	
50	FLUX_APER	Flux vector within fixed circular aperture(s)	[count]	- Idac catalogues: apertures are 16 (3") and 25 (4.7") pixels diameter. - cat chi2-RSC catalogues: apertures are SNLS (7.5 * <i>FWHM</i> ), 10 (1.86"), 12, 14, 16, 18, 20, 22, 24, 26, 28, 30, 32, 34, 36, 38, 40, 42, 44, 46, 48, 50, 52, 54, 56, 58, 60 (11.16") pixels diameter.
51	FLUXERR_APER	RMS error vector for aperture flux(es)	[count]	
52	MAG_APER	Fixed aperture magnitude vector	[mag]	Given for apertures defined by FLUX_APER
53	MAGERR_APER	RMS error vector for fixed aperture mag.	[mag]	
54	FLUX_AUTO	Flux within a Kron-like elliptical aperture	[count]	

**Table 29:** Description of parameters listed in T0007 catalogues (cond't).

Id	Parameter	Description	Units	Comments
55	FLUXERR_AUTO	RMS error for AUTO flux	[count]	
56	MAG_AUTO	Kron-like elliptical aperture magnitude	[mag]	
57	MAGERR_AUTO	RMS error for AUTO magnitude	[mag]	
58	FLUX_PETRO	Flux within a Petrosian-like elliptical aperture	[count]	
59	FLUXERR_PETRO	RMS error for Petrosian flux	[count]	
60	MAG_PETRO	Petrosian-like elliptical aperture magnitude	[mag]	
61	MAGERR_PETRO	RMS error for PETROSian magnitude	[mag]	
62	FLUX_RADIUS	Fraction-of-light radii	[pixel]	Radii that contain 20%, 50% and 80% of the total flux.
63	KRON_RADIUS	Kron apertures in units of A or B		
64	PETRO_RADIUS	Petrosian apertures in units of A or B		
65	BACKGROUND	Background at centroid position	[count]	
66	THRESHOLD	Detection threshold above background	[count]	
67	MU_THRESHOLD	Detection threshold above background	[mag/arcsec <sup>2</sup> ]	
68	FLUX_MAX	Peak flux above background	[count]	
69	MU_MAX	Peak surface brightness above background	[mag/arcsec <sup>2</sup> ]	
70	ISOAREA_IMAGE	Isophotal area above Analysis threshold	[pixel <sup>2</sup> ]	
71	ISOAREAF_IMAGE	Isophotal area (filtered) above Detection threshold	[pixel <sup>2</sup> ]	
72	ISOAREA_WORLD	Isophotal area above Analysis threshold	[deg <sup>2</sup> ]	
73	ISOAREAF_WORLD	Isophotal area (filtered) above Detection threshold	[deg <sup>2</sup> ]	
74	FLAGS	Extraction flags		
75	CLASS_STAR	S/G classifier output		
76	FLAG_MASK	Bit flag for star-galaxy separation, saturation and masking		
77	DK_CELL	Refined color term cell number		
78	FLAG_IFILTER	i-filter flag (0 is the old i filter, 1 is the new i filter)		
79	CFHTLS_TILE	CFHTLS tile of the detection		

**Table 30:** Description of parameters listed in T0007 catalogues (cont'd).

## 6.4 The QualityFITS input and output products

QualityFITS is a Terapix quality assessment tool for FITS images. During CFHTLS T0007 production, it is used to assess whether individual CFHT input images and the CFHTLS output stacks meet the survey specifications. QualityFITS also produces the input weight-map images as well as the input .ldac catalogues.

The quality assessments are done from a visual inspection of QualityFITS outputs and from a series of statistics, tables and plots. An overview and a quick-look image quality assessments can be made using the QualityFITS web page. This “ID-card” for each image is produced automatically and is used to grade all images through the Youpi user interface<sup>27</sup>.

The information returned by QualityFITS depends on the type of images (Multi-extension fits (MEF) or single extension FITS, the type of detectors (single CCD, mosaic of CCDs) and the origin of images. Depending on the steps of the processing (evaluation of input images or of final stacks), they are referenced as QualityFITS-in (or QFITS-in) or QualityFITS-out (or QFITS-out) products.

As a general rule any CFHT images entering or leaving the Terapix center is passes through QualityFITS-in or QualityFITS-out processing steps. 7042 CFHTLS input images and the 2276 T0007 output images were evaluated using this tool.

The QualityFITS data products are images, tables and plots:

- the FITS weight-map image, using WeightWatcher (Marmo & Bertin, 2008), in a multiple or single extension FITS format, like the input image;
- the .ldac catalogue, using SExtractor;
- an analysis of the shape and spatial variation of the PSF using PSFEX, sampled over the whole field (QualityFITS-out), or CCD by CCD for a mosaic (as for QualityFITS-in in the case of MegaCam input images);
- an analysis of the sky background over the whole field of CCD by CCD for a mosaic;
- an analysis of galaxy and stellar counts, based on an automatic blind star-galaxy separation from a  $r_h$ <sup>28</sup>-magnitude diagram. The counts are shown on separate plots and compared to expectations: for the galaxies, they are compared to published results of CFHTLS Deep galaxy counts with the MegaCam filters; for stars, the counts are compared to Bahcall-Soneira models (Bahcall & Soneira, 1981);
- an analysis of the astrometry of images, using SCAMP. For CFHT input images (QualityFITS-in), the astrometry analysis is approximate, and just relies on the FITS keywords. For CFHTLS stacks (QualityFITS-out), the analysis is based on a comparison between the CFHTLS and the 2MASS source catalogues;
- a properly oriented (in case of reversed detector images due to flipped positions of output amplifiers), scaled and astrometrically calibrate binned view of each CCD and of the whole MegaCam field;

---

<sup>27</sup><http://youpi.terapix.fr>

<sup>28</sup>half-light radius

- close up views of the central and the four corner regions of the MegaCam image. The views are unbinned 512×512 pixels JPEG sub-images of the five regions, but is sometimes expanded to 1024×1024 pixels when necessary;
- a series of tables that contain information from the image FITS header, or statistics on the seeing, the background, the number of detections, either over the whole image or CCD by CCD for a mosaic.

The QualityFITS output files are all public. The QualityFITS QA pages are available from the synoptic table. The T0007 synoptic table is a convenient way to have a quick look at the images.

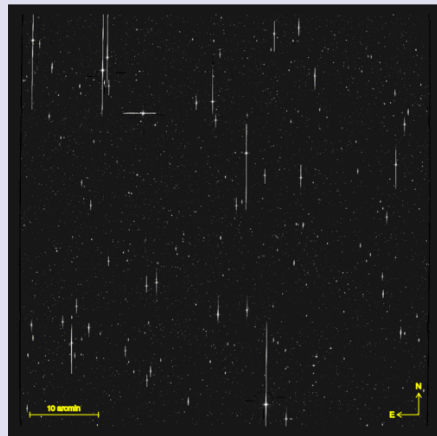


### Evaluation of CFHTLS\_W\_i\_222054+002300\_T0007

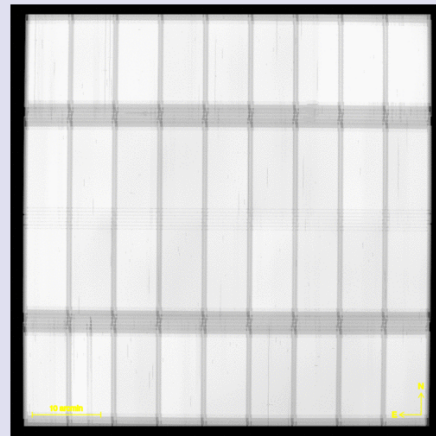
raw image weight map  
background map PSF map  
Galaxy counts histogram Galaxy selection rh-mag  
Star counts histogram Star selection rh-mag  
PSF orientation diagram and ellipticity map  
Reference astrometric errors  
subimages  
Summary table [csv]  
Processed on 29-12-2011 23:11:29 by condor2 with qualityFITS v.1.13.12 in 409 s send bug reports to magnard@iap.fr

Keyword	Value
ORIGIN	CFHT
TELESCOP	CFHT 3.6m
DETECTOR	MegaCam
INSTRUME	MegaPrime
DATE	2010-11-28T19:00:40

Keyword	Value
OBJECT	w4.+2-1
EXPTIME	5.535909000E+03
FILTER	i.MP9701
EQUINOX	2000.0000

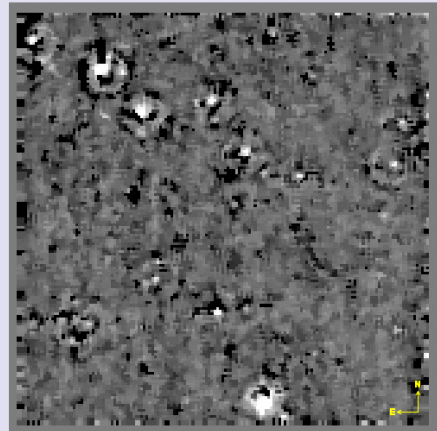


Raw mosaic image

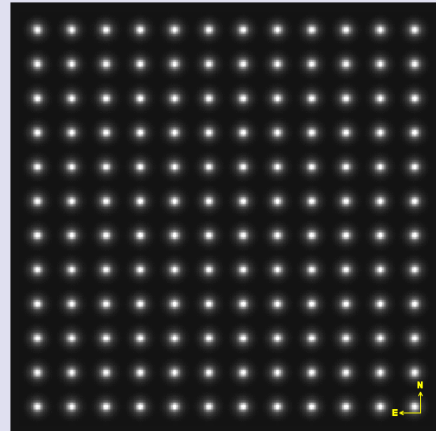


Mosaic of weightmap

Note to Internet Explorer users: IE is unable to render properly the transparency in PNG images. Prefer mozilla. Cf. test.



mosaic of backgrounds (gamma=2.2)  
mesh size = 64 pixels



mosaic of PSF

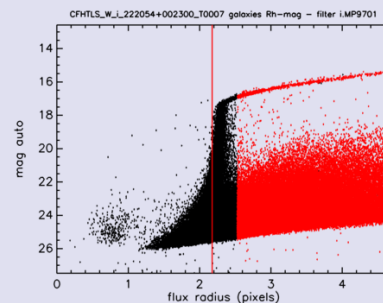
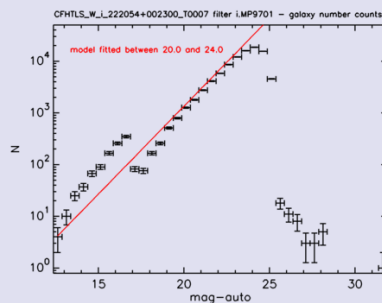


**Figure 48:** QFITS-out page of the W4 CFHTLS\_W\_i\_222054+002300 stack. The top table summarises the images origin and the nature of the stack. The next images show, from top left to bottom right: binned images of the stack, its weight-map, and the sky background; the PSF over the MegaCam field. The plots at the bottom show the galaxy counts (left) derived from the .1dac catalogue. The galaxies are extracted from a blind selection of the sources shown on the right  $r_h - mag$  plot (red points). The red line on the galaxy count plot is the expectation.

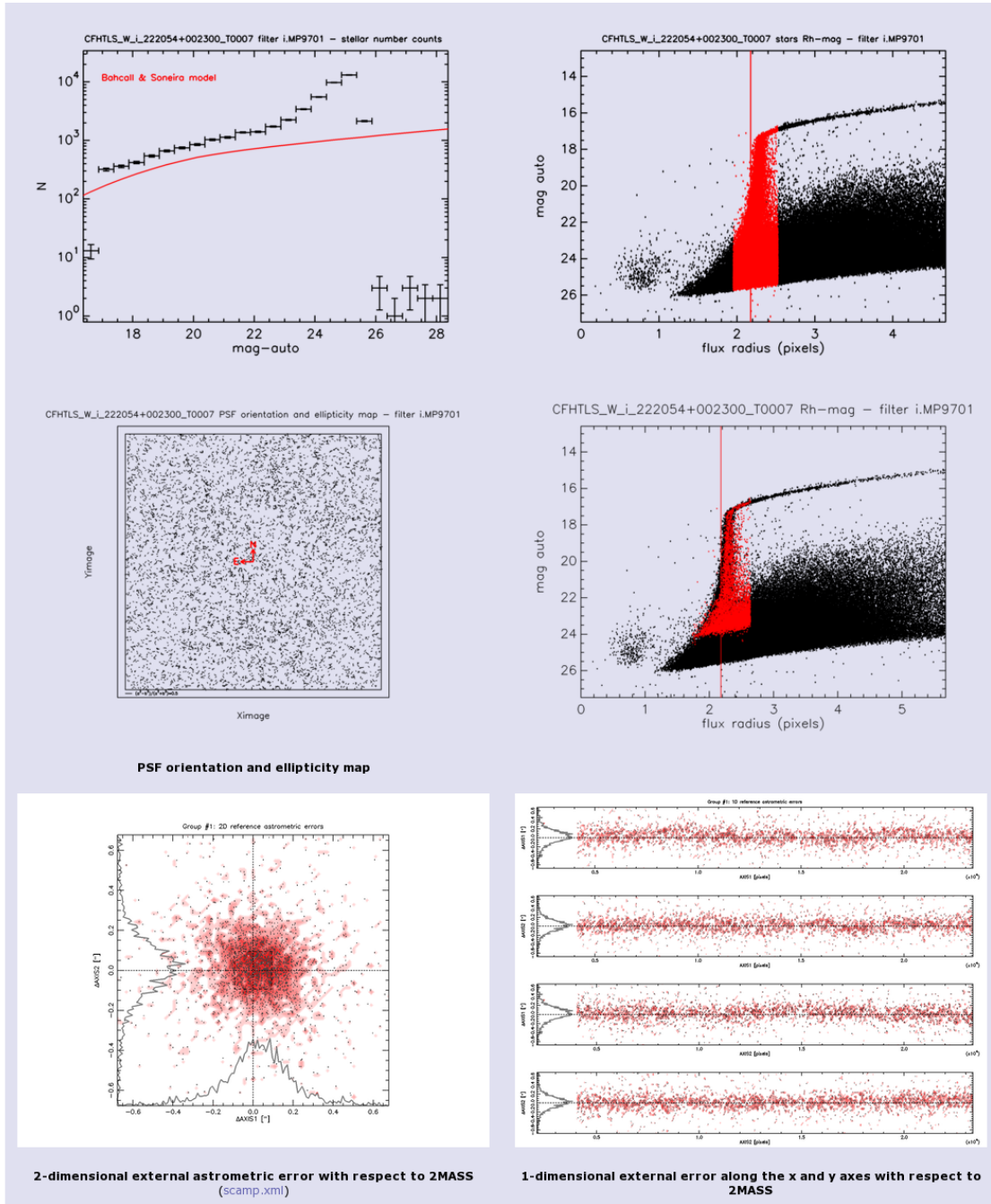
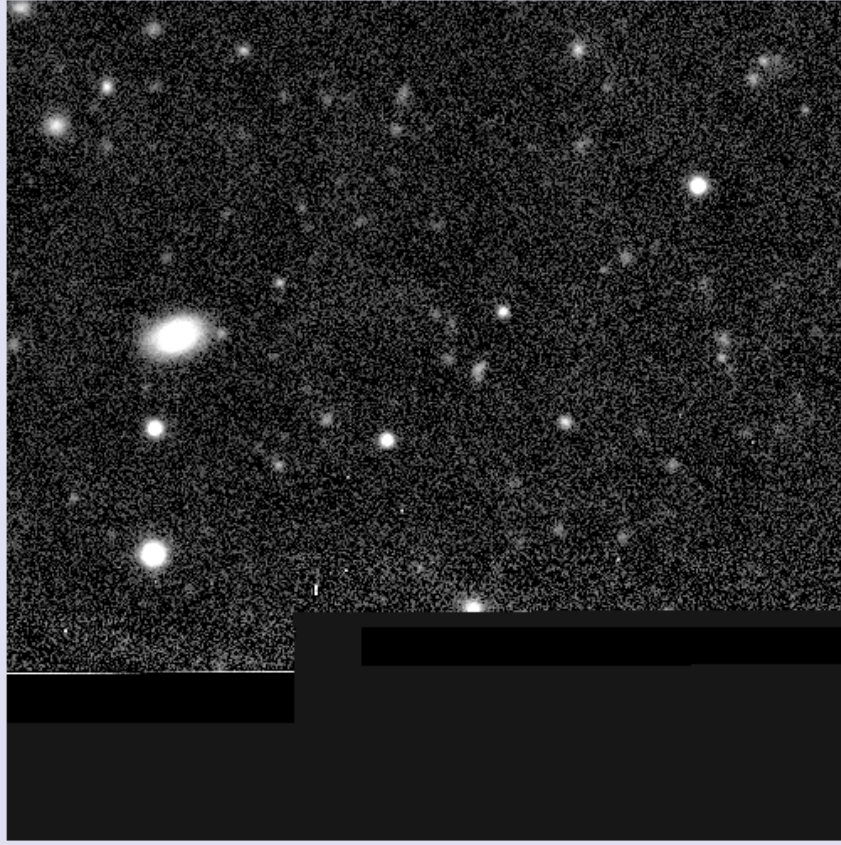


**Figure 49:** QFITS-out page of the same field (cont'd). The clickable plots show, from top left to bottom right, the stellar-counts (left) derived from a blind selection of red sources shown on the right  $r_h - magnitude$  plot. The red line is the predictions of the Bahcall-Soneira model. The plot on the middle panel shows the amplitude  $((a^2 - b^2)/(a^2 + b^2) = \text{length of lines})$  and the orientation (= orientation of lines) of the stellar ellipticity vectors over the MegaCam field. The selected sources are the red points shown on the right  $r_h - magnitude$  plot. The plots at the bottom are the 2-dimensional (left) and 1-dimensional astrometric errors of sources with respect to the 2MASS catalogue. They are produced by running SCAMP in a simple diagnostic mode (-MATCH N -SOLVE\_ASTROM N -SOLVE\_PHOTOM N).



Summary of scamp astrometric statistics	
AstromChi2_Internal_HighSN	0
AstromChi2_Reference	1.97
AstromChi2_Reference_HighSN	1.97
AstromNDets_Internal_HighSN	2504
AstromNDets_Reference	2506

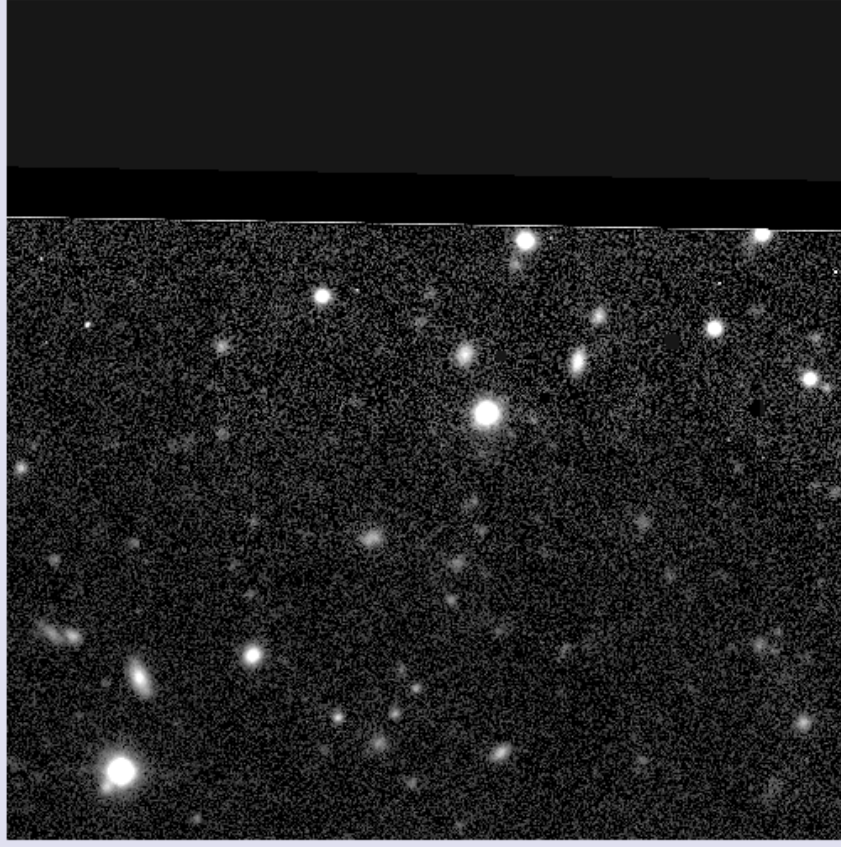


subimage1 CFHTLS\_W\_I\_222054+002300\_T0007[0] (EXT\_0)

4x4 binned chip	background (ADU)	sigma_bkg (mag/arcsec <sup>2</sup> )	nsexdet	seeing (pix)	FRseeing (arcsec)	seeing loaded	schiz2
pixel (1,1) is at lower left	-0.0	1.7	151438	3.521	4.354	0.655	0.810
EXT_0		-0.16					8390
							6402
							1.36

qualityFITS command line : /usr/local/bin/qualityFITS -vw --pass2 --scamp --subim 500 CFHTLS\_W\_I\_222054+002300\_T0007.fits --weight CFHTLS\_W\_I\_222054+002300\_T0007\_weight.fits --sexldac CFHTLS\_W\_I\_222054+002300\_T0007.ldac --background CFHTLS\_W\_I\_222054+002300\_T0007\_mbkkg.fits --logfile CFHTLS\_W\_I\_222054+002300\_T0007\_log --filterfile /data/fci6/raid2/hudelot/CFHTLS/T0007/raide/fci6/raide/raide\_filters\_magcam.dat -c /data/fci6/raid2/hudelot/CFHTLS/T0007/Wide/Rescale199\_apCorr/QFITS-out/qualityFITS-out\_T0007.rc

Summary of scamp astrometric statistics	
AstromNDets_Reference_HighSN	2504
AstromSigma_Internal_HighSN (arcsec)	0 0
AstromSigma_Reference (arcsec)	0.23 0.22
AstromSigma_Reference_HighSN (arcsec)	0.22 0.22



subimage2 CFHTLS\_W\_I\_222054+002300\_T0007[0] (EXT\_0)

4x4 binned chip	background (ADU)	sigma_bkg (mag/arcsec <sup>2</sup> )	nsexdet	seeing (pix)	FRseeing (arcsec)	seeing loaded	schiz2
pixel (1,1) is at lower left	-0.0	1.7	151438	3.521	4.354	0.655	0.810
EXT_0		-0.16					8390
							6402
							1.36

qualityFITS command line : /usr/local/bin/qualityFITS -vw --pass2 --scamp --subim 500 CFHTLS\_W\_I\_222054+002300\_T0007.fits --weight CFHTLS\_W\_I\_222054+002300\_T0007\_weight.fits --sexldac CFHTLS\_W\_I\_222054+002300\_T0007.ldac --background CFHTLS\_W\_I\_222054+002300\_T0007\_mbkkg.fits --logfile CFHTLS\_W\_I\_222054+002300\_T0007\_log --filterfile /data/fci6/raid2/hudelot/CFHTLS/T0007/raide/fci6/raide/raide\_filters\_magcam.dat -c /data/fci6/raid2/hudelot/CFHTLS/T0007/Wide/Rescale199\_apCorr/QFITS-out/qualityFITS-out\_T0007.rc

## 6.5 Transfer to CADC and CDS

### 6.5.1 Data products at CADC

The data products that are archived and distributed by CADC are all MD5 checksummed by TERAPIX prior to delivery to CADC. The MD5-checksum is calculated again immediately before and after the transfer, and the checksum values are all preserved in the CADC archive. TERAPIX verified the integrity of the whole T0007 release by comparing the TERAPIX and CADC checksum values. The checksums can be downloaded by the CFHTLS users so any user can verify that the images are not corrupted after the transfer from CADC to his own disk.

Note that prior to transfer all data are now compressed using gzip. There is no longer RICE compressed data in the T0007 archived because all weight-map and stack images are not 16-bit Integer FITS files. CFHTLS users also expressed a preference for gzipped data.

### 6.5.2 Data products at CDS

The Centre de Donnees astronomiques de Strasbourg (CDS) (Genova et al., 2000) provides several products derived from the CFHTLS T0007 surveys:

- The catalog of observations: two tables (II/317/cfhtls\_w, II/317/cfhtls\_d), for Wide and Deep surveys respectively (fields W1-W4: 35,651,677 sources; fields D1-D4: 2,293,851 sources). This catalog is available via the VizieR catalog service (Ochsenbein et al., 2000) for any Web users and for Virtual-observatory compatible tools such as Aladin (Bonnarel et al., 2000) or Topcat (Taylor, 2005). This catalog has been also integrated in the CDS cross-match service (Pineau et al., 2011) allowing it to be easily correlated with any other catalogue at the CDS;
- 10 multi-resolution all-sky previews (one preview per *ugriz* band and one per survey (Wide, Deep) and two coloured multi-resolution all-sky previews (based on *ugi* bands). Each preview allows one to zoom and pan into the four fields of the CFHTLS (W1-W4 for the Wide survey, and D1-D4 for the Deep survey) combined as a unique global sky (see Figure 51). These multi-resolution all-sky previews can be visualised by Aladin or other compatible tools. These all-sky previews has been generated from 9 recursive HEALPix sky tessellations from 52 to 0.2'' pixel angular resolution (HEALPix Norder 3 to 11) using a bilinear resampling from the original images to the deeper HEALPix grid (Norder 11). A weighted average based on the distance to the border has been applied on the pixels found in the original image overlap regions. Pixels from HEALPix order N is the average value of the 4 corresponding HEALPix pixels of the order N+1. The all-sky previews are delivered in JPEG-encoded tiles (8 bits pixel values - compressed) and in FITS encoded tiles (true pixel values) (Fernique et al., 2010).

These products are available through the following links :

- VizieR direct access<sup>29</sup>
- CDS Xmatch<sup>30</sup>
- Alladin<sup>31</sup> : (Menu File => Allsky => Image => Optical => CFHTLS, see illustration)

<sup>29</sup><http://vizier.u-strasbg.fr/viz-bin/VizieR?-source=CFHTLS-T0007>

<sup>30</sup><http://cdsxmatch.u-strasbg.fr/xmatch>

<sup>31</sup><http://aladin.u-strasbg.fr>



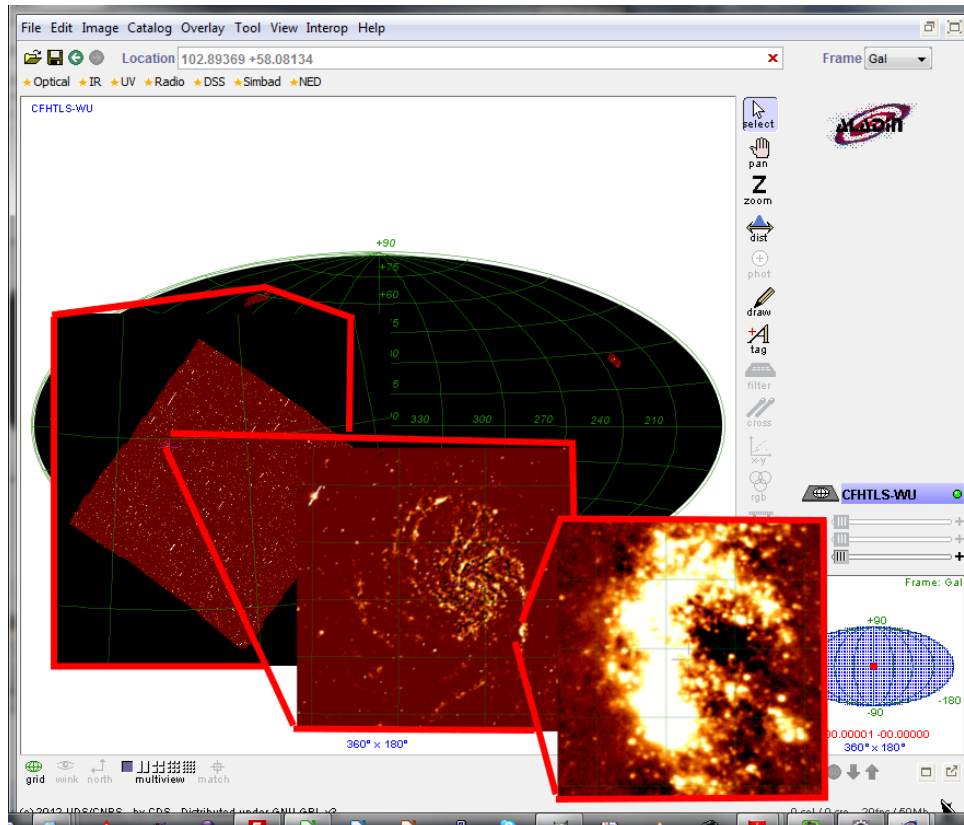
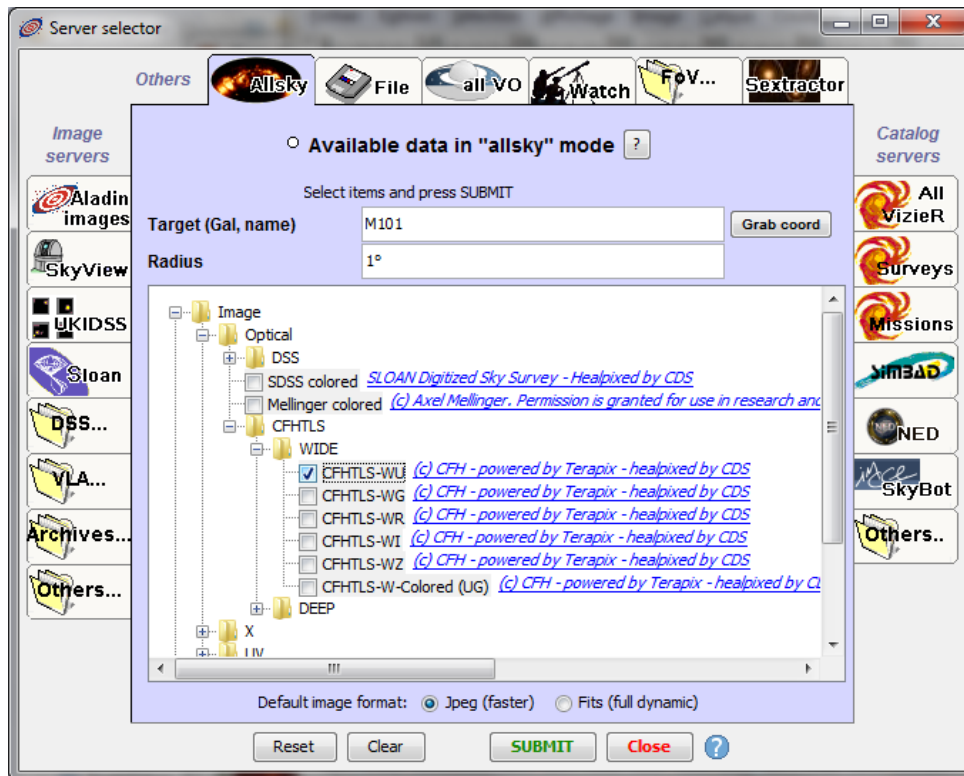


**Figure 51:** Upper panel: CFHTLS all-sky previews available via Aladin server. Lower Panel: From the whole sky view to M101: an example of CFHTLS Wide  $u$ -band multi-resolution all-sky preview.

## 7 Acknowledgements

We thank Emmanuel Bertin for practical advice on the use of the AstrOmatic software suite; the CFHT staff, in particular the QSO team; the SNLS team, in particular Pierre Astier, Ray Carlberg, Julien Guy, Chris Pritchett, Raynald Pain; CADAM, in particular JJ Kavelaars and John Ouellette; the CDS in Strasbourg; the CFHTLS Data Operation Group and the CFHTLS Steering Group. Terapix is funded by the French national research agency (CNRS/INSU), the Programme National Cosmologie et Galaxies (PNCG), the Service d’Astrophysique of the Commissariat à l’Energie Atomique (CEA/SAp), the Institut d’Astrophysique de Paris (IAP), the Agence National de la Recherche (ANR) grants ECOSSTAT, DESIR and TG\_REGALDIS, and the European FP5 RTD contracts “Astrowise” and “AVO” (Astrophysical Virtual Observatory).

Funding for SDSS-III has been provided by the Alfred P. Sloan Foundation, the Participating Institutions, the National Science Foundation, and the U.S. Department of Energy Office of Science. The SDSS-III web site is <http://www.sdss3.org/>.

SDSS-III is managed by the Astrophysical Research Consortium for the Participating Institutions of the SDSS-III Collaboration including the University of Arizona, the Brazilian Participation Group, Brookhaven National Laboratory, University of Cambridge, Carnegie Mellon University, University of Florida, the French Participation Group, the German Participation Group, Harvard University, the Instituto de Astrofísica de Canarias, the Michigan State/Notre Dame/JINA Participation Group, Johns Hopkins University, Lawrence Berkeley National Laboratory, Max Planck Institute for Astrophysics, Max Planck Institute for Extraterrestrial Physics, New Mexico State University, New York University, Ohio State University, Pennsylvania State University, University of Portsmouth, Princeton University, the Spanish Participation Group, University of Tokyo, University of Utah, Vanderbilt University, University of Virginia, University of Washington, and Yale University.

This survey makes use of data products from the Two Micron All Sky Survey, which is a joint project of the University of Massachusetts and the Infrared Processing and Analysis Center/California Institute of Technology, funded by the National Aeronautics and Space Administration and the National Science Foundation.

# A CFHTLS T0007 Wide supplementary information

## A.1 Complete list of Wide stacks coordinates, filters and exposure time

**Table 31:** The CFHTLS T0007 Wide stack list. Stacks are listed by Cartesian Ident name (column #1). Field coordinates are provided in columns #2 and #3. Column #4 gives the filters in which stacks were observed (important especially for i/y filters). The last five columns quote the total exposure times of T0007 stacks provided by TERAPIX. Highlighted entries denote exposure time and/or filter changes as compared to T0006 due to the VIPERS-DDT exposures. The relative positions of all fields of the list are shown in Fig. 20. The complete set of CFHTLS input images combined into each stack are listed in Appendix A.2.

W Cartesian Ident name	CFHTLS Ident name	RA [J2000]	DEC [J2000]	Filters	Exp. Time $u^*$ [s]	Exp. Time $g$ [s]	Exp. Time $r$ [s]	Exp. Time $i/y$ [s]	Exp. Time $z$ [s]
W1(-4 - 4)	020241-104400	02:02:41.15	-10:44:00	$u^*, g, r, y, z$	3000.0	2500.0	2000.0	7380.0	3600.0
W1(-4 - 3)	020241-094800	02:02:41.15	-09:48:00	$u^*, g, r, i, z$	3000.0	3000.0	2000.0	4305.0	3600.0
W1(-4 - 2)	020241-085200	02:02:41.15	-08:52:00	$u^*, g, r, i, z$	3000.0	2500.0	2000.0	4920.0	4200.0
W1(-4 - 1)	020241-075600	02:02:41.15	-07:56:00	$u^*, g, r, i, z$	3000.0	2500.0	2000.0	4305.0	3600.0
W1(-4 - 0)	020241-070000	02:02:41.15	-07:00:00	$u^*, g, r, i, z$	3000.0	2500.0	2000.0	4305.0	3600.0
W1(-4 + 1)	020241-060400	02:02:41.15	-06:04:00	$u^*, g, r, i, z$	3000.0	2500.0	2000.0	4305.0	3600.0
W1(-4 + 2)	020241-050800	02:02:41.15	-05:08:00	$u^*, g, r, i, z$	3000.0	3000.0	2000.0	4305.0	3600.0
W1(-4 + 3)	020241-041200	02:02:41.15	-04:12:00	$u^*, g, r, i, z$	3000.0	2500.0	2000.0	4305.0	3600.0
W1(-3 - 4)	020631-104400	02:06:30.86	-10:44:00	$u^*, g, r, y, z$	3000.0	2500.0	2000.0	4305.0	3600.0
W1(-3 - 3)	020631-094800	02:06:30.86	-09:48:00	$u^*, g, r, i, z$	3000.0	2500.0	2000.0	4305.0	3600.0
W1(-3 - 2)	020631-085200	02:06:30.86	-08:52:00	$u^*, g, r, i, z$	3000.0	2500.0	2000.0	4305.0	3600.0
W1(-3 - 1)	020631-075600	02:06:30.86	-07:56:00	$u^*, g, r, i, z$	3000.0	2500.0	2000.0	4920.0	3600.0
W1(-3 - 0)	020631-070000	02:06:30.86	-07:00:00	$u^*, g, r, i, z$	3000.0	6500.0	2000.0	4305.0	3600.0
W1(-3 + 1)	020631-060400	02:06:30.86	-06:04:00	$u^*, g, r, i, z$	3000.0	3500.0	2000.0	3690.0	3600.0
W1(-3 + 2)	020631-050800	02:06:30.86	-05:08:00	$u^*, g, r, i, z$	3000.0	2500.0	2000.0	4305.0	6600.0
W1(-3 + 3)	020631-041200	02:06:30.86	-04:12:00	$u^*, g, r, i, z$	3000.0	2500.0	2000.0	4305.0	3600.0
W1(-2 - 4)	021021-104400	02:10:20.58	-10:44:00	$u^*, g, r, y, z$	3600.0	2500.0	2000.0	4305.0	3600.0
W1(-2 - 3)	021021-094800	02:10:20.58	-09:48:00	$u^*, g, r, i, z$	3000.0	2500.0	2000.0	4305.0	3600.0
W1(-2 - 2)	021021-085200	02:10:20.58	-08:52:00	$u^*, g, r, i, z$	3000.0	2500.0	2500.0	4305.0	3600.0
W1(-2 - 1)	021021-075600	02:10:20.58	-07:56:00	$u^*, g, r, i, z$	3000.0	2500.0	2500.0	4305.0	3600.0
W1(-2 - 0)	021021-070000	02:10:20.58	-07:00:00	$u^*, g, r, i, z$	3000.0	2500.0	2500.0	4305.0	3600.0
W1(-2 + 1)	021021-060400	02:10:20.58	-06:04:00	$u^*, g, r, i, z$	3000.0	2500.0	2000.0	3690.0	3600.0
W1(-2 + 2)	021021-050800	02:10:20.58	-05:08:00	$u^*, g, r, i, z$	3000.0	2500.0	2000.0	4305.0	3600.0
W1(-2 + 3)	021021-041200	02:10:20.58	-04:12:00	$u^*, g, r, i, z$	3000.0	2500.0	2000.0	4305.0	3600.0
W1(-1 - 4)	021410-104400	02:14:10.29	-10:44:00	$u^*, g, r, y, z$	3000.0	2500.0	2000.0	4305.0	3600.0
W1(-1 - 3)	021410-094800	02:14:10.29	-09:48:00	$u^*, g, r, i, z$	3000.0	2500.0	2000.0	4305.0	3600.0
W1(-1 - 2)	021410-085200	02:14:10.29	-08:52:00	$u^*, g, r, i, z$	3000.0	2500.0	2000.0	4920.0	3600.0
W1(-1 - 1)	021410-075600	02:14:10.29	-07:56:00	$u^*, g, r, i, z$	3000.0	2500.0	2000.0	4305.0	3600.0
W1(-1 - 0)	021410-070000	02:14:10.29	-07:00:00	$u^*, g, r, i, z$	3000.0	2500.0	2000.0	4305.0	3600.0
W1(-1 + 1)	021410-060400	02:14:10.29	-06:04:00	$u^*, g, r, i, z$	3600.0	3500.0	2000.0	4305.0	3600.0
W1(-1 + 2)	021410-050800	02:14:10.29	-05:08:00	$u^*, g, r, i, z$	3000.0	2500.0	2500.0	4305.0	6601.0
W1(-1 + 3)	021410-041200	02:14:10.29	-04:12:00	$u^*, g, r, i, z$	3000.0	2500.0	2000.0	3690.0	6000.0
W1(-0 - 4)	021800-104400	02:18:00.00	-10:44:00	$u^*, g, r, y, z$	3000.0	2500.0	2000.0	4305.0	3600.0
W1(-0 - 3)	021800-094800	02:18:00.00	-09:48:00	$u^*, g, r, i, z$	3000.0	3500.0	2000.0	4305.0	3600.0
W1(-0 - 2)	021800-085200	02:18:00.00	-08:52:00	$u^*, g, r, i, z$	3000.0	2500.0	3000.0	4305.0	3600.0
W1(-0 - 1)	021800-075600	02:18:00.00	-07:56:00	$u^*, g, r, i, z$	3000.0	2500.0	2000.0	4305.0	3600.0
W1(-0 - 0)	021800-070000	02:18:00.00	-07:00:00	$u^*, g, r, i, z$	3000.0	2500.0	2000.0	4920.0	3600.0
W1(-0 + 1)	021800-060400	02:18:00.00	-06:04:00	$u^*, g, r, i, z$	3000.0	2500.0	2500.0	4305.0	6601.0
W1(-0 + 2)	021800-050800	02:18:00.00	-05:08:00	$u^*, g, r, i, z$	3000.0	3000.0	2000.0	4305.0	6000.0
W1(-0 + 3)	021800-041200	02:18:00.00	-04:12:00	$u^*, g, r, i, z$	3000.0	2500.0	2000.0	4305.0	6000.0
W1(+1 - 4)	022150-104400	02:21:49.71	-10:44:00	$u^*, g, r, y, z$	3000.0	2500.0	2000.0	4305.0	3600.0
W1(+1 - 3)	022150-094800	02:21:49.71	-09:48:00	$u^*, g, r, i, z$	3000.0	2500.0	2000.0	4305.0	3600.0
W1(+1 - 2)	022150-085200	02:21:49.71	-08:52:00	$u^*, g, r, i, z$	3000.0	2500.0	2000.0	4920.0	3600.0
W1(+1 - 1)	022150-075600	02:21:49.71	-07:56:00	$u^*, g, r, y, z$	3000.0	2500.0	2000.0	4920.0	3600.0
W1(+1 - 0)	022150-070000	02:21:49.71	-07:00:00	$u^*, g, r, i, z$	3000.0	3000.0	2000.0	4305.0	3600.0
W1(+1 + 1)	022150-060400	02:21:49.71	-06:04:00	$u^*, g, r, y, z$	3000.0	4500.0	2000.0	3690.0	7201.0
W1(+1 + 2)	022150-050800	02:21:49.71	-05:08:00	$u^*, g, r, i, z$	3000.0	2500.0	2000.0	4305.0	6001.0

Continued on next page

Table 31 – Continued from previous page

W Cartesian Ident name	CFHTLS Ident name	RA [J2000]	DEC [J2000]	Filters	Exp. Time $u^*$ [s]	Exp. Time $g$ [s]	Exp. Time $r$ [s]	Exp. Time $i/y$ [s]	Exp. Time $z$ [s]
W1(+1 + 3)	022150–041200	02:21:49.71	–04:12:00	$u^*, g, r, i, z$	3000.0	2500.0	2500.0	4920.0	6001.0
W1(+2 – 4)	022539–104400	02:25:39.42	–10:44:00	$u^*, g, r, y, z$	3000.0	2500.0	2000.0	4305.0	3600.0
W1(+2 – 3)	022539–094800	02:25:39.42	–09:48:00	$u^*, g, r, i, z$	3000.0	2500.0	2000.0	4305.0	4200.0
W1(+2 – 2)	022539–085200	02:25:39.42	–08:52:00	$u^*, g, r, i, z$	3000.0	2500.0	2000.0	4305.0	3600.0
W1(+2 – 1)	022539–075600	02:25:39.42	–07:56:00	$u^*, g, r, i, z$	3000.0	2500.0	2000.0	3690.0	4200.0
W1(+2 – 0)	022539–070000	02:25:39.42	–07:00:00	$u^*, g, r, i, z$	3000.0	2500.0	3000.0	3690.0	3600.0
W1(+2 + 1)	022539–060400	02:25:39.42	–06:04:00	$u^*, g, r, y, z$	3000.0	2500.0	2000.0	<b>2100.0</b>	6000.0
W1(+2 + 2)	022539–050800	02:25:39.42	–05:08:00	$u^*, g, r, y, z$	<b>6600.0</b>	2500.0	2000.0	4920.0	6000.0
W1(+2 + 3)	022539–041200	02:25:39.42	–04:12:00	$u^*, g, r, i, z$	5950.0	2500.0	3000.0	4340.0	7200.0
W1(+3 – 4)	022929–104400	02:29:29.14	–10:44:00	$u^*, g, r, y, z$	3000.0	2500.0	2000.0	4305.0	3600.0
W1(+3 – 3)	022929–094800	02:29:29.14	–09:48:00	$u^*, g, r, i, z$	3000.0	2500.0	2500.0	4305.0	3600.0
W1(+3 – 2)	022929–085200	02:29:29.14	–08:52:00	$u^*, g, r, i, z$	4200.0	2500.0	2000.0	4305.0	3600.0
W1(+3 – 1)	022929–075600	02:29:29.14	–07:56:00	$u^*, g, r, i, z$	3000.0	2500.0	2000.0	4920.0	3600.0
W1(+3 – 0)	022929–070000	02:29:29.14	–07:00:00	$u^*, g, r, i, z$	3000.0	2500.0	2000.0	4340.0	7201.0
W1(+3 + 1)	022929–060400	02:29:29.14	–06:04:00	$u^*, g, r, y, z$	3000.0	<b>4450.0</b>	2000.0	3075.0	3600.0
W1(+3 + 2)	022929–050800	02:29:29.14	–05:08:00	$u^*, g, r, y, z$	4800.0	<b>3950.0</b>	2500.0	<b>1500.0</b>	3600.0
W1(+3 + 3)	022929–041200	02:29:29.14	–04:12:00	$u^*, g, r, i, z$	3000.0	2500.0	2000.0	3720.0	3600.0
W1(+4 – 4)	023319–104400	02:33:18.85	–10:44:00	$u^*, g, r, y, z$	3000.0	2500.0	2000.0	7380.0	3600.0
W1(+4 – 3)	023319–094800	02:33:18.85	–09:48:00	$u^*, g, r, i, z$	3000.0	3000.0	2000.0	4305.0	3600.0
W1(+4 – 2)	023319–085200	02:33:18.85	–08:52:00	$u^*, g, r, i, z$	3000.0	2500.0	2000.0	4305.0	3600.0
W1(+4 – 1)	023319–075600	02:33:18.85	–07:56:00	$u^*, g, r, i, z$	3000.0	2500.0	2000.0	4305.0	3600.0
W1(+4 – 0)	023319–070000	02:33:18.85	–07:00:00	$u^*, g, r, i, z$	3000.0	2500.0	2000.0	4960.0	3600.0
W1(+4 + 1)	023319–060400	02:33:18.85	–06:04:00	$u^*, g, r, i, z$	3000.0	<b>3950.0</b>	2000.0	4340.0	3600.0
W1(+4 + 2)	023319–050800	02:33:18.85	–05:08:00	$u^*, g, r, y, z$	3000.0	<b>4531.0</b>	2000.0	3075.0	3600.0
W1(+4 + 3)	023319–041200	02:33:18.85	–04:12:00	$u^*, g, r, i, z$	3000.0	2500.0	2000.0	3720.0	3600.0
W2(–1 – 1)	085011–051100	08:50:11.37	–05:11:00	$u^*, g, r, i, z$	3000.0	3000.0	2000.0	4305.0	3600.0
W2(–1 – 0)	085011–041500	08:50:11.37	–04:15:00	$u^*, g, r, i, z$	3000.0	2500.0	2000.0	4305.0	3600.0
W2(–1 + 1)	085011–031900	08:50:11.37	–03:19:00	$u^*, g, r, i, z$	3000.0	4000.0	2500.0	4305.0	3600.0
W2(–1 + 2)	085011–022300	08:50:11.37	–02:23:00	$u^*, g, r, i, z$	3000.0	3000.0	2000.0	4305.0	3600.0
W2(–1 + 3)	085011–012700	08:50:11.37	–01:27:00	$u^*, g, r, i, z$	3000.0	2500.0	2500.0	3690.0	3600.0
W2(–0 – 1)	085400–051100	08:54:00.00	–05:11:00	$u^*, g, r, i, z$	3000.0	2500.0	2000.0	4305.0	3600.0
W2(–0 – 0)	085400–041500	08:54:00.00	–04:15:00	$u^*, g, r, i, z$	3600.0	3000.0	2000.0	4305.0	4200.0
W2(–0 + 1)	085400–031900	08:54:00.00	–03:19:00	$u^*, g, r, i, z$	3000.0	2500.0	2000.0	4305.0	3600.0
W2(–0 + 2)	085400–022300	08:54:00.00	–02:23:00	$u^*, g, r, i, z$	3000.0	3000.0	2000.0	4305.0	3600.0
W2(–0 + 3)	085400–012700	08:54:00.00	–01:27:00	$u^*, g, r, i, z$	3000.0	2500.0	3000.0	4305.0	3600.0
W2(+1 – 1)	085749–051100	08:57:48.63	–05:11:00	$u^*, g, r, i, z$	3000.0	2500.0	2000.0	3690.0	3600.0
W2(+1 – 0)	085749–041500	08:57:48.63	–04:15:00	$u^*, g, r, i, z$	3000.0	2500.0	2000.0	4305.0	3600.0
W2(+1 + 1)	085749–031900	08:57:48.63	–03:19:00	$u^*, g, r, y, z$	3000.0	3000.0	3000.0	4305.0	3600.0
W2(+1 + 2)	085749–022300	08:57:48.63	–02:23:00	$u^*, g, r, i, z$	3600.0	3000.0	2000.0	4305.0	3600.0
W2(+1 + 3)	085749–012700	08:57:48.63	–01:27:00	$u^*, g, r, i, z$	3000.0	3000.0	2000.0	3690.0	3600.0
W2(+2 – 1)	090137–051100	09:01:37.26	–05:11:00	$u^*, g, r, i, z$	3000.0	2500.0	2000.0	4305.0	3600.0
W2(+2 – 0)	090137–041500	09:01:37.26	–04:15:00	$u^*, g, r, i, z$	3000.0	2500.0	2000.0	4305.0	3600.0
W2(+2 + 1)	090137–031900	09:01:37.26	–03:19:00	$u^*, g, r, i, z$	3000.0	3000.0	2000.0	4305.0	3600.0
W2(+2 + 2)	090137–022300	09:01:37.26	–02:23:00	$u^*, g, r, y, z$	3000.0	3000.0	2000.0	4305.0	3600.0
W2(+2 + 3)	090137–012700	09:01:37.26	–01:27:00	$u^*, g, r, i, z$	3000.0	2500.0	2000.0	4305.0	3600.0
W2(+3 – 1)	090526–051100	09:05:25.89	–05:11:00	$u^*, g, r, i, z$	3000.0	2500.0	2000.0	4305.0	3600.0
W2(+3 – 0)	090526–041500	09:05:25.89	–04:15:00	$u^*, g, r, i, z$	3000.0	2500.0	2000.0	4305.0	3600.0
W2(+3 + 1)	090526–031900	09:05:25.89	–03:19:00	$u^*, g, r, i, z$	3000.0	2500.0	2000.0	3690.0	3600.0
W2(+3 + 2)	090526–022300	09:05:25.89	–02:23:00	$u^*, g, r, i, z$	3000.0	2500.0	2000.0	4325.0	7201.0
W2(+3 + 3)	090526–012700	09:05:25.89	–01:27:00	$u^*, g, r, i, z$	3000.0	2500.0	2000.0	4305.0	3600.0
W3(–3 – 3)	140016+514231	14:00:16.28	+51:42:31	$u^*, g, r, i, z$	3001.0	2500.0	2000.0	4306.0	3601.0
W3(–3 – 2)	135955+523831	13:59:55.42	+52:38:31	$u^*, g, r, i, z$	3000.0	2500.0	2000.0	4306.0	4201.0
W3(–3 – 1)	135933+533431	13:59:33.41	+53:34:31	$u^*, g, r, i, z$	3000.0	2500.0	2000.0	3720.0	3601.0
W3(–3 – 0)	135910+543031	13:59:10.19	+54:30:31	$u^*, g, r, i, z$	3000.0	2500.0	2000.0	4306.0	3601.0
W3(–3 + 1)	135846+552631	13:58:45.65	+55:26:31	$u^*, g, r, y, z$	3001.0	2500.0	2000.0	4306.0	3601.0
W3(–3 + 2)	135820+562231	13:58:19.70	+56:22:31	$u^*, g, r, i, z$	3000.0	2500.0	2500.0	4306.0	3601.0
W3(–3 + 3)	135752+571831	13:57:52.22	+57:18:31	$u^*, g, r, i, z$	3000.0	2501.0	2000.0	4306.0	3601.0
W3(–2 – 3)	140609+514231	14:06:08.85	+51:42:31	$u^*, g, r, i, z$	3000.0	2500.0	2000.0	4306.0	3601.0
W3(–2 – 2)	140555+523831	14:05:54.95	+52:38:31	$u^*, g, r, i, z$	3001.0	2500.0	2000.0	4306.0	3601.0

Continued on next page

Table 31 – Continued from previous page

W Cartesian Ident name	CFHTLS Ident name	RA [J2000]	DEC [J2000]	Filters	Exp. Time $u^*$ [s]	Exp. Time $g$ [s]	Exp. Time $r$ [s]	Exp. Time $i/y$ [s]	Exp. Time $z$ [s]
W3(-2 - 1)	140540+533431	14:05:40.27	+53:34:31	$u^*, g, r, y, z$	3000.0	2500.0	2000.0	4306.0	3601.0
W3(-2 - 0)	140525+543031	14:05:24.79	+54:30:31	$u^*, g, r, i, z$	3000.0	2500.0	2000.0	3691.0	3601.0
W3(-2 + 1)	140509+552631	14:05:08.43	+55:26:31	$u^*, g, r, y, z$	3000.0	2501.0	2501.0	4306.0	3601.0
W3(-2 + 2)	140451+562231	14:04:51.13	+56:22:31	$u^*, g, r, i, z$	3000.0	2501.0	2000.0	3691.0	3601.0
W3(-2 + 3)	140433+571831	14:04:32.82	+57:18:31	$u^*, g, r, y, z$	3000.0	2501.0	3001.0	4306.0	3601.0
W3(-1 - 3)	141202+514231	14:12:01.43	+51:42:31	$u^*, g, r, i, z$	3000.0	2500.0	2000.0	6152.0	3601.0
W3(-1 - 2)	141155+523831	14:11:54.47	+52:38:31	$u^*, g, r, i, z$	3000.0	2501.0	2501.0	4306.0	3601.0
W3(-1 - 1)	141147+533431	14:11:47.14	+53:34:31	$u^*, g, r, i, z$	3001.0	2500.0	2000.0	4306.0	3601.0
W3(-1 - 0)	141139+543031	14:11:39.40	+54:30:31	$u^*, g, r, i, z$	3000.0	2500.0	2000.0	4306.0	3601.0
W3(-1 + 1)	141131+552631	14:11:31.22	+55:26:31	$u^*, g, r, i, z$	3000.0	2501.0	2001.0	3691.0	3601.0
W3(-1 + 2)	141123+562231	14:11:22.56	+56:22:31	$u^*, g, r, i, z$	3000.0	2501.0	2001.0	4306.0	3601.0
W3(-1 + 3)	141113+571831	14:11:13.41	+57:18:31	$u^*, g, r, y, z$	3001.0	2501.0	2000.0	4306.0	3601.0
W3(-0 - 3)	141754+514231	14:17:54.00	+51:42:31	$u^*, g, r, i, z$	3000.0	2500.0	3001.0	4341.0	3601.0
W3(-0 - 2)	141754+523831	14:17:54.00	+52:38:31	$u^*, g, r, i, z$	3000.0	2500.0	2501.0	4341.0	3601.0
W3(-0 - 1)	141754+533431	14:17:54.00	+53:34:31	$u^*, g, r, i, z$	3001.0	2500.0	2500.0	3721.0	3601.0
W3(-0 - 0)	141754+543031	14:17:54.00	+54:30:31	$u^*, g, r, i, z$	3000.0	2500.0	2000.0	4341.0	3601.0
W3(-0 + 1)	141754+552631	14:17:54.00	+55:26:31	$u^*, g, r, i, z$	3000.0	2501.0	2000.0	4306.0	3601.0
W3(-0 + 2)	141754+562231	14:17:54.00	+56:22:31	$u^*, g, r, i, z$	3001.0	2501.0	2001.0	4306.0	3601.0
W3(-0 + 3)	141754+571831	14:17:54.00	+57:18:31	$u^*, g, r, i, z$	3001.0	2501.0	2000.0	4306.0	3601.0
W3(+1 - 3)	142347+514231	14:23:46.57	+51:42:31	$u^*, g, r, i, z$	3000.0	3001.0	2501.0	4341.0	4201.0
W3(+1 - 2)	142354+523831	14:23:53.53	+52:38:31	$u^*, g, r, i, z$	3001.0	2501.0	2000.0	4341.0	3601.0
W3(+1 - 1)	142401+533431	14:24:00.86	+53:34:31	$u^*, g, r, i, z$	3000.0	2501.0	2000.0	4341.0	6002.0
W3(+1 - 0)	142409+543031	14:24:08.61	+54:30:31	$u^*, g, r, i, z$	3001.0	2501.0	2000.0	4341.0	5401.0
W3(+1 + 1)	142417+552631	14:24:16.79	+55:26:31	$u^*, g, r, i, z$	3001.0	2500.0	2000.0	4306.0	3601.0
W3(+1 + 2)	142425+562231	14:24:25.44	+56:22:31	$u^*, g, r, i, z$	6001.0	2501.0	2000.0	4306.0	3601.0
W3(+1 + 3)	142435+571831	14:24:34.59	+57:18:31	$u^*, g, r, i, z$	3001.0	2501.0	2000.0	4306.0	3601.0
W3(+2 - 3)	142939+514231	14:29:39.15	+51:42:31	$u^*, g, r, i, z$	3001.0	2501.0	2000.0	4961.0	4201.0
W3(+2 - 2)	142953+523831	14:29:53.05	+52:38:31	$u^*, g, r, i, z$	3000.0	3501.0	2000.0	4341.0	3600.0
W3(+2 - 1)	143008+533431	14:30:07.72	+53:34:31	$u^*, g, r, i, z$	3000.0	2501.0	2000.0	4961.0	3601.0
W3(+2 - 0)	143023+543031	14:30:23.21	+54:30:31	$u^*, g, r, i, z$	3001.0	2501.0	2000.0	4306.0	3601.0
W3(+2 + 1)	143040+552631	14:30:39.57	+55:26:31	$u^*, g, r, i, z$	3001.0	2500.0	2000.0	4306.0	4801.0
W3(+2 + 2)	143057+562231	14:30:56.87	+56:22:31	$u^*, g, r, i, z$	3001.0	2501.0	2000.0	4306.0	3601.0
W3(+2 + 3)	143115+571831	14:31:15.18	+57:18:31	$u^*, g, r, i, z$	3001.0	2500.0	2000.0	4306.0	3601.0
W3(+3 - 3)	143532+514231	14:35:31.73	+51:42:31	$u^*, g, r, i, z$	3001.0	2500.0	2000.0	3691.0	3601.0
W3(+3 - 2)	143553+523831	14:35:52.59	+52:38:31	$u^*, g, r, i, z$	3000.0	2500.0	2000.0	3691.0	3601.0
W3(+3 - 1)	143615+533431	14:36:14.59	+53:34:31	$u^*, g, r, y, z$	3000.0	2500.0	2000.0	4306.0	3601.0
W3(+3 - 0)	143638+543031	14:36:37.81	+54:30:31	$u^*, g, r, i, z$	3000.0	2500.0	2000.0	4306.0	3601.0
W3(+3 + 1)	143702+552631	14:37:02.35	+55:26:31	$u^*, g, r, i, z$	3001.0	2501.0	2000.0	4306.0	3601.0
W3(+3 + 2)	143728+562231	14:37:28.30	+56:22:31	$u^*, g, r, y, z$	3001.0	2500.0	2000.0	4921.0	3601.0
W3(+3 + 3)	143756+571831	14:37:55.78	+57:18:31	$u^*, g, r, i, z$	3001.0	2500.0	2000.0	4306.0	3601.0
W4(+2 - 2)	222054-003100	22:20:53.78	-00:31:00	$u^*, g, r, i, z$	3000.0	2500.0	2000.0	7995.0	7800.0
W4(+2 - 1)	222054+002300	22:20:53.77	+00:23:00	$u^*, g, r, i, z$	3000.0	2500.0	2000.0	4305.0	7200.0
W4(+2 + 0)	222054+011900	22:20:53.88	+01:19:00	$u^*, g, r, i, z$	3000.0	2500.0	2000.0	4305.0	3600.0
W4(+1 - 2)	221706-003100	22:17:05.77	-00:31:00	$u^*, g, r, i, z$	3000.0	2500.0	2000.0	3690.0	3600.0
W4(+1 - 1)	221706+002300	22:17:05.77	+00:23:00	$u^*, g, r, i, z$	3000.0	2500.0	2000.0	8611.0	3600.0
W4(+1 + 0)	221706+011900	22:17:05.82	+01:19:00	$u^*, g, r, i, z$	3000.0	2500.0	2000.0	4305.0	3600.0
W4(+1 + 1)	221706+021500	22:17:05.94	+02:15:00	$u^*, g, r, i, z$	3000.0	2500.0	2000.0	4305.0	3600.0
W4(+0 - 2)	221318-003100	22:13:17.76	-00:31:00	$u^*, g, r, i, z$	3000.0	5000.0	2000.0	4305.0	3600.0
W4(+0 - 1)	221318+002300	22:13:17.76	+00:23:00	$u^*, g, r, i, z$	3000.0	5000.0	2000.0	4305.0	3600.0
W4(+0 + 0)	221318+011900	22:13:17.76	+01:19:00	$u^*, g, r, i, z$	3000.0	2500.0	2500.0	4305.0	7200.0
W4(+0 + 1)	221318+021500	22:13:17.76	+02:15:00	$u^*, g, r, i, z$	3000.0	2500.0	2000.0	4305.0	3600.0
W4(-1 - 2)	220930-003100	22:09:29.75	-00:31:00	$u^*, g, r, i, z$	3000.0	2500.0	3000.0	4305.0	3600.0
W4(-1 - 1)	220930+002300	22:09:29.76	+00:23:00	$u^*, g, r, y, z$	3000.0	5500.0	2000.0	4305.0	3600.0
W4(-1 + 0)	220930+011900	22:09:29.70	+01:19:00	$u^*, g, r, i, z$	3000.0	2500.0	2000.0	4305.0	3600.0
W4(-1 + 1)	220930+021500	22:09:29.59	+02:15:00	$u^*, g, r, y, z$	3000.0	5000.0	2000.0	4305.0	3600.0
W4(-1 + 2)	220930+031100	22:09:29.41	+03:11:00	$u^*, g, r, y, z$	3000.0	2500.0	2000.0	4305.0	3600.0
W4(-1 + 3)	220930+040700	22:09:29.17	+04:07:00	$u^*, g, r, y, z$	3000.0	2500.0	2000.0	4305.0	3600.0
W4(-2 + 0)	220542+011900	22:05:41.64	+01:19:00	$u^*, g, r, i, z$	3000.0	2500.0	2500.0	7995.0	3600.0
W4(-2 + 1)	220542+021500	22:05:41.41	+02:15:00	$u^*, g, r, i, z$	3000.0	2500.0	2000.0	4305.0	3600.0
W4(-2 + 2)	220542+031100	22:05:41.06	+03:11:00	$u^*, g, r, y, z$	3000.0	2500.0	2000.0	4305.0	3600.0

Continued on next page

Table 31 – Continued from previous page

W Cartesian Ident name	CFHTLS Ident name	RA [J2000]	DEC [J2000]	Filters	Exp. Time $u^*$ [s]	Exp. Time $g$ [s]	Exp. Time $r$ [s]	Exp. Time $i/y$ [s]	Exp. Time $z$ [s]
W4(-2 + 3)	220542+040700	22:05:40.58	+04:07:00	$u^*, g, r, y, z$	3000.0	2500.0	2000.0	4305.0	3600.0
W4(-3 + 0)	220154+011900	22:01:53.58	+01:19:00	$u^*, g, r, i, z$	3000.0	2500.0	2000.0	4305.0	3600.0
W4(-3 + 1)	220154+021500	22:01:53.23	+02:15:00	$u^*, g, r, i, z$	4200.0	2500.0	2000.0	4305.0	3600.0
W4(-3 + 2)	220154+031100	22:01:52.70	+03:11:00	$u^*, g, r, i, z$	3000.0	2500.0	2000.0	4305.0	3600.0
W4(-3 + 3)	220154+040700	22:01:51.99	+04:07:00	$u^*, g, r, y, z$	3000.0	3000.0	2000.0	4305.0	3600.0
W4(+2 - 2)	222054-003100	22:20:53.78	-00:31:00	$u^*, g, r, i, z$	3000.0	2500.0	2000.0	7995.0	7800.0
W4(+2 - 1)	222054+002300	22:20:53.77	+00:23:00	$u^*, g, r, i, z$	3000.0	2500.0	2000.0	4305.0	7200.0
W4(+2 + 0)	222054+011900	22:20:53.88	+01:19:00	$u^*, g, r, i, z$	3000.0	2500.0	2000.0	4305.0	3600.0
W4(+1 - 2)	221706-003100	22:17:05.77	-00:31:00	$u^*, g, r, i, z$	3000.0	2500.0	2000.0	3690.0	3600.0
W4(+1 - 1)	221706+002300	22:17:05.77	+00:23:00	$u^*, g, r, i, z$	3000.0	2500.0	2000.0	8611.0	3600.0
W4(+1 + 0)	221706+011900	22:17:05.82	+01:19:00	$u^*, g, r, i, z$	3000.0	2500.0	2000.0	4305.0	3600.0
W4(+1 + 1)	221706+021500	22:17:05.94	+02:15:00	$u^*, g, r, i, z$	3000.0	2500.0	2000.0	4305.0	3600.0
W4(+0 - 2)	221318-003100	22:13:17.76	-00:31:00	$u^*, g, r, i, z$	3000.0	5000.0	2000.0	4305.0	3600.0
W4(+0 - 1)	221318+002300	22:13:17.76	+00:23:00	$u^*, g, r, i, z$	3000.0	5000.0	2000.0	4305.0	3600.0
W4(+0 + 0)	221318+011900	22:13:17.76	+01:19:00	$u^*, g, r, i, z$	3000.0	2500.0	2500.0	4305.0	7200.0
W4(+0 + 1)	221318+021500	22:13:17.76	+02:15:00	$u^*, g, r, i, z$	3000.0	2500.0	2000.0	4305.0	3600.0
W4(-1 - 2)	220930-003100	22:09:29.75	-00:31:00	$u^*, g, r, i, z$	3000.0	2500.0	3000.0	4305.0	3600.0
W4(-1 - 1)	220930+002300	22:09:29.76	+00:23:00	$u^*, g, r, y, z$	3000.0	5500.0	2000.0	4305.0	3600.0
W4(-1 + 0)	220930+011900	22:09:29.70	+01:19:00	$u^*, g, r, i, z$	3000.0	2500.0	2000.0	4305.0	3600.0
W4(-1 + 1)	220930+021500	22:09:29.59	+02:15:00	$u^*, g, r, y, z$	3000.0	5000.0	2000.0	4305.0	3600.0
W4(-1 + 2)	220930+031100	22:09:29.41	+03:11:00	$u^*, g, r, y, z$	3000.0	2500.0	2000.0	4305.0	3600.0
W4(-1 + 3)	220930+040700	22:09:29.17	+04:07:00	$u^*, g, r, y, z$	3000.0	2500.0	2000.0	4305.0	3600.0
W4(-2 + 0)	220542+011900	22:05:41.64	+01:19:00	$u^*, g, r, i, z$	3000.0	2500.0	2500.0	7995.0	3600.0
W4(-2 + 1)	220542+021500	22:05:41.41	+02:15:00	$u^*, g, r, i, z$	3000.0	2500.0	2000.0	4305.0	3600.0
W4(-2 + 2)	220542+031100	22:05:41.06	+03:11:00	$u^*, g, r, y, z$	3000.0	2500.0	2000.0	4305.0	3600.0
W4(-2 + 3)	220542+040700	22:05:40.58	+04:07:00	$u^*, g, r, y, z$	3000.0	2500.0	2000.0	4305.0	3600.0
W4(-3 + 0)	220154+011900	22:01:53.58	+01:19:00	$u^*, g, r, i, z$	3000.0	2500.0	2000.0	4305.0	3600.0
W4(-3 + 1)	220154+021500	22:01:53.23	+02:15:00	$u^*, g, r, i, z$	4200.0	2500.0	2000.0	4305.0	3600.0
W4(-3 + 2)	220154+031100	22:01:52.70	+03:11:00	$u^*, g, r, i, z$	3000.0	2500.0	2000.0	4305.0	3600.0
W4(-3 + 3)	220154+040700	22:01:51.99	+04:07:00	$u^*, g, r, y, z$	3000.0	3000.0	2000.0	4305.0	3600.0

## A.2 List of images in each Wide stack

**Table 32:** Full list of CFHTLS input images included in each Wide stacks. Highlighted entries denote new images or filter change as compared to T0006 (due to VIPERS-DDT data). The corresponding exposure times, or any details regarding each stack, are quoted in Tables 31, and in the T0007 synoptic table

W Cartesian Ident Name	Filter	CFHT odometer number of input images combined in stacks
W1(-4-4)	<i>u</i> *	1022212,1022213,1022214,1022215,1022216
	<i>g</i>	942766,942767,942768,942769,942770
	<i>r</i>	816609,816610,1014659,1014660
	<i>y</i>	967664,967665,967666,967894,967895,967896,1030576,1030578,1030579,1030580,1030581,1038680
	<i>z</i>	1037804,1037805,1037806,1037807,1037808,1037809
W1(-4-3)	<i>u</i> *	1022217,1022218,1022219,1022220,1022221
	<i>g</i>	862819,862822,862823,862824,862956,862957
	<i>r</i>	814948,814949,1014657,1014658
	<i>i</i>	880193,880194,880195,880196,880197,880198,880199
	<i>z</i>	1038038,1038039,1038040,1038041,1038042,1038043
W1(-4-2)	<i>u</i> *	1030705,1030706,1030708,1030710,1030748
	<i>g</i>	879742,879743,879744,879745,879746
	<i>r</i>	814942,814943,1014655,1014656
	<i>i</i>	880200,880201,880203,880204,880205,880206,880207,880208
	<i>z</i>	1038045,1038046,1038350,1038351,1038353,1038356,1038357
W1(-4-1)	<i>u</i> *	1030698,1030699,1030701,1030704,1038673
	<i>g</i>	879977,879978,879979,879980,879981
	<i>r</i>	811173,811174,811181,811186
	<i>i</i>	880209,880210,880211,880212,880213,880214,880215
	<i>z</i>	1038355,1038358,1038359,1038360,1038361,1038362
W1(-4-0)	<i>u</i> *	1030595,1030596,1030597,1030696,1030697
	<i>g</i>	880967,880968,880969,880970,880971
	<i>r</i>	814940,814941,1014651,1014652
	<i>i</i>	880434,880436,880437,880438,880439,880440,880441
	<i>z</i>	1038476,1038477,1038478,1038479,1038480,1038481
W1(-4+1)	<i>u</i> *	1030590,1030591,1030592,1030593,1038672
	<i>g</i>	880972,880973,880974,880975,880976
	<i>r</i>	810510,810511,1014649,1014650
	<i>i</i>	880977,880978,880979,880980,880981,880982,880983
	<i>z</i>	1038482,1038483,1038484,1038485,1038486,1038487
W1(-4+2)	<i>u</i> *	1030585,1030586,1030587,1030588,1030589
	<i>g</i>	883305,883306,885065,885317,885318,885319
	<i>r</i>	810504,810505,1014467,1014468
	<i>i</i>	881254,881255,881256,881257,881258,881259,881260
	<i>z</i>	1038488,1038489,1038490,1038491,1038493,1038661
W1(-4+3)	<i>u</i> *	1030476,1030477,1038669,1038670,1038671
	<i>g</i>	885422,885423,885424,885425,1031327
	<i>r</i>	810496,810497,1014465,1014466
	<i>i</i>	881261,881262,881263,881264,881265,881266,881267
	<i>z</i>	1038494,1038495,1038496,1038497,1038498,1038499
W1(-3-4)	<i>u</i> *	1030749,1030778,1030779,1030780,1030781
	<i>g</i>	942771,942772,942773,942774,942775
	<i>r</i>	816607,816608,1021185,1021186
	<i>y</i>	964850,964851,964852,964853,964854,964855,964856
	<i>z</i>	1037798,1037799,1037800,1037801,1037802,1037803
W1(-3-3)	<i>u</i> *	1030468,1030469,1030470,1030471,1030472
	<i>g</i>	872207,872208,872209,872210,872211
	<i>r</i>	814956,814957,1014463,1014464
	<i>i</i>	879636,879638,879639,879640,879641,879642,879643
	<i>z</i>	1030196,1030197,1030198,1030199,1030200,1030201
W1(-3-2)	<i>u</i> *	1022616,1022617,1022618,1022619,1022620
	<i>g</i>	872212,872213,872214,872215,872216
	<i>r</i>	810486,810487,1014461,1014462
	<i>i</i>	879644,879645,879646,879647,879648,879649,879650
	<i>z</i>	1030190,1030191,1030192,1030193,1030194,1030195

Continued on next page

Table 32 – Continued from previous page

W Cartesian Ident Name	Filter	CFHT odometer number of input images combined in stacks
W1(-3-1)	$u^*$	1022611,1022612,1022613,1022614,1022615
	$g$	872217,872218,872219,872220,872222
	$r$	810488,810516,1014459,1014460
	$i$	879747,879748,879749,879750,879753,879982,879983,879984
	$z$	1030075,1030076,1030077,1030078,1030079,1030080
W1(-3-0)	$u^*$	1030463,1030464,1030465,1030466,1030467
	$g$	872277,872279,872280,872281,872282,872283,872284,872285,872286,872287,872289,872290,872291
	$r$	810491,810517,1014008,1014009
	$i$	879985,879986,879987,879988,879989,879991,879992
	$z$	1030069,1030070,1030071,1030072,1030073,1030074
W1(-3+1)	$u^*$	1022472,1022473,1022475,1022476,1022610
	$g$	875012,875013,875014,875015,875016,875017,875018
	$r$	810492,810493,1014006,1014007
	$i$	880087,880088,880089,880091,880092,880093
	$z$	1030063,1030064,1030065,1030066,1030067,1030068
W1(-3+2)	$u^*$	1022467,1022470,1022471,1022608,1022609
	$g$	875122,875123,875124,875125,875126
	$r$	810494,810495,1013887,1013888
	$i$	880094,880095,880096,880097,880098,880099,880100
	$z$	1022623,1022624,1022625,1022626,1022627,1030057,1030058,1030059,1030060,1030061,1030062
W1(-3+3)	$u^*$	1022462,1022463,1022464,1022465,1022466
	$g$	879631,879632,879633,879634,879635
	$r$	809745,809746,1013885,1013886
	$i$	880101,880102,880103,880104,880105,880106,880107
	$z$	1022602,1022603,1022604,1022605,1022606,1022607
W1(-2-4)	$u^*$	1030783,1030784,1030787,1030788,1030789,1030790
	$g$	942777,942778,942779,942781,942782
	$r$	816405,816406,1021187,1021188
	$y$	964843,964844,964845,964846,964847,964848,964849
	$z$	1033066,1033067,1033068,1033069,1033070,1033071
W1(-2-3)	$u^*$	955734,955735,955736,955737,955738
	$g$	872201,872202,872203,872205,872206
	$r$	814962,814963,1022114,1022115
	$i$	875622,875623,875627,875783,875784,875785,875786
	$z$	964970,964971,964972,964973,964974,964975
W1(-2-2)	$u^*$	948436,948437,948438,948439,948440
	$g$	827404,827405,827406,827407,827408
	$r$	810417,810484,810485,1022477,1022478
	$i$	827409,827411,827412,827413,827414,827415,827416
	$z$	948613,948614,948615,948616,948617,948618
W1(-2-1)	$u^*$	948328,948329,948330,948331,948332
	$g$	821835,821836,821837,821838,821839
	$r$	809512,809612,809613,1022621,1022622
	$i$	821845,821846,821847,821848,821849,821850,821851
	$z$	947407,947409,955003,955004,955005,955006
W1(-2-0)	$u^*$	948311,948312,948313,948314,948315
	$g$	821598,821599,821600,821602,821603
	$r$	809506,809610,809611,1022481,1022482
	$i$	821604,821608,821609,821610,821612,821613,821614
	$z$	947392,947393,947395,947396,947397,947398
W1(-2+1)	$u^*$	947860,947861,947862,947863,947864
	$g$	821593,821594,821595,821596,821597
	$r$	809500,809501,1022225,1022226
	$i$	820501,820502,820565,820566,820567,820568
	$z$	942131,942132,942133,942134,942143,942197
W1(-2+2)	$u^*$	947855,947856,947857,947858,947859
	$g$	820488,820489,820490,820491,820492
	$r$	806863,806864,1022222,1022223
	$i$	820493,820494,820495,820496,820497,820498,820499
	$z$	890897,890898,890899,890900,890901,890902

Continued on next page



Table 32 – Continued from previous page

W Cartesian Ident Name	Filter	CFHT odometer number of input images combined in stacks
W1(-2+3)	$u^*$	947845,947846,947847,947848,947849
	$g$	820483,820484,820485,820486,820487
	$r$	806861,806862,1022479,1022480
	$i$	820409,820410,820411,820412,820413,820414,820415
	$z$	891213,891214,891215,891216,891217,891218
W1(-1-4)	$u^*$	1030791,1030792,1030793,1030794,1030795
	$g$	948431,948432,948433,948434,948435
	$r$	816403,816404,1021189,1021190
	$y$	964005,964006,964007,964008,964009,964010,964011
W1(-1-3)	$z$	1033060,1033061,1033062,1033063,1033064,1033065
	$u^*$	955393,955394,955395,955396,955397
	$g$	870647,870648,870649,870650,870802
	$r$	814969,814970,1022112,1022113
	$i$	875435,875436,875437,875438,875439,875441,875442
W1(-1-2)	$z$	964962,964963,964964,964966,964967,964968
	$u^*$	947850,947851,947852,947853,947854
	$g$	827417,827418,827419,827420,827421
	$r$	810415,810416,1021976,1021977
W1(-1-1)	$i$	831270,831271,831272,831273,831274,831275,831276,831277
	$z$	890762,890763,890764,890765,890767,890768
	$u^*$	942315,942316,942317,942318,942319
	$g$	821840,821841,821842,821843,821844
	$r$	809518,809519,1021974,1021975
W1(-1-0)	$i$	821852,821853,821854,821855,821856,821857,821858
	$z$	880680,880681,880682,880683,880684,880685
	$u^*$	889435,889436,889437,889438,889439
	$g$	820397,820398,820399,820400,820401
	$r$	806859,806860,1021972,1021973
W1(-1+1)	$i$	820402,820403,820404,820405,820406,820407,820408
	$z$	874465,874466,874467,874468,874469,874470
	$u^*$	880764,883008,883009,883011,883012,1031324
	$g$	816622,816784,819864,819865,819866,819867,819868
	$r$	806857,806858,1021970,1021971
W1(-1+2)	$i$	821586,821587,821588,821589,821590,821591,821592
	$z$	874117,874460,874461,874462,874463,874464
	$u^*$	765305,765306,765307,765308,765309
	$g$	765310,765316,765317,765318,765319
	$r$	759164,765302,765303,1021968,1021969
W1(-1+3)	$i$	764947,764948,764949,764950,764951,764952,764953
	$z$	765761,765762,765763,765764,765765,765766,766294,766295,766296,766297,766298
	$u^*$	765365,765366,765367,765368,765369
	$g$	765354,765358,765359,765362,765363
	$r$	758894,758895,1021966,1021967
W1(-0-4)	$i$	762828,762832,762833,762834,762835,762836
	$z$	765371,765372,765373,765374,765375,766359,766360,766361,766362,766363
	$u^*$	1030962,1030963,1030964,1030965,1030966
	$g$	942215,942216,942217,942219,942220
	$r$	816397,816398,1021191,1021192
W1(-0-3)	$y$	963763,963764,963765,963766,963767,963768,963769
	$z$	1037792,1037793,1037794,1037795,1037796,1037797
	$u^*$	948622,948623,948626,955391,955392
	$g$	863927,864040,870641,870642,870643,870644,870645
	$r$	814975,814976,1022110,1022111
W1(-0-2)	$i$	863913,863914,863920,863922,863923,863924,863925
	$z$	963435,963436,963437,963438,963439,963440
	$u^*$	947503,947504,947505,947506,947507
	$g$	827422,827423,827424,827425,827426
	$r$	810993,810994,810995,810996,1021978,1021979
	$i$	831160,831161,831162,831163,831164,831165,831166
	$z$	890351,890352,890353,890354,890355,890356

Continued on next page

Table 32 – Continued from previous page

W Cartesian Ident Name	Filter	CFHT odometer number of input images combined in stacks
W1(-0-1)	$u^*$	942205,942206,942207,942208,942209
	$g$	826625,826626,826627,826628,826629
	$r$	809614,809615,1021830,1021831
	$i$	826519,826520,826521,826522,826523,826524,826525
	$z$	880664,880665,880666,880668,880669,880670
W1(-0-0)	$u^*$	889633,889634,889635,889636,889637
	$g$	816413,816414,816415,816416,816509
	$r$	806855,806856,1021832,1021833
	$i$	816895,819719,819720,819721,819722,819723,819724,819725
	$z$	874471,874472,874473,874474,874475,874476
W1(-0+1)	$u^*$	761701,761702,761703,761704,761705
	$g$	761321,761322,761323,761324,761325
	$r$	759155,761326,761327,1021834,1021835
	$i$	762493,762494,762495,762496,762497,762498,762499
	$z$	765767,765768,765769,765770,765771,765772,766289,766290,766291,766292,766293
W1(-0+2)	$u^*$	761981,761982,761983,761984,761985
	$g$	762628,765155,765156,765157,765158,765159
	$r$	759153,759154,1021962,1021963
	$i$	762474,762475,762476,762477,762478,762479,762480
	$z$	764800,764801,764802,764803,764804,766177,766178,766179,766180,766181
W1(-0+3)	$u^*$	761970,761971,761972,761973,761974
	$g$	762623,762624,762625,762626,762627
	$r$	758577,758578,1021964,1021965
	$i$	762390,762391,762392,762393,762394,762395,762396
	$z$	764795,764796,764797,764798,764799,766170,766171,766172,766173,766174
W1(+1-4)	$u^*$	1030967,1030968,1030969,1030970,1030971
	$g$	942210,942211,942212,942213,942214
	$r$	815808,816392,1021193,1021194
	$y$	963756,963757,963758,963759,963760,963761,963762
	$z$	1032875,1032876,1032877,1032878,1032879,1032880
W1(+1-3)	$u^*$	948451,948619,948620,948621,1031326
	$g$	863283,863284,863285,863286,863287
	$r$	815132,815133,1022108,1022109
	$i$	875443,875444,875445,875446,875447,875489,875490
	$z$	955020,955021,955212,955213,955214,955215
W1(+1-2)	$u^*$	947498,947499,947500,947501,947502
	$g$	827325,827326,827327,827328,827329
	$r$	809776,809777,1021980,1021981
	$i$	830980,831153,831154,831155,831156,831157,831158,831159
	$z$	889306,889307,889308,889309,889310,889311
W1(+1-1)	$u^*$	883299,883300,883301,883302,883303
	$g$	826630,826631,826645,826646,826647
	$r$	809620,809621,1021828,1021829
	$y$	1030480,1038662,1038663,1038664,1038665,1038666,1038667,1038668
	$z$	884123,884124,884125,884126,884127,884128
W1(+1-0)	$u^*$	942076,942077,942080,942081,942082
	$g$	816407,816408,816409,816410,816411,816412
	$r$	806761,806762,1021814,1021815
	$i$	819869,819870,819871,819872,819873,819874,819875
	$z$	831420,831421,831422,831423,831532,831533
W1(+1+1)	$u^*$	761469,761470,761471,761472,761473
	$g$	761197,761198,761199,761200,761320,761582,761583,761584,761585
	$r$	758575,758576,1021683,1021684
	$y$	1030457,1030458,1030459,1030460,1030461,1030462
	$z$	761588,761592,761696,761697,761698,761699,761700,766164,766165,766166,766167,766168
W1(+1+2)	$u^*$	761838,761839,761840,761841,761842
	$g$	761826,761827,761828,761829,761830
	$r$	758401,758402,1021681,1021682
	$i$	760933,760934,760935,760936,760938,760939,760940
	$z$	764954,764955,764956,764957,764958,765858,765859,765860,765861,765862

Continued on next page

Table 32 – Continued from previous page

W Cartesian Ident Name	Filter	CFHT odometer number of input images combined in stacks
W1(+1+3)	$u^*$	761832,761833,761834,761835,761836
	$g$	728058,728059,728060,728061,728062
	$r$	779979,779980,780209,1021679,1021680
	$i$	758566,758567,758568,758569,758570,758571,758572,758573
	$z$	761059,761060,761061,761062,761063,765851,765852,765853,765854,765855
W1(+2-4)	$u^*$	1030972,1030973,1030974,1030975,1030976
	$g$	942050,942051,942052,942053,942075
	$r$	815620,815622,1021195,1021196
	$y$	963132,963133,963134,963135,963136,963137,963138
	$z$	1032233,1032234,1032235,1032236,1032237,1032238
W1(+2-3)	$u^*$	948441,948442,948443,948444,948445
	$g$	863090,863091,863092,863093,863094
	$r$	815138,815139,1022106,1022107
	$i$	875613,875614,875616,875617,875618,875619,875620
	$z$	960408,962895,962896,962897,962898,962899,962900
W1(+2-2)	$u^*$	947399,947400,947401,947402,1031325
	$g$	827313,827314,827315,827316,827317
	$r$	809770,809771,1021982,1021983
	$i$	827318,827319,827320,827321,827322,827323,827324
	$z$	885304,885306,885307,885308,885309,885310
W1(+2-1)	$u^*$	942200,942201,942202,942203,942204
	$g$	826736,826737,826738,826739,826740
	$r$	809626,809627,1021826,1021827
	$i$	826729,826731,826732,826733,826734,826735
	$z$	881347,884117,884118,884119,884120,884121,884122
W1(+2-0)	$u^*$	934919,934920,934921,935068,935200
	$g$	732957,732958,732959,732960,732961
	$r$	729725,729726,806759,806760,1021816,1021817
	$i$	816763,816764,816765,816766,816768,816769
	$z$	879864,879865,879866,879867,879868,879869
W1(+2+1)	$u^*$	761975,761976,761977,761978,761979
	$g$	728046,728047,728048,728049,728050
	$r$	727579,727580,1021673,1021674
	$y$	<b>1110944,1110945,1118156,1118157,1118158,1118159,1118308</b>
	$z$	764693,764694,764695,764696,764697,765846,765847,765848,765849,765850
W1(+2+2)	$u^*$	758888,758889,758890,758891,758892, <b>1110668,1110669,1110670,1110671,1110672,1110673</b>
	$g$	727461,727462,727463,727464,727465
	$r$	727459,727460,1021675,1021676
	$y$	1030300,1030301,1030302,1030303,1030305,1030306,1038678,1038679
	$z$	760942,760943,760944,760945,760946,765774,765775,765776,765777,765778
W1(+2+3)	$u^*$	719023,719024,719025,719026,719027,719028,719029
	$g$	715499,715500,715501,715502,715503
	$r$	715071,715072,715073,715074,1021677,1021678
	$i$	715226,715227,715228,715229,715230,715231,715232
	$z$	718692,718693,718694,718695,718696,718697,718698,718699,718700
W1(+3-4)	$u^*$	1030977,1030978,1030979,1030980,1030981
	$g$	934780,934781,934782,934783,934784
	$r$	815614,815615,1021370,1021371
	$y$	963125,963126,963127,963128,963129,963130,963131
	$z$	1032227,1032228,1032229,1032230,1032231,1032232
W1(+3-3)	$u^*$	948333,948334,948335,948446,948447
	$g$	863085,863086,863087,863088,863089
	$r$	815145,815273,815274,1022104,1022105
	$i$	874623,874624,874625,874626,874627,874628,874629
	$z$	948635,948636,948637,948638,955017,955018
W1(+3-2)	$u^*$	942325,942326,942397,942398,942399,942400,942401
	$g$	827307,827308,827309,827310,827311
	$r$	809764,809765,1022102,1022103
	$i$	827300,827301,827302,827303,827304,827305,827306
	$z$	885067,885068,885069,885070,885071,885072

Continued on next page

Table 32 – Continued from previous page

W Cartesian Ident Name	Filter	CFHT odometer number of input images combined in stacks
W1(+3-1)	$u^*$	942045,942046,942047,942048,942049
	$g$	826741,826742,826743,826744,826745
	$r$	809632,809633,1021824,1021825
	$i$	826746,826747,826748,826749,826750,826751,826752,826753
	$z$	880424,880425,880430,880431,880432,880435
W1(+3-0)	$u^*$	832185,832186,832187,832188,832189
	$g$	724440,724441,724442,724443,724444
	$r$	720440,720441,1021818,1021819
	$i$	720087,720088,720089,720090,720091,720092,720093
	$z$	832484,832485,832486,832487,832488,832489,832713,832714,832715,832716,832717,832719
W1(+3+1)	$u^*$	831522,831523,831524,831525,831526
	$g$	719196,719197,719198,719199,719200,719202, <b>1118579,1118580,1118581,1118582,1118583</b>
	$r$	719194,719195,1021671,1021672
	$y$	1030206,1030207,1030208,1038675,1038804
	$z$	831967,831968,831969,831970,831971,831972
W1(+3+2)	$u^*$	820092,826810,826811,831517,831518,831519,831520,831521
	$g$	724435,724436,724437,724438,724439, <b>1119117,1119118,1119119,1119120,1119121</b>
	$r$	719958,720444,720445,1021551,1021552
	$y$	<b>1118742,1118743,1118744,1118745,1118746</b>
	$z$	831862,831863,831864,831865,831866,831867
W1(+3+3)	$u^*$	816625,816626,816903,816904,1031323
	$g$	719946,719947,719948,719949,719950
	$r$	719944,719945,1021505,1021506
	$i$	719951,719952,719953,719954,719955,719956
	$z$	831631,831632,831633,831634,831635,831636
W1(+4-4)	$u^*$	1031188,1031189,1031190,1031191,1038674
	$g$	934914,934915,934916,934917,934918
	$r$	815289,816391,1021501,1021502
	$y$	962886,962887,962889,962890,962892,1030598,1030599,1030600,1030796,1030797,1030798,1030799
	$z$	1032881,1032882,1032883,1032884,1032885,1032886
W1(+4-3)	$u^*$	942402,942403,942404,948448,948449
	$g$	862721,863278,863279,863280,863281,863282
	$r$	815279,815287,1022100,1022101
	$i$	862611,862612,862613,862614,862615,862616,862617
	$z$	942760,942761,942762,942763,942764,942765
W1(+4-2)	$u^*$	942320,942321,942322,942323,942324
	$g$	826648,826649,826650,826651,826652
	$r$	810325,810326,1022098,1022099
	$i$	826960,826961,827067,827068,827069,827070,827071
	$z$	884609,884610,884611,884612,884613,884614
W1(+4-1)	$u^*$	940656,940658,941955,941956,942044
	$g$	826954,826955,826956,826957,826958
	$r$	810323,810324,1021822,1021823
	$i$	826819,826820,826821,826822,826823,826824,826825
	$z$	879878,879879,879880,879881,879882,879883
W1(+4-0)	$u^*$	832057,832058,832059,832060,832061
	$g$	724447,724448,724449,724450,724451
	$r$	720442,720443,1021820,1021821
	$i$	720102,720103,720104,720105,720106,720108,720109,720110
	$z$	832478,832479,832480,832481,832482,832483
W1(+4+1)	$u^*$	831857,831858,831859,831860,831861
	$g$	724612,724613,724614,724615,724616, <b>1118892,1118893,1118894,1118895,1118896</b>
	$r$	724371,724372,1021669,1021670
	$i$	723402,723403,723404,723405,723406,723407,723408
	$z$	832190,832191,832192,832193,832194,832195
W1(+4+2)	$u^*$	831626,831627,831628,831629,831630
	$g$	724606,724608,724609,724610,724611, <b>1118408,1118865,1118866,1118867,1118868,1118869,1118891</b>
	$r$	724369,724370,1021667,1021668
	$y$	1030216,1030217,1030218,1038676,1038677
	$z$	832062,832063,832064,832065,832066,832067

Continued on next page

Table 32 – Continued from previous page

W Cartesian Ident Name	Filter	CFHT odometer number of input images combined in stacks
W1(+4+3)	$u^*$	831527,831528,831529,831530,831531
	$g$	715504,715505,715506,715507,715820
	$r$	715075,715076,1021503,1021504
	$i$	720022,720023,720024,720025,720026,720027
	$z$	831973,831974,831975,831976,831977,831978
W2(-1-1)	$u^*$	906869,906870,906871,906872,906873
	$g$	881306,883362,883363,883364,883365,883366
	$r$	832209,832210,967608,967609
	$i$	832213,832214,832215,832216,832217,832218,832219
	$z$	900138,900139,900140,900141,900142,900143
W2(-1-0)	$u^*$	906775,906776,906777,906867,906868
	$g$	831665,831666,831667,831668,831669
	$r$	831656,831657,967606,967607
	$i$	831658,831659,831660,831661,831662,831663,831664
	$z$	900132,900133,900134,900135,900136,900137
W2(-1+1)	$u^*$	906177,906178,906179,906180,906181
	$g$	831313,831315,831316,831333,831334,831335,831336,831337
	$r$	831309,831310,831311,967604,967605
	$i$	831201,831202,831203,831204,831205,831206,831207
	$z$	900126,900127,900128,900129,900130,900131
W2(-1+2)	$u^*$	898948,898949,898951,898952,898953
	$g$	831195,831196,831197,831198,831199,831200
	$r$	831193,831194,967602,967603
	$i$	830746,830747,830748,830749,830750,830751,830752
	$z$	900037,900038,900039,900040,900041,900042
W2(-1+3)	$u^*$	898954,898955,898956,898957,898958
	$g$	731002,731003,731004,731005,731006
	$r$	730895,731000,731001,962772,962773
	$i$	775337,775339,775349,789017,789018,789019
	$z$	900031,900032,900033,900034,900035,900036
W2(-0-1)	$u^*$	963593,963594,963596,963597,987072
	$g$	881290,881291,881292,881293,881294
	$r$	832102,832103,967600,967601
	$i$	832086,832087,832088,832089,832090,832091,832092
	$z$	960992,960993,960994,960995,960996,960997
W2(-0-0)	$u^*$	905607,905608,905609,905610,905611,905612
	$g$	831561,831562,831563,831564,831565,831566
	$r$	831654,831655,967598,967599
	$i$	831549,831550,831551,831552,831553,831554,831555
	$z$	899551,899552,899553,899554,899555,899556,899557
W2(-0+1)	$u^*$	896035,896036,896037,896038,896039
	$g$	826673,826674,826675,826676,826677
	$r$	826541,826542,967596,967597
	$i$	830739,830740,830741,830742,830743,830744,830745
	$z$	899368,899369,899370,899371,899372,899373
W2(-0+2)	$u^*$	895798,895799,895800,895801,895802
	$g$	826839,826840,826841,826842,826843,826844
	$r$	826539,826540,967594,967595
	$i$	826665,826666,826667,826668,826669,826670,826671
	$z$	899140,899141,899142,899144,899145,899146
W2(-0+3)	$u^*$	895793,895794,895795,895796,895797
	$g$	789020,789021,789022,789023,789024
	$r$	730652,730653,777838,777839,962770,962771
	$i$	784772,784773,784774,784775,784776,784777,784778
	$z$	896289,896290,896291,896292,896293,896294
W2(+1-1)	$u^*$	963346,963347,963348,963349,963350
	$g$	880241,880242,880243,880244,880245
	$r$	832100,832101,967592,967593
	$i$	832093,832094,832095,832096,832097,832098
	$z$	960423,960424,960425,960428,960429,960431

Continued on next page

Table 32 – Continued from previous page

W Cartesian Ident Name	Filter	CFHT odometer number of input images combined in stacks
W2(+1-0)	$u^*$	905696,905697,905698,905699,905700
	$g$	831556,831557,831558,831559,831560
	$r$	831547,831548,967590,967591
	$i$	831433,831434,831435,831436,831437,831438,831439
	$z$	899558,899559,899560,899561,899562,899563
W2(+1+1)	$u^*$	896030,896031,896032,896033,896034
	$g$	789148,826660,826661,826662,826663,826664
	$r$	777631,777632,963359,963360,963372,963373
	$y$	986922,986923,986924,986925,986926,987068,987069
	$z$	889524,889525,889526,889527,889528,889529
W2(+1+2)	$u^*$	890112,890113,890114,890115,890117,890120
	$g$	774795,774796,774797,774798,774799,774800
	$r$	777305,777306,963157,963161
	$i$	777301,777302,777303,777304,777309,777310,777311
	$z$	889336,889337,889338,889339,889340,889341
W2(+1+3)	$u^*$	890107,890108,890109,890110,890111
	$g$	774288,774289,774293,774294,774295,774296
	$r$	777307,777308,962768,962769
	$i$	775154,775155,775158,775159,775161,775162
	$z$	889343,889344,889345,889346,889347,889348
W2(+2-1)	$u^*$	963166,963167,963168,963169,963170
	$g$	880237,880238,880239,880476,880477
	$r$	831997,831998,967588,967589
	$i$	832006,832007,832008,832009,832010,832011,832012
	$z$	956125,956126,956127,956128,956129,956130
W2(+2-0)	$u^*$	905819,905820,905821,905822,905823
	$g$	831347,831348,831349,831350,831351
	$r$	831345,831346,967586,967587
	$i$	831338,831339,831340,831341,831342,831343,831344
	$z$	899564,899565,899566,899568,899569,899570
W2(+2+1)	$u^*$	896025,896026,896027,896028,896029
	$g$	774116,774117,774118,774119,774120,774121
	$r$	774129,774130,962801,962802
	$i$	774122,774123,774124,774125,774126,774127,774128
	$z$	889530,889531,889532,889533,889534,889535
W2(+2+2)	$u^*$	890407,890408,890409,890410,890411
	$g$	774281,774282,774283,774284,774285,774286
	$r$	731035,731036,963159,963160
	$y$	1038712,1038713,1038714,1038840,1038841,1038842,1038843
	$z$	889350,889351,889352,889353,889354,889355
W2(+2+3)	$u^*$	895788,895789,895790,895791,895792
	$g$	731007,731008,731009,731010,731011
	$r$	730922,962766,962767,987075
	$i$	777315,777316,777317,777318,777446,777447,777448
	$z$	895598,895599,895600,896295,896296,896297
W2(+3-1)	$u^*$	963052,963053,963054,963055,963056
	$g$	880225,880226,880227,880228,880229
	$r$	831995,831996,967584,967585
	$i$	831999,832000,832001,832002,832003,832004,832005
	$z$	955447,955448,955449,955450,955451,955452
W2(+3-0)	$u^*$	905935,905936,905937,905938,905939
	$g$	739202,739203,739204,739205,739650
	$r$	730941,730942,963591,963592
	$i$	784765,784766,784767,784768,784769,784770,784771
	$z$	899936,899937,899938,899939,899940,899941
W2(+3+1)	$u^*$	890565,890566,890567,890568,890569
	$g$	733290,733291,733292,733293,733294
	$r$	730939,730940,963164,963165
	$i$	777312,777313,777314,777442,777443,777445
	$z$	889356,889357,889358,889359,889360,889361

Continued on next page

Table 32 – Continued from previous page

W Cartesian Ident Name	Filter	CFHT odometer number of input images combined in stacks
W2(+3+2)	$u^*$	890560,890561,890562,890563,890564
	$g$	732998,732999,733000,733001,733002
	$r$	730738,730739,963162,963163
	$i$	732380,732381,732382,732383,781182,781183,781184
	$z$	781185,781186,781187,781188,781189,781190,781191,781192,781195,781196,781197,781198
W2(+3+3)	$u^*$	895593,895594,895595,895596,895597
	$g$	732991,732992,732993,732994,732996
	$r$	732760,732762,962764,962765
	$i$	784758,784759,784760,784761,784762,784763,784764
	$z$	895572,895573,895574,895575,895576,895577
W3(-3-3)	$u^*$	850250,850251,850252,850253,850254
	$g$	792941,792942,792943,792944,792945
	$r$	792446,792447,967513,967514
	$i$	793316,793317,793318,793319,793320,793321,793322
	$z$	850441,850442,850443,850444,850445,850446
W3(-3-2)	$u^*$	850245,850246,850247,850248,850249
	$g$	793176,793177,793178,793179,793180
	$r$	792448,792449,967515,967516
	$i$	793323,793324,793325,793326,793327,793328,793329
	$z$	850255,850256,850257,850258,850259,850260,850261
W3(-3-1)	$u^*$	905718,905719,905720,905721,905722
	$g$	708589,708590,708591,708592,708593
	$r$	708586,708587,967972,967973
	$i$	708704,708705,708706,708707,708708,708709
	$z$	850962,850963,850964,850965,850966,850967
W3(-3-0)	$u^*$	905849,905850,905851,905852,905853
	$g$	793330,793331,793332,793333,793334
	$r$	792953,792954,967981,967982
	$i$	793456,793457,793458,793459,793460,793461,793462
	$z$	850956,850957,850958,850959,850960,850961
W3(-3+1)	$u^*$	918225,918226,918227,918228,918229
	$g$	800976,800977,800978,800979,800980
	$r$	797257,797258,974334,974335
	$y$	986927,986928,986929,986930,986931,986932,986933
	$z$	905021,905022,905023,905024,905025,905026
W3(-3+2)	$u^*$	918977,918978,918979,918980,918981
	$g$	800982,800983,800984,800985,800986
	$r$	797662,797663,974350,974675,974676
	$i$	797761,797762,797763,797764,797765,797766,797767
	$z$	905499,905500,905501,905502,905503,905504
W3(-3+3)	$u^*$	975448,975449,975450,994906,994907
	$g$	849609,849610,849611,849612,849613
	$r$	844750,844751,975587,975588
	$i$	845231,845232,845233,845234,845235,845236,845237
	$z$	964907,964908,964909,964910,964911,964912
W3(-2-3)	$u^*$	899071,899072,899075,994908,994909
	$g$	788717,788718,789050,789051,789052
	$r$	781209,781210,967613,967614
	$i$	792946,792947,792948,792949,792950,792951,792952
	$z$	850359,850360,850361,850362,850364,850365
W3(-2-2)	$u^*$	850348,850349,850350,850351,850352
	$g$	788842,788843,788844,788845,788846
	$r$	780551,780553,967611,967612
	$i$	793051,793052,793053,793054,793055,793056,793057
	$z$	850353,850354,850355,850356,850357,850358
W3(-2-1)	$u^*$	905723,905724,905725,905726,905727
	$g$	788847,788848,788849,788850,788851
	$r$	781217,781218,967970,967971
	$y$	987079,987080,987081,987082,987083,987084,987085
	$z$	851164,851165,851166,851167,851168,851170

Continued on next page

Table 32 – Continued from previous page

W Cartesian Ident Name	Filter	CFHT odometer number of input images combined in stacks
W3(-2-0)	$u^*$	905854,905855,905856,905857,905858
	$g$	792935,792936,792937,792938,792939
	$r$	781219,781220,967983,967984
	$i$	793065,793066,793068,793069,793070,793071
	$z$	851171,851172,851174,851175,851176,851177
W3(-2+1)	$u^*$	918456,918457,918458,918459,918460
	$g$	796972,796973,796974,796975,796981
	$r$	796979,796980,973413,974332,974333
	$y$	987093,987094,987095,987096,987097,987098,987099
	$z$	905027,905028,905029,905030,905031,905032
W3(-2+2)	$u^*$	919084,919085,919086,919087,919088
	$g$	802356,802357,802358,802359,802360
	$r$	797670,797671,974677,974678
	$i$	845099,845100,845101,845102,845103,845104
	$z$	906682,906683,906684,906685,906686,906687
W3(-2+3)	$u^*$	975577,975578,975579,975580,975581
	$g$	849614,849615,849616,849617,849618
	$r$	845365,845366,975457,975458,975589,975590
	$y$	987086,987087,987088,987089,987090,987091,987092
	$z$	965362,965363,965364,965365,965366,965367
W3(-1-3)	$u^*$	850753,850754,850755,850756,850757
	$g$	788200,788201,788202,788203,788204
	$r$	777535,777536,967615,967616
	$i$	789162,789163,789164,789165,789166,789167,789168,789169,789170,789171
	$z$	850758,850759,850760,850761,850762,850763
W3(-1-2)	$u^*$	850851,850852,850853,850854,850855
	$g$	788205,789173,789174,789176,789177
	$r$	781215,781216,967871,967966,967967
	$i$	792430,792431,792432,792433,792434,792435,792438
	$z$	850856,850857,850858,850859,850860,850861
W3(-1-1)	$u^*$	905729,905730,905731,905732,905733
	$g$	792425,792426,792427,792428,792429
	$r$	781213,781214,967968,967969
	$i$	792439,792440,792441,792442,792443,792444,792445
	$z$	850862,850863,850864,850865,850866,850867
W3(-1-0)	$u^*$	905859,905860,905861,905862,905863
	$g$	788853,788854,788857,789053,789054
	$r$	781211,781212,967985,967986
	$i$	792617,792618,792619,792620,792621,792622,792623
	$z$	853250,853251,853252,853253,853254,853255
W3(-1+1)	$u^*$	918461,918462,918463,918464,918465
	$g$	796967,796968,796969,796970,796971
	$r$	796977,796978,973411,973412
	$i$	796982,796983,796984,796985,796986,796987
	$z$	905034,905035,905036,905038,905039,905040
W3(-1+2)	$u^*$	919089,919090,919091,919092,919093
	$g$	802361,802362,802363,802364,802365
	$r$	802664,802665,974987,974988
	$i$	845105,845106,845107,845108,845109,845110,845111
	$z$	906780,906781,906782,906783,906784,906785
W3(-1+3)	$u^*$	975905,975906,975907,975908,975909
	$g$	849619,849620,849621,849622,849623
	$r$	845367,845368,975595,975596
	$y$	986956,986957,986958,986959,986960,986961,986962
	$z$	964459,964460,964461,964462,964463,964464
W3(-0-3)	$u^*$	918116,918117,918118,918119,918120
	$g$	707655,707656,707657,707658,707659
	$r$	707662,707663,973397,973781,974184,974185
	$i$	705484,705485,705486,705487,705488,705489,705490
	$z$	905014,905015,905016,905017,905018,905019

Continued on next page



Table 32 – Continued from previous page

W Cartesian Ident Name	Filter	CFHT odometer number of input images combined in stacks
W3(-0-2)	$u^*$	912457,912458,912459,912460,912461
	$g$	707554,707555,707556,707557,707558
	$r$	707559,707560,973350,973395,973396
	$i$	705403,705404,705405,705406,705407,705408,705409
	$z$	895845,895846,895847,895848,895849,895850
W3(-0-1)	$u^*$	905987,905988,905989,905990,905991
	$g$	707434,707435,707436,707437,707438
	$r$	707432,707433,973348,973926,973927
	$i$	705391,705397,705398,705399,705400,705401
	$z$	895517,895520,895522,895525,895526,895527
W3(-0-0)	$u^*$	905982,905983,905984,905985,905986
	$g$	707276,707277,707278,707279,707280
	$r$	707274,707275,973346,973347
	$i$	705244,705245,705246,705247,705248,705249,705250
	$z$	853918,853919,853920,853921,853922,853923
W3(-0+1)	$u^*$	918466,918467,918468,918589,918590
	$g$	796616,796617,796618,796619,796620
	$r$	796623,796624,973409,973410
	$i$	796626,796744,796745,796746,796747,796748,796749
	$z$	905224,905225,905226,905227,905228,905229
W3(-0+2)	$u^*$	919602,919603,919604,919605,919606
	$g$	802366,802367,802368,802369,802370
	$r$	802671,802672,974989,974990
	$i$	844865,844866,844867,844868,844869,844870,844871
	$z$	906810,906811,906812,906813,906814,906815
W3(-0+3)	$u^*$	979597,979598,979599,979600,979601
	$g$	849695,849696,849697,849698,849699
	$r$	845369,845370,975593,975594
	$i$	849624,849625,849626,849627,849628,849629,849630
	$z$	964178,964179,964180,964181,964182,964458
W3(+1-3)	$u^*$	918982,918983,918984,918985,918986
	$g$	739209,739210,739211,739212,739216,739218
	$r$	739207,739208,973400,974186,974187
	$i$	742622,742880,742881,742882,742883,742884,742885
	$z$	906521,906654,906655,906656,906657,906658,906659
W3(+1-2)	$u^*$	918842,918843,918844,918845,918846
	$g$	742886,742887,742888,742889,742890
	$r$	742236,742237,973401,973402
	$i$	743062,743063,743065,743066,743067,743068,743069
	$z$	906515,906516,906517,906518,906519,906520
W3(+1-1)	$u^*$	918837,918838,918839,918840,918841
	$g$	745141,745142,745143,745144,745145
	$r$	745147,745148,973403,973404
	$i$	743070,743071,743072,743073,743074,743075,743076
	$z$	906355,906356,906357,906358,906508,906509,906510,906511,906513,906514
W3(+1-0)	$u^*$	918596,918597,918598,918599,918600
	$g$	742892,742893,742894,742895,742896
	$r$	745149,745150,973405,973406
	$i$	743078,743079,743080,743081,743082,743083,743084
	$z$	906234,906235,906236,906349,906350,906351,906352,906353,906354
W3(+1+1)	$u^*$	918591,918592,918593,918594,918595
	$g$	796611,796612,796613,796614,796615
	$r$	796621,796622,973407,973408
	$i$	796485,796486,796487,796488,796489,796490,796491
	$z$	905230,905231,905233,905234,905235,905236
W3(+1+2)	$u^*$	919758,919759,919760,919761,919762,974999,975000,975001,975002,975003
	$g$	844738,844739,844740,844741,844742
	$r$	780364,780365,974991,974992
	$i$	797645,797646,797647,797648,797649,797650,797651
	$z$	907094,907095,907096,907097,907098,907099

Continued on next page

Table 32 – Continued from previous page

W Cartesian Ident Name	Filter	CFHT odometer number of input images combined in stacks
W3(+1+3)	$u^*$	975910,975911,975912,975913,975914
	$g$	849700,849701,849702,849703,849704
	$r$	845477,845478,975591,975592
	$i$	849705,849706,849772,849773,849774,849775,849776
	$z$	963929,963930,963931,964175,964176,964177
W3(+2-3)	$u^*$	975221,975222,975223,975224,975225
	$g$	750105,750106,750107,750187,750188
	$r$	745594,745595,975013,975014
	$i$	743140,745587,745588,745589,745590,745591,745592,745593
	$z$	918131,918132,918133,918134,918135,918136,918137
W3(+2-2)	$u^*$	975131,975132,975133,975134,975135
	$g$	750322,750323,750959,750960,750961,750962,750963
	$r$	750965,750967,975011,975012
	$i$	745599,745600,745601,745602,745604,745605,745606
	$z$	918125,918126,918127,918128,918129,918130
W3(+2-1)	$u^*$	975004,975005,975006,975007,975008
	$g$	753782,753783,753784,753785,753786
	$r$	753780,755116,975009,975010
	$i$	751034,751197,751198,751199,751200,751201,751202,751203
	$z$	918027,918028,918029,918030,918031,918032
W3(+2-0)	$u^*$	973921,973922,973923,973924,973925
	$g$	755117,755118,755119,755120,755244
	$r$	753788,753789,974997,974998
	$i$	789056,789057,789058,789059,789060,789061,789062
	$z$	918021,918022,918023,918024,918025,918026
W3(+2+1)	$u^*$	973916,973917,973918,973919,973920
	$g$	796351,796352,796608,796609,796610
	$r$	780366,780367,974995,974996
	$i$	793809,793810,793811,793812,793813,793814,793815
	$z$	912552,912553,917941,917942,917943,917944,917945,917946
W3(+2+2)	$u^*$	973911,973912,973913,973914,973915
	$g$	802666,802667,802668,802669,802670
	$r$	802673,802674,974993,974994
	$i$	844743,844744,844745,844746,844747,844748,844749
	$z$	917935,917936,917937,917938,917939,917940
W3(+2+3)	$u^*$	979602,979603,979604,979605,979606
	$g$	849767,849768,849769,849770,849771
	$r$	845479,845480,975235,975236
	$i$	849777,849778,849779,849780,849781,849782,849783
	$z$	963923,963924,963925,963926,963927,963928
W3(+3-3)	$u^*$	975226,975227,975228,975229,975230
	$g$	859218,859219,859623,859624,859625
	$r$	852994,852995,975115,975116
	$i$	853622,853623,853624,853625,853626,853739
	$z$	930854,930855,930856,930857,930858,930859
W3(+3-2)	$u^*$	975582,975583,975584,975585,975586
	$g$	860019,860020,860021,987108,987109
	$r$	852996,852997,975117,975118
	$i$	853849,853912,853913,853914,853915,853916
	$z$	930860,930861,930862,930863,930864,930865
W3(+3-1)	$u^*$	980090,980091,980092,980093,980094
	$g$	890597,890600,890601,890603,890604
	$r$	852998,852999,975119,975120
	$y$	987229,987230,987231,987232,987233,987234,987235
	$z$	931000,931001,931002,931003,931004,931005
W3(+3-0)	$u^*$	979853,979854,979855,979856,979857
	$g$	899066,899067,899068,899069,899070
	$r$	853000,853001,975122,975123
	$i$	899485,899486,899487,899488,899489,899490,899491
	$z$	931006,931007,931008,931009,931010,987110

Continued on next page

Table 32 – Continued from previous page

W Cartesian Ident Name	Filter	CFHT odometer number of input images combined in stacks
W3(+3+1)	$u^*$	975915,975916,975917,975918,975919
	$g$	899576,899577,899578,899579,899580
	$r$	853002,853003,975136,975137
	$i$	900058,900059,900060,900061,900062,900063,900064
	$z$	931115,931116,931117,931118,931119,931120
W3(+3+2)	$u^*$	980095,980096,980097,980098,980099
	$g$	899971,899972,899973,899974,899975
	$r$	853004,853005,975231,975232
	$y$	987236,987237,987238,987239,987240,987241,987242,987243
	$z$	931121,931122,931123,931124,931125,931126
W3(+3+3)	$u^*$	981430,981431,981432,981433,981434
	$g$	905494,905495,905496,905497,905498
	$r$	853006,853007,975233,975234
	$i$	900166,900167,900168,900169,900170,900171,900172
	$z$	964913,964914,964915,964916,964917,964918
W4(-3+0)	$u^*$	934901,934902,934903,934904,934905
	$g$	930784,930785,930786,930787,930788
	$r$	919694,919695,988176,988177
	$i$	918162,918163,918164,918165,918265,918266,918267
	$z$	918919,918920,918921,918922,918923,918924
W4(-3+1)	$u^*$	934712,934730,934891,934892,934893,934894,934895
	$g$	930908,930909,930910,930911,930912
	$r$	930675,930676,987485,987486
	$i$	918268,918269,918270,918271,918272,918273,918391
	$z$	919025,919026,919027,919028,919029,919030
W4(-3+2)	$u^*$	935165,935166,935167,935168,935169
	$g$	919445,919446,919447,919448,919449
	$r$	930768,930769,987279,987280
	$i$	918392,918393,918394,918395,918396,918397,918398
	$z$	919031,919032,919033,919034,919035,919036
W4(-3+3)	$u^*$	935185,935186,935187,935188,935189
	$g$	935326,935438,935439,935440,935441,935442
	$r$	934411,934412,987128,987129
	$y$	995422,995423,995424,995425,995426,995427,995428
	$z$	931298,931299,931300,931301,931302,931303
W4(-2+0)	$u^*$	934896,934897,934898,934899,934900
	$g$	850526,850527,850528,850529,850530
	$r$	850531,850532,996131,996133,996134
	$i$	853639,853640,853641,853642,853643,853647,853648,862673,862674,862675,862676,862677,862678
	$z$	874406,874407,874408,874409,874410,874411
W4(-2+1)	$u^*$	934402,934403,934404,934405,934406
	$g$	919130,919131,919132,919133,919134
	$r$	919450,919451,996142,996143
	$i$	918155,918156,918157,918158,918159,918160,918161
	$z$	918912,918913,918915,918916,918917,918918
W4(-2+2)	$u^*$	934906,934907,934908,934909,934910
	$g$	935299,935300,935301,935302,935303
	$r$	930770,930771,987643,987644
	$y$	995150,995151,995152,995153,995154,995281,995282
	$z$	919688,919689,919690,919691,919692,919693
W4(-2+3)	$u^*$	935180,935181,935182,935183,935184
	$g$	935321,935322,935323,935324,935325
	$r$	934409,934410,987806,987807
	$y$	995672,995673,995674,995675,995676,995677,995678
	$z$	931148,931149,931150,931151,931152,931153
W4(-1-2)	$u^*$	864142,864143,864144,864145,864146
	$g$	860225,860228,860229,860230,860231
	$r$	851200,851202,996280,996282,996284,996286
	$i$	862697,862698,862699,862700,862701,862702,862703
	$z$	864136,864137,864138,864139,864140,864141

Continued on next page

Table 32 – Continued from previous page

W Cartesian Ident Name	Filter	CFHT odometer number of input images combined in stacks
W4(-1-1)	$u^*$	870363,870364,870365,870366,870367
	$g$	860601,860602,860603,860604,860605,862806,862807,862808,862809,862918,862919
	$r$	850808,850809,996449,996450
	$y$	995679,995680,995681,995682,995885,995886,995887
	$z$	870155,870156,870157,870158,870159,870160
W4(-1+0)	$u^*$	930774,930775,930776,930777,930778
	$g$	859940,859941,859942,859943,859944
	$r$	850996,850997,996146,996147
	$i$	859945,859946,859947,859949,859951,859952,859953
	$z$	859723,859724,859725,859726,859727,859728
W4(-1+1)	$u^*$	934397,934398,934399,934400,934401
	$g$	853649,853650,853651,853652,853653,862692,862693,862694,862695,862696
	$r$	850286,850287,996144,996145
	$y$	996018,996019,996020,996021,996022,996023,996024
	$z$	875403,875404,875405,875406,875407,875408
W4(-1+2)	$u^*$	935170,935171,935172,935173,935174
	$g$	935304,935305,935306,935307,935308
	$r$	930772,930773,987645,987646
	$y$	995283,995284,995285,995286,995287,995288,995289
	$z$	931043,931044,931050,931051,931052,931053
W4(-1+3)	$u^*$	935175,935176,935177,935178,935179
	$g$	935316,935317,935318,935319,935320
	$r$	934407,934408,987804,987805
	$y$	995290,995291,995292,995293,995419,995420,995421
	$z$	931054,931055,931056,931057,931058,931059
W4(+0-2)	$u^*$	864147,864148,864149,864150,864151
	$g$	853285,853286,853287,853288,853289,862801,862802,862803,862804,862805
	$r$	851127,851128,996451,996452
	$i$	862597,862598,862599,862600,862601,862602,862603
	$z$	863984,863985,863986,863987,863988,863989
W4(+0-1)	$u^*$	870368,870369,870371,870372,996025
	$g$	853290,853291,853292,853293,853294,862920,862921,862922,862923,862924
	$r$	850994,850995,996453,996454
	$i$	862794,862795,862796,862797,862798,862799,862800
	$z$	870357,870358,870359,870360,870361,870362
W4(+0+0)	$u^*$	872170,872171,872173,872175,872176
	$g$	860077,860078,860079,860080,860081
	$r$	851189,851190,851191,996455,996456
	$i$	863246,863247,863248,863249,863250,863251,863252
	$z$	860606,860607,860608,860609,860610,860611,872158,872159,872160,872161,872162,872163
W4(+0+1)	$u^*$	934392,934393,934394,934395,934396
	$g$	860188,860189,860190,860191,860192
	$r$	851192,851193,996457,996458
	$i$	863445,863446,863447,863448,863449,863450,863451
	$z$	879612,879613,879614,879615,879616,879617
W4(+1-2)	$u^*$	863902,863903,863904,863905,863906
	$g$	850998,850999,851000,851001,851002
	$r$	850000,850001,996629,996630
	$i$	859675,859676,859677,859678,859679,859681
	$z$	863896,863897,863898,863899,863900,863901
W4(+1-1)	$u^*$	870499,870500,870501,870502,870504
	$g$	851003,851004,851005,851006,851007
	$r$	850102,850103,996627,996628
	$i$	860594,860595,860596,860597,860598,860599,860600,863044,863045,863046,863047,863048,863049,863050
	$z$	870493,870494,870495,870496,870497,870498
W4(+1+0)	$u^*$	872242,872243,872244,872245,872246
	$g$	851129,851130,851131,851132,851194
	$r$	850638,850639,996625,996626
	$i$	863051,863052,863053,863054,863055,863056,863057
	$z$	872057,872058,872059,872060,872061,872062

Continued on next page

Table 32 – *Continued from previous page*

W Cartesian Ident Name	Filter	CFHT odometer number of input images combined in stacks
W4(+1+1)	$u^*$	930779,930780,930781,930782,930783
	$g$	851195,851196,851197,851198,851199
	$r$	850636,850637,996623,996624
	$i$	863253,863254,863255,863256,863257,863258,863259
	$z$	879618,879619,879621,879622,879623,879624
W4(+2-2)	$u^*$	858903,858905,858906,858907,859955
	$g$	850104,850105,850106,850107,850108
	$r$	849847,849848,996631,996632
	$i$	853569,853584,853585,853586,853587,853588,862590,862591,862592,862593,862594,862595,862596
	$z$	853577,853578,853579,853580,853581,853582,853583,863977,863978,863980,863981,863982,863983
W4(+2-1)	$u^*$	858908,858909,858910,858911,858912
	$g$	850220,850221,850222,850223,850224
	$r$	849849,849850,996633,996634
	$i$	860082,860083,860084,860085,860086,860087,860088
	$z$	853787,853788,853789,853790,853791,853792,870699,870700,870701,870702,870706,870707
W4(+2+0)	$u^*$	872069,872070,872071,872072,872073
	$g$	850281,850282,850283,850284,850285
	$r$	849998,849999,996635,996636
	$i$	860413,860414,860415,860416,860417,860418,860419
	$z$	871416,871417,871418,871419,871420,871421

## A.3 CFHTLS T0007 Wide configuration files

### A.3.1 SCAMP configuration files for T0007 Wide

#### SCAMP internal astrometric reference catalogue run (W1) :

```
# Default configuration file for SCAMP 1.5.5
# EB 2009-04-10
# Last modified for CFHTLS-T0007-W1 (Megacam):
# YG 2010-12-13

#----- Field grouping -----
FGROUP_RADIUS      1.0          # Max dist (deg) between field groups

#----- Reference catalogs -----
REF_SERVER         cocatl.u-strasbg.fr # Internet addresses of catalog servers
REF_PORT           1660          # Ports to connect to catalog servers
CDSCLIENT_EXEC    aclient       # CDSclient executable
ASTREF_CATALOG     2MASS         # NONE, FILE, USNO-A1, USNO-A2, USNO-B1,
                                # GSC-1.3, GSC-2.2, UCAC-1, UCAC-2,
                                # NOMAD-1, 2MASS, DENIS-3,
                                # SDSS-R3, SDSS-R5 or SDSS-R6
ASTREF_BAND        DEFAULT      # Photom. band for astr.ref.magnitudes
                                # or DEFAULT, BLUEST, or REDDEST
ASTREFCAT_NAME     astrefcat.cat  # Local astrometric reference catalogs
ASTREFCENT_KEYS    X_WORLD,Y_WORLD # Local ref.cat.centroid parameters
ASTREFERR_KEYS     ERRA_WORLD,ERRB_WORLD,ERRTHETA_WORLD
                                # Local ref.cat.error ellipse parameters
ASTREFMAG_KEY      MAG          # Local ref.cat.magnitude parameter
SAVE_REFCATALOG    N            # Save ref catalogs in FITS-LDAC format?
REFOUT_CATPATH     .            # Save path for reference catalogs

#----- Merged output catalogs -----
MERGEDOUTCAT_NAME  CFHTLS-T0007-W1_SCamp_astr_ref.cat
                                # Merged output catalog filename
MERGEDOUTCAT_TYPE  FITS_LDAC     # NONE, ASCII_HEAD, ASCII, FITS_LDAC

#----- Pattern matching -----
MATCH              Y            # Do pattern-matching (Y/N) ?
MATCH_NMAX         0            # Max.number of detections for MATCHing
                                # (0=auto)
PIXSCALE_MAXERR    1.2          # Max scale-factor uncertainty
POSANGLE_MAXERR    5.0          # Max position-angle uncertainty (deg)
POSITION_MAXERR    1.0          # Max positional uncertainty (arcmin)
MATCH_RESOL        0            # Matching resolution (arcsec); 0=auto
MATCH_FLIPPED      N            # Allow matching with flipped axes?
MOSAIC_TYPE        SAME_CRVAL    # UNCHANGED, SAME_CRVAL, SHARE_PROJAXIS,
                                # FIX_FOCALPLANE or LOOSE
FIXFOCALPLANE_NMIN 1            # Min number of dets for FIX_FOCALPLANE

#----- Cross-identification -----
CROSSID_RADIUS     2.0          # Cross-id initial radius (arcsec)

#----- Astrometric solution -----
SOLVE_Astrom       Y            # Compute astrometric solution (Y/N) ?
ASTRINSTRU_KEY     FILTER,QRUNID # FITS keyword(s) defining the astrom
STABILITY_TYPE     INSTRUMENT    # EXPOSURE, GROUP, INSTRUMENT or FILE
CENTROID_KEYS      XWIN_IMAGE,YWIN_IMAGE # Cat. parameters for centroiding
CENTROIDERR_KEYS   ERRRAWIN_IMAGE,ERRBWIN_IMAGE,ERRTHETAWIN_IMAGE
                                # Cat. params for centroid err ellipse
DISTORT_KEYS       XWIN_IMAGE,YWIN_IMAGE # Cat. parameters or FITS keywords
```

```

DISTORT_GROUPS      1,1          # Polynom group for each context key
DISTORT_DEGREES    3            # Polynom degree for each group
ASTREF_WEIGHT      1.0          # Relative weight of ref.astrom.cat.
ASTRCLIP_NSIGMA    3.0          # Astrom. clipping threshold in sigmas
CORRECT_COLOURSHIFTS N          # Correct for colour shifts (Y/N)?

#----- Photometric solution -----
SOLVE_PHOTOM       Y            # Compute photometric solution (Y/N) ?
MAGZERO_OUT        30.0          # Magnitude zero-point(s) in output
MAGZERO_INTERR     0.01          # Internal mag.zero-point accuracy
MAGZERO_REFERR     0.03          # Photom.field mag.zero-point accuracy
PHOTINSTRU_KEY     FILTER        # FITS keyword(s) defining the photom.
MAGZERO_KEY        PHOT_C        # FITS keyword for the mag zero-point
EXPOTIME_KEY       EXPTIME       # FITS keyword for the exposure time (s)
AIRMASS_KEY        AIRMASS       # FITS keyword for the airmass
EXTINCT_KEY        PHOT_K        # FITS keyword for the extinction coeff
PHOTOMFLAG_KEY     PHOTFLAG      # FITS keyword for the photometry flag
PHOTFLUX_KEY       FLUX_AUTO      # Catalog param. for the flux measurement
PHOTFLUXERR_KEY    FLUXERR_AUTO   # Catalog parameter for the flux error
PHOTCLIP_NSIGMA    3.0          # Photom.clipping threshold in sigmas

#----- Check-plots -----
CHECKPLOT_CKEY     SCAMPCOL       # FITS keyword for PLPLOT field colour
CHECKPLOT_DEV      PNG            # NULL, XWIN, TK, PS, PSC, XFIG, PNG,
                                # JPEG, AQT, PDF or SVG
CHECKPLOT_RES      1600,1200      # Check-plot resolution (0 = default)
CHECKPLOT_ANTIALIAS Y            # Anti-aliasing using convert (Y/N) ?
CHECKPLOT_TYPE     DISTORTION,ASTR_INTERROR2D,ASTR_INTERROR1D,ASTR_REFERROR2D,
ASTR_REFERROR1D,ASTR_CHI2,PHOT_ERROR,PHOT_ERRORVSMAG,
PHOT_ZPCORR,PHOT_ZPCORR3D
CHECKPLOT_NAME     distort,astr_interror2d,astr_interror1d,astr_referror2d,
astr_referror1d,astr_chi2,psphot_error,phot_errorvsmag,
phot_zpcorr,phot_zpcorr3d
                                # Check-plot filename(s)

#----- Check-images -----
CHECKIMAGE_TYPE    NONE           # NONE, AS_PAIR, AS_REFPAIR, or AS_XCORR
CHECKIMAGE_NAME    check.fits     # Check-image filename(s)

#----- Miscellaneous -----
SN_THRESHOLDS     10.0,100.0     # S/N thresholds (in sigmas) for all and
                                # high-SN sample
FWHM_THRESHOLDS   0.0,100.0      # FWHM thresholds (in pixels) for sources
FLAGS_MASK        0x00f0         # Rejection mask on SEX FLAGS
WEIGHTFLAGS_MASK  0x00ff         # Rejection mask on SEX FLAGS_WEIGHT
IMAFLAGS_MASK     0x0            # Rejection mask on SEX IMAFLAGS_ISO
AHEADER_GLOBAL    /usr/share/scamp/megacam.ahead
AHEADER_SUFFIX    .ahead         # Filename of the global INPUT header
                                # Filename extension for additional
                                # INPUT headers
HEADER_SUFFIX     .head          # Filename extension for OUTPUT headers
HEADER_TYPE       NORMAL         # NORMAL or FOCAL_PLANE
VERBOSE_TYPE      LOG            # QUIET, NORMAL, LOG or FULL
WRITE_XML         Y              # Write XML file (Y/N)?
XML_NAME          CFHTLS-T0007-W1_SCamp_astr_ref.xml
                                # Filename for XML output
XSL_URL           scamp.xsl      # Filename for XSL style-sheet
NTHREADS         0               # Number of simultaneous threads for
                                # the SMP version of SCAMP
                                # 0 = automatic

```

## SCAMP astrometric run using internal astrometric reference catalogue (W1) :

```

# Default configuration file for SCAMP 1.5.5
# EB 2009-04-10
# Last modified for CFHTLS-T0007-W1 (Megacam):
# YG 2010-12-14

#----- Field grouping -----
FGROUP_RADIUS      1.0          # Max dist (deg) between field groups

#----- Reference catalogs -----
REF_SERVER          cocat1.u-strasbg.fr # Internet addresses of catalog servers
REF_PORT            1660          # Ports to connect to catalog servers
CDSCLIENT_EXEC     aclient       # CDSclient executable
ASTREF_CATALOG      FILE         # NONE, FILE, USNO-A1, USNO-A2, USNO-B1,
                                # GSC-1.3, GSC-2.2, UCAC-1, UCAC-2,
                                # NOMAD-1, 2MASS, DENIS-3,
                                # SDSS-R3, SDSS-R5 or SDSS-R6
ASTREF_BAND         DEFAULT      # Photom. band for astr.ref.magnitudes
                                # or DEFAULT, BLUEST, or REDDEST
ASTREFCAT_NAME      CFHTLS-T0007-W1_SCamp_astr_ref.cat
                                # Local astrometric reference catalogs
ASTREFCENT_KEYS     X_WORLD,Y_WORLD # Local ref.cat.centroid parameters
ASTREFERR_KEYS      ERRA_WORLD, ERRB_WORLD, ERRTHETA_WORLD
                                # Local ref.cat.error ellipse parameters
ASTREFMAG_KEY       MAG          # Local ref.cat.magnitude parameter
SAVE_REFCATALOG     N           # Save ref catalogs in FITS-LDAC format?
REFOUT_CATPATH      .           # Save path for reference catalogs

#----- Merged output catalogs -----
MERGEDOUTCAT_NAME   scamp.cat     # Merged output catalog filename
MERGEDOUTCAT_TYPE   NONE         # NONE, ASCII_HEAD, ASCII, FITS_LDAC

#----- Pattern matching -----
MATCH               Y           # Do pattern-matching (Y/N) ?
MATCH_NMAX          0           # Max.number of detections for MATCHing
                                # (0=auto)
PIXSCALE_MAXERR     1.2         # Max scale-factor uncertainty
POSANGLE_MAXERR     5.0         # Max position-angle uncertainty (deg)
POSITION_MAXERR     1.0         # Max positional uncertainty (arcmin)
MATCH_RESOL         0           # Matching resolution (arcsec); 0=auto
MATCH_FLIPPED       N           # Allow matching with flipped axes?
MOSAIC_TYPE         SAME_CRVAL   # UNCHANGED, SAME_CRVAL, SHARE_PROJAXIS,
                                # FIX_FOCALPLANE or LOOSE
FIXFOCALPLANE_NMIN 1           # Min number of dets for FIX_FOCALPLANE

#----- Cross-identification -----
CROSSID_RADIUS      2.0         # Cross-id initial radius (arcsec)

#----- Astrometric solution -----
SOLVE_Astrom        Y           # Compute astrometric solution (Y/N) ?
ASTRINSTRU_KEY      FILTER,QRUNID # FITS keyword(s) defining the astrom
STABILITY_TYPE      INSTRUMENT  # EXPOSURE, GROUP, INSTRUMENT or FILE
CENTROID_KEYS       XWIN_IMAGE,YWIN_IMAGE # Cat. parameters for centroiding
CENTROIDERR_KEYS    ERRRAWIN_IMAGE,ERRBWIN_IMAGE,ERRTHETAWIN_IMAGE
                                # Cat. params for centroid err ellipse
DISTORT_KEYS        XWIN_IMAGE,YWIN_IMAGE # Cat. parameters or FITS keywords
DISTORT_GROUPS      1,1         # Polynom group for each context key
DISTORT_DEGREES     3           # Polynom degree for each group
ASTREF_WEIGHT        1.0        # Relative weight of ref.astrom.cat.
ASTRCLIP_NSIGMA     3.0        # Astrom. clipping threshold in sigmas
CORRECT_COLOURSHIFTS N         # Correct for colour shifts (Y/N)?

```



```

#----- Photometric solution -----
SOLVE_PHOTOM          Y          # Compute photometric solution (Y/N) ?
MAGZERO_OUT           30.0       # Magnitude zero-point(s) in output
MAGZERO_INTERR        0.01       # Internal mag.zero-point accuracy
MAGZERO_REFERR        0.03       # Photom.field mag.zero-point accuracy
PHOTINSTRU_KEY        FILTER     # FITS keyword(s) defining the photom.
MAGZERO_KEY           PHOT_C     # FITS keyword for the mag zero-point
EXPOTIME_KEY          EXPTIME    # FITS keyword for the exposure time (s)
AIRMASS_KEY           AIRMASS    # FITS keyword for the airmass
EXTINCT_KEY           PHOT_K     # FITS keyword for the extinction coeff
PHOTOMFLAG_KEY        PHOTFLAG   # FITS keyword for the photometry flag
PHOTFLUX_KEY          FLUX_AUTO   # Catalog param. for the flux measurement
PHOTFLUXERR_KEY       FLUXERR_AUTO # Catalog parameter for the flux error
PHOTCLIP_NSIGMA      3.0        # Photom.clipping threshold in sigmas

#----- Check-plots -----
CHECKPLOT_CKEY         SCAMPCOL   # FITS keyword for PLPLOT field colour
CHECKPLOT_DEV         PNG        # NULL, XWIN, TK, PS, PSC, XFIG, PNG,
                                # JPEG, AQT, PDF or SVG
CHECKPLOT_RES         1600,1200   # Check-plot resolution (0 = default)
CHECKPLOT_ANTIALIAS   Y          # Anti-aliasing using convert (Y/N) ?
CHECKPLOT_TYPE        DISTORTION,ASTR_INTERROR2D,ASTR_INTERROR1D,ASTR_REFERROR2D,
                                ASTR_REFERROR1D,ASTR_CHI2,PHOT_ERROR,PHOT_ERRORVSMAG,
                                PHOT_ZPCORR,PHOT_ZPCORR3D
CHECKPLOT_NAME        distort,astr_interror2d,astr_interror1d,astr_referror2d,
                                astr_referror1d,astr_chi2,psphot_error,phot_errorvsmag,
                                phot_zpcorr,phot_zpcorr3d
                                # Check-plot filename(s)

#----- Check-images -----
CHECKIMAGE_TYPE       NONE       # NONE, AS_PAIR, AS_REPAIR, or AS_XCORR
CHECKIMAGE_NAME       check.fits  # Check-image filename(s)

#----- Miscellaneous -----
SN_THRESHOLDS        10.0,100.0  # S/N thresholds (in sigmas) for all and
                                # high-SN sample
FWHM_THRESHOLDS      0.0,100.0   # FWHM thresholds (in pixels) for sources
FLAGS_MASK            0x00f0     # Rejection mask on SEX FLAGS
WEIGHTFLAGS_MASK     0x00ff     # Rejection mask on SEX FLAGS_WEIGHT
IMAFLAGS_MASK        0x0        # Rejection mask on SEX IMAFLAGS_ISO
AHEADER_GLOBAL       /usr/share/scamp/megacam.ahead
                                # Filename of the global INPUT header
AHEADER_SUFFIX       .ahead      # Filename extension for additional
                                # INPUT headers
HEADER_SUFFIX        .head       # Filename extension for OUTPUT headers
HEADER_TYPE          NORMAL      # NORMAL or FOCAL_PLANE
VERBOSE_TYPE         LOG        # QUIET, NORMAL, LOG or FULL
WRITE_XML            Y          # Write XML file (Y/N)?
XML_NAME             CFHTLS-T0007-W1_SCamp_ast_rz.xml
                                # Filename for XML output
XSL_URL              scamp.xsl   # Filename for XSL style-sheet
NTHREADS             0          # Number of simultaneous threads for
                                # the SMP version of SCAMP
                                # 0 = automatic

```

## SCAMP astrometric run using external astrometric reference catalogue (W2,W3,W4) :

```

# Default configuration file for SCAMP 1.5.5
# EB 2009-04-10
# Last modified for CFHTLS-T0007-W2 (Megacam):
# YG 2010-10-22

#----- Field grouping -----
FGROUP_RADIUS      1.0          # Max dist (deg) between field groups

#----- Reference catalogs -----
REF_SERVER          cocat1.u-strasbg.fr # Internet addresses of catalog servers
REF_PORT            1660          # Ports to connect to catalog servers
CDSCIENT_EXEC       aclient       # CDSCient executable
ASTREF_CATALOG      2MASS         # NONE, FILE, USNO-A1, USNO-A2, USNO-B1,
                                # GSC-1.3, GSC-2.2, UCAC-1, UCAC-2,
                                # NOMAD-1, 2MASS, DENIS-3,
                                # SDSS-R3, SDSS-R5 or SDSS-R6
ASTREF_BAND         DEFAULT       # Photom. band for astr.ref.magnitudes
                                # or DEFAULT, BLUEST, or REDDEST
ASTREFCAT_NAME      astrefcat.cat  # Local astrometric reference catalogs
ASTREFCENT_KEYS     X_WORLD,Y_WORLD # Local ref.cat.centroid parameters
ASTREFERR_KEYS      ERRA_WORLD, ERRB_WORLD, ERRTHETA_WORLD
                                # Local ref.cat.error ellipse parameters
ASTREFMAG_KEY       MAG           # Local ref.cat.magnitude parameter
SAVE_REFCATALOG     N             # Save ref catalogs in FITS-LDAC format?
REFOUT_CATPATH      .            # Save path for reference catalogs

#----- Merged output catalogs -----
MERGEDOUTCAT_NAME   scamp.cat      # Merged output catalog filename
MERGEDOUTCAT_TYPE   NONE          # NONE, ASCII_HEAD, ASCII, FITS_LDAC

#----- Pattern matching -----
MATCH               Y             # Do pattern-matching (Y/N) ?
MATCH_NMAX          0            # Max.number of detections for MATCHING
                                # (0=auto)
PIXSCALE_MAXERR     1.2          # Max scale-factor uncertainty
POSANGLE_MAXERR     5.0          # Max position-angle uncertainty (deg)
POSITION_MAXERR     1.0          # Max positional uncertainty (arcmin)
MATCH_RESOL         0            # Matching resolution (arcsec); 0=auto
MATCH_FLIPPED       N            # Allow matching with flipped axes?
MOSAIC_TYPE         SAME_CRVAL    # UNCHANGED, SAME_CRVAL, SHARE_PROJAXIS,
                                # FIX_FOCALPLANE or LOOSE
FIXFOCALPLANE_NMIN 1            # Min number of dets for FIX_FOCALPLANE

#----- Cross-identification -----
CROSSID_RADIUS      2.0          # Cross-id initial radius (arcsec)

#----- Astrometric solution -----
SOLVE_ASTROM        Y            # Compute astrometric solution (Y/N) ?
ASTRINSTRU_KEY      FILTER,QRUNID # FITS keyword(s) defining the astrom
STABILITY_TYPE      INSTRUMENT    # EXPOSURE, GROUP, INSTRUMENT or FILE
CENTROID_KEYS       XWIN_IMAGE,YWIN_IMAGE # Cat. parameters for centroiding
CENTROIDERR_KEYS    ERRRAWIN_IMAGE,ERRBWIN_IMAGE,ERRTHETAWIN_IMAGE
                                # Cat. params for centroid err ellipse
DISTORT_KEYS        XWIN_IMAGE,YWIN_IMAGE # Cat. parameters or FITS keywords
DISTORT_GROUPS      1,1          # Polynom group for each context key
DISTORT_DEGREES     3            # Polynom degree for each group
ASTREF_WEIGHT       1.0          # Relative weight of ref.astrom.cat.
ASTRCLIP_NSIGMA     3.0          # Astrom. clipping threshold in sigmas
CORRECT_COLOURSHIFTS N          # Correct for colour shifts (Y/N)?

```

```

#----- Photometric solution -----
SOLVE_PHOTOM          Y          # Compute photometric solution (Y/N) ?
MAGZERO_OUT           30.0       # Magnitude zero-point(s) in output
MAGZERO_INTERR        0.01       # Internal mag.zero-point accuracy
MAGZERO_REFERR        0.03       # Photom.field mag.zero-point accuracy
PHOTINSTRU_KEY        FILTER     # FITS keyword(s) defining the photom.
MAGZERO_KEY           PHOT_C     # FITS keyword for the mag zero-point
EXPOTIME_KEY          EXPTIME    # FITS keyword for the exposure time (s)
AIRMASS_KEY           AIRMASS    # FITS keyword for the airmass
EXTINCT_KEY           PHOT_K     # FITS keyword for the extinction coeff
PHOTOMFLAG_KEY        PHOTFLAG   # FITS keyword for the photometry flag
PHOTFLUX_KEY          FLUX_AUTO   # Catalog param. for the flux measurement
PHOTFLUXERR_KEY       FLUXERR_AUTO # Catalog parameter for the flux error
PHOTCLIP_NSIGMA      3.0        # Photom.clipping threshold in sigmas

#----- Check-plots -----
CHECKPLOT_CKEY        SCAMPCOL   # FITS keyword for PLPLOT field colour
CHECKPLOT_DEV         PSC,PNG    # NULL, XWIN, TK, PS, PSC, XFIG, PNG,
                                # JPEG, AQT, PDF or SVG
CHECKPLOT_RES         1600,1200  # Check-plot resolution (0 = default)
CHECKPLOT_ANTIALIAS   Y          # Anti-aliasing using convert (Y/N) ?
CHECKPLOT_TYPE        DISTORTION,ASTR_INTERROR2D,ASTR_INTERROR1D,ASTR_REFERROR2D,
                                ASTR_REFERROR1D,ASTR_CHI2,PHOT_ERROR,PHOT_ERRORVSMAG,
                                PHOT_ZPCORR,PHOT_ZPCORR3D
CHECKPLOT_NAME        distort,astr_interror2d,astr_interror1d,astr_referror2d,
                                astr_referror1d,astr_chi2,psphot_error,phot_errorvsmag,
                                phot_zpcorr,phot_zpcorr3d
                                # Check-plot filename(s)

#----- Check-images -----
CHECKIMAGE_TYPE       NONE       # NONE, AS_PAIR, AS_REFPAIR, or AS_XCORR
CHECKIMAGE_NAME       check.fits  # Check-image filename(s)

#----- Miscellaneous -----
SN_THRESHOLDS        10.0,100.0  # S/N thresholds (in sigmas) for all and
                                # high-SN sample
FWHM_THRESHOLDS      0.0,100.0  # FWHM thresholds (in pixels) for sources
FLAGS_MASK            0x00f0     # Rejection mask on SEX FLAGS
WEIGHTFLAGS_MASK     0x00ff     # Rejection mask on SEX FLAGS_WEIGHT
IMAFLAGS_MASK        0x0        # Rejection mask on SEX IMAFLAGS_ISO
AHEADER_GLOBAL       /usr/share/scamp/megacam.ahead
                                # Filename of the global INPUT header
AHEADER_SUFFIX       .ahead     # Filename extension for additional
                                # INPUT headers
HEADER_SUFFIX        .head      # Filename extension for OUTPUT headers
HEADER_TYPE          NORMAL     # NORMAL or FOCAL_PLANE
VERBOSE_TYPE         LOG        # QUIET, NORMAL, LOG or FULL
WRITE_XML            Y          # Write XML file (Y/N)?
XML_NAME             CFHTLS-T0007-W2_SCamp_astr.xml
                                # Filename for XML output
XSL_URL              scamp.xsl  # Filename for XSL style-sheet
NTHREADS             0          # Number of simultaneous threads for
                                # the SMP version of SCAMP
                                # 0 = automatic

```

## SCAMP photometric run (W1,W2,W3,W4) :

```
# Default configuration file for SCAMP 1.5.5
# EB 2009-04-10
# Last modified for CFHTLS-T0007-W4 (Megacam):
# YG 2010-10-27

#----- Field grouping -----
FGROUP_RADIUS      1.0          # Max dist (deg) between field groups

#----- Reference catalogs -----
REF_SERVER          cocat1.u-strasbg.fr # Internet addresses of catalog servers
REF_PORT            1660          # Ports to connect to catalog servers
CDSCIENT_EXEC       aclient       # CDSCient executable
ASTREF_CATALOG      2MASS         # NONE, FILE, USNO-A1, USNO-A2, USNO-B1,
                                     # GSC-1.3, GSC-2.2, UCAC-1, UCAC-2,
                                     # NOMAD-1, 2MASS, DENIS-3,
                                     # SDSS-R3, SDSS-R5 or SDSS-R6
ASTREF_BAND         DEFAULT       # Photom. band for astr.ref.magnitudes
                                     # or DEFAULT, BLUEST, or REDDEST
ASTREFCAT_NAME      astrefcat.cat  # Local astrometric reference catalogs
ASTREFCENT_KEYS     X_WORLD,Y_WORLD # Local ref.cat.centroid parameters
ASTREFERR_KEYS      ERRA_WORLD, ERRB_WORLD, ERRTHETA_WORLD
                                     # Local ref.cat.error ellipse parameters
ASTREFMAG_KEY       MAG           # Local ref.cat.magnitude parameter
SAVE_REFCATALOG     N             # Save ref catalogs in FITS-LDAC format?
REFOUT_CATPATH      .             # Save path for reference catalogs

#----- Merged output catalogs -----
MERGEDOUTCAT_NAME   scamp.cat      # Merged output catalog filename
MERGEDOUTCAT_TYPE   NONE          # NONE, ASCII_HEAD, ASCII, FITS_LDAC

#----- Pattern matching -----
MATCH               N             # Do pattern-matching (Y/N) ?
MATCH_NMAX          0             # Max.number of detections for MATCHING
                                     # (0=auto)
PIXSCALE_MAXERR     1.2           # Max scale-factor uncertainty
POSANGLE_MAXERR     5.0           # Max position-angle uncertainty (deg)
POSITION_MAXERR     1.0           # Max positional uncertainty (arcmin)
MATCH_RESOL         0             # Matching resolution (arcsec); 0=auto
MATCH_FLIPPED       N             # Allow matching with flipped axes?
MOSAIC_TYPE         UNCHANGED     # UNCHANGED, SAME_CRVAL, SHARE_PROJAXIS,
                                     # FIX_FOCALPLANE or LOOSE
FIXFOCALPLANE_NMIN 1             # Min number of dets for FIX_FOCALPLANE

#----- Cross-identification -----
CROSSID_RADIUS      2.0          # Cross-id initial radius (arcsec)

#----- Astrometric solution -----
SOLVE_ASTROM        N             # Compute astrometric solution (Y/N) ?
ASTRINSTRU_KEY      FILTER,QRUNID # FITS keyword(s) defining the astrom
STABILITY_TYPE      INSTRUMENT    # EXPOSURE, GROUP, INSTRUMENT or FILE
CENTROID_KEYS       XWIN_IMAGE,YWIN_IMAGE # Cat. parameters for centroiding
CENTROIDERR_KEYS    ERRRAWIN_IMAGE,ERRBWIN_IMAGE,ERRTHETAWIN_IMAGE
                                     # Cat. params for centroid err ellipse
DISTORT_KEYS        XWIN_IMAGE,YWIN_IMAGE # Cat. parameters or FITS keywords
DISTORT_GROUPS      1,1           # Polynom group for each context key
DISTORT_DEGREES     3             # Polynom degree for each group
ASTREF_WEIGHT        1.0          # Relative weight of ref.astrom.cat.
ASTRCLIP_NSIGMA     3.0          # Astrom. clipping threshold in sigmas
CORRECT_COLOURSHIFTS N           # Correct for colour shifts (Y/N)?
```

```

#----- Photometric solution -----
SOLVE_PHOTOM          Y          # Compute photometric solution (Y/N) ?
MAGZERO_OUT           30.0       # Magnitude zero-point(s) in output
MAGZERO_INTERR        0.01       # Internal mag.zero-point accuracy
MAGZERO_REFERR        0.03       # Photom.field mag.zero-point accuracy
PHOTINSTRU_KEY        FILTER     # FITS keyword(s) defining the photom.
MAGZERO_KEY           PHOT_C     # FITS keyword for the mag zero-point
EXPOTIME_KEY          EXPTIME    # FITS keyword for the exposure time (s)
AIRMASS_KEY           AIRMASS    # FITS keyword for the airmass
EXTINCT_KEY           PHOT_K     # FITS keyword for the extinction coeff
PHOTOMFLAG_KEY        PHOTFLAG   # FITS keyword for the photometry flag
PHOTFLUX_KEY          FLUX_AUTO   # Catalog param. for the flux measurement
PHOTFLUXERR_KEY       FLUXERR_AUTO # Catalog parameter for the flux error
PHOTCLIP_NSIGMA       3.0       # Photom.clipping threshold in sigmas

#----- Check-plots -----
CHECKPLOT_CKEY        SCAMPCOL   # FITS keyword for PLPLOT field colour
CHECKPLOT_DEV         PNG        # NULL, XWIN, TK, PS, PSC, XFIG, PNG,
                                # JPEG, AQT, PDF or SVG
CHECKPLOT_RES         1600,1200  # Check-plot resolution (0 = default)
CHECKPLOT_ANTIALIAS   Y          # Anti-aliasing using convert (Y/N) ?
CHECKPLOT_TYPE        DISTORTION,ASTR_INTERROR2D,ASTR_INTERROR1D,ASTR_REFERROR2D,
                                ASTR_REFERROR1D,ASTR_CHI2,PHOT_ERROR,PHOT_ERRORVSMAG,
                                PHOT_ZPCORR,PHOT_ZPCORR3D
CHECKPLOT_NAME        distort,astr_interror2d,astr_interror1d,astr_referror2d,
                                astr_referror1d,astr_chi2,psphot_error,phot_errorvsmag,
                                phot_zpcorr,phot_zpcorr3d
                                # Check-plot filename(s)

#----- Check-images -----
CHECKIMAGE_TYPE       NONE       # NONE, AS_PAIR, AS_REFPAIR, or AS_XCORR
CHECKIMAGE_NAME       check.fits  # Check-image filename(s)

#----- Miscellaneous -----
SN_THRESHOLDS        10.0,100.0  # S/N thresholds (in sigmas) for all and
                                # high-SN sample
FWHM_THRESHOLDS      0.0,100.0  # FWHM thresholds (in pixels) for sources
FLAGS_MASK            0x00f0     # Rejection mask on SEX FLAGS
WEIGHTFLAGS_MASK     0x00ff     # Rejection mask on SEX FLAGS_WEIGHT
IMAFLAGS_MASK        0x0        # Rejection mask on SEX IMAFLAGS_ISO
AHEADER_GLOBAL       /usr/share/scamp/megacam.ahead
                                # Filename of the global INPUT header
AHEADER_SUFFIX       .ahead     # Filename extension for additional
                                # INPUT headers
HEADER_SUFFIX        .head      # Filename extension for OUTPUT headers
HEADER_TYPE          NORMAL     # NORMAL or FOCAL_PLANE
VERBOSE_TYPE         LOG        # QUIET, NORMAL, LOG or FULL
WRITE_XML            Y          # Write XML file (Y/N)?
XML_NAME             CFHTLS-T0007-W4_SCamp_phot.xml
                                # Filename for XML output
XSL_URL              scamp.xsl   # Filename for XSL style-sheet
NTHREADS             0          # Number of simultaneous threads for
                                # the SMP version of SCAMP
                                # 0 = automatic

```

### A.3.2 SWarp stack configuration file for T0007 Wide

```

# Default configuration file for SWarp 2.17.6
# EB 2009-04-09
#
# Last modified for CFHTLS-T0007 (Megacam):
# YG 2010-11-02

#----- Output -----
IMAGEOUT_NAME      CFHTLS_W_z_022929-075600_T0007.fits
                   # Output filename
WEIGHTOUT_NAME     CFHTLS_W_z_022929-075600_T0007_weight.fits
                   # Output weight-map filename

HEADER_ONLY        N          # Only a header as an output file (Y/N)?
HEADER_SUFFIX      .head     # Filename extension for additional headers

#----- Input Weights -----
WEIGHT_TYPE        MAP_WEIGHT # BACKGROUND,MAP_RMS,MAP_VARIANCE
                   # or MAP_WEIGHT
WEIGHT_SUFFIX      _weight.fits # Suffix to use for weight-maps
WEIGHT_IMAGE       # Weightmap filename if suffix not used
                   # (all or for each weight-map)
WEIGHT_THRESH      # Bad pixel weight-threshold

#----- Co-addition -----
COMBINE            Y          # Combine resampled images (Y/N)?
COMBINE_TYPE       MEDIAN    # MEDIAN,AVERAGE,MIN,MAX,WEIGHTED,CHI2
                   # or SUM
BLANK_BADPIXELS    N          # Set to 0 pixels having a weight of 0

#----- Astrometry -----
CELESTIAL_TYPE     NATIVE    # NATIVE, PIXEL, EQUATORIAL,
                   # GALACTIC,ECLIPTIC, or SUPERGALACTIC
PROJECTION_TYPE    TAN       # Any WCS projection code or NONE
PROJECTION_ERR     0.001     # Maximum projection error (in output
                   # pixels), or 0 for no approximation
CENTER_TYPE        MANUAL    # MANUAL, ALL or MOST
CENTER             02:29:29.14,-07:56:00 # Coordinates of the image center
PIXELSCALE_TYPE    MANUAL    # MANUAL,FIT,MIN,MAX or MEDIAN
PIXEL_SCALE        0.186    # Pixel scale
IMAGE_SIZE         19354,19354 # Image size (0 = AUTOMATIC)

#----- Resampling -----
RESAMPLE           Y          # Resample input images (Y/N)?
RESAMPLE_DIR       .         # Directory path for resampled images
RESAMPLE_SUFFIX    .resamp.fits # filename extension for resampled images
RESAMPLING_TYPE    LANCZOS3  # NEAREST,BILINEAR,LANCZOS2,LANCZOS3
                   # or LANCZOS4 (1 per axis)
OVERSAMPLING       0         # Oversampling in each dimension
                   # (0 = automatic)
INTERPOLATE        Y          # Interpolate bad input pixels (Y/N)?
                   # (all or for each image)
FSCALASTRO_TYPE    VARIABLE  # NONE,FIXED, or VARIABLE
FSCALE_KEYWORD     FLXSCALE  # FITS keyword for the multiplicative
                   # factor applied to each input image
FSCALE_DEFAULT     1.0       # Default FSCALE value if not in header
GAIN_KEYWORD       GAIN      # FITS keyword for effect. gain (e-/ADU)
GAIN_DEFAULT       0.0       # Default gain if no FITS keyword found
                   # 0 = infinity (all or for each image)
SATLEV_KEYWORD     SATURATE  # FITS keyword for saturation level (ADU)
SATLEV_DEFAULT     50000.0   # Default saturation if no FITS keyword

```

```

#----- Background subtraction -----
SUBTRACT_BACK      Y          # Subtraction sky background (Y/N)?
                        # (all or for each image)
BACK_TYPE          AUTO      # AUTO or MANUAL
                        # (all or for each image)
BACK_DEFAULT       0.0      # Default background value in MANUAL
                        # (all or for each image)
BACK_SIZE          32       # Background mesh size (pixels)
                        # (all or for each image)
BACK_FILTERSIZE    7        # Background map filter range (meshes)
                        # (all or for each image)
BACK_FILTTHRESH   0.0      # Threshold above which the background-
                        # map filter operates

#----- Memory management -----
VMEM_DIR           .        # Directory path for swap files
VMEM_MAX           2047     # Maximum amount of virtual memory (MB)
MEM_MAX            128     # Maximum amount of usable RAM (MB)
COMBINE_BUFSIZE    400     # RAM dedicated to co-addition(MB)

#----- Miscellaneous -----
DELETE_TMPFILES    Y        # Delete temporary resampled FITS files
                        # (Y/N)?

COPY_KEYWORDS      FILTER,INSTRUME,TELESCOP,DETECTOR,OBSERVER,PHOT_C,PHOT_K,
OBJECT,DATE_OBS,ORIGIN,SEEING,REL_DATE
                        # List of FITS keywords to propagate
                        # from the input to the output headers
WRITE_FILEINFO     N        # Write information about each input
                        # file in the output image header?
WRITE_XML          Y        # Write XML file (Y/N)?
XML_NAME           CFHTLS_w_z_022929-075600_T0007_SWarp.xml
                        # Filename for XML output
XSL_URL            swarp.xsl # Filename for XSL style-sheet
VERBOSE_TYPE       NORMAL   # QUIET,NORMAL or FULL
NNODES             1        # Number of nodes (for clusters)
NODE_INDEX         0        # Node index (for clusters)

NTHREADS          0        # Number of simultaneous threads for
                        # the SMP version of SWarp
                        # 0 = automatic

```

### A.3.3 SWarp chi2-image configuration file for T0007 Wide

```

# Default configuration file for SWarp 2.17.6
# EB 2009-04-09
#
# Last modified for CFHTLS-T0007 chi2 (Megacam):
# YG 2010-12-14

#----- Output -----
IMAGEOUT_NAME      CFHTLS_W_gri_022929-075600_T0007.fits
                   # Output filename
WEIGHTOUT_NAME     CFHTLS_W_gri_022929-075600_T0007_weight.fits
                   # Output weight-map filename

HEADER_ONLY        N          # Only a header as an output file (Y/N)?
HEADER_SUFFIX      .head     # Filename extension for additional headers

#----- Input Weights -----
WEIGHT_TYPE        MAP_WEIGHT # BACKGROUND, MAP_RMS, MAP_VARIANCE
                   # or MAP_WEIGHT
WEIGHT_SUFFIX      _weight.fits # Suffix to use for weight-maps
WEIGHT_IMAGE       # Weightmap filename if suffix not used
                   # (all or for each weight-map)
WEIGHT_THRESH      # Bad pixel weight-threshold

#----- Co-addition -----
COMBINE            Y          # Combine resampled images (Y/N)?
COMBINE_TYPE       CHI2      # MEDIAN, AVERAGE, MIN, MAX, WEIGHTED, CHI2
                   # or SUM
BLANK_BADPIXELS    N          # Set to 0 pixels having a weight of 0

#----- Astrometry -----
CELESTIAL_TYPE     NATIVE     # NATIVE, PIXEL, EQUATORIAL,
                   # GALACTIC, ECLIPTIC, or SUPERGALACTIC
PROJECTION_TYPE    TAN        # Any WCS projection code or NONE
PROJECTION_ERR     0.001      # Maximum projection error (in output
                   # pixels), or 0 for no approximation
CENTER_TYPE        MANUAL     # MANUAL, ALL or MOST
CENTER             02:29:29.14,-07:56:00 # Coordinates of the image center
PIXELSCALE_TYPE    MANUAL     # MANUAL, FIT, MIN, MAX or MEDIAN
PIXEL_SCALE        0.186     # Pixel scale
IMAGE_SIZE         19354,19354 # Image size (0 = AUTOMATIC)

#----- Resampling -----
RESAMPLE           Y          # Resample input images (Y/N)?
RESAMPLE_DIR       .          # Directory path for resampled images
RESAMPLE_SUFFIX    .resamp.fits # filename extension for resampled images
RESAMPLING_TYPE    LANCZOS3   # NEAREST, BILINEAR, LANCZOS2, LANCZOS3
                   # or LANCZOS4 (1 per axis)
OVERSAMPLING       0          # Oversampling in each dimension
                   # (0 = automatic)
INTERPOLATE        Y          # Interpolate bad input pixels (Y/N)?
                   # (all or for each image)
FSCALASTRO_TYPE    VARIABLE   # NONE, FIXED, or VARIABLE
FSCALE_KEYWORD     FLXSCALE   # FITS keyword for the multiplicative
                   # factor applied to each input image
FSCALE_DEFAULT     1.0        # Default FSCALE value if not in header
GAIN_KEYWORD       GAIN       # FITS keyword for effect. gain (e-/ADU)
GAIN_DEFAULT       0.0        # Default gain if no FITS keyword found
                   # 0 = infinity (all or for each image)
SATLEV_KEYWORD     SATURATE   # FITS keyword for saturation level (ADU)
SATLEV_DEFAULT     50000.0    # Default saturation if no FITS keyword

```



```

#----- Background subtraction -----
SUBTRACT_BACK      Y          # Subtraction sky background (Y/N)?
                        # (all or for each image)
BACK_TYPE          AUTO      # AUTO or MANUAL
                        # (all or for each image)
BACK_DEFAULT       0.0       # Default background value in MANUAL
                        # (all or for each image)
BACK_SIZE          64        # Background mesh size (pixels)
                        # (all or for each image)
BACK_FILTERSIZE    3         # Background map filter range (meshes)
                        # (all or for each image)
BACK_FILTTHRESH   0.0       # Threshold above which the background-
                        # map filter operates

#----- Memory management -----
VMEM_DIR           .         # Directory path for swap files
VMEM_MAX           2047      # Maximum amount of virtual memory (MB)
MEM_MAX            4096      # Maximum amount of usable RAM (MB)
COMBINE_BUFSIZE    1024     # RAM dedicated to co-addition(MB)

#----- Miscellaneous -----
DELETE_TMPFILES    Y         # Delete temporary resampled FITS files
                        # (Y/N)?

COPY_KEYWORDS      OBJECT,FILTER,TELESCOP,INSTRUME,DETECTOR
                        # List of FITS keywords to propagate
                        # from the input to the output headers
WRITE_FILEINFO     Y         # Write information about each input
                        # file in the output image header?
WRITE_XML          Y         # Write XML file (Y/N)?
XML_NAME           CFHTLS_W_gri_022929-075600-T0007_SWarp_chi2.xml
                        # Filename for XML output
XSL_URL            swarp.xsl # Filename for XSL style-sheet
VERBOSE_TYPE       NORMAL    # QUIET,NORMAL or FULL
NNODES             1         # Number of nodes (for clusters)
NODE_INDEX         0         # Node index (for clusters)

NTHREADS           0         # Number of simultaneous threads for
                        # the SMP version of SWarp
                        # 0 = automatic

```

### A.3.4 SExtractor .ldac catalogue configuration file for T0007 Wide

```

# Default configuration file for SExtractor 2.11.0
# EB 2010-02-11
#
# Last modified for SExtr stack.ldac MAG_APER(1):
# YG 2011-01-28

#----- Catalog -----
CATALOG_NAME      CFHTLS_W_r_141754+543031_T0007.ldac
                  # name of the output catalog
CATALOG_TYPE      FITS_LDAC
                  # NONE,ASCII,ASCII_HEAD, ASCII_SKYCAT,
                  # ASCII_VOTABLE, FITS_1.0 or FITS_LDAC
PARAMETERS_NAME   sextr-stack_APER1.param
                  # name of the file containing catalog contents

#----- Extraction -----
DETECT_TYPE       CCD
                  # CCD (linear) or PHOTO (with gamma correction)
DETECT_MINAREA    3
                  # min. number of pixels above threshold
DETECT_MAXAREA    0
                  # max. number of pixels above threshold (0=unlimited)
THRESH_TYPE       RELATIVE
                  # threshold type: RELATIVE (in sigmas)
                  # or ABSOLUTE (in ADUs)
DETECT_THRESH     1.0
                  # <sigmas> or <threshold>,<ZP> in mag.arcsec-2
ANALYSIS_THRESH   1.0
                  # <sigmas> or <threshold>,<ZP> in mag.arcsec-2
FILTER            Y
                  # apply filter for detection (Y or N)?
FILTER_NAME       default-auto.conv
                  # name of the file containing the filter
FILTER_THRESH     32
                  # Threshold[s] for retina filtering
DEBLEND_NTHRESH   32
                  # Number of deblending sub-thresholds
DEBLEND_MINCONT   0.002
                  # Minimum contrast parameter for deblending
CLEAN             Y
                  # Clean spurious detections? (Y or N)?
CLEAN_PARAM       1.0
                  # Cleaning efficiency
MASK_TYPE         CORRECT
                  # type of detection MASKing: can be one of
                  # NONE, BLANK or CORRECT

#----- WEIGHTing -----
WEIGHT_TYPE       MAP_WEIGHT
                  # type of WEIGHTing: NONE, BACKGROUND,
                  # MAP_RMS, MAP_VAR or MAP_WEIGHT
WEIGHT_IMAGE      CFHTLS_W_r_141754+543031_T0007_weight.fits
                  # weight-map filename
WEIGHT_GAIN       Y
                  # modulate gain (E/ADU) with weights? (Y/N)
WEIGHT_THRESH     0
                  # weight threshold[s] for bad pixels

#----- FLAGging -----
FLAG_IMAGE        flag.fits
                  # filename for an input FLAG-image
FLAG_TYPE         OR
                  # flag pixel combination: OR, AND, MIN, MAX
                  # or MOST

#----- Photometry -----
PHOT_APERTURES    34.853
                  # MAG_APER aperture diameter(s) in pixels
PHOT_AUTOPARAMS  2.5, 3.5
                  # MAG_AUTO parameters: <Kron_fact>,<min_radius>
PHOT_PETROPARAMS 2.0, 3.5
                  # MAG_PETRO parameters: <Petrosian_fact>,
                  # <min_radius>
PHOT_AUTOAPERS    0.0,0.0
                  # <estimation>,<measurement> minimum apertures
                  # for MAG_AUTO and MAG_PETRO
PHOT_FLUXFRAC     0.2,0.5,0.8
                  # flux fraction[s] used for FLUX_RADIUS
SATUR_LEVEL       50000.0
                  # level (in ADUs) at which arises saturation
SATUR_KEY         TOTO
                  # keyword for saturation level (in ADUs)
MAG_ZEROPOINT     30.0
                  # magnitude zero-point
MAG_GAMMA         4.0
                  # gamma of emulsion (for photographic scans)
GAIN              0.0
                  # detector gain in e-/ADU
GAIN_KEY          GAIN
                  # keyword for detector gain in e-/ADU
PIXEL_SCALE       0
                  # size of pixel in arcsec (0=use FITS WCS info)

```

```

#----- Star/Galaxy Separation -----
SEEING_FWHM      0.9          # stellar FWHM in arcsec
STARNNW_NAME     default-auto.nnw # Neural-Network_Weight table filename

#----- Background -----
BACK_TYPE        AUTO          # AUTO or MANUAL
BACK_VALUE       0.0           # Default background value in MANUAL mode
BACK_SIZE        128           # Background mesh: <size> or <width>,<height>
BACK_FILTERSIZE  3             # Background filter: <size> or <width>,<height>
BACKPHOTO_TYPE   GLOBAL        # can be GLOBAL or LOCAL
BACKPHOTO_THICK  24           # thickness of the background LOCAL annulus
BACK_FILTTHRESH  0.0           # Threshold above which the background-
# map filter operates

#----- Check Image -----
CHECKIMAGE_TYPE  MINIBACKGROUND # can be NONE, BACKGROUND, BACKGROUND_RMS,
# MINIBACKGROUND, MINIBACK_RMS, -BACKGROUND,
# FILTERED, OBJECTS, -OBJECTS, SEGMENTATION,
# or APERTURES
CHECKIMAGE_NAME  CFHTLS_W_r_141754+543031_T0007_mbkg.fits
# Filename for the check-image

#----- Memory (change with caution!) -----
MEMORY_OBJSTACK  3000          # number of objects in stack
MEMORY_PIXSTACK  300000        # number of pixels in stack
MEMORY_BUFSIZE   1024          # number of lines in buffer

#----- ASSOCIation -----
ASSOC_NAME       sky.list      # name of the ASCII file to ASSOCIate
ASSOC_DATA       2,3,4         # columns of the data to replicate (0=all)
ASSOC_PARAMS     2,3,4         # columns of xpos,ypos[,mag]
ASSOC_RADIUS     2.0           # cross-matching radius (pixels)
ASSOC_TYPE       NEAREST       # ASSOCIation method: FIRST, NEAREST, MEAN,
# MAG_MEAN, SUM, MAG_SUM, MIN or MAX
ASSOCSELEC_TYPE  MATCHED       # ASSOC selection type: ALL, MATCHED or -MATCHED

#----- Miscellaneous -----
VERBOSE_TYPE     NORMAL        # can be QUIET, NORMAL or FULL
HEADER_SUFFIX    .head         # Filename extension for additional headers
WRITE_XML        Y             # Write XML file (Y/N)?
XML_NAME         CFHTLS_W_r_141754+543031_T0007_SExtr_ldac.xml
# Filename for XML output
XSL_URL         sextractor.xsl # Filename for XSL style-sheet
NTHREADS        1             # 1 single thread
FITS_UNSIGNED    N             # Treat FITS integer values as unsigned (Y/N)?
INTERP_MAXXLG   16            # Max. lag along X for 0-weight interpolation
INTERP_MAXYLG   16            # Max. lag along Y for 0-weight interpolation
INTERP_TYPE      ALL           # Interpolation type: NONE, VAR_ONLY or ALL

#----- Experimental Stuff -----
PSF_NAME         default.psf    # File containing the PSF model
PSF_NMAX         2             # Max.number of PSFs fitted simultaneously
PATTERN_TYPE     RINGS-HARMONIC # can RINGS-QUADPOLE, RINGS-OCTOPOLE,
# RINGS-HARMONICS or GAUSS-LAGUERRE
SOM_NAME         default.som    # File containing Self-Organizing Map weights

```

### A.3.5 SExtractor DUAL MODE .cat catalogue configuration file for T0007 Wide

```

# Default configuration file for SExtractor 2.8.6
# EB 2009-04-09
#
# Last modified for CFHTLS-T0007 chi2 (Megacam):
# PH 2011-06-09

#----- Catalog -----
CATALOG_NAME      CFHTLS_W_r_141754+543031_T0007.cat
                  # name of the output catalog
CATALOG_TYPE      ASCII_HEAD      # NONE,ASCII,ASCII_HEAD, ASCII_SKYCAT,
                  # ASCII_VOTABLE, FITS_1.0 or FITS_LDAC
PARAMETERS_NAME   sextr-chi2_APER27.param # name of the file containing catalog contents

#----- Extraction -----
DETECT_TYPE       CCD              # CCD (linear) or PHOTO (with gamma correction)
DETECT_MINAREA    3                # minimum number of pixels above threshold
THRESH_TYPE       ABSOLUTE         # threshold type: RELATIVE (in sigmas)
                  # or ABSOLUTE (in ADUs)
DETECT_THRESH     0.4              # <sigmas> or <threshold>,<ZP> in mag.arcsec-2
ANALYSIS_THRESH   0.4              # <sigmas> or <threshold>,<ZP> in mag.arcsec-2
FILTER            Y                # apply filter for detection (Y or N)?
FILTER_NAME       default-autochi2.conv # name of the file containing the filter
FILTER_THRESH     # Threshold[s] for retina filtering
DEBLEND_NTHRESH   32              # Number of deblending sub-thresholds
DEBLEND_MINCONT   0.002           # Minimum contrast parameter for deblending
CLEAN             Y                # Clean spurious detections? (Y or N)?
CLEAN_PARAM       1.0             # Cleaning efficiency
MASK_TYPE         CORRECT          # type of detection MASKing: can be one of
                  # NONE, BLANK or CORRECT

#----- WEIGHTing -----
WEIGHT_TYPE       MAP_WEIGHT,MAP_WEIGHT # type of WEIGHTing: NONE, BACKGROUND,
                  # MAP_RMS, MAP_VAR or MAP_WEIGHT
WEIGHT_IMAGE      CFHTLS_W_gri_141754+543031_T0007_weight.fits,
                  CFHTLS_W_r_141754+543031_T0007_weight.fits
                  # weight-map filename
WEIGHT_GAIN       Y                # modulate gain (E/ADU) with weights? (Y/N)
WEIGHT_THRESH     # weight threshold[s] for bad pixels

#----- FLAGging -----
FLAG_IMAGE        flag.fits        # filename for an input FLAG-image
FLAG_TYPE         OR               # flag pixel combination: OR, AND, MIN, MAX
                  # or MOST

#----- Photometry -----
PHOT_APERTURES    10.,12.,14.,16.,18.,20.,22.,24.,26.,28.,30.,32.,34.,36.,38.,
                  40.,42.,44.,46.,48.,50.,52.,54.,56.,58.,60.,34.853
                  # MAG_APER aperture diameter(s) in pixels
PHOT_AUTOPARAMS   2.5, 3.5        # MAG_AUTO parameters: <Kron_fact>,<min_radius>
PHOT_PETROPARAMS  2.0, 3.5        # MAG_PETRO parameters: <Petrosian_fact>,
                  # <min_radius>
PHOT_AUTOAPERS    16.0,16.0       # <estimation>,<measurement> minimum apertures
                  # for MAG_AUTO and MAG_PETRO
PHOT_FLUXFRAC     0.2,0.5,0.8     # flux fraction[s] used for FLUX_RADIUS
SATUR_LEVEL       50000.0         # level (in ADUs) at which arises saturation
SATUR_KEY         TOTO            # keyword for saturation level (in ADUs)
MAG_ZEROPOINT     30.0           # magnitude zero-point
MAG_GAMMA         4.0            # gamma of emulsion (for photographic scans)
GAIN              0.0            # detector gain in e-/ADU
GAIN_KEY          GAIN           # keyword for detector gain in e-/ADU
PIXEL_SCALE       0              # size of pixel in arcsec (0=use FITS WCS info)

```

```

#----- Star/Galaxy Separation -----
SEEING_FWHM      0.9          # stellar FWHM in arcsec
STARNW_NAME      default-autochi2.nnw  # Neural-Network_Weight table filename

#----- Background -----
BACK_TYPE        AUTO          # AUTO or MANUAL
BACK_VALUE       0.0          # Default background value in MANUAL mode
BACK_SIZE        256          # Background mesh: <size> or <width>,<height>
BACK_FILTERSIZE  9            # Background filter: <size> or <width>,<height>
BACKPHOTO_TYPE   LOCAL        # can be GLOBAL or LOCAL
BACKPHOTO_THICK  30          # thickness of the background LOCAL annulus
BACK_FILTTHRESH  0.0          # Threshold above which the background-
                                # map filter operates

#----- Check Image -----
CHECKIMAGE_TYPE  MINIBACKGROUND  # can be NONE, BACKGROUND, BACKGROUND_RMS,
                                # MINIBACKGROUND, MINIBACK_RMS, -BACKGROUND,
                                # FILTERED, OBJECTS, -OBJECTS, SEGMENTATION,
                                # or APERTURES
CHECKIMAGE_NAME  CFHTLS_W_r_141754+543031_T0007_mbkgs_chi2.fits
                                # Filename for the check-image

#----- Memory (change with caution!) -----
MEMORY_OBJSTACK  5000         # number of objects in stack
MEMORY_PIXSTACK  1000000     # number of pixels in stack
MEMORY_BUFSIZE   1024        # number of lines in buffer

#----- ASSOCIation -----
ASSOC_NAME       sky.list     # name of the ASCII file to ASSOCIate
ASSOC_DATA       2,3,4        # columns of the data to replicate (0=all)
ASSOC_PARAMS     2,3,4        # columns of xpos,ypos[,mag]
ASSOC_RADIUS     2.0         # cross-matching radius (pixels)
ASSOC_TYPE       NEAREST     # ASSOCIation method: FIRST, NEAREST, MEAN,
                                # MAG_MEAN, SUM, MAG_SUM, MIN or MAX
ASSOCSELEC_TYPE  MATCHED     # ASSOC selection type: ALL, MATCHED or -MATCHED

#----- Miscellaneous -----
VERBOSE_TYPE     NORMAL      # can be QUIET, NORMAL or FULL
WRITE_XML        Y           # Write XML file (Y/N)?
XML_NAME         CFHTLS_W_r_141754+543031_T0007_SExtr_chi2.xml
                                # Filename for XML output
XSL_URL          sextractor.xsl # Filename for XSL style-sheet
NTHREADS        0           # Number of simultaneous threads for
                                # the SMP version of SExtractor
                                # 0 = automatic
FITS_UNSIGNED    N           # Treat FITS integer values as unsigned (Y/N)?
INTERP_MAXXLG   16          # Max. lag along X for 0-weight interpolation
INTERP_MAXYLAG  16          # Max. lag along Y for 0-weight interpolation
INTERP_TYPE      ALL         # Interpolation type: NONE, VAR_ONLY or ALL

#----- Experimental Stuff -----
PSF_NAME         default.psf  # File containing the PSF model
PSF_NMAX         9           # Max.number of PSFs fitted simultaneously
PSFDISPLAY_TYPE  SPLIT       # Catalog type for PSF-fitting: SPLIT or VECTOR
PATTERN_TYPE     RINGS-HARMONIC
                                # can RINGS-QUADPOLE, RINGS-OCTOPOLE,
                                # RINGS-HARMONICS or GAUSS-LAGUERRE
SOM_NAME         default.som  # File containing Self-Organizing Map weights

```

## B CFHTLS T0007 Deep supplementary information

### B.1 Rescaling factors applied to deep stacks

Filter	u		g		r		i		y		z	
	D-25	D85	D-25	D85	D-25	D85	D-25	D85	D-25	D85	D-25	D85
D1-MED	0.015	0.016	0.013	0.011	0.026	0.023	0.023	0.032	0.034	0.013	0.015	0.019
D2-MED	0.027	0.005	0.010	0.010	0.021	0.016	0.028	0.032	0.017	0.031	0.019	0.018
D3-MED	0.026	0.026	0.005	0.007	0.012	0.016	0.029	0.021	0.016	0.020	0.010	0.011
D4-MED	-0.003	0.007	0.003	0.013	0.019	0.014	0.018	0.027	0.023	0.028	0.014	0.017
D1-SIG	0.026	0.027	0.023	0.026	0.035	0.035	0.037	0.039	0.036	0.032	0.028	0.032
D2-SIG	0.035	0.024	0.021	0.022	0.027	0.028	0.037	0.037	0.027	0.031	0.030	0.030
D3-SIG	0.030	0.035	0.019	0.023	0.026	0.028	0.039	0.036	0.027	0.028	0.026	0.024
D4-SIG	0.014	0.017	0.016	0.023	0.023	0.026	0.032	0.035	0.030	0.033	0.026	0.027

**Table 33:** Rescaling factors which were applied to each individual deep stack. Magnitude offsets,  $\delta_{\text{SNLS}}$ , between SNLS tertiary standards and CFHTLS stacks. These magnitude offsets are used to compute a rescaling factor using Equation 5.

## B.2 CFHTLS T0007 Deep configuration files

### B.2.1 SCAMP configuration files for T0007 Deep

#### SCAMP internal astrometric reference catalogue run (D1,D2,D3,D4) :

```
# Default configuration file for SCAMP 1.5.5
# EB 2009-04-10
# Last modified for CFHTLS-T0007-D3 (Megacam):
# YG 2011-05-27

#----- Field grouping -----
FGROUP_RADIUS          1.0          # Max dist (deg) between field groups

#----- Reference catalogs -----
REF_SERVER              cocatl.u-strasbg.fr # Internet addresses of catalog servers
REF_PORT                1660          # Ports to connect to catalog servers
CDSCLIENT_EXEC         aclient       # CDSclient executable
ASTREF_CATALOG          2MASS         # NONE, FILE, USNO-A1, USNO-A2, USNO-B1,
# GSC-1.3, GSC-2.2, UCAC-1, UCAC-2,
# NOMAD-1, 2MASS, DENIS-3,
# SDSS-R3, SDSS-R5 or SDSS-R6
ASTREF_BAND             DEFAULT       # Photom. band for astr.ref.magnitudes
# or DEFAULT, BLUEST, or REDDEST
ASTREFCAT_NAME          astrefcat.cat  # Local astrometric reference catalogs
ASTREFCENT_KEYS        X_WORLD,Y_WORLD # Local ref.cat.centroid parameters
ASTREFERR_KEYS         ERRA_WORLD,ERRB_WORLD,ERRTHETA_WORLD
# Local ref.cat.error ellipse parameters
ASTREFMAG_KEY          MAG           # Local ref.cat.magnitude parameter
SAVE_REFCATALOG        N             # Save ref catalogs in FITS-LDAC format?
REFOUT_CATPATH         .             # Save path for reference catalogs

#----- Merged output catalogs -----
MERGEDOUTCAT_NAME      CFHTLS-T0007-D3_SCamp_astr_ref.cat
# Merged output catalog filename
MERGEDOUTCAT_TYPE      FITS_LDAC     # NONE, ASCII_HEAD, ASCII, FITS_LDAC

#----- Pattern matching -----
MATCH                  Y             # Do pattern-matching (Y/N) ?
MATCH_NMAX             0             # Max.number of detections for MATCHing
# (0=auto)
PIXSCALE_MAXERR        1.2          # Max scale-factor uncertainty
POSANGLE_MAXERR        5.0          # Max position-angle uncertainty (deg)
POSITION_MAXERR        1.0          # Max positional uncertainty (arcmin)
MATCH_RESOL            0            # Matching resolution (arcsec); 0=auto
MATCH_FLIPPED          N            # Allow matching with flipped axes?
MOSAIC_TYPE            SAME_CRVAL    # UNCHANGED, SAME_CRVAL, SHARE_PROJAXIS,
# FIX_FOCALPLANE or LOOSE
FIXFOCALPLANE_NMIN    1            # Min number of dets for FIX_FOCALPLANE

#----- Cross-identification -----
CROSSID_RADIUS         2.0          # Cross-id initial radius (arcsec)

#----- Astrometric solution -----
SOLVE_Astrom           Y            # Compute astrometric solution (Y/N) ?
ASTRINSTRU_KEY         FILTER,QRUNID # FITS keyword(s) defining the astrom
STABILITY_TYPE         INSTRUMENT    # EXPOSURE, GROUP, INSTRUMENT or FILE
CENTROID_KEYS          XWIN_IMAGE,YWIN_IMAGE # Cat. parameters for centroiding
CENTROIDERR_KEYS       ERRRAWIN_IMAGE,ERRBWIN_IMAGE,ERRTHETAWIN_IMAGE
# Cat. params for centroid err ellipse
DISTORT_KEYS           XWIN_IMAGE,YWIN_IMAGE # Cat. parameters or FITS keywords
```

```

DISTORT_GROUPS      1,1          # Polynom group for each context key
DISTORT_DEGREES    3            # Polynom degree for each group
ASTREF_WEIGHT      1.0          # Relative weight of ref.astrom.cat.
ASTRCLIP_NSIGMA   3.0          # Astrom. clipping threshold in sigmas
CORRECT_COLOURSHIFTS N         # Correct for colour shifts (Y/N)?

#----- Photometric solution -----
SOLVE_PHOTOM      Y            # Compute photometric solution (Y/N) ?
MAGZERO_OUT       30.0         # Magnitude zero-point(s) in output
MAGZERO_INTERR    0.01         # Internal mag.zero-point accuracy
MAGZERO_REFERR    0.03         # Photom.field mag.zero-point accuracy
PHOTINSTRU_KEY    FILTER       # FITS keyword(s) defining the photom.
MAGZERO_KEY       PHOT_C       # FITS keyword for the mag zero-point
EXPOTIME_KEY      EXPTIME      # FITS keyword for the exposure time (s)
AIRMASS_KEY       AIRMASS      # FITS keyword for the airmass
EXTINCT_KEY       PHOT_K       # FITS keyword for the extinction coeff
PHOTOMFLAG_KEY    PHOTFLAG     # FITS keyword for the photometry flag
PHOTFLUX_KEY      FLUX_AUTO     # Catalog param. for the flux measurement
PHOTFLUXERR_KEY   FLUXERR_AUTO  # Catalog parameter for the flux error
PHOTCLIP_NSIGMA  3.0          # Photom.clipping threshold in sigmas

#----- Check-plots -----
CHECKPLOT_CKEY    SCAMPCOL      # FITS keyword for PLPLOT field colour
CHECKPLOT_DEV     PNG           # NULL, XWIN, TK, PS, PSC, XFIG, PNG,
                                # JPEG, AQT, PDF or SVG
CHECKPLOT_RES     1600,1200     # Check-plot resolution (0 = default)
CHECKPLOT_ANTIALIAS Y          # Anti-aliasing using convert (Y/N) ?
CHECKPLOT_TYPE    DISTORTION,ASTR_INTERROR2D,ASTR_INTERROR1D,ASTR_REFERROR2D,
ASTR_REFERROR1D,ASTR_CHI2,PHOT_ERROR,PHOT_ERRORVSMAG,
PHOT_ZPCORR,PHOT_ZPCORR3D
CHECKPLOT_NAME    distort,astr_interror2d,astr_interror1d,astr_referror2d,
astr_referror1d,astr_chi2,psphot_error,phot_errorvsmag,
phot_zpcorr,phot_zpcorr3d
                                # Check-plot filename(s)

#----- Check-images -----
CHECKIMAGE_TYPE   NONE          # NONE, AS_PAIR, AS_REFPAIR, or AS_XCORR
CHECKIMAGE_NAME   check.fits    # Check-image filename(s)

#----- Miscellaneous -----
SN_THRESHOLDS    10.0,100.0    # S/N thresholds (in sigmas) for all and
                                # high-SN sample
FWHM_THRESHOLDS  0.0,100.0     # FWHM thresholds (in pixels) for sources
FLAGS_MASK       0x00f0        # Rejection mask on SEX FLAGS
WEIGHTFLAGS_MASK 0x00ff        # Rejection mask on SEX FLAGS_WEIGHT
IMAFLAGS_MASK    0x0           # Rejection mask on SEX IMAFLAGS_ISO
AHEADER_GLOBAL   /usr/share/scamp/megacam.ahead
AHEADER_SUFFIX   .ahead        # Filename of the global INPUT header
                                # Filename extension for additional
                                # INPUT headers
HEADER_SUFFIX    .head         # Filename extension for OUTPUT headers
HEADER_TYPE      NORMAL        # NORMAL or FOCAL_PLANE
VERBOSE_TYPE     LOG           # QUIET, NORMAL, LOG or FULL
WRITE_XML        Y             # Write XML file (Y/N)?
XML_NAME         CFHTLS-T0007-D3_SCamp_astrom_ref.xml
                                # Filename for XML output
XSL_URL          scamp.xsl     # Filename for XSL style-sheet
NTHREADS        0             # Number of simultaneous threads for
                                # the SMP version of SCAMP
                                # 0 = automatic

```



## SCAMP astrometric run using internal astrometric reference catalogue (D1,D2,D3,D4) :

```

# Default configuration file for SCAMP 1.5.5
# EB 2009-04-10
# Last modified for CFHTLS-T0007-D3 (Megacam):
# YG 2011-02-21

#----- Field grouping -----
FGROUP_RADIUS      1.0          # Max dist (deg) between field groups

#----- Reference catalogs -----
REF_SERVER          cocat1.u-strasbg.fr # Internet addresses of catalog servers
REF_PORT            1660          # Ports to connect to catalog servers
CDSCLIENT_EXEC     aclient       # CDSclient executable
ASTREF_CATALOG      FILE         # NONE, FILE, USNO-A1, USNO-A2, USNO-B1,
                                # GSC-1.3, GSC-2.2, UCAC-1, UCAC-2,
                                # NOMAD-1, 2MASS, DENIS-3,
                                # SDSS-R3, SDSS-R5 or SDSS-R6
ASTREF_BAND         DEFAULT      # Photom. band for astr.ref.magnitudes
                                # or DEFAULT, BLUEST, or REDDEST
ASTREFCAT_NAME      CFHTLS-T0007-D3_SCamp_astr_ref.cat
                                # Local astrometric reference catalogs
ASTREFCENT_KEYS     X_WORLD,Y_WORLD # Local ref.cat.centroid parameters
ASTREFERR_KEYS      ERRA_WORLD, ERRB_WORLD, ERRTHETA_WORLD
                                # Local ref.cat.error ellipse parameters
ASTREFMAG_KEY       MAG          # Local ref.cat.magnitude parameter
SAVE_REFCATALOG     N           # Save ref catalogs in FITS-LDAC format?
REFOUT_CATPATH      .           # Save path for reference catalogs

#----- Merged output catalogs -----
MERGEDOUTCAT_NAME   scamp.cat     # Merged output catalog filename
MERGEDOUTCAT_TYPE   NONE         # NONE, ASCII_HEAD, ASCII, FITS_LDAC

#----- Pattern matching -----
MATCH               Y           # Do pattern-matching (Y/N) ?
MATCH_NMAX          0           # Max.number of detections for MATCHing
                                # (0=auto)
PIXSCALE_MAXERR     1.2         # Max scale-factor uncertainty
POSANGLE_MAXERR     5.0         # Max position-angle uncertainty (deg)
POSITION_MAXERR     1.0         # Max positional uncertainty (arcmin)
MATCH_RESOL         0           # Matching resolution (arcsec); 0=auto
MATCH_FLIPPED       N           # Allow matching with flipped axes?
MOSAIC_TYPE         SAME_CRVAL   # UNCHANGED, SAME_CRVAL, SHARE_PROJAXIS,
                                # FIX_FOCALPLANE or LOOSE
FIXFOCALPLANE_NMIN 1           # Min number of dets for FIX_FOCALPLANE

#----- Cross-identification -----
CROSSID_RADIUS      2.0         # Cross-id initial radius (arcsec)

#----- Astrometric solution -----
SOLVE_ASTROM        Y           # Compute astrometric solution (Y/N) ?
ASTRINSTRU_KEY      FILTER,QRUNID # FITS keyword(s) defining the astrom
STABILITY_TYPE      INSTRUMENT  # EXPOSURE, GROUP, INSTRUMENT or FILE
CENTROID_KEYS       XWIN_IMAGE,YWIN_IMAGE # Cat. parameters for centroiding
CENTROIDERR_KEYS    ERRRAWIN_IMAGE,ERRBWIN_IMAGE,ERRTHETAWIN_IMAGE
                                # Cat. params for centroid err ellipse
DISTORT_KEYS        XWIN_IMAGE,YWIN_IMAGE # Cat. parameters or FITS keywords
DISTORT_GROUPS      1,1         # Polynom group for each context key
DISTORT_DEGREES     3           # Polynom degree for each group
ASTREF_WEIGHT        1.0         # Relative weight of ref.astrom.cat.
ASTRCLIP_NSIGMA     3.0         # Astrom. clipping threshold in sigmas
CORRECT_COLOURSHIFTS N         # Correct for colour shifts (Y/N)?

```

```

#----- Photometric solution -----
SOLVE_PHOTOM          Y          # Compute photometric solution (Y/N) ?
MAGZERO_OUT           30.0       # Magnitude zero-point(s) in output
MAGZERO_INTERR        0.01       # Internal mag.zero-point accuracy
MAGZERO_REFERR        0.03       # Photom.field mag.zero-point accuracy
PHOTINSTRU_KEY        FILTER      # FITS keyword(s) defining the photom.
MAGZERO_KEY           PHOT_C      # FITS keyword for the mag zero-point
EXPOTIME_KEY          EXPTIME     # FITS keyword for the exposure time (s)
AIRMASS_KEY           AIRMASS     # FITS keyword for the airmass
EXTINCT_KEY           PHOT_K      # FITS keyword for the extinction coeff
PHOTOMFLAG_KEY        PHOTFLAG    # FITS keyword for the photometry flag
PHOTFLUX_KEY          FLUX_AUTO    # Catalog param. for the flux measurement
PHOTFLUXERR_KEY       FLUXERR_AUTO # Catalog parameter for the flux error
PHOTCLIP_NSIGMA      3.0         # Photom.clipping threshold in sigmas

#----- Check-plots -----
CHECKPLOT_CKEY        SCAMPCOL     # FITS keyword for PLPLOT field colour
CHECKPLOT_DEV         PNG          # NULL, XWIN, TK, PS, PSC, XFIG, PNG,
                                     # JPEG, AQT, PDF or SVG
CHECKPLOT_RES         1600,1200    # Check-plot resolution (0 = default)
CHECKPLOT_ANTIALIAS   Y           # Anti-aliasing using convert (Y/N) ?
CHECKPLOT_TYPE        DISTORTION,ASTR_INTERROR2D,ASTR_INTERROR1D,ASTR_REFERROR2D,
ASTR_REFERROR1D,ASTR_CHI2,PHOT_ERROR,PHOT_ERRORVSMAG,
PHOT_ZPCORR,PHOT_ZPCORR3D
CHECKPLOT_NAME        distort,astr_interror2d,astr_interror1d,astr_referror2d,
astr_referror1d,astr_chi2,psphot_error,phot_errorvsmag,
phot_zpcorr,phot_zpcorr3d
                                     # Check-plot filename(s)

#----- Check-images -----
CHECKIMAGE_TYPE       NONE        # NONE, AS_PAIR, AS_REPAIR, or AS_XCORR
CHECKIMAGE_NAME       check.fits   # Check-image filename(s)

#----- Miscellaneous -----
SN_THRESHOLDS        10.0,100.0   # S/N thresholds (in sigmas) for all and
                                     # high-SN sample
FWHM_THRESHOLDS      0.0,100.0    # FWHM thresholds (in pixels) for sources
FLAGS_MASK           0x00f0       # Rejection mask on SEX FLAGS
WEIGHTFLAGS_MASK     0x00ff       # Rejection mask on SEX FLAGS_WEIGHT
IMAFLAGS_MASK        0x0          # Rejection mask on SEX IMAFLAGS_ISO
AHEADER_GLOBAL       /usr/share/scamp/megacam.ahead
                                     # Filename of the global INPUT header
AHEADER_SUFFIX       .ahead       # Filename extension for additional
                                     # INPUT headers
HEADER_SUFFIX        .head        # Filename extension for OUTPUT headers
HEADER_TYPE          NORMAL       # NORMAL or FOCAL_PLANE
VERBOSE_TYPE         LOG          # QUIET, NORMAL, LOG or FULL
WRITE_XML            Y           # Write XML file (Y/N)?
XML_NAME             CFHTLS-T0007-D3_SCamp_ast_g.xml
                                     # Filename for XML output
XSL_URL              scamp.xsl    # Filename for XSL style-sheet
NTHREADS            0            # Number of simultaneous threads for
                                     # the SMP version of SCAMP
                                     # 0 = automatic

```

## SCAMP photometric run (D1,D2,D3,D4) :

```

# Default configuration file for SCAMP 1.5.5
# EB 2009-04-10
# Last modified for CFHTLS-T0007-D3 (Megacam):
# YG 2011-06-10

#----- Field grouping -----
FGROUP_RADIUS      1.0          # Max dist (deg) between field groups

#----- Reference catalogs -----
REF_SERVER         cocat1.u-strasbg.fr # Internet addresses of catalog servers
REF_PORT           1660           # Ports to connect to catalog servers
CDSCLIENT_EXEC    aclient        # CDSclient executable
ASTREF_CATALOG     FILE          # NONE, FILE, USNO-A1, USNO-A2, USNO-B1,
                                # GSC-1.3, GSC-2.2, UCAC-1, UCAC-2,
                                # NOMAD-1, 2MASS, DENIS-3,
                                # SDSS-R3, SDSS-R5 or SDSS-R6
ASTREF_BAND        DEFAULT       # Photom. band for astr.ref.magnitudes
                                # or DEFAULT, BLUEST, or REDDEST
ASTREFCAT_NAME     CFHTLS-T0007-D3_SCamp_astr_ref.cat
                                # Local astrometric reference catalogs
ASTREFCENT_KEYS    X_WORLD,Y_WORLD # Local ref.cat.centroid parameters
ASTREFERR_KEYS     ERRA_WORLD, ERRB_WORLD, ERRTHETA_WORLD
                                # Local ref.cat.error ellipse parameters
ASTREFMAG_KEY      MAG           # Local ref.cat.magnitude parameter
SAVE_REFCATALOG    N            # Save ref catalogs in FITS-LDAC format?
REFOUT_CATPATH     .            # Save path for reference catalogs

#----- Merged output catalogs -----
MERGEDOUTCAT_NAME  scamp.cat      # Merged output catalog filename
MERGEDOUTCAT_TYPE  NONE          # NONE, ASCII_HEAD, ASCII, FITS_LDAC

#----- Pattern matching -----
MATCH              N            # Do pattern-matching (Y/N) ?
MATCH_NMAX         0           # Max.number of detections for MATCHing
                                # (0=auto)
PIXSCALE_MAXERR    1.2         # Max scale-factor uncertainty
POSANGLE_MAXERR    5.0         # Max position-angle uncertainty (deg)
POSITION_MAXERR    1.0         # Max positional uncertainty (arcmin)
MATCH_RESOL        0           # Matching resolution (arcsec); 0=auto
MATCH_FLIPPED      N           # Allow matching with flipped axes?
MOSAIC_TYPE        UNCHANGED    # UNCHANGED, SAME_CRVAL, SHARE_PROJAXIS,
                                # FIX_FOCALPLANE or LOOSE
FIXFOCALPLANE_NMIN 1           # Min number of dets for FIX_FOCALPLANE

#----- Cross-identification -----
CROSSID_RADIUS     2.0         # Cross-id initial radius (arcsec)

#----- Astrometric solution -----
SOLVE_Astrom       N           # Compute astrometric solution (Y/N) ?
ASTRINSTRU_KEY     FILTER,QRUNID # FITS keyword(s) defining the astrom
STABILITY_TYPE     INSTRUMENT   # EXPOSURE, GROUP, INSTRUMENT or FILE
CENTROID_KEYS      XWIN_IMAGE,YWIN_IMAGE # Cat. parameters for centroiding
CENTROIDERR_KEYS   ERRRAWIN_IMAGE,ERRBWIN_IMAGE,ERRTHETAWIN_IMAGE
                                # Cat. params for centroid err ellipse
DISTORT_KEYS       XWIN_IMAGE,YWIN_IMAGE # Cat. parameters or FITS keywords
DISTORT_GROUPS     1,1         # Polynom group for each context key
DISTORT_DEGREES    3           # Polynom degree for each group
ASTREF_WEIGHT      1.0         # Relative weight of ref.astrom.cat.
ASTRCLIP_NSIGMA   3.0         # Astrom. clipping threshold in sigmas
CORRECT_COLOURSHIFTS N        # Correct for colour shifts (Y/N)?

```

```

#----- Photometric solution -----
SOLVE_PHOTOM          Y          # Compute photometric solution (Y/N) ?
MAGZERO_OUT           30.0       # Magnitude zero-point(s) in output
MAGZERO_INTERR        0.01      # Internal mag.zero-point accuracy
MAGZERO_REFERR        0.03      # Photom.field mag.zero-point accuracy
PHOTINSTRU_KEY        FILTER     # FITS keyword(s) defining the photom.
MAGZERO_KEY           PHOT_C     # FITS keyword for the mag zero-point
EXPOTIME_KEY          EXPTIME    # FITS keyword for the exposure time (s)
AIRMASS_KEY           AIRMASS    # FITS keyword for the airmass
EXTINCT_KEY           PHOT_K     # FITS keyword for the extinction coeff
PHOTOMFLAG_KEY        PHOTFLAG   # FITS keyword for the photometry flag
PHOTFLUX_KEY          FLUX_AUTO   # Catalog param. for the flux measurement
PHOTFLUXERR_KEY       FLUXERR_AUTO # Catalog parameter for the flux error
PHOTCLIP_NSIGMA      3.0        # Photom.clipping threshold in sigmas

#----- Check-plots -----
CHECKPLOT_CKEY        SCAMPCOL    # FITS keyword for PLPLOT field colour
CHECKPLOT_DEV         PNG         # NULL, XWIN, TK, PS, PSC, XFIG, PNG,
                                # JPEG, AQT, PDF or SVG
CHECKPLOT_RES         1600,1200   # Check-plot resolution (0 = default)
CHECKPLOT_ANTIALIAS   Y          # Anti-aliasing using convert (Y/N) ?
CHECKPLOT_TYPE        DISTORTION,ASTR_INTERROR2D,ASTR_INTERROR1D,ASTR_REFERROR2D,
                                ASTR_REFERROR1D,ASTR_CHI2,PHOT_ERROR,PHOT_ERRORVSMAG,
                                PHOT_ZPCORR,PHOT_ZPCORR3D
CHECKPLOT_NAME        distort,astr_interror2d,astr_interror1d,astr_referror2d,
                                astr_referror1d,astr_chi2,psphot_error,phot_errorvsmag,
                                phot_zpcorr,phot_zpcorr3d
                                # Check-plot filename(s)

#----- Check-images -----
CHECKIMAGE_TYPE       NONE        # NONE, AS_PAIR, AS_REPAIR, or AS_XCORR
CHECKIMAGE_NAME       check.fits  # Check-image filename(s)

#----- Miscellaneous -----
SN_THRESHOLDS        10.0,100.0  # S/N thresholds (in sigmas) for all and
                                # high-SN sample
FWHM_THRESHOLDS      0.0,100.0   # FWHM thresholds (in pixels) for sources
FLAGS_MASK            0x00f0     # Rejection mask on SEX FLAGS
WEIGHTFLAGS_MASK     0x00ff     # Rejection mask on SEX FLAGS_WEIGHT
IMAFLAGS_MASK        0x0        # Rejection mask on SEX IMAFLAGS_ISO
AHEADER_GLOBAL       /usr/share/scamp/megacam.ahead
                                # Filename of the global INPUT header
AHEADER_SUFFIX       .ahead      # Filename extension for additional
                                # INPUT headers
HEADER_SUFFIX        .head       # Filename extension for OUTPUT headers
HEADER_TYPE          NORMAL      # NORMAL or FOCAL_PLANE
VERBOSE_TYPE         LOG         # QUIET, NORMAL, LOG or FULL
WRITE_XML            Y          # Write XML file (Y/N)?
XML_NAME             CFHTLS-T0007-D3_SCamp_phot_g.xml
                                # Filename for XML output
XSL_URL              scamp.xsl   # Filename for XSL style-sheet
NTHREADS             0          # Number of simultaneous threads for
                                # the SMP version of SCAMP
                                # 0 = automatic

```

## B.2.2 SWarp stack configuration file for T0007 Deep

```
# Default configuration file for SWarp 2.17.6
# EB 2009-04-09
#
# Last modified for CFHTLS-T0007 (Megacam):
# YG 2011-09-01

#----- Output -----
IMAGEOUT_NAME      CFHTLS_D-85_g_221531-174356_T0007.fits
                   # Output filename
WEIGHTOUT_NAME     CFHTLS_D-85_g_221531-174356_T0007_weight.fits
                   # Output weight-map filename

HEADER_ONLY        N          # Only a header as an output file (Y/N)?
HEADER_SUFFIX      .head     # Filename extension for additional headers

#----- Input Weights -----
WEIGHT_TYPE        MAP_WEIGHT # BACKGROUND, MAP_RMS, MAP_VARIANCE
                   # or MAP_WEIGHT
WEIGHT_SUFFIX      _weight.fits # Suffix to use for weight-maps
WEIGHT_IMAGE       # Weightmap filename if suffix not used
                   # (all or for each weight-map)
WEIGHT_THRESH      # Bad pixel weight-threshold

#----- Co-addition -----
COMBINE            Y          # Combine resampled images (Y/N)?
COMBINE_TYPE       MEDIAN    # MEDIAN, AVERAGE, MIN, MAX, WEIGHTED, CHI2
                   # or SUM
BLANK_BADPIXELS    N          # Set to 0 pixels having a weight of 0

#----- Astrometry -----
CELESTIAL_TYPE     NATIVE     # NATIVE, PIXEL, EQUATORIAL,
                   # GALACTIC, ECLIPTIC, or SUPERGALACTIC
PROJECTION_TYPE    TAN        # Any WCS projection code or NONE
PROJECTION_ERR     0.001     # Maximum projection error (in output
                   # pixels), or 0 for no approximation
CENTER_TYPE        MANUAL     # MANUAL, ALL or MOST
CENTER             22:15:31,-17:43:56 # Coordinates of the image center
PIXELSCALE_TYPE    MANUAL     # MANUAL, FIT, MIN, MAX or MEDIAN
PIXEL_SCALE        0.186     # Pixel scale
IMAGE_SIZE         19354,19354 # Image size (0 = AUTOMATIC)

#----- Resampling -----
RESAMPLE           Y          # Resample input images (Y/N)?
RESAMPLE_DIR       .          # Directory path for resampled images
RESAMPLE_SUFFIX    .resamp.fits # filename extension for resampled images
RESAMPLING_TYPE    LANCZOS3   # NEAREST, BILINEAR, LANCZOS2, LANCZOS3
                   # or LANCZOS4 (1 per axis)
OVERSAMPLING       0          # Oversampling in each dimension
                   # (0 = automatic)
INTERPOLATE        Y          # Interpolate bad input pixels (Y/N)?
                   # (all or for each image)
FSCALASTRO_TYPE    VARIABLE   # NONE, FIXED, or VARIABLE
FSCALE_KEYWORD     FLXSCALE   # FITS keyword for the multiplicative
                   # factor applied to each input image
FSCALE_DEFAULT     1.0        # Default FSCALE value if not in header
GAIN_KEYWORD       GAIN       # FITS keyword for effect. gain (e-/ADU)
GAIN_DEFAULT       0.0        # Default gain if no FITS keyword found
                   # 0 = infinity (all or for each image)
SATLEV_KEYWORD     SATURATE   # FITS keyword for saturation level (ADU)
SATLEV_DEFAULT     50000.0    # Default saturation if no FITS keyword
```

```

#----- Background subtraction -----
SUBTRACT_BACK      Y          # Subtraction sky background (Y/N)?
                        # (all or for each image)
BACK_TYPE          AUTO      # AUTO or MANUAL
                        # (all or for each image)
BACK_DEFAULT       0.0      # Default background value in MANUAL
                        # (all or for each image)
BACK_SIZE          128      # Background mesh size (pixels)
                        # (all or for each image)
BACK_FILTERSIZE    3        # Background map filter range (meshes)
                        # (all or for each image)
BACK_FILTTHRESH   0.0      # Threshold above which the background-
                        # map filter operates

#----- Memory management -----
VMEM_DIR           .        # Directory path for swap files
VMEM_MAX           2047     # Maximum amount of virtual memory (MB)
MEM_MAX            128      # Maximum amount of usable RAM (MB)
COMBINE_BUFSIZE    400      # RAM dedicated to co-addition(MB)

#----- Miscellaneous -----
DELETE_TMPFILES    Y        # Delete temporary resampled FITS files
                        # (Y/N)?

COPY_KEYWORDS      FILTER,INSTRUME,TELESCOP,DETECTOR,OBSERVER,PHOT_C,PHOT_K,
OBJECT,DATE_OBS,ORIGIN,SEEING,REL_DATE
                        # List of FITS keywords to propagate
                        # from the input to the output headers
WRITE_FILEINFO     N        # Write information about each input
                        # file in the output image header?
WRITE_XML          Y        # Write XML file (Y/N)?
XML_NAME           CFHTLS_D-85_g_221531-174356_T0007_Swarp.xml
                        # Filename for XML output
XSL_URL            swarp.xsl # Filename for XSL style-sheet
VERBOSE_TYPE       NORMAL   # QUIET,NORMAL or FULL
NNODES             1        # Number of nodes (for clusters)
NODE_INDEX         0        # Node index (for clusters)
NTHREADS           0        # Number of simultaneous threads for
                        # the SMP version of SWarp
                        # 0 = automatic

```

### B.2.3 SWarp chi2-image configuration file for T0007 Deep

```

# Default configuration file for SWarp 2.17.6
# EB 2009-04-09
#
# Last modified for CFHTLS-T0007 chi2 (Megacam):
# YG 2011-09-22

#----- Output -----
IMAGEOUT_NAME      CFHTLS_D-85_gri_221531-174356_T0007.fits
                   # Output filename
WEIGHTOUT_NAME     CFHTLS_D-85_gri_221531-174356_T0007_weight.fits
                   # Output weight-map filename

HEADER_ONLY        N          # Only a header as an output file (Y/N)?
HEADER_SUFFIX      .head     # Filename extension for additional headers

#----- Input Weights -----
WEIGHT_TYPE        MAP_WEIGHT # BACKGROUND,MAP_RMS,MAP_VARIANCE
                   # or MAP_WEIGHT
WEIGHT_SUFFIX      _weight.fits # Suffix to use for weight-maps
WEIGHT_IMAGE       # Weightmap filename if suffix not used
                   # (all or for each weight-map)
WEIGHT_THRESH      # Bad pixel weight-threshold

#----- Co-addition -----
COMBINE            Y          # Combine resampled images (Y/N)?
COMBINE_TYPE       CHI2      # MEDIAN,AVERAGE,MIN,MAX,WEIGHTED,CHI2
                   # or SUM
BLANK_BADPIXELS    N          # Set to 0 pixels having a weight of 0

#----- Astrometry -----
CELESTIAL_TYPE     NATIVE     # NATIVE, PIXEL, EQUATORIAL,
                   # GALACTIC,ECLIPTIC, or SUPERGALACTIC
PROJECTION_TYPE    TAN        # Any WCS projection code or NONE
PROJECTION_ERR     0.001      # Maximum projection error (in output
                   # pixels), or 0 for no approximation
CENTER_TYPE        MANUAL     # MANUAL, ALL or MOST
CENTER             22:15:31,-17:43:56 # Coordinates of the image center
PIXELSCALE_TYPE    MANUAL     # MANUAL,FIT,MIN,MAX or MEDIAN
PIXEL_SCALE        0.186      # Pixel scale
IMAGE_SIZE         19354,19354 # Image size (0 = AUTOMATIC)

#----- Resampling -----
RESAMPLE           Y          # Resample input images (Y/N)?
RESAMPLE_DIR       .          # Directory path for resampled images
RESAMPLE_SUFFIX    .resamp.fits # filename extension for resampled images
RESAMPLING_TYPE    LANCZOS3   # NEAREST,BILINEAR,LANCZOS2,LANCZOS3
                   # or LANCZOS4 (1 per axis)
OVERSAMPLING       0          # Oversampling in each dimension
                   # (0 = automatic)
INTERPOLATE        Y          # Interpolate bad input pixels (Y/N)?
                   # (all or for each image)
FSCALASTRO_TYPE    VARIABLE   # NONE,FIXED, or VARIABLE
FSCALE_KEYWORD     FLXSCALE   # FITS keyword for the multiplicative
                   # factor applied to each input image
FSCALE_DEFAULT     1.0        # Default FSCALE value if not in header
GAIN_KEYWORD       GAIN       # FITS keyword for effect. gain (e-/ADU)
GAIN_DEFAULT       0.0        # Default gain if no FITS keyword found
                   # 0 = infinity (all or for each image)
SATLEV_KEYWORD     SATURATE   # FITS keyword for saturation level (ADU)
SATLEV_DEFAULT     50000.0    # Default saturation if no FITS keyword

```

```

#----- Background subtraction -----
SUBTRACT_BACK      Y          # Subtraction sky background (Y/N)?
                    # (all or for each image)
BACK_TYPE          AUTO       # AUTO or MANUAL
                    # (all or for each image)
BACK_DEFAULT       0.0       # Default background value in MANUAL
                    # (all or for each image)
BACK_SIZE          64        # Background mesh size (pixels)
                    # (all or for each image)
BACK_FILTERSIZE    3         # Background map filter range (meshes)
                    # (all or for each image)
BACK_FILTTHRESH    0.0       # Threshold above which the background-
                    # map filter operates

#----- Memory management -----
VMEM_DIR           .         # Directory path for swap files
VMEM_MAX           2047      # Maximum amount of virtual memory (MB)
MEM_MAX            4096      # Maximum amount of usable RAM (MB)
COMBINE_BUFSIZE    1024     # RAM dedicated to co-addition(MB)

#----- Miscellaneous -----
DELETE_TMPFILES    Y         # Delete temporary resampled FITS files
                    # (Y/N)?

COPY_KEYWORDS      OBJECT,FILTER # List of FITS keywords to propagate
                    # from the input to the output headers
WRITE_FILEINFO     Y         # Write information about each input
                    # file in the output image header?
WRITE_XML          Y         # Write XML file (Y/N)?
XML_NAME           CFHTLS_D-85_gri_221531-174356_T0007_SWarp_chi2.xml
                    # Filename for XML output
XSL_URL            swarp.xsl  # Filename for XSL style-sheet
VERBOSE_TYPE       NORMAL    # QUIET,NORMAL or FULL
NNODES             1         # Number of nodes (for clusters)
NODE_INDEX         0         # Node index (for clusters)
NTHREADS           0         # Number of simultaneous threads for
                    # the SMP version of SWarp
                    # 0 = automatic

```



## B.2.4 SExtractor .ldac catalogue configuration file for T0007 Deep

```

# Default configuration file for SExtractor 2.11.0
# EB 2010-02-11
#
# Last modified for SExtr stack.ldac MAG_APER(1):
# YG 2011-01-28

#----- Catalog -----
CATALOG_NAME      CFHTLS_D-85_y_100028+021230_T0007.ldac
                  # name of the output catalog
CATALOG_TYPE      FITS_LDAC
                  # NONE,ASCII,ASCII_HEAD, ASCII_SKYCAT,
                  # ASCII_VOTABLE, FITS_1.0 or FITS_LDAC
PARAMETERS_NAME   sextr-stack_APER1.param
                  # name of the file containing catalog contents

#----- Extraction -----
DETECT_TYPE       CCD
                  # CCD (linear) or PHOTO (with gamma correction)
DETECT_MINAREA    3
                  # min. number of pixels above threshold
DETECT_MAXAREA    0
                  # max. number of pixels above threshold (0=unlimited)
THRESH_TYPE       RELATIVE
                  # threshold type: RELATIVE (in sigmas)
                  # or ABSOLUTE (in ADUs)
DETECT_THRESH     1.0
                  # <sigmas> or <threshold>,<ZP> in mag.arcsec-2
ANALYSIS_THRESH   1.0
                  # <sigmas> or <threshold>,<ZP> in mag.arcsec-2
FILTER            Y
                  # apply filter for detection (Y or N)?
FILTER_NAME       default-auto.conv
                  # name of the file containing the filter
FILTER_THRESH     32
                  # Threshold[s] for retina filtering
DEBLEND_NTHRESH   32
                  # Number of deblending sub-thresholds
DEBLEND_MINCONT   0.002
                  # Minimum contrast parameter for deblending
CLEAN             Y
                  # Clean spurious detections? (Y or N)?
CLEAN_PARAM       1.0
                  # Cleaning efficiency
MASK_TYPE         CORRECT
                  # type of detection MASKing: can be one of
                  # NONE, BLANK or CORRECT

#----- WEIGHTing -----
WEIGHT_TYPE       MAP_WEIGHT
                  # type of WEIGHTing: NONE, BACKGROUND,
                  # MAP_RMS, MAP_VAR or MAP_WEIGHT
WEIGHT_IMAGE      CFHTLS_D-85_y_100028+021230_T0007_weight.fits
                  # weight-map filename
WEIGHT_GAIN       Y
                  # modulate gain (E/ADU) with weights? (Y/N)
WEIGHT_THRESH     0
                  # weight threshold[s] for bad pixels

#----- FLAGging -----
FLAG_IMAGE        flag.fits
                  # filename for an input FLAG-image
FLAG_TYPE         OR
                  # flag pixel combination: OR, AND, MIN, MAX
                  # or MOST

#----- Photometry -----
PHOT_APERTURES    27.7139
                  # MAG_APER aperture diameter(s) in pixels
PHOT_AUTOPARAMS  2.5, 3.5
                  # MAG_AUTO parameters: <Kron_fact>,<min_radius>
PHOT_PETROPARAMS 2.0, 3.5
                  # MAG_PETRO parameters: <Petrosian_fact>,
                  # <min_radius>
PHOT_AUTOAPERS    0.0,0.0
                  # <estimation>,<measurement> minimum apertures
                  # for MAG_AUTO and MAG_PETRO
PHOT_FLUXFRAC     0.2,0.5,0.8
                  # flux fraction[s] used for FLUX_RADIUS
SATUR_LEVEL       50000.0
                  # level (in ADUs) at which arises saturation
SATUR_KEY         TOTO
                  # keyword for saturation level (in ADUs)
MAG_ZEROPOINT     30.0
                  # magnitude zero-point
MAG_GAMMA         4.0
                  # gamma of emulsion (for photographic scans)
GAIN              0.0
                  # detector gain in e-/ADU
GAIN_KEY          GAIN
                  # keyword for detector gain in e-/ADU
PIXEL_SCALE       0
                  # size of pixel in arcsec (0=use FITS WCS info)

```

```

#----- Star/Galaxy Separation -----
SEEING_FWHM      0.9          # stellar FWHM in arcsec
STARNNW_NAME     default-auto.nnw # Neural-Network_Weight table filename

#----- Background -----
BACK_TYPE        AUTO          # AUTO or MANUAL
BACK_VALUE       0.0           # Default background value in MANUAL mode
BACK_SIZE        128           # Background mesh: <size> or <width>,<height>
BACK_FILTERSIZE  3             # Background filter: <size> or <width>,<height>
BACKPHOTO_TYPE   GLOBAL        # can be GLOBAL or LOCAL
BACKPHOTO_THICK  24            # thickness of the background LOCAL annulus
BACK_FILTTHRESH  0.0           # Threshold above which the background-
                                # map filter operates

#----- Check Image -----
CHECKIMAGE_TYPE  MINIBACKGROUND # MINIBACKGROUND, MINIBACK_RMS, -BACKGROUND,
                                # FILTERED, OBJECTS, -OBJECTS, SEGMENTATION,
                                # or APERTURES
CHECKIMAGE_NAME  CFHTLS_D-85_y_100028+021230_T0007_mbgk.fits
                                # Filename for the check-image

#----- Memory (change with caution!) -----
MEMORY_OBJSTACK  3000          # number of objects in stack
MEMORY_PIXSTACK  3000000       # number of pixels in stack
MEMORY_BUFSIZE   1024          # number of lines in buffer

#----- ASSOCIation -----
ASSOC_NAME       sky.list       # name of the ASCII file to ASSOCIate
ASSOC_DATA       2,3,4          # columns of the data to replicate (0=all)
ASSOC_PARAMS     2,3,4          # columns of xpos,ypos[,mag]
ASSOC_RADIUS     2.0           # cross-matching radius (pixels)
ASSOC_TYPE       NEAREST        # ASSOCIation method: FIRST, NEAREST, MEAN,
                                # MAG_MEAN, SUM, MAG_SUM, MIN or MAX
ASSOCSELEC_TYPE  MATCHED        # ASSOC selection type: ALL, MATCHED or -MATCHED

#----- Miscellaneous -----
VERBOSE_TYPE     NORMAL         # can be QUIET, NORMAL or FULL
HEADER_SUFFIX    .head          # Filename extension for additional headers
WRITE_XML        Y              # Write XML file (Y/N)?
XML_NAME         CFHTLS_W_r_021021-104400_T0007_SExtr_ldac.xml
                                # Filename for XML output
XSL_URL          sextractor.xsl # Filename for XSL style-sheet
NTHREADS         1              # 1 single thread
FITS_UNSIGNED    N              # Treat FITS integer values as unsigned (Y/N)?
INTERP_MAXXLG    16             # Max. lag along X for 0-weight interpolation
INTERP_MAXYLAG   16             # Max. lag along Y for 0-weight interpolation
INTERP_TYPE      ALL            # Interpolation type: NONE, VAR_ONLY or ALL

#----- Experimental Stuff -----
PSF_NAME         default.psf    # File containing the PSF model
PSF_NMAX         2              # Max.number of PSFs fitted simultaneously
PATTERN_TYPE     RINGS-HARMONIC # can RINGS-QUADPOLE, RINGS-OCTOPOLE,
                                # RINGS-HARMONICS or GAUSS-LAGUERRE
SOM_NAME         default.som    # File containing Self-Organizing Map weights

```

## B.2.5 SExtractor DUAL MODE .cat catalogue configuration file for T0007 Deep

```

# Default configuration file for SExtractor 2.8.6
# EB 2009-04-09
#
# Last modified for CFHTLS-T0007 chi2 (Megacam):
# YG 2011-09-24

#----- Catalog -----
CATALOG_NAME      CFHTLS_D-25_g_022559-042940_T0007.cat
                  # name of the output catalog
CATALOG_TYPE      ASCII_HEAD      # NONE,ASCII,ASCII_HEAD, ASCII_SKYCAT,
                  # ASCII_VOTABLE, FITS_1.0 or FITS_LDAC
PARAMETERS_NAME   sextr-chi2_APER27.param # name of the file containing catalog contents

#----- Extraction -----
DETECT_TYPE       CCD              # CCD (linear) or PHOTO (with gamma correction)
DETECT_MINAREA    3                # minimum number of pixels above threshold
THRESH_TYPE       ABSOLUTE         # threshold type: RELATIVE (in sigmas)
                  # or ABSOLUTE (in ADUs)
DETECT_THRESH     0.4              # <sigmas> or <threshold>,<ZP> in mag.arcsec-2
ANALYSIS_THRESH   0.4              # <sigmas> or <threshold>,<ZP> in mag.arcsec-2
FILTER            Y                # apply filter for detection (Y or N)?
FILTER_NAME       default-autochi2.conv # name of the file containing the filter
FILTER_THRESH     # Threshold[s] for retina filtering
DEBLEND_NTHRESH   32              # Number of deblending sub-thresholds
DEBLEND_MINCONT   0.002           # Minimum contrast parameter for deblending
CLEAN             Y                # Clean spurious detections? (Y or N)?
CLEAN_PARAM       1.0             # Cleaning efficiency
MASK_TYPE         CORRECT          # type of detection MASKing: can be one of
                  # NONE, BLANK or CORRECT

#----- WEIGHting -----
WEIGHT_TYPE       MAP_WEIGHT,MAP_WEIGHT # type of WEIGHting: NONE, BACKGROUND,
                  # MAP_RMS, MAP_VAR or MAP_WEIGHT
WEIGHT_IMAGE      CFHTLS_D-25_gri_022559-042940_T0007_weight.fits,
                  CFHTLS_D-25_g_022559-042940_T0007_weight.fits
                  # weight-map filename
WEIGHT_GAIN       Y                # modulate gain (E/ADU) with weights? (Y/N)
WEIGHT_THRESH     # weight threshold[s] for bad pixels

#----- FLAGging -----
FLAG_IMAGE        flag.fits        # filename for an input FLAG-image
FLAG_TYPE         OR               # flag pixel combination: OR, AND, MIN, MAX
                  # or MOST

#----- Photometry -----
PHOT_APERTURES    10.,12.,14.,16.,18.,20.,22.,24.,26.,28.,30.,32.,34.,36.,38.,
                  40.,42.,44.,46.,48.,50.,52.,54.,56.,58.,60.,26.471
                  # MAG_APER aperture diameter(s) in pixels
PHOT_AUTOPARAMS   2.5, 3.5        # MAG_AUTO parameters: <Kron_fact>,<min_radius>
PHOT_PETROPARAMS  2.0, 3.5        # MAG_PETRO parameters: <Petrosian_fact>,
                  # <min_radius>
PHOT_AUTOAPERS    16.0,16.0       # <estimation>,<measurement> minimum apertures
                  # for MAG_AUTO and MAG_PETRO
PHOT_FLUXFRAC     0.2,0.5,0.8     # flux fraction[s] used for FLUX_RADIUS
SATUR_LEVEL       50000.0         # level (in ADUs) at which arises saturation
SATUR_KEY         TOTO            # keyword for saturation level (in ADUs)
MAG_ZEROPOINT     30.0           # magnitude zero-point
MAG_GAMMA         4.0            # gamma of emulsion (for photographic scans)
GAIN              0.0            # detector gain in e-/ADU
GAIN_KEY          GAIN           # keyword for detector gain in e-/ADU
PIXEL_SCALE       0              # size of pixel in arcsec (0=use FITS WCS info)

```

```

#----- Star/Galaxy Separation -----
SEEING_FWHM      0.9          # stellar FWHM in arcsec
STAR_NW_NAME     default-autochi2.nnw # Neural-Network_Weight table filename

#----- Background -----
BACK_TYPE        AUTO          # AUTO or MANUAL
BACK_VALUE       0.0          # Default background value in MANUAL mode
BACK_SIZE        256          # Background mesh: <size> or <width>,<height>
BACK_FILTERSIZE  9            # Background filter: <size> or <width>,<height>
BACKPHOTO_TYPE   LOCAL        # can be GLOBAL or LOCAL
BACKPHOTO_THICK  30           # thickness of the background LOCAL annulus
BACK_FILTTHRESH  0.0         # Threshold above which the background-
                               # map filter operates

#----- Check Image -----
CHECKIMAGE_TYPE  MINIBACKGROUND # can be NONE, BACKGROUND, BACKGROUND_RMS,
                               # MINIBACKGROUND, MINIBACK_RMS, -BACKGROUND,
                               # FILTERED, OBJECTS, -OBJECTS, SEGMENTATION,
                               # or APERTURES
CHECKIMAGE_NAME  CFHTLS_D-25_g_022559-042940_T0007_mbk_g_chi2.fits
                               # Filename for the check-image

#----- Memory (change with caution!) -----
MEMORY_OBJSTACK  5000         # number of objects in stack
MEMORY_PIXSTACK  1000000      # number of pixels in stack
MEMORY_BUFSIZE   1024        # number of lines in buffer

#----- ASSOCIation -----
ASSOC_NAME       sky.list     # name of the ASCII file to ASSOCIate
ASSOC_DATA       2,3,4        # columns of the data to replicate (0=all)
ASSOC_PARAMS     2,3,4        # columns of xpos,ypos[,mag]
ASSOC_RADIUS     2.0         # cross-matching radius (pixels)
ASSOC_TYPE       NEAREST      # ASSOCIation method: FIRST, NEAREST, MEAN,
                               # MAG_MEAN, SUM, MAG_SUM, MIN or MAX
ASSOCSELEC_TYPE  MATCHED     # ASSOC selection type: ALL, MATCHED or -MATCHED

#----- Miscellaneous -----
VERBOSE_TYPE     NORMAL       # can be QUIET, NORMAL or FULL
WRITE_XML        Y            # Write XML file (Y/N)?
XML_NAME         CFHTLS_D-25_g_022559-042940_T0007_SExtr_chi2.xml
                               # Filename for XML output
XSL_URL          sextractor.xsl # Filename for XSL style-sheet
NTHREADS        0            # Number of simultaneous threads for
                               # the SMP version of SExtractor
                               # 0 = automatic
FITS_UNSIGNED    N            # Treat FITS integer values as unsigned (Y/N)?
INTERP_MAXLAG    16           # Max. lag along X for 0-weight interpolation
INTERP_MAXYLAG   16           # Max. lag along Y for 0-weight interpolation
INTERP_TYPE      ALL          # Interpolation type: NONE, VAR_ONLY or ALL

#----- Experimental Stuff -----
PSF_NAME         default.psf   # File containing the PSF model
PSF_NMAX         9            # Max.number of PSFs fitted simultaneously
PSFDISPLAY_TYPE  SPLIT        # Catalog type for PSF-fitting: SPLIT or VECTOR
PATTERN_TYPE     RINGS-HARMONIC # can RINGS-QUADPOLE, RINGS-OCTOPOLE,
                               # RINGS-HARMONICS or GAUSS-LAGUERRE
SOM_NAME         default.som   # File containing Self-Organizing Map weights

```

## Acronyms & Abbreviations

---

---

ASCII	American Standard Code for Information Interchange (ASCII) table format
CADC	The Canadian Astronomy Data Center
CCD	Charge Coupled Device
CFHT	Canada-France-Hawaii Telescope
CFHTLS	Canada-France-Hawaii Telescope Legacy Survey
COSMOS	Cosmological Evolution Survey
FITS	Flexible Image Transport System (FITS) file format
FoV	Field of View
FWHM	Full Width at Half Maximum
LDAC	Leiden Data Analysis Center (LDAC) catalogue format
MEF	Multi-Extension FITS (MEF) file format
PSF	Point Spread Function
PSFEx	PSF Extractor
QA	Quality Assessment
QC	Quality Control
QSO	Queued Service Observations (QSO)
SCAMP	Software for Calibrating AstroMetry and Photometry
SDSS	Sloan Digital Sky Survey
SDSS-DR8	SDSS 8th Data Release
SExtractor	Source Extractor
SLR	Stellar Locus Regression
SNLS	SuperNova Legacy Survey
SNR	Signal to Noise Ratio
T0006	CFHTLS 6th Data Release
T0007	CFHTLS 7th Data Release

---

## Acronyms & Abbreviations (cont.)

---

USNO	United States Naval Observatory
VIMOS	Visible MultiObject Spectrograph
VIPERS	VIMOS Public Extra Galactic Observation Survey
XML	Extensible Markup Language (XML) table format
Youpi	“YOUpi is your processing Pipeline”
ZP(s)	Zero Point(s)
2MASS	The Two Micron All Sky Survey

---

---

## References

- Astier, P., et al. 2006, *A&A*, 447, 31
- Bahcall, J. N., & Soneira, R. M. 1981, *ApJS*, 47, 357
- Bertin, E. 2006, in *ASP Conference Series*, Vol. 351, *ADASS XV*, ed. C. Gabriel, C. Arviset, D. Ponz, & S. Enrique, 112
- Bertin, E. 2009, in *Memorie della Società Astronomica Italiana*, Vol. 80, 422
- Bertin, E. 2011, in *ASP Conference Series*, Vol. 442, *ADASS XX*, ed. I. N. Evans, A. Accomazzi, D. J. Mink, & A. H. Rots, 435
- Bertin, E., Mellier, Y., Radovich, M., Missonnier, G., Didelon, P., & Morin, B. 2002, in *ASP Conference Series*, Vol. 281, *ADASS XI*, ed. D. A. Bohlender, D. Durand, & T. H. Handley, 228
- Bonnarel, F., et al. 2000, *A&AS*, 143, 33
- Boulade, O., et al. 2000, in *SPIE Conference Series*, ed. M. Iye & A. F. Moorwood, Vol. 4008, 657
- Capak, P., et al. 2007, *ApJS*, 172, 99
- Fernique, P., Oberto, A., Boch, T., & Bonnarel, F. 2010, in *Astronomical Society of the Pacific Conference Series*, Vol. 434, *Astronomical Data Analysis Software and Systems XIX*, ed. Y. Mizumoto, K.-I. Morita, & M. Ohishi, 163
- Genova, F., et al. 2000, *A&AS*, 143, 1
- Holtzman, J. A., et al. 2008, *AJ*, 136, 2306
- Kron, R. G. 1980, *ApJS*, 43, 305
- Landolt, A. U. 1992, *AJ*, 104, 340
- Magnier, E. A., & Cuillandre, J.-C. 2004, *PASP*, 116, 449
- Marmo, C., & Bertin, E. 2008, in *ASP Conference Series*, Vol. 394, *ADASS XVII*, ed. R. W. Argyle, P. S. Bunclark, & J. R. Lewis, 619
- McCracken, H. J., et al. 2003, *A&A*, 410, 17
- Ochsenbein, F., Bauer, P., & Marcout, J. 2000, *A&AS*, 143, 23
- Oke, J. B. 1974, *ApJS*, 27, 21
- Oke, J. B., & Gunn, J. E. 1983, *ApJ*, 266, 713
- Pickles, A. J. 1998, *PASP*, 110, 863
- Pineau, F.-X., Boch, T., & Derriere, S. 2011, in *Astronomical Society of the Pacific Conference Series*, Vol. 442, *Astronomical Data Analysis Software and Systems XX*, ed. I. N. Evans, A. Accomazzi, D. J. Mink, & A. H. Rots, 85
- Regnault, N., et al. 2009, *A&A*, 506, 999

- Schlegel, D. J., Finkbeiner, D. P., & Davis, M. 1998, ApJ, 500, 525
- Schultheis, M., Robin, A. C., Reylé, C., McCracken, H. J., Bertin, E., Mellier, Y., & Le Fèvre, O. 2006, A&A, 447, 185
- Sesar, B., Jurić, M., & Ivezić, Ž. 2011, ApJ, 731, 4
- Skrutskie, M. F., et al. 2006, AJ, 131, 1163
- Smith, J. A., et al. 2002, AJ, 123, 2121
- Szalay, A. S., Connolly, A. J., & Szokoly, G. P. 1999, AJ, 117, 68
- Taylor, M. B. 2005, in Astronomical Society of the Pacific Conference Series, Vol. 347, Astronomical Data Analysis Software and Systems XIV, ed. P. Shopbell, M. Britton, & R. Ebert, 29
- Westera, P., Lejeune, T., Buser, R., Cuisinier, F., & Bruzual, G. 2002, A&A, 381, 524